DEVELOPMENT OF A PERFORMANCE-BASED SEISMIC DESIGN PHILOSOPHY FOR MID-RISE WOODFRAME CONSTRUCTION

NEESWOOD

SIMPLIFIED DIRECT DISPLACEMENT DESIGN OF SIX-STORY NEESWOOD CAPSTONE BUILDING AND PRE-TEST SEISMIC PERFORMANCE ASSESSMENT

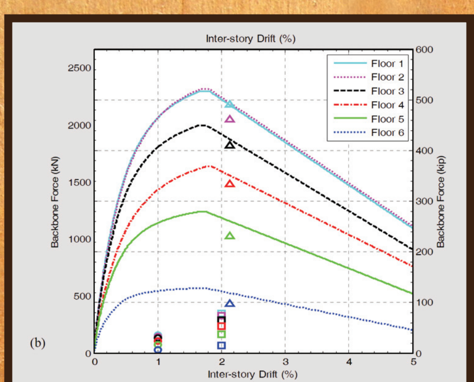

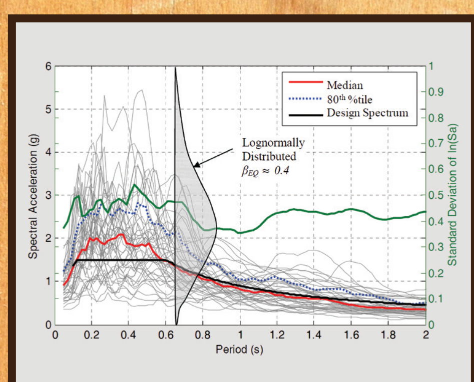

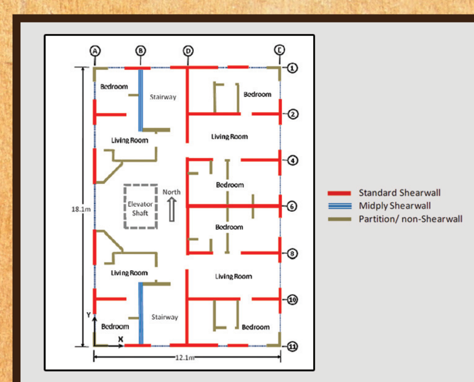

By
WeiChiang Pang, David Rosowsky
John van de Lindt and Shiling Pei

Technical Report MCEER-10-0002 ■ May 28, 2010

This research was conducted at Texas A&M University and Colorado State University and was supported by the National Science Foundation under Grant No. CMMI-0529903 (NEES Research) and CMMI-0402490 (NEES Operations).

Sponsored by the
National Science Foundation
NSF Grant Number CMMI-0529903 and CMMI-0402490

Project Title
Development of a Performance-Based Seismic Design
Philosophy for Mid-Rise Woodframe Construction

Project Team
Colorado State University
University of Delaware
University at Buffalo, State University of New York
Rensselaer Polytechnic Institute
Texas A&M University

Web Site
www.engr.colostate.edu/NEESWood

DISCLAIMER

NEESWood Report No. 5

Simplified Direct Displacement Design of Six-Story NEESWood Capstone Building and Pre-Test Seismic Performance Assessment

by

WeiChiang Pang,[1] David Rosowsky,[2] John van de Lindt[3] and Shiling Pei[4]

Publication Date: May 28, 2010
Submittal Date: December 14, 2009

Technical Report MCEER-10-0002

NSF Grant Numbers CMMI-0529903 and CMMI-0402490

1 Assistant Professor, Civil Engineering Department, Clemson University; former Post-doctoral Researcher, Zachry Department of Civil Engineering, Texas A&M University
2 Professor and Dean of Engineering, Department of Civil & Environmental Engineering, Rensselaer Polytechnic Institute; former A.P. Florence Wiley Chair Professor and Department Head, Zachry Department of Civil Engineering, Texas A&M University
3 Associate Professor, Department of Civil Engineering, Colorado State University
4 Graduate Student, Department of Civil Engineering, Colorado State University

MCEER
University at Buffalo, State University of New York
Red Jacket Quadrangle, Buffalo, NY 14261
Phone: (716) 645-3391; Fax (716) 645-3399
E-mail: *mceer@buffalo.edu*; WWW Site: *http://mceer.buffalo.edu*

Project Overview

NEESWood: Development of a Performance-Based Seismic Design Philosophy for Mid-Rise Woodframe Construction

While woodframe structures have historically performed well with regard to life safety in regions of moderate to high seismicity, these types of low-rise structures have sustained significant structural and nonstructural damage in recent earthquakes. To date, the height of woodframe construction has been limited to approximately four stories, mainly due to a lack of understanding of the dynamic response of taller (mid-rise) woodframe construction, nonstructural limitations such as material fire requirements, and potential damage considerations for nonstructural finishes. Current building code requirements for engineered wood construction around the world are not based on a global seismic design philosophy. Rather, wood elements are designed independently of each other without considering the influence of their stiffness and strength on the other structural components of the structural system. Furthermore, load paths in woodframe construction arising during earthquake shaking are not well understood. These factors, rather than economic considerations, have limited the use of wood to low-rise construction and, thereby, have reduced the economical competitiveness of the wood industry in the U.S. and abroad relative to the steel and concrete industry. This project sought to take on the challenge of developing a direct displacement based seismic design philosophy that provides the necessary mechanisms to safely increase the height of woodframe structures in active seismic zones of the U.S. as well as mitigating damage to low-rise woodframe structures. This was accomplished through the development of a new seismic design philosophy that will make mid-rise woodframe construction a competitive option in regions of moderate to high seismicity. Such a design philosophy falls under the umbrella of the performance-based design paradigm.

In Year 1 of the NEESWood Project, a full-scale seismic benchmark test of a two-story woodframe townhouse unit that required the simultaneous use of the two three-dimensional shake tables at the University of Buffalo's NEES node was performed. As the largest full-scale three-dimensional shake table test ever performed in the U.S., the results of this series of shake table tests on the townhouse serve as a benchmark for both woodframe performance and nonlinear models for seismic analysis of woodframe structures. These efficient analysis tools provide a platform upon which to build the direct displacement based design (DDBD) philosophy. The DDBD methodology relies on the development of key performance requirements such as limiting inter-story deformations. The method incorporates the use of economical seismic protection systems such as supplemental dampers and base isolation systems in order to further increase energy dissipation capacity and/or increase the natural period of the woodframe buildings.

The societal impacts of this new DDBD procedure, aimed at increasing the height of woodframe structures equipped with economical seismic protection systems, is also investigated within the scope of this NEESWood project. Following the development of the DDBD philosophy for mid-rise (and all) woodframe structures, it was applied to the seismic design of a mid-rise (six-story) multi-family residential woodframe condominium/apartment building. This mid-rise woodframe structure was constructed and tested at full-scale in a series of shake table tests on the E-Defense (Miki) shake table in Japan. The use of the E-Defense shake table, the largest 3-D shake table in the world, was necessary to accommodate the height and payload of the mid-rise building.

This report presents a simplified direct displacement design (DDD) procedure which was used to design the shear walls for a six-story woodframe structure. This structure, referred to as the NEESWood Capstone Building, was designed to meet four performance expectations: damage limitation, life-safety, far-field collapse prevention, and near-fault collapse prevention. A series of nonlinear time history analyses were performed using suites of both far-field and near-fault ground motion records to verify that design requirements were met. The distributions of inter-story drifts obtained from these time history analyses confirmed that the building met all four performance expectations, thereby validating the DDD procedure. Additionally, collapse analysis in accordance with the Applied Technology Council project 63 (ATC-63) methodology was performed. The results of incremental dynamic analyses confirmed that the building had an adequate capacity or margin against collapse, as dictated by the ATC-63 methodology.

Project Team

John W. van de Lindt, Ph.D., Principal Investigator: Associate Professor, Department of Civil Engineering, Colorado State University, Fort Collins, CO 80523-1372; *jwv@engr.colostate.edu*.

Rachel A. Davidson, Ph.D., Co-Principal Investigator: Associate Professor, Department of Civil and Environmental Engineering, University of Delaware, Newark, DE 19716-3120; *rdavidso@udel.edu.*

Andre Filiatrault, Ph.D. Eng., Co-Principal Investigator: Professor Department of Civil, Structural, and Environmental Engineering, State University of New York at Buffalo, Buffalo, New York 14261; *af36@buffalo.edu*.

David V. Rosowsky, Ph.D., Co-Principal Investigator: A.P. Florence Wiley Chair Professor and Department Head, Texas A&M University, Department of Civil Engineering, College Station, TX 77843-3136; *rosowsky@tamu.edu*.

Michael D. Symans, Ph.D., Co-Principal Investigator: Associate Professor, Department of Civil and Environmental Engineering, Rensselaer Polytechnic Institute, 110 8th Street, Troy, NY 12180-3590; *symans@rpi.edu*.

ABSTRACT

This report presents a simplified direct displacement design (DDD) procedure which was used to design the shear walls for a six-story woodframe structure. The building will be tested in the final phase of a Network for Earthquake Engineering Simulation (NEES) project. Specifically, *NEESWood Capstone Building* was designed to meet four performance expectations: damage limitation, life-safety, far-field collapse prevention, and near-fault collapse prevention. The performance expectations are defined in terms of combinations of inter-story drift limits and prescribed seismic hazard levels associated with predefined non-exceedance probabilities. To verify that design requirements were met, a series of nonlinear time-history analyses (NLTHA) were performed using suites of both far-field and near-fault ground motion records. The distributions of inter-story drifts obtained from the NLTHA confirm that the Capstone Building designed using DDD meets all four target performance expectations, thereby validating the DDD procedure. Additionally, collapse analysis in accordance with the recently proposed Applied Technology Council project 63 (ATC-63) methodology was performed. The results of incremental dynamic analyses confirmed that the Capstone Building designed using the DDD procedure has adequate capacity or margin against collapse, as dictated by the ATC-63 methodology.

ACKNOWLEDGEMENTS

The authors gratefully acknowledge the Principal Investigators of the NEESWood Project who supported the preparation and design of the NEESWood Capstone Building: Andre Filiatrault at University at Buffalo, Michael Symans at Rensselaer Polytechnic Institute and Rachel Davidson at University of Delaware. The authors also thank Dr. Erol Karacabeyli and Dr. Chun Ni at the FPInnovations, Forintek Division for providing midply shear wall test data and reviewing an earlier draft of this report.

TABLE OF CONTENTS

TABLE OF CONTENTS (CONT'D)

List of Figures

LIST OF FIGURES (CONT'D)

LIST OF FIGURES (CONT'D)

List of Figures (Cont'd)

LIST OF TABLES

List of Tables (Cont'd)

LIST OF TABLES (CONT'D)

NOTATIONS

$ACMR$ = Adjusted Collapse Margin Ratio (CMR × SSF)

α = Stiffness and Strength Degradation Parameter for Shear Wall Reloading Curves; Modeling Parameter for the Modified Stewart Hysteretic Model

B_ζ = Damping Reduction Factor

β = Stiffness and Strength Degradation Parameter for Shear Wall Reloading Curves; Modeling Parameter for the Modified Stewart Hysteretic Model

β_{EQ} = Ground Motion Uncertainty

β_{DS} = Design Procedure Uncertainty

β_R = Total Uncertainty (include Ground Motion, Design Procedure, Test Data and Modeling Uncertainties)

β_{TOT} = Total/Composite Uncertainty (ATC-63 Collapse Margin Analysis)

β_v = Story Shear Factor

C_c = Design Base Shear Coefficient

C_{NE} = Adjustment Factor for Non-exceedance Probability

C_t = Approximate Period Parameter

C_v = Vertical Distribution Factor for Design Base Shear

CMR = Collapse Margin Ratio

DBE = Design Basis Earthquake

Δ = Displacement

Δ_{eff} = Target Design Displacement at the Effective Height of the *Substitute Structure*

Δ_{it} = Inter-story Displacement

Δ_o = Story Displacement (Relative to Ground)

Δ_t = Target Displacement

Δ_u = Displacement at the Point of Maximum Force on the Shear Wall Backbone Curve; Modeling Parameter for the Modified Stewart Hysteretic Model

Δ_{un} = Maximum Displacement of the Previous Hysteresis Loops; Modeling Parameter for the Modified Stewart Hysteretic Model

Δ_{ult} = Displacement at Ultimate Base Shear (Pushover Analysis)

$\Delta_{60\%}$ = Roof Displacement at which the Base Shear is 60% of the Peak Base Shear (Pushover Analysis)

E_{loop} = Energy Dissipated by the Nonlinear Shear Wall in One Complete Hysteresis Cycle/Loop

E_{So} = Strain Energy of the Linear-elastic System at Target Displacement, Δ_t

F = Equivalent Lateral Force

F_0 = Force Intercept of the Asymptotic Line ($r_1K_0\Delta + F_0$) for the Shear Wall Backbone Curve; Modeling Parameter for the Modified Stewart Hysteretic Model

F_b = Shear Wall Backbone Force

F_i = Force Intercept of the Pinched Line ($r_4K_0\Delta + F_I$); Modeling Parameter for the Modified Stewart Hysteretic Model

$\Phi(.)$ = Cumulative Density Function of a Standard Normal Distribution

$\Phi^{-1}(.)$ = Inverse Cumulative Density Function of a Standard Normal Distribution

g = Gravitational Constant

h_{eff} = Effective Height of the *Substitute Structure*

h_o = Story Height (Relative to the Ground)

h_s = Story Height (Including the Thickness of the Floor or Roof Diaphragm)

H = Seismic Hazard Level

I_E = Occupancy Important Factor

K_{eff} = Effective Secant Stiffness of the *Substitute Structure*

K_0 = Initial Tangent Stiffness

K_P = Reloading Stiffness; Modeling Parameter for the Modified Stewart Hysteretic Model

K_S = Secant Stiffness

λ = Logarithmic Median (Parameter for Lognormal Distribution)

M_o = Overturning Moment

MCE = Maximum Credible Earthquake

μ_c = Ductility Factor (Pushover Analysis)

N_S = Total Number of Stories

NE_t = Design/Target Non-exceedance Probability

P_f = Collapse/failure Probability

P_{NE} = Non-exceedance Probability

R = Response Modification Factor

r_1 = Asymptotic Tangent Stiffness Ratio of the Nonlinear Ascending Branch of the Shear Wall Backbone Curve; Modeling Parameter for the Modified Stewart Hysteretic Model

r_2 = Stiffness Ratio of the Linear Descending Branch of the Shear Wall Backbone Curve; Modeling Parameter for the Modified Stewart Hysteretic Model

r_3 = Stiffness Ratio of Unloading Path; Modeling Parameter of the Modified Stewart Hysteretic Model

r_4 = Stiffness Ratio of the Pinched Line ($r_4K_0\Delta + F_I$); Modeling Parameter for the Modified Stewart Hysteretic Model

S_{DS} = Short-period Spectral Acceleration for Design Basis Earthquake (DBE)

S_{D1} = 1-second Spectral Acceleration for Design Basis Earthquake (DBE)

S_{SS} = Short-period Spectral Acceleration for Short Return Period Earthquake (SRE)

S_{S1} = 1-second Spectral Acceleration for Short Return Period Earthquake (SRE)

S_{MCE} = MCE Spectral Acceleration at the Upper Limit of the Approximate Period T_u

S_{CT} = Spectral Acceleration at T_u that causes 50% of the analyses/cases to Collapse.

S_{MS} = Short-period Spectral Acceleration for Maximum Credible Earthquake (MCE)

S_{M1} = 1-second Spectral Acceleration for Maximum Credible Earthquake (MCE)

$\vec{S}_X$ = Design Spectral Acceleration Adjusted for Non-exceedance Probability

SRE = Short Return Period Earthquake

SSF = Spectral Shape Factor

T_a = Approximate Fundamental Period (Defined in the ASCE/SEI-7)

T_S = S_{XS}/S_{X1}; Short-period Transition Period; Upper Bound Period of the Plateau Region of the Design Acceleration Response Spectrum

T_0 = 0.2 S_{XS}/S_{X1}; Lower Bound Period of the Plateau Region of the Design Acceleration Response Spectrum

T_u = Upper Limit of the Approximate Fundamental Period (Defined in the ASCE/SEI-7)

θ = Drift (Percentage of Story Height)

θ_{eff} = Target Design Drift at the Effective Height of the *Substitute Structure*

θ_{eq50} = Equivalent 50% Non-exceedance Drift Limit

θ_{it} = Inter-story Drift (Percentage of Story Height)

θ_{lim} = Design/Target Inter-story Drift Limit (Percentage of Story Height)

V_b = Base Shear

V_{max} = Maximum Base Shear (Pushover Analysis)

V_s = Story Shear

V_{ult} = Ultimate Base Shear in a Pushover Analysis (defined at the point where the Base Shear deteriorates to 80% of the Peak Base Shear)

V/W = Base Shear-to-Total Building Weight Ratio

W = Seismic Weight

W_{eff} = Effective Seismic Weight of the *Substitute Structure*

x = Exponent for the Approximate Period Equation (in the ASCE/SEI-7)

ξ = Logarithmic Standard Deviation (Parameter for Lognormal Distribution)

ζ_{hyst} = Hysteretic Damping (Fraction of Critical Damping)

ζ_{int} = Intrinsic Damping (Fraction of Critical Damping)

ζ_{eff} = Effective Viscous Damping (Fraction of Critical Damping)

1. INTRODUCTION

In the United States (US), multi-story residential and commercial structures such as multi-family apartments, condominiums and hotels/motels are often light-frame wood (also known as *woodframe*) construction. For multi-story construction, if woodframe is selected over other structural systems it is because of its fast construction speed and low construction cost (Cheung 2008). Although woodframe construction provides an economical alternative for multi-story buildings, the current US building codes make it difficult to exceed five stories (ICC 2006) in general, and even four stories in some jurisdictions. The height limitation reflects the lack of knowledge of the dynamic response of taller wood buildings under lateral loadings (e.g., wind and earthquake loads), as well as fire safety considerations and other local district land use regulations. Such height restrictions have limited the use of wood for multi-story construction in the US. Nevertheless, many other industrialized countries permit the construction of taller wood buildings (i.e., more than five stories). For example, New Zealand does not have building height restrictions for wood construction. Canada and England have recently revised their building codes to allow the construction of wood buildings of up to six and eight stories, respectively (Craig 2008). In the US, the timber engineering design and research communities are in the process of developing new design guidelines and procedures that will enable building taller woodframe structures, including those in seismic regions such as the Pacific Northwest where wood has a strong industry hold. One such effort is the NEESWood project which focuses on the development of a performance-based seismic design (PBSD) procedure for mid-rise woodframe construction in regions of moderate to high seismicity (van de Lindt et al. 2008).

As part of the NEESWood project, a series of full-scale seismic tests of a two-story Benchmark Woodframe Building were conducted at the University at Buffalo (UB) Network for Earthquake Engineering Simulation (NEES) site (Christovasilis et al. 2007). The Benchmark Building was designed in accordance with the *Uniform Building Code* (ICBO 1988). The test building was representative of a typical townhouse structure built in the 1980's and located in the Western US. In order to establish the relationship between the fundamental period (or lateral stiffness) and the contribution of the non-structural elements, shake table tests were conducted at different stages of construction (e.g., wood structural elements only, wood structural elements and gypsum wall board, and the complete structure including the exterior stucco). The test data collected in the Benchmark Building test included (1) force and deformation measurements of the shear walls and non-load bearing walls, (2) tension force and uplift measurements of the anchor bolts and hold-downs, (3) sill plate slippage, and (4) absolute acceleration measurements. In addition, damage to the structural and non-structural components, such as the gypsum wall boards (GWB) and exterior stucco, were visually inspected and documented at the end of each stage of testing. The Benchmark test results and findings were used to develop numerical tools and validate a preliminary version of a new direct displacement design (DDD) procedure for PBSD of multi-story woodframe buildings (Pang and Rosowsky 2009). The DDD procedure was then used to design the shear walls of a six-story woodframe building, which will be constructed and tested at full-scale in the final phase of the NEESWood project.

1.1 Description of the Six-story NEESWood Capstone Building

The architectural layout (Figures 1 to 4) and building design parameters (e.g., the location of bearing walls) determined based on the 2006 *International Building Code* (ICC 2006) served as the starting point for the displacement-based seismic design of the six-story NEESWood Capstone Building. The plan dimensions of the building are approximately 18.1 m (59.5 ft) in the longitudinal direction and 12.1 m (39.8 ft) in the transverse direction. The height of the building from the base to the top of the roof parapet is approximately 17.5 m (57.5 ft), with a story clear height of 2.74 m (9 ft) for the 1st story and a story clear height of 2.44m (8 ft) for 2nd to 6th stories (Figure 1-4). The thickness of the floor system is approximately 25.4 cm (10 in) and the roof diaphragm thickness is 38.1 cm (15 in). The total living space of the test building is approximately 1350 m^2 (14500 ft^2). There are 23 living units with four apartment units on each floor except for the 6th floor which contains a large luxury penthouse and two regular apartment units (Figures 1 to 3). The total seismic weight of the as-designed building was estimated to be 2734 kN (615 kips). A series of full-scale shake table tests of the NEESWood Capstone building are scheduled to be conducted on the E-defense (Miki City) shake table in Japan in July 2009.

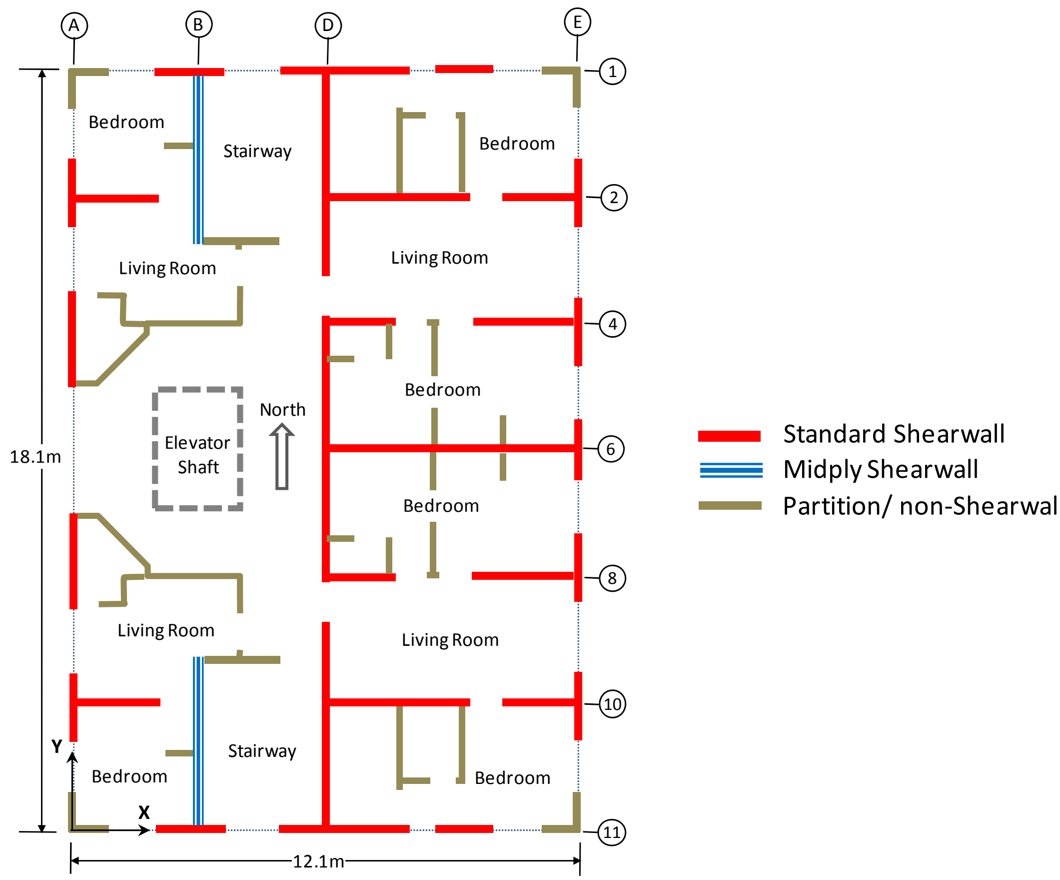

Figure 1-1: Plan view of the six-story NEESWood Capstone Building for 1st floor.

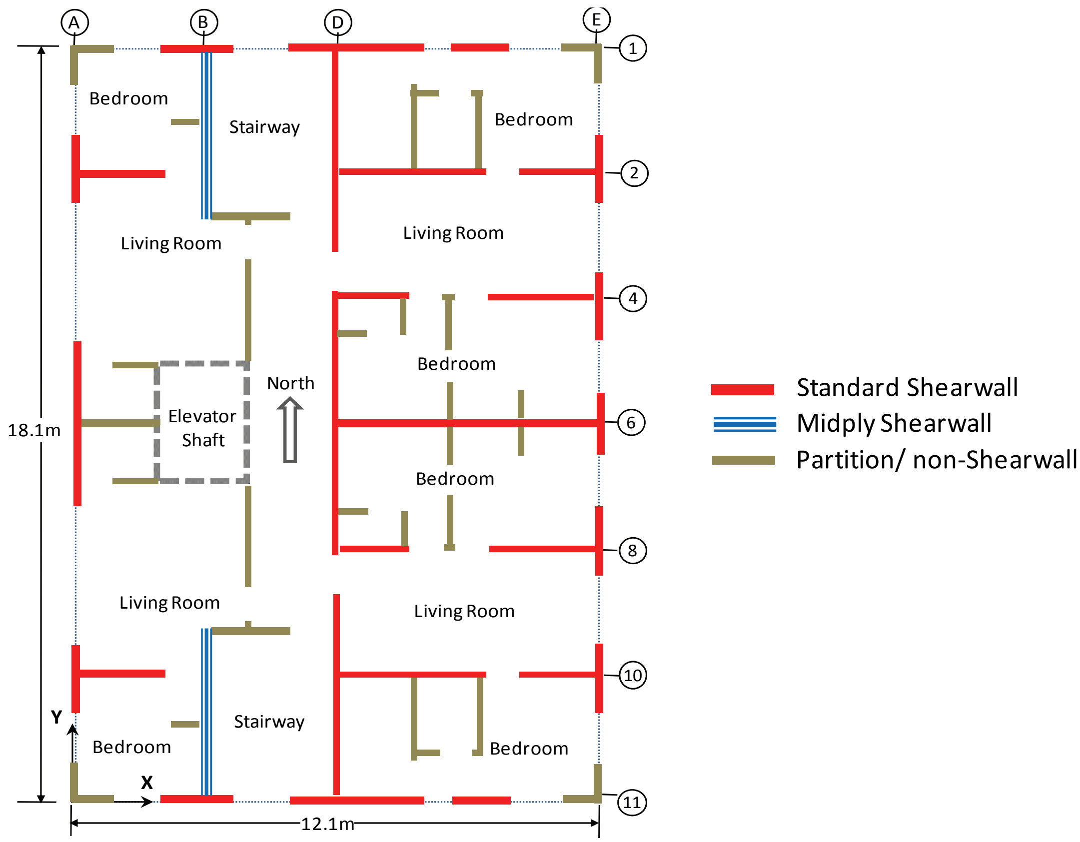

Figure 1-2: Plan view of the six-story NEESWood Capstone Building for 2nd to 5th floors.

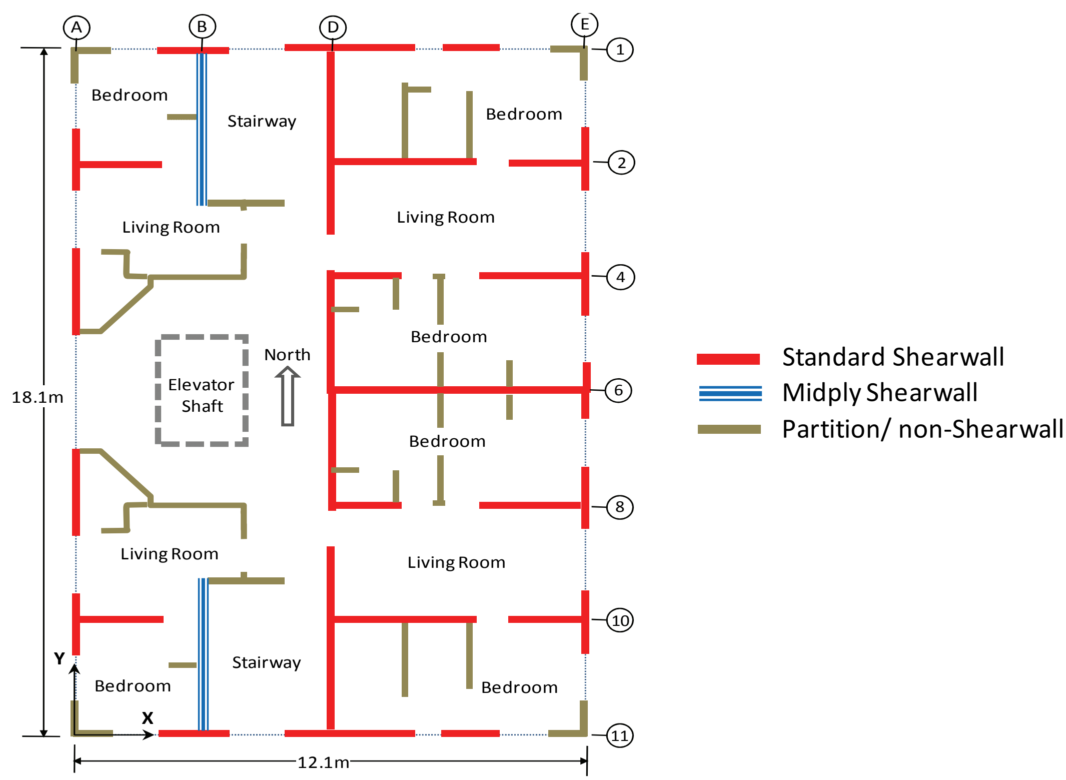

Figure 1-3: Plan view of the six-story NEESWood Capstone Building for 6th floor.

(a)

(b)

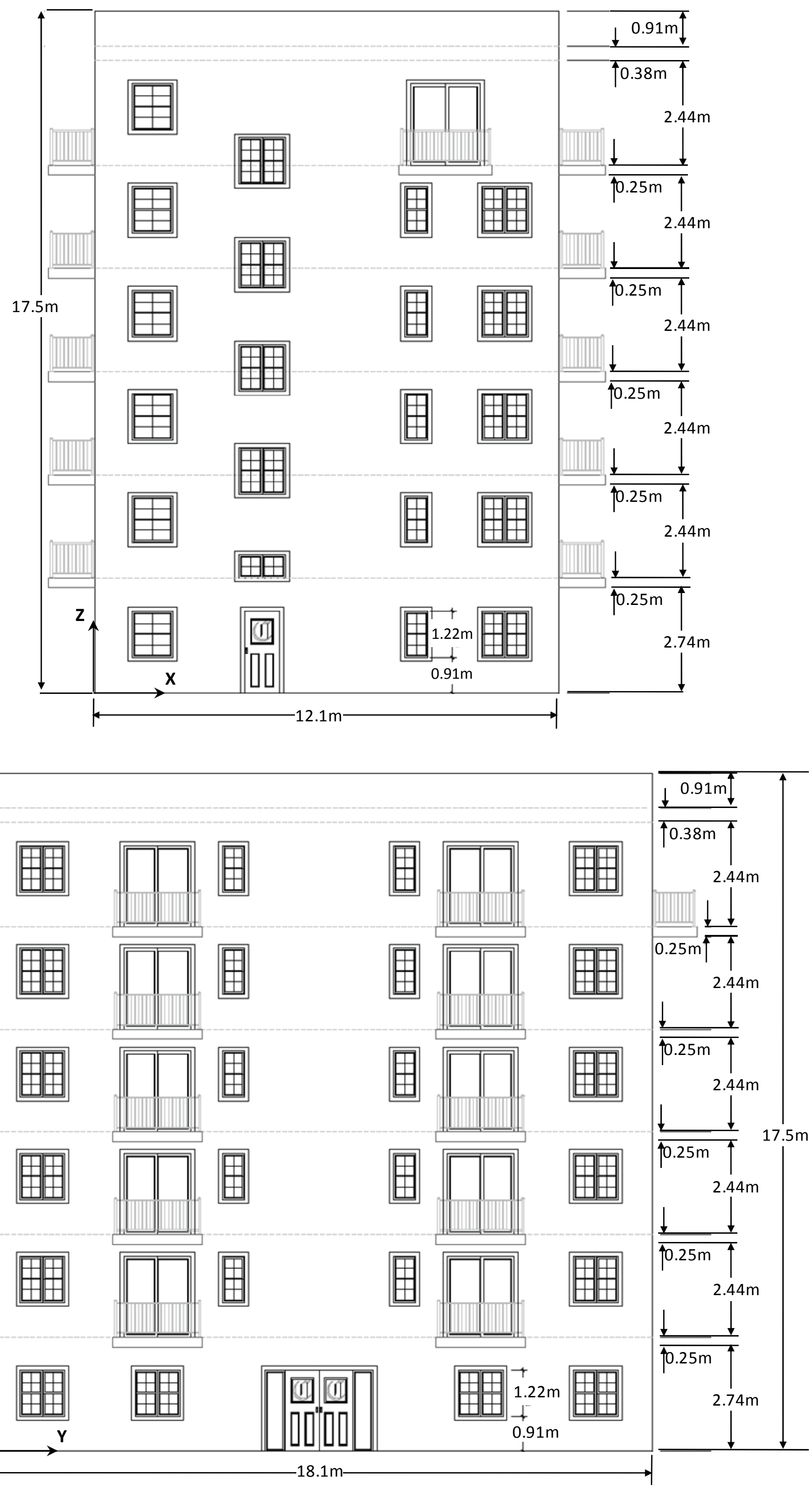

Figure 1-4: Elevation views of the six-story NEESWood Capstone Building, (a) south elevation and (b) west elevation.

2. PERFORMANCE EXPECTATIONS

The six-story Capstone Building was designed to meet the four performance requirements listed in Table 2-1. Each performance requirement is specified by a probability of non-exceedance of an inter-story drift limit at a specified level of seismic hazard. The performance requirement is given by the following expression:

$$P_{NE}(\theta < \theta_{\lim} \mid H) \geq NE_t \tag{1}$$

where θ and θ_{lim} are the inter-story drift and target drift limit, respectively. The term $P_{NE}(.)$ is the non-exceedance probability of the inter-story drift at a prescribed hazard level (seismic intensity, H) and NE_t is the target/design non-exceedance probability. ASCE/SEI-41, *Seismic Rehabilitation of Existing Buildings* (ASCE 2006), provides guidelines for design and retrofit of structures by specifying three performance levels namely immediate occupancy (IO), life safety (LS), and collapse prevention (CP). The IO, LS, and CP definitions correspond to the performance expectations for Levels 1 to 3 (Table 2-1) and the hazard levels are associated with earthquakes having 50%, 10% and 2% exceedance probabilities in 50 years, respectively. The performance levels/expectations selected by the NEESWood project team and used for designing the Capstone Building are based on the ASCE/SEI-41 guidelines with some modifications. According to ASCI/SEI-41, the inter-story drift limits for wood shear walls for the IO, LS, and CP limit states are 1%, 2% and 3%, respectively. The non-exceedance probabilities for the aforementioned drift limits are assumed to be 50% (median) since the NE probabilities are not explicitly defined in ASCE/SEI-41.

Table 2-1: Performance expectations for NEESWood Capstone Building.

Performance Level	Seismic Hazard	Performance Expectations	
		Inter-story Drift Limit	Non-exceedance Probability
Level 1	50%/50yr	1%	50%
Level 2	10%/50yr	2%	50%
Level 3	2%/50yr	4%	80%
Level 4	Near-Fault	7%	50%

Based on observations made during the NEESWood Benchmark test, *non-structural damage* such as cracking of stucco and GWB occurred at inter-story drifts between 0.5% and 1%, and possible *life-safety* related failures such as total splitting of sill plates, buckling of GWB at door/window openings and separation of GWB from the ceiling were reported at drifts greater than 2% (Christovasilis et al. 2007). Hence, the 1% and 2% drift limits for the IO and LS limit states, respectively, were adopted for the Levels 1 and 2 performance expectations without any modifications. It should be noted that while a 1% drift limit with a 50% NE probability was considered to be an "acceptable" drift limit in terms of limiting financial loss, a lower drift limit (e.g., 0.5%) combined with a higher NE probability (e.g. 80%) may be specified in the proposed DDD approach if it is determined that a more stringent damage limitation limit state should be considered.

At Level 3 (2%/50yr hazard), a drift limit of 4% combined with an 80% NE probability was used as the design performance expectation. The 4% drift limit was based on the Benchmark test results for a ground motion representative of 2%/50yr hazard level where a maximum inter-story drift of 3.5% was recorded under a ground motion representative of 2%/50yr hazard level. At 3.5% drift, the test structure retained about 75% of its lateral initial stiffness and did not exhibit any visible sign of incipient collapse. Hence, the 4% drift limit was selected for Level 3. In the proposed NEESWood performance expectations, buildings located near fault lines are required to meet the Level 4 performance requirement, namely a 7% drift limit with a 50% NE probability, when subjected to a suite of near-fault ground motions with strong velocity pulses. The 7% drift limit was based on the collapse analysis of woodframe buildings (Christovasilis et al. 2009) using incremental dynamic analysis (IDA) (Vamvatsikos and Cornell 2002) and has been used in the ATC-63 project to evaluate the collapse probability of wood buildings (ATC 2008).

2.1 Design Spectra

The Capstone Building is assumed to be located in Southern California and founded on stiff soil (Site Class D). The design 5% damping spectral acceleration values for seismic hazard Levels 1 to 3 are shown in Table 2-2 and the horizontal acceleration design spectra determined in accordance with ASCE/SEI-41 (2006) are shown in Figure 2-1. The determination of the design spectral acceleration parameters for the 50%/50yr earthquake is given in Appendix A. These far-field response spectra (for sites located > 10 km from fault rupture) were used in the simplified DDD procedure to design the Capstone Building. Note that the near-fault response spectrum was not specifically determined or used in the design process. However, a suite of un-scaled near-fault ground motions (Krawinkler et al. 2003) were used in the NLTHA to verify the design of the Capstone Building at Level 4.

Table 2-2: Design spectral acceleration values for 5% damping.

Hazard Level	Intensity (% of DBE)	Exceedance Probability	Spectral Acceleration Short-period S_{XS}[a] (g)	Spectral Acceleration 1-second S_{X1}[a] (g)	T_0[b] (s)	T_S[c] (s)
Short Return Period Earthquake (SRE)	44%	50%/50yr	0.44	0.26	0.12	0.59
Design Basis Earthquake (DBE)	100%	10%/50yr	1.00	0.60	0.12	0.60
Maximum Credible Earthquake (MCE)	150%	2%/50yr	1.50	0.90	0.12	0.60

[a] X = M = Maximum Credible Earthquake
D = Design Basis Earthquake
S = Short Return Period Earthquake
[b] $T_0 = 0.2\, S_{XS}/S_{X1}$
[c] $T_S = S_{XS}/S_{X1}$

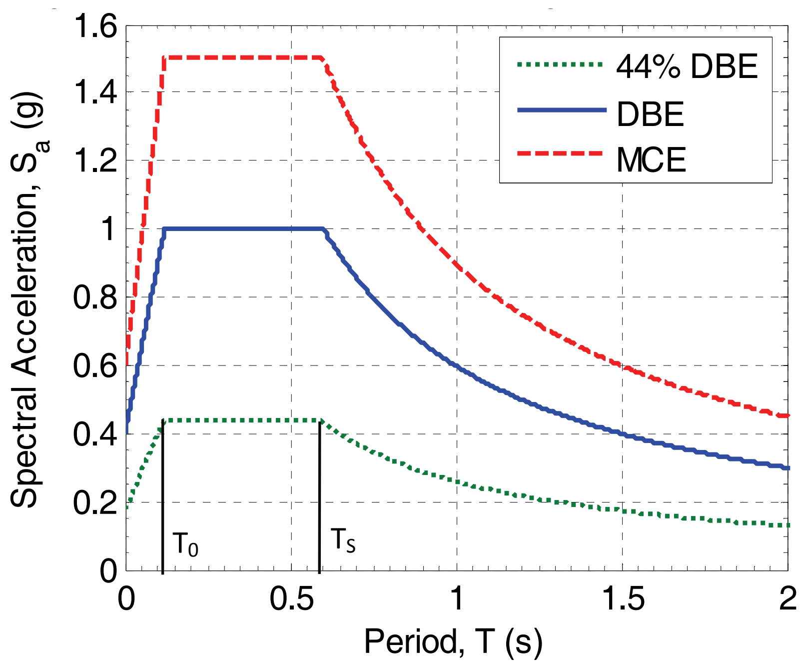

Figure 2-1: Design acceleration response spectra for 5% damping.

3. STANDARD AND MIDPLY SHEAR WALLS

The Capstone Building is constructed with North American style engineered light-frame wood shear walls with tie-down systems to restrain uplift forces caused by the overturning moments. The shear walls are built with nominal 51 mm × 152 mm (2 in. × 6 in.) Douglas Fir and Spruce Pine Fir studs spaced at 406 mm (16 in.) on-center and 10d common nails (3.76 mm in diameter (0.148 in.)) are used to fasten the 11.9 mm (15/32 in.) thick Oriented Strand Board (OSB) to the framing members. The Capstone Building is built almost entirely using conventional North American style stud wall systems (referred as *standard* walls in this paper), except for an interior wall line parallel to the longitudinal direction in which very high shear capacity is required (see Figures 1 and 2) along which a new system known as *midply* construction is used (Varoglu et al. 2007). The midply wall system consists of standard shear wall components but the sheathing is sandwiched between studs that are rotated 90 degrees with respect to those in standard walls and the sheathing is attached to the wide faces of the studs (see Figure 3-1). The sheathing nails in midply walls are driven through studs at one side of the sheathing panel and into studs on the opposite side of the panel resulting in fasteners working in double-shear.

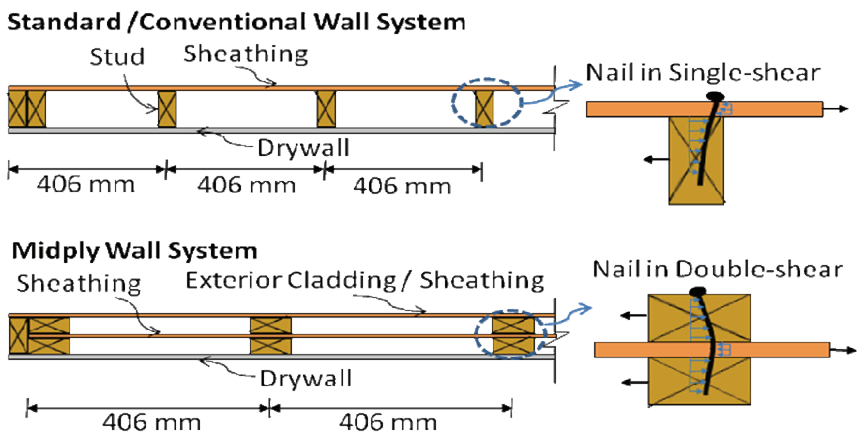

Figure 3-1: Cross-section of standard and midply walls.

The complete shear wall backbone curve is required in the simplified DDD procedure. Both standard and midply shear walls were modeled using the M-CASHEW program, a Matlab version of the CASHEW (Cyclic Analysis of Wood SHEar Walls) program (Folz and Filiatrault 2001a). The M-CASHEW program can be used to predict the load-displacement response at the top of the wall by modeling the relative movements of the shear wall components (panels and framing members) and the individual load-slip response of nails. The backbone response of a wood shear wall is given by the following five-parameter equation which consists of a nonlinear logarithmic ascending branch and a linear descending (softening) branch:

$$F_b(\Delta) = \begin{cases} \left[1 - e^{-\frac{K_0}{F_0}\Delta}\right]\left(r_1 K_0 \Delta + F_0\right) & \text{for} \quad \Delta \leq \Delta_u \\ F_u + r_2 K_0 (\Delta - \Delta_u) & \text{for} \quad \Delta > \Delta_u \end{cases} \tag{2}$$

The backbone parameters are depicted graphically in Figure 3-2.

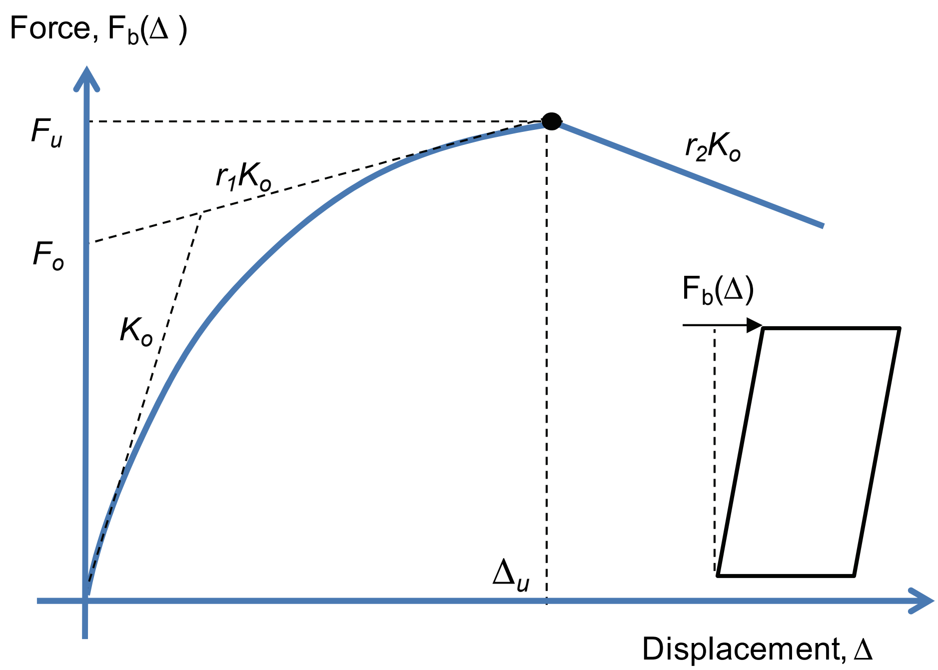

Figure 3-2: Shear wall backbone parameters.

3.1 Connector Parameters

In the M-CASHEW model, the nails are modeled using a modified Stewart hysteretic model (Stewart 1987) which includes hysteresis pinching, strength and stiffness degradation (

Figure **3-3**). The hysteretic parameters for the sheathing nails and dry wall screws are shown in Table 3-1. Note that the hysteretic parameters for 8d box (2.87 mm in diameter) and 10d common (3.76 mm in diameter) nails were determined by fitting actual cyclic nail test data. The double-shear connector parameters, however, were calibrated by modifying the single-shear nail parameters to match the midply wall test results by Varoglu et. al (2007).

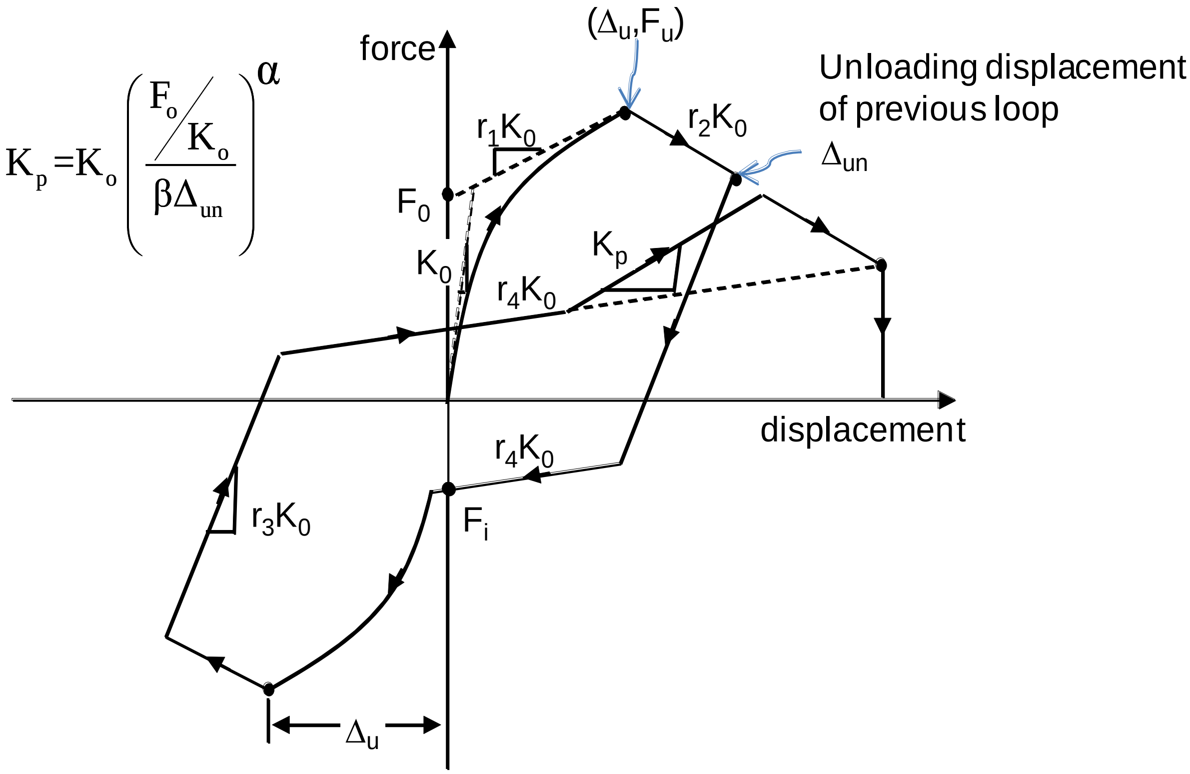

Figure 3-3: Modified Stewart hysteretic model (nonlinear spring).

Table 3-1: Connector parameters for nails in single- and double-shear.

Shear Mode	K_o (kN/mm)	r_1	r_2	r_3	r_4	F_o (kN)	F_i (kN)	Δ_u (mm)	α	β
8d box nail (2.87 mm dia.) and 9.5 mm OSB										
Single[(a)]	0.85	0.035	-0.049	1.40	0.015	0.801	0.187	12.19	0.8	1.1
Double	1.71	0.035	-0.0392	1.40	0.015	1.601	0.187	9.75	0.8	1.1
10d common nail (3.76 mm dia.) and 11.9 mm OSB										
Single[(b)]	1.55	0.0289	-0.0268	1.04	0.0094	0.979	0.133	8.64	0.73	1.4
Double	3.11	0.0289	-0.0214	1.04	0.0094	1.957	0.133	6.91	0.73	1.4
#6 bugle head dry wall screw (3.61 mm dia. × 31.75 mm long) and 12.7 mm GWB										
Single[(c)]	2.63	0.018	-0.015	1.1	0.002	0.423	0.044	3.56	0.8	1.1

(a) Based on the nail test results for nominal 51 mm (2 in.) thick framing member attached to 9.5 mm (3/8 in.) thick OSB using 8d box gun nails (Folz 2001).

(b) Based on the cyclic and monotonic nail test results for nominal 51 mm (2 in.) thick Hem Fir stud attached to 11.9 mm (15/32") thick OSB using 10d common nail (Coyne 2007).

(c) The connector parameters were estimated by matching the M-CASHEW model backbone responses to the actual GWB-only wall test results obtained from the CUREE Task 1.3.1 Test Group 12 (Gatto and Uang 2001) and CUREE Task 1.4.4 Test Group 19 (Pardoen et al. 2003).

Figure 3-4 shows a 2.44 m × 2.44 m (8 ft. × 8 ft.) midply shear wall (test M47-01) constructed with nominal 51 mm (2 in.) thick Spruce Pine Fir studs spaced at 610 mm (24 in.) on-center. Sheathing nails were spaced at 102 mm (4 in.) on-center along the panel edges and 203 mm (8 in.) along the interior studs. Power-driven nails, 3 mm (0.118 in.) in diameter and 82 mm (3.23 in.) in length, were used. Since connector data was not available for the actual power-driven nails used to construct the midply test specimen, the parameters of the 8d box nail (having similar diameter) tested in single-shear were used to model the test wall. To account for the double-shear effects, the backbone parameters of the nail in single-shear were modified by multiplying K_o and F_o parameters by 2, and multiplying Δ_u and r_1 parameters by 0.8 (Table 3-1). This assumption is validated by comparing the hysteretic loops predicted by M-CASHEW with those from the actual midply wall test (Figure 3-4). Using the same approach, the parameters for the 10d common nail in double-shear were estimated and used to generate the midply backbone parameters used in the displacement-based design of the Capstone Building.

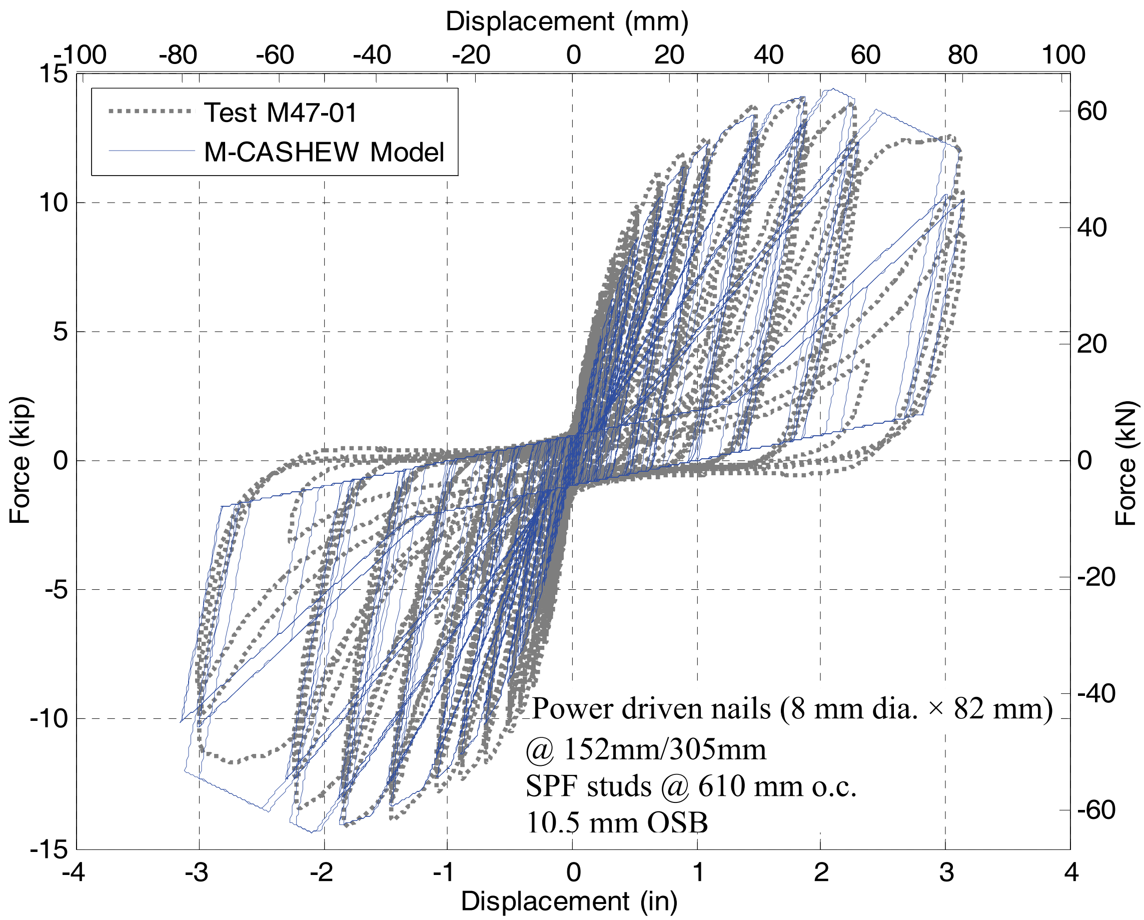

Figure 3-4: Model-predicted and test hysteretic loops of midply wall.

For the gypsum-to-wood framing connection (dry wall screw), a set of five backbone parameters (K_o, F_o, r_1, r_2 and Δ) were determined such that the model predicted backbone curve matched the experimental results from the monotonic pushover test of two 2.44 m × 2.44 m (8ft × 8ft) shear walls sheathed with 12 mm (1/2 in.) thick GWB on one-side only (Gatto and Uang 2001) (Figure 3-5). The remaining hysteretic parameters (r_3, r_4, α and β) were calibrated based on other cyclic response of shear walls sheathed with GWB (McMullin and Merrick 2001).

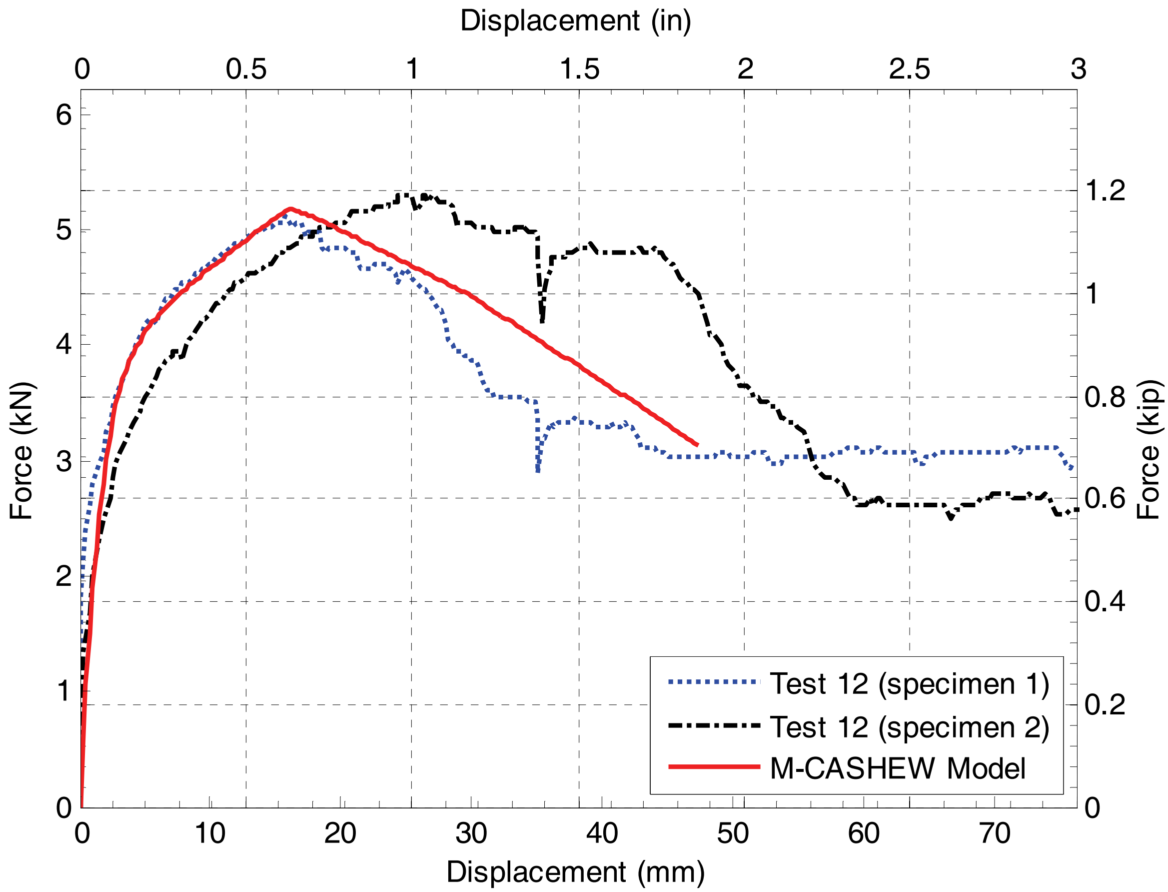

Figure 3-5: Experimental monotonic curves and model predicted backbone curve of 2.44 m × 2.44 m shear wall with 12 mm thick gypsum wallboard.

3.2 Shear Wall Backbone Database

Using the single- and double-shear 10d nail parameters presented in Table 3-1, the nonlinear shear spring elements of standard and midply shear walls were constructed using the M-CASHEW program. Similarly, the shear spring elements for the GWB walls were constructed using the single-shear dry wall screw parameters listed in Table 3-1. These shear spring elements were used to generate the displacement-based shear wall design table / database. The shear wall database contains the backbone parameters for 2.74 m (9 ft) and 2.44 m (8 ft) tall standard and midply shear walls with field nail spacing of 305 mm (12 in.) and edge nail spacings of 51, 76, 102 and 152 mm (2, 3, 4, and 6 in.) are shown in Table 3-2. The shear wall database can also be presented in graphical format (e.g., Figure 3-6). Also shown in Table 3-2 are the backbone parameters for walls sheathed with only 12.7 mm (1/2 in.) thick GWB (i.e., no structural sheathing) connected by 31.75 mm (1.25 in.) long #6 bugle head drywall screws at 406 mm (16 in.) on-center. The backbone curve for a wall sheathed with OSB on one side and drywall on the opposite side can be approximated by summing the OSB and GWB backbone curves. This modeling approach has been used by others (White and Ventura 2006; Folz and Filiatrault 2001b; Kim and Rosowsky 2005). The complete shear wall database for 2.44 m (8 ft) and 2.74 m (9 ft) tall walls can be found in Appendix B.

Table 3-2: Displacement-based shear wall design table for unit wall width (per m).

Wall Height (m)	Wall Type/ Panel Layer	Edge Nail Spacing (mm)	K_o (kN/mm)	F_u (kN)	Backbone Force at Different Drift Levels (kN)				
					0.5%	1.0%	2.0%	3.0%	4.0%
2.74	Standard[(a)]	51	2.269	31.68	19.42	26.68	31.6	27.36	22.92
		76	1.861	21.37	14.41	18.75	21.22	18.05	14.88
		102	1.586	16.40	11.49	14.53	16.13	13.69	11.24
		152	1.138	11.20	8.12	10.13	11.01	9.44	7.87
	Midply[(b)]	51	2.890	61.53	29.82	46.39	61.52	53.09	44.66
		76	2.514	41.81	23.83	34.75	40.95	35.5	30.05
		102	2.208	31.83	19.76	27.69	30.79	26.77	22.75
		152	1.813	21.70	14.85	19.69	20.93	18.27	15.60
	GWB[(c)]	406	0.743	2.03	1.95	1.85	1.37	0.88	0.39
2.44	Standard[(a)]	51	2.432	32.2	19.15	26.82	32.05	28.13	23.82
		76	2.176	21.94	14.8	19.17	21.87	18.7	15.52
		102	1.740	16.75	11.64	14.91	16.58	14.18	11.79
		152	1.356	11.41	8.34	10.3	11.27	9.65	8.03
	Midply[(b)]	51	2.971	63.47	28.28	45.33	62.69	55.8	47.52
		76	2.633	42.67	22.94	34.33	41.95	36.58	31.21
		102	2.396	32.26	19.42	27.56	31.5	27.54	23.57
		152	1.988	22.11	14.79	19.87	21.38	18.76	16.14
	GWB[(c)]	406	1.231	2.11	2.04	1.88	1.30	0.73	0.16

(a) Standard wall model is built with 11.9 mm thick OSB connected to framing members by 10d common nails (3.76 mm dia.) in single-shear.
(b) Midply wall model is built with 11.9 mm thick OSB connected to framing members by 10d common nails (3.76mm dia.) in double-shear
(c) Gypsum wall board model is built with 12.7 mm thick GWB connected to framing members by #6 bugle head drywall screws (3.61 mm dia.) in single-shear.

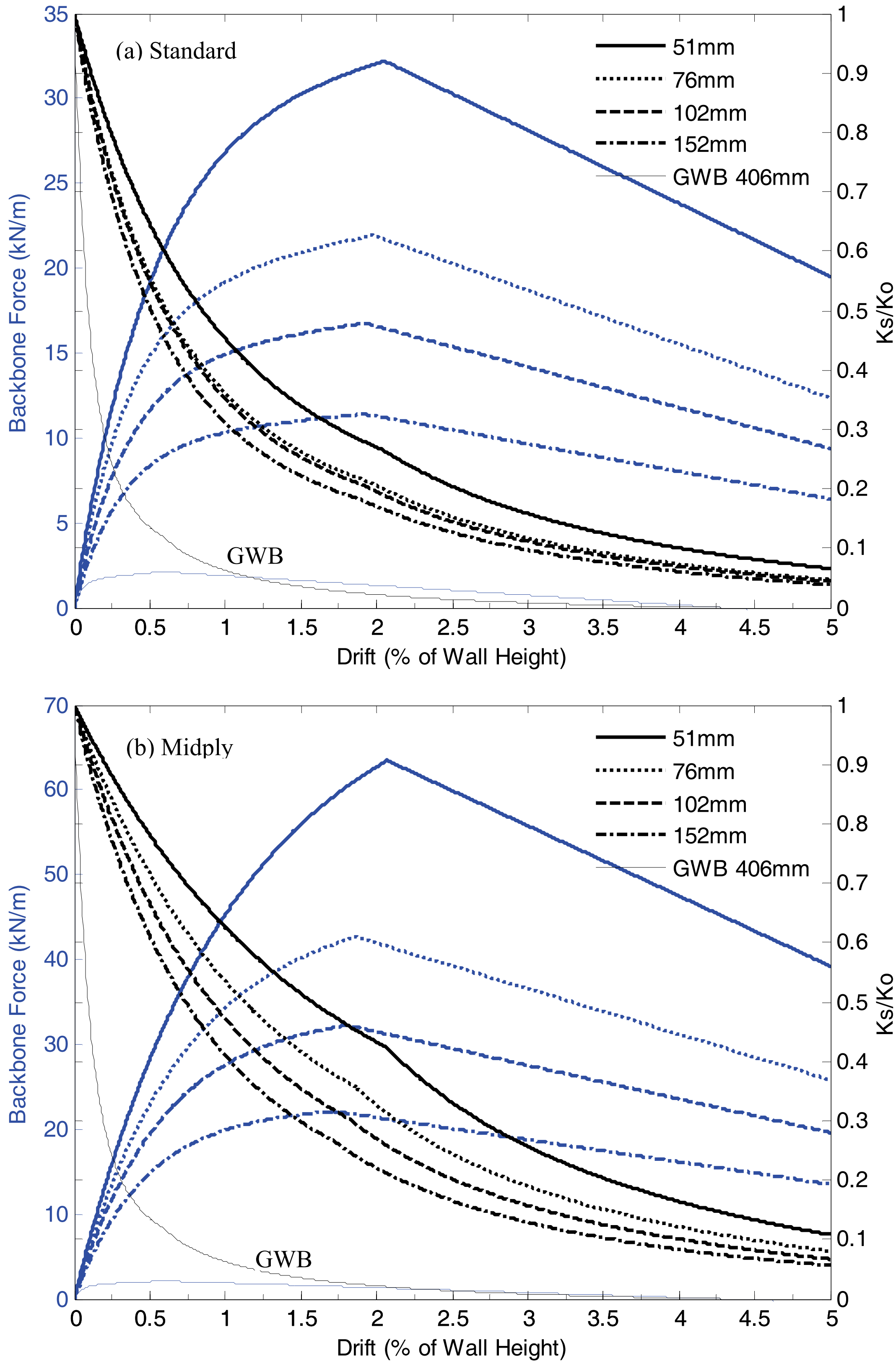

Figure 3-6: Shear wall backbone and K_s/K_o curves for 2.44m (8 ft) tall (a) standard and (b) midply walls built with 10d common nails and 11.9 mm OSB.

3.3 Hysteretic Damping Model for Wood Shear Walls

Hysteretic damping, ξ_{hyst}, in the wood shear wall can be estimated using the following equation:

$$\zeta_{hyst} = \frac{1}{4\pi}\frac{E_{loop}}{E_{So}} = \frac{1}{2\pi}\frac{E_{loop}}{K_s \Delta_t^2} \tag{3}$$

where E_{loop} is the energy dissipated by the actual nonlinear shear wall in one complete cycle and E_{So} is the strain energy of the linear-elastic system at the target displacement, Δ_t and secant stiffness, K_s, determined at Δ_t. Figure 3-7 shows the determination of hysteretic damping for the APA shear wall test designated *2004-14 8dcom* (Martin 2004) at a target displacement of 56.8 mm.

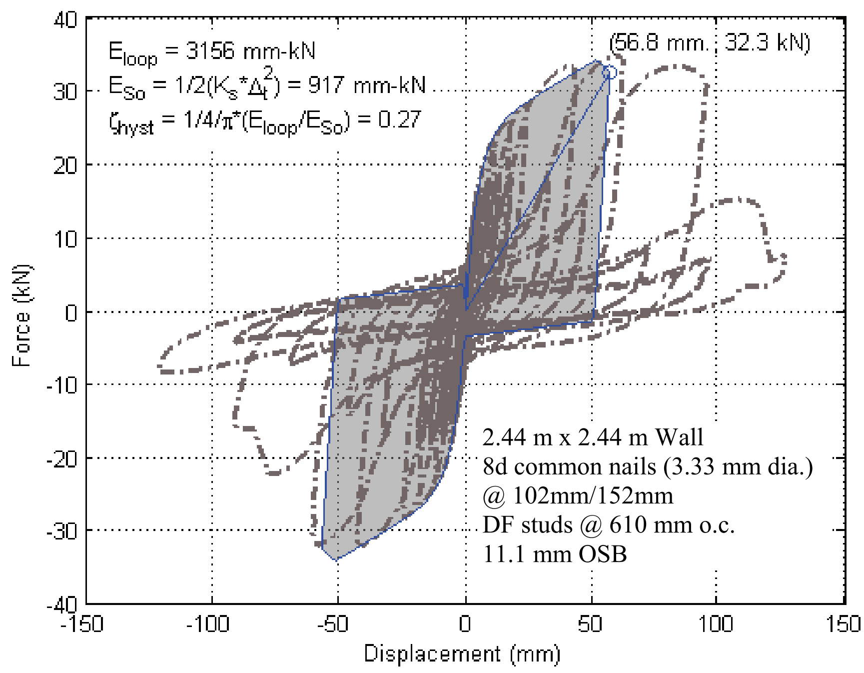

Figure 3-7: Determination of hysteretic damping of wood shear wall.

The actual test hysteretic loops were first fitted to the 10-parameter modified Stewart model. Next, the fitted wall parameters were used to generate nonlinear hysteretic loops at different target displacements and the hysteretic damping values were calculated using equation

(3). Using the same approach, hysteretic damping values for standard and midply shear walls tested by different laboratories (Martin and Skaggs 2003; Varoglu et al. 2007; Pardoen et al. 2003) were calculated and plotted in Figure 3-8. The results show that the hysteretic damping can be characterized using the secant-to-initial stiffness ratio (K_o/K_s) :

$$\zeta_{hyst} = 0.32e^{-1.38\frac{K_s}{K_o}} \tag{4}$$

Once a target/design wall drift limit has been selected, the secant-to-initial stiffness ratio can be calculated (or interpolated) using the displacement-based shear wall design database (Table 3-2) and the resulting equivalent hysteretic damping ratio can be computed using equation (4). Other studies of hysteretic damping based on the results of cyclic pushover analyses of woodframe structures suggested an equivalent viscous damping ratio of about 18% of critical when the lateral stiffness of the structure degrades to 33% of its initial stiffness (Filiatrault et al. 2003). At K_s/K_o of 0.33, the damping model proposed in this study yields an equivalent hysteretic damping of 20% (Figure 3-8) which is very close to the value suggested by Filiatrault et al. (2003).

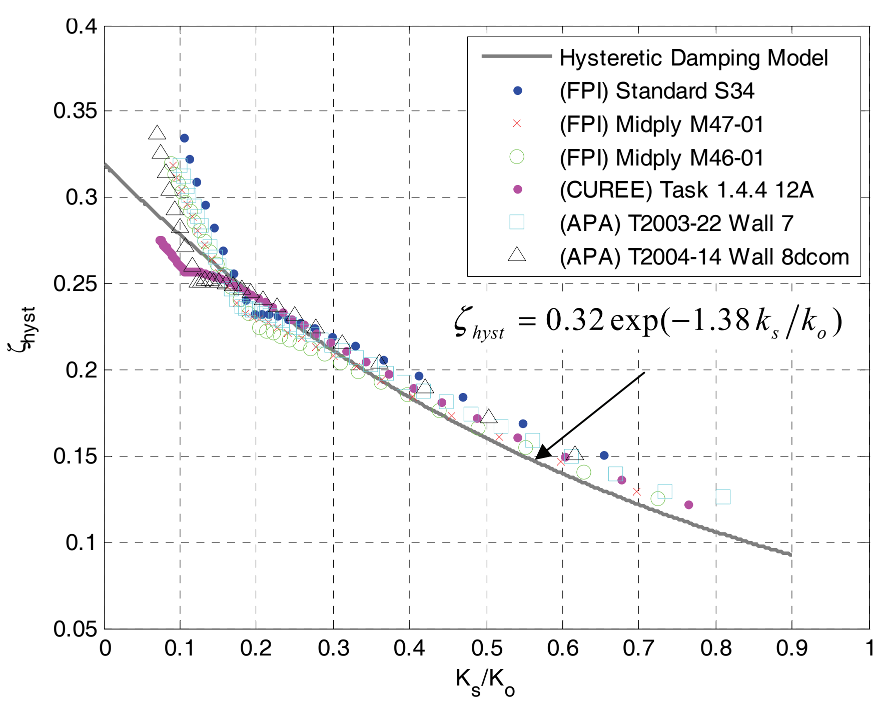

Figure 3-8: Equivalent hysteretic damping model.

4. SIMPLIFIED DIRECT DISPLACEMENT DESIGN (DDD) PROCEDURE

The DDD procedure used to design the shear walls of the six-story NEESWood Capstone Building is a simplified version of the *original* DDD procedure (Pang and Rosowsky 2009). The *original* DDD procedure was intended to meet specified drift limits with a 50% non-exceedance probability (median) and inter-story drifts are estimated using a normalized modal analysis which includes contributions from all vibration modes. The main advantages of the new simplified DDD procedure are that (1) it does not require modal analysis and thus allows the design to be completed using a spreadsheet, and (2) it allows consideration of drift limit non-exceedance probabilities other than 50%. Table 4-1 summarizes the information used to calculate the design forces for Performance Level 3. These design forces were obtained using the simplified DDD procedure, which is described in the following sections. The complete details of the DDD calculations for Performance Levels 1 to 3 are given in Appendix C.

Table 4-1: Summary of DDD calculations for design Level 3.

Story	h_s (m)	h_o (m)	θ_{it} (%)	W (kN)	Δ_{it} (mm)	Δ_o (mm)	$W^*\Delta_o$ (kN-mm)	C_v	β_v	$C_v{}^*h_o$ (m)	$W^*\Delta_o^2$ x10^3 (kN-mm^2)	V_s (kN)	K_s (kN/mm)	F (kN)	F^*h_o (kN-m)
1	3.05	3.05	2.13	502	65	65	32554	0.059	1.000	0.18	2111	2185	33.68	129	393.9
2	2.74	5.79	2.13	474	58	123	58401	0.106	0.941	0.61	7196	2055	35.21	232	1342.6
3	2.74	8.53	2.13	474	58	182	86064	0.156	0.835	1.33	15629	1823	31.24	342	2915.8
4	2.74	11.28	2.13	474	58	240	113727	0.207	0.678	2.33	27290	1482	25.39	451	5091.4
5	2.74	14.02	2.13	505	58	298	150597	0.274	0.472	3.84	44928	1030	17.65	598	8382.0
6	2.74	16.76	2.13	305	58	357	108965	0.198	0.198	3.32	38868	433	7.41	433	7251.4
Σ				2734	Δ_{eff} =	247	550308	1.000	h_{eff} =	11.62	136022			2185	25377.1

Step 1: Determine adjustment factor for specified non-exceedance (NE) probability at the design drift limit.

The inter-story drift limit for seismic hazard Level 3 (MCE) is 4% with an 80% non-exceedance probability. All other hazard levels were associated with 50% NE probabilities (i.e., median values). The design spectrum specified in both ASCE/SEI-7 (2005) and ASCE/SEI-41 (2006) represents the median demand for the specified hazard level. In order to design for a target non-exceedance probability of inter-story drift greater than the median, the design spectral value must be adjusted upward to reflect the increase in the design non-exceedance probability. The design spectral acceleration adjusted for NE probability, $\overline{S}_X$, is equal to the product of the code-specified spectral acceleration value (median) and the adjustment factor, C_{NE}:

$$\overline{S}_X = C_{NE} S_X \tag{5}$$

The factor C_{NE} is assumed to be lognormally distributed with a median value of 1.0 (assuming that the code specified median value is unbiased) and a logarithmic standard deviation, β_R, which accounts for the uncertainty of the ground motions, β_{EQ}, as well as the uncertainty associated with the design procedure (i.e., simplified DDD procedure), β_{DS}:

$$\beta_R = \sqrt{\beta_{EQ}^{\ 2} + \beta_{DS}^{\ 2}} \tag{6}$$

Figure 4-1 shows the response spectra of the ATC-63 far-field ground motion ensemble scaled to the MCE level (Level 3) and the logarithmic standard deviation of the response spectra, β_{EQ}. The uncertainty due to the ground motion varies from about 0.35 to 0.5. Following the ATC-63 study, a fixed value of 0.4 was assumed for the β_{EQ}. The simplified DDD procedure does not explicitly account for a number of factors that might affect the actual inter-story drift response such as torsion, higher mode effects, anchor tiedown system (continuous rod) elongation and compression of the chord members, or flexible diaphragms. The uncertainties introduced into the analysis arising from these assumptions/simplifications, β_{DS}, was assumed to be 0.6 and the total uncertainty β_R, rounded up to the nearest 0.05, was determined to be 0.75 using equation (6).

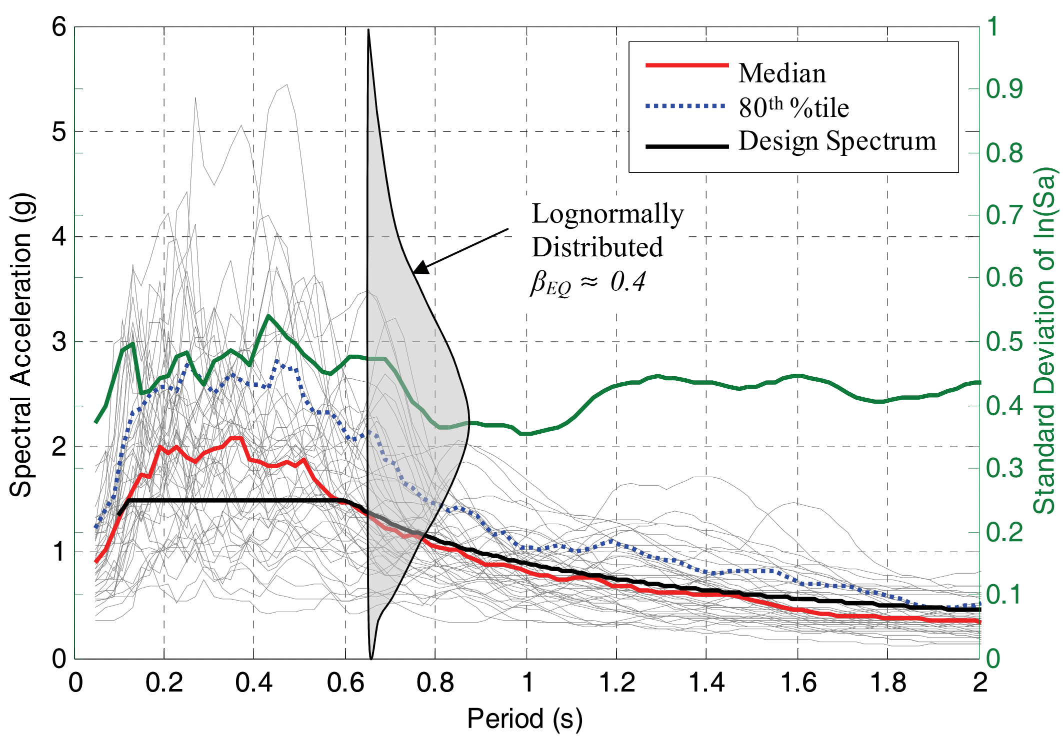

Figure 4-1: ATC-63 far-field ground motion ensemble scaled to the Level 3 (MCE) design spectrum.

The adjustment factor for the NE probability can be determined using the inverse of the lognormal cumulative distribution function (CDF) with median value of 1.0 (logarithmic median = 0).

$$C_{NE} = \exp[\Phi^{-1}(NE_t)\beta_R + \ln(1)] = \exp[\Phi^{-1}(NE_t)\beta_R] \qquad (7)$$

where $\Phi^{-1}(.)$ is the inverse CDF of the standard normal distribution. Figure 4-2 shows two CDFs with logarithmic standard deviations of 0.40 and 0.75. The CDF with logarithmic standard deviation, β_R, of 0.40 includes only the ground motion uncertainty while the CDF with β_R of 0.75 includes both the ground motion and the design procedure uncertainties. The CDF with the higher logarithmic standard deviation (i.e., 0.75) has a greater dispersion and it produces a larger adjustment factor, C_{NE}. Using equation (7), the C_{NE} factor for the Capstone Building Level 3 design with 80% non-exceedance probability was determined to be 1.88 (Figure 4-2).

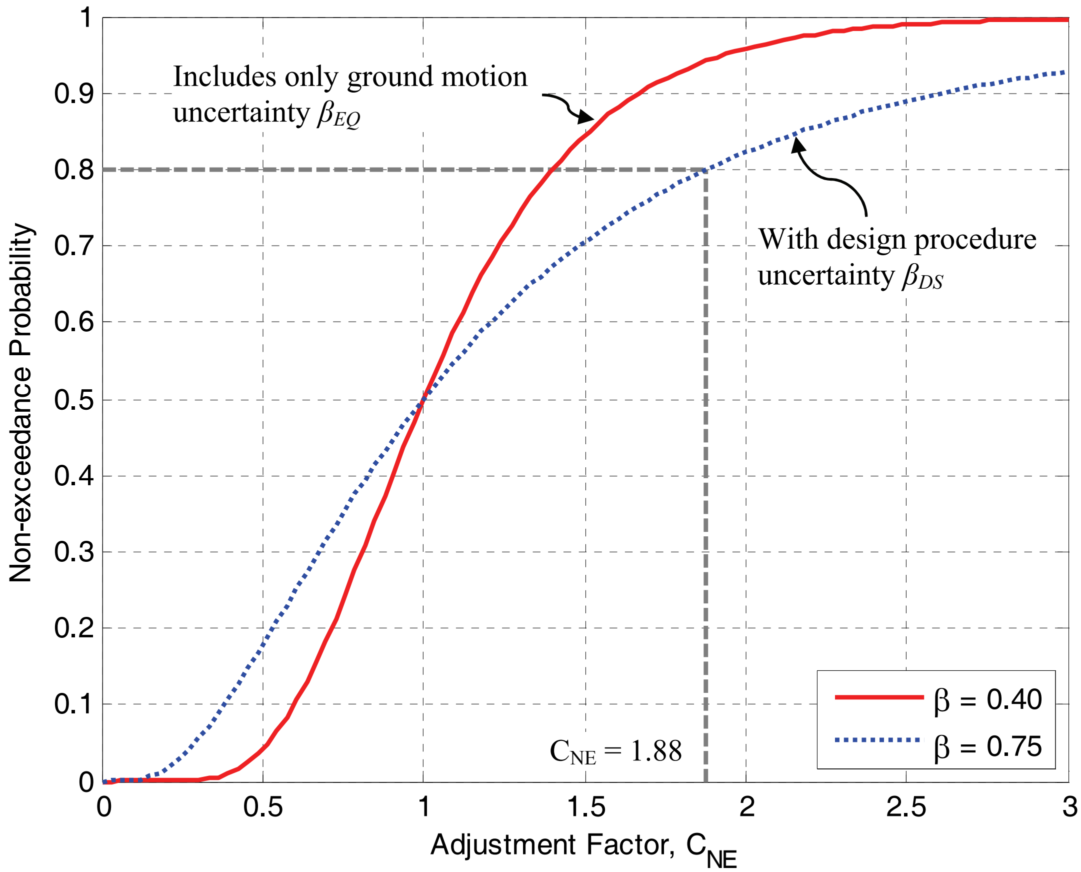

Figure 4-2: Adjustment factor for non-exceedance probability.

Step 2: Select a design inter-story drift.

The proposed NEESWood drift limit for seismic hazard Level 3 is 4%. The design inter-story drift adjusted for NE probability was $4\%/C_{NE} = 2.13\%$, an equivalent 50% NE drift limit, θ_{eq50}. Figure 4-3 shows the target peak inter-story drift curve for seismic hazard Level 3. Note that the median of the new peak inter-story drift distribution curve is equal to θ_{eq50}. The equivalent 50% NE inter-story drift limit was used in the displacement-based design of the six-story building (Table 4-1). While a constant inter-story drift limit was used throughout the design of the six-story Capstone Building, the procedure allows different inter-story drift limits to be assigned to each story if desired.

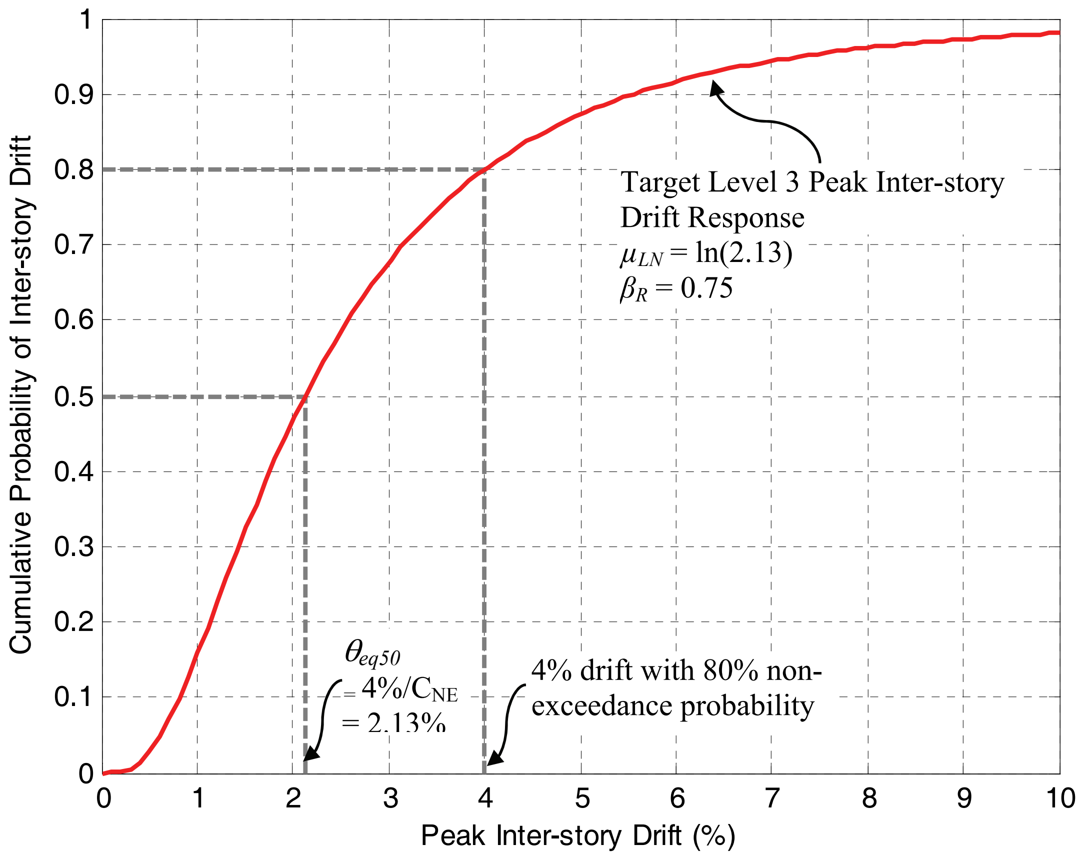

Figure 4-3: Target peak inter-story drift distribution curve.

Step 3: Calculate the vertical distribution factors for base shear, C_v, as:

$$C_{v_j} = \frac{W_j \Delta_{oj}}{\sum_i W_i \Delta_{oi}} \tag{8}$$

Where subscript i is the floor number, W is the lumped seismic weight of the floor or the roof diaphragm and Δ_o is the target floor displacement relative to the ground (Figure 4-4). The seismic weights listed in Table 4-1 were estimated based on the tributary area of the shear walls (i.e., half of the wall weight was assigned to the floor above and half to the floor below).

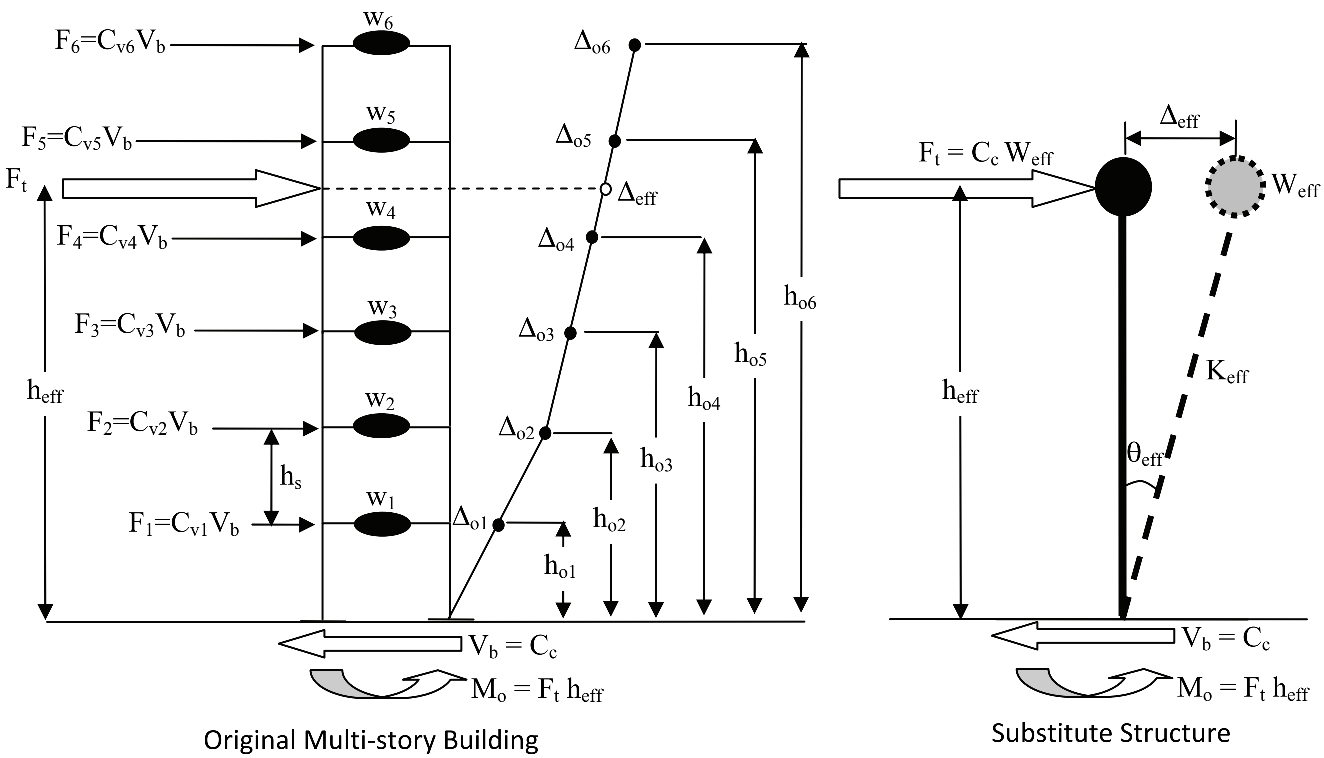

Figure 4-4: Example 6-story building and substitute structure for DDD procedure.

Step 4: Calculate the effective height, h_{eff}, for the *substitute structure* modeled as a single-degree-of-freedom (SDOF) system.

The effective height is located at the centroid of the assumed lateral force distribution and is calculated as:

$$h_{eff} = \frac{\sum_i C_{v_i} h_{oi}}{\sum_i C_{v_i} = 1} = \sum_i C_{v_i} h_{oi} \tag{9}$$

where β_{vi} is the story shear factor computed as the sum of the vertical distribution factors, c_{vi}, on and above the i^{th} floor and h_o is the floor height with respect to the ground. For typical multi-story buildings with approximately equal story heights and seismic weights at each story, the ratio of effective-to-roof height generally is about 0.7. The effective height for the six-story Capstone Building was determined to be 11.62 m (see Table 4-1), or 0.69 times the roof height (16.76 m).

Step 5: Use interpolation to obtain the target displacement at the effective height, Δ_{eff}, or target drift at effective height, θ_{eff}.

The effective height, 11.62 m (38.11 ft), for the NEESWood Capstone Building is located between levels 4 and 5 (Table 4-1). Using interpolation, the effective displacement with respect to the ground level is 247 mm (9.73 inches).

Step 6: Calculate the effective seismic weight, W_{eff}, of the substitute structure:

$$W_{eff} = \frac{\left(\sum_i W_i \Delta_{oi}\right)^2}{\sum_i W_i \Delta_{oi}^2} \tag{10}$$

The $\sum_i W_i \Delta_{oi}$ and $\sum_i W_i \Delta_{oi}^2$ terms are shown in last row of Table 4-1. The effective seismic weight for the six-story NEESWood Capstone Building is $(550308)^2/(136022\times10^3)$ = 2226 kN (500.5 kip). For most mid-rise buildings of regular plan, the effective seismic weight usually is about 80% of the total seismic weight. For the Capstone Building, the effective seismic weight is 81% of its total weight.

Step 7: Determine the damping reduction factor, B_ζ, per ASCE/SEI-41 (2006) section 1.6.1.5 as:

$$B_\zeta = \frac{4}{5.6 - \ln(100\zeta_{eff})} \tag{11}$$

where ζ_{eff} is the effective viscous damping as a fraction of the critical damping, computed as the sum of the hysteretic damping of the shear walls, ζ_{hyst} (see equation (4)), and the intrinsic damping, ξ_{int},

$$\zeta_{eff} = \zeta_{\text{int}} + \zeta_{hyst} \tag{12}$$

In the design of the six-story NEESWood Capstone Building, 5% intrinsic damping was assumed. The intrinsic damping accounts for the damping contributions of building components other than the shear walls (e.g., gypsum partition walls and floor diaphragms). At the equivalent

50% NE inter-story drift limit (2.13%), and assuming most walls are built with a 51 mm (2 in.) or 76 mm (3 in.) perimeter nailing, the K_s/K_o ratio is about 0.30 (from Figure 3-6, Table 3-2 or). Substituting K_s/K_o of 0.30 into the equivalent hysteretic damping equation (4) gives an estimated hysteretic damping of 0.21. The total equivalent viscous damping, including the intrinsic damping, therefore is 0.26. Using equation (11), the damping reduction factor therefore is 1.71.

Step 8. Determine the design base shear coefficient, C_c, using the capacity spectrum approach as:

$$C_c = \min \begin{cases} \dfrac{C_{NE} S_{XS}}{B_\zeta} \\ \dfrac{g}{4\pi^2 \Delta_{eff}} \left(\dfrac{C_{NE} S_{X1}}{B_\zeta} \right)^2 \end{cases} \tag{13}$$

Equation (13) is the solution for the intersection between the demand and the capacity spectra (Shama and Mander 2003) (Figure 4-5). For seismic hazard Level 3, the spectral design values for short-period, S_{MS}, and 1-second period, S_{M1}, are 0.9 and 1.5 g, respectively (Table 2-2). The first term of equation (13) is for a structure having a secant period (at the design displacement, Δ_{eff}) less than or equal to the short-period, T_s, defined in Section 11.4 of ASCE/SEI-7 (2005). For most mid-rise buildings, where the secant periods are generally greater than T_s but less than T_L, the second term usually governs the design. The long-period transition period, T_L, can be obtained from ASCE/SEI-7 (2005). Using equation (13), the base shear coefficient for seismic hazard level 3 therefore is 0.981.

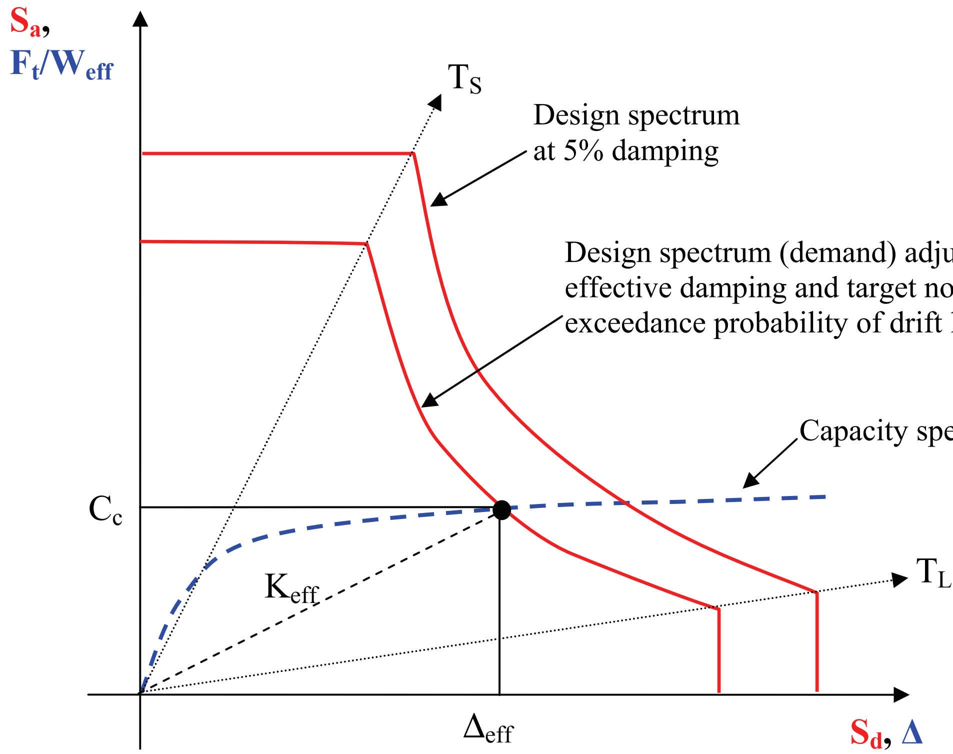

Figure 4-5: Determination of the design base shear coefficient using capacity spectrum approach.

Step 9. Calculate design forces

Once the base shear coefficient is obtained, the base shear, lateral forces, story shears, overturning moments and the required story secant stiffnesses are calculated as:

Base shear, V_b

$$V_b = C_c W_{eff} \tag{14}$$

Equivalent static lateral forces, F_i

$$F_i = C_{v_i} C_c W_{eff} = C_{v_i} V_b \tag{15}$$

Story shears, V_{s_i}

$$V_{s_i} = \sum_{j=i}^{N_S} C_{v_j} V_b = \beta_{v_i} V_b \tag{16}$$

Overturning moment, M_{o_i}

$$M_{o_i} = \sum_{j=i}^{N_S} F_j \left(h_{o_j} - h_{o_i} \right) \tag{17}$$

where N_s is the total number of stories (i.e., six for the Capstone Building).

Effective secant stiffness (SDOF), K_{eff}

$$K_{eff} = \frac{C_c W_{eff}}{\theta_{eff} h_{eff}} = \frac{C_c W_{eff}}{\Delta_{eff}} \tag{18}$$

Required secant stiffness for each story,

$$K_{s_i} = \frac{V_{S_i}}{\Delta_{it_i}} \tag{19}$$

From Table 4-1, the design base shear and overturning moment are approximately 2185 kN (491 kips) and 25377 kN-m (18718 kip-ft), respectively. The required effective secant stiffness of the building at the target drift limit, computed using equation (18), is 8.84 kN/mm (50.47 kip/in). The effective secant period, computed as $2\pi/\sqrt{(g \times K_{eff}/W_{eff})}$, therefore is 1.01 s. Recall that the secant-to-initial stiffness ratio of 0.30 was assumed when determining the hysteretic damping, the minimum initial design stiffness therefore is $K_{eff}/0.30$ = 29.46 kN/mm (168.23 kip/in) and the associated initial period is 0.55 second.

Step 10. Select shear walls to meet the design story shears

The design points, or expected design inter-story drift and required story shear pairs (θ_{it} and V_s), are shown in Table 4-1. Shear wall nailing schedules were selected from the shear wall database (Table 3-2 or Figure 3-6). Shear wall backbone forces were taken from the "2% drift" column since the equivalent 50% NE inter-story drift was determined to be 2.13% for seismic hazard Level 3. The design story shears were distributed to wall lines according to their tributary areas. Direct summation of the equivalent stiffness of shear wall segments was used to generate the story backbone curves. Note that this assumes no torsion and that all shear walls at the same floor level experience the same drift. The nailing patterns for the shear walls for each floor were determined such that the story backbone curve was above the design points (i.e., design NE 50% drift and required story shear pairs) associated with that floor (see Figure 4-6). The required story shears, determined using equation (16), for Levels 1 to 3 are listed in Table 4-2 (see Appendix C for details). The complete shear wall nail schedules for stories 1 to 6 are provided in Appendix D. In the 1st story, most of the *standard* shear walls are sheathed with two layers of OSB (one layer on each side of the wall) attached using nails with either a 51 mm (2 in.) or 76 mm (3 in.) edge spacing (see Appendix D). At wall line B (parallel to the longitudinal direction) in the 1st story, double-layer midply shear walls with 76 mm (3 in.) edge nail spacing were used.

Table 4-2: Design 50% NE drift limits and required story shears for Performance Levels 1 to 3.

Performance Level Seismic Hazard	Level 1 50%/50yr		Level 2 10%/50yr		Level 3 2%/50yr	
Story	Drift Limit (%)	V_s (kN)	Drift Limit (%)	Vs (kN)	Drift Limit (%)	V_s (kN)
1	1.00	158.2	2.00	349.1	2.13	2184.6
2	1.00	148.9	2.00	328.5	2.13	2055.3
3	1.00	132.1	2.00	291.4	2.13	1823.5
4	1.00	107.3	2.00	236.8	2.13	1481.8
5	1.00	74.6	2.00	164.7	2.13	1030.4
6	1.00	31.3	2.00	69.1	2.13	432.6

(a)

(b)

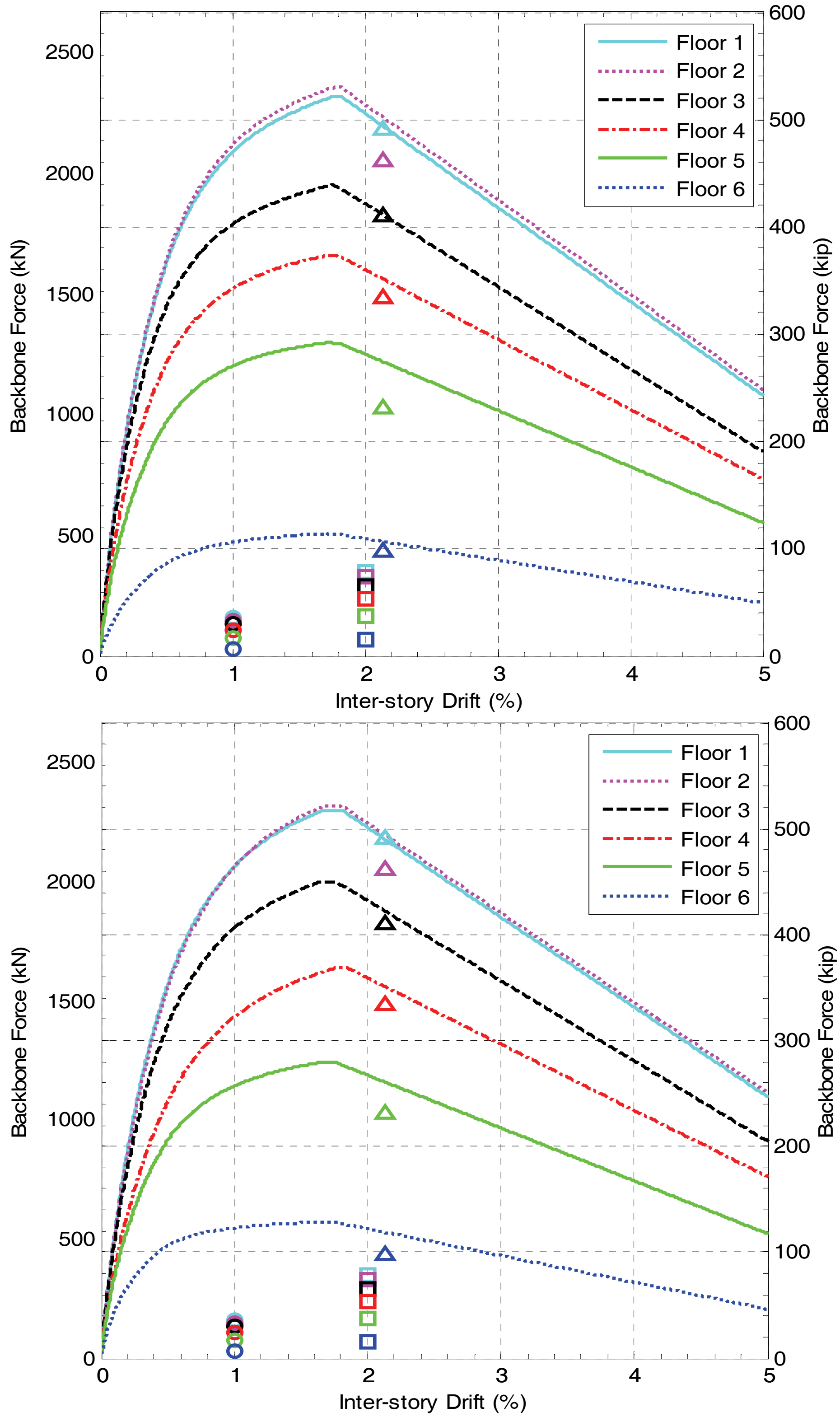

Figure 4-6: Design points for seismic hazard Level 3 and inter-story backbone curves (a) transverse direction and (b) longitudinal direction.

4.1 Comparison between Force-based Design (FBD) and Displacement-based Design (DDD)

In force-based design (FBD) procedure, the design base shear equation in the current edition of International Building Code (ICC 2006) is:

$$V_b = \frac{S_a\left(T_a\right) I_E W}{R} \tag{20}$$

where W is the total seismic weight and I_E is the occupancy important factor. For the six-story Capstone Building, the total seismic weight was estimated to be 2734 kN (615 kip) and $I_E = 1$ was assumed. R is the response modification factor which is equal to 6.5 for light-frame wood shear wall system. $S_a(T_a)$ is the design spectral acceleration at the approximate fundamental period of the building, T_a. The approximate fundamental period of the six-story building determined using the empirical equation provided in the ASCE/SEI 7-05 (ASCE 2005) is 0.40s.

$$T_a = C_t h_n^{\ x} \tag{21}$$

where h_n is the roof height of the structure (55 ft or 16.76 m) and C_t is the approximate period parameter which is equal to 0.0488 or 0.02 when the building height is expressed in SI or US customary units, respectively. For woodframe structures, the exponent x is equal to 0.75. Note that the design hazard level for the FBD procedure is the same as the NEESWood seismic hazard Level 2. Therefore, the design spectral acceleration, $S_a(T_a$=0.40s), is equal to 1.0 g (Figure 2-1).

The design forces, determined using the FBD procedure, are summarized in Table 4-3. The FBD base shear and overturning moment are 421 kN (95 kip) and 4886 m-kN (3604 ft-kip), respectively. According to the FBD procedure, the design base shear-to-total building weight ratio, V/W, is 0.154 (Table 4-4). Note that the seismic hazard associated with the FBD procedure is the same as the NEESWood seismic hazard Level 2. The DDD V/W ratio for seismic hazard Level 2 is 0.128 which is slightly lower than the FBD V/W ratio. However, Figure 4-6 shows that the controlling design level is seismic hazard Level 3. In order to satisfy the design requirement for Performance Level 3 (i.e., 4% drift limit with 80% NE probability), the six-story Capstone Building must have a maximum base shear capacity of at least 79.9% of the total building weight. Note that the FBD procedure considers only one design requirement/objective. Furthermore, the FBD base shear ratio is computed as $1/R$ which means the V/W ratio is a constant value for all buildings with light-frame wood shear wall systems. On the other hand, the DDD V/W ratios are function of the design requirements (i.e., seismic hazard level, drift limit and target NE probability). This means that, using the DDD procedure, structures can be designed to meet owners' specifications or needs that are beyond the current code requirement.

Table 4-3: Design forces for force-based procedure.

Story	W (kN)	h_o (m)	$W*h_o$ (kN-m)	$W*h_o/\Sigma(W*h_o)$	F (kN)	V_s (kN)	$F*h_o$ (m-kN)	kN/m^2	F/W
1	502	3.05	1530	0.059	24.88	420.6	75.8	1.910	0.050
2	474	5.79	2745	0.106	44.64	395.7	258.5	1.797	0.094
3	474	8.53	4045	0.156	65.78	351.1	561.4	1.595	0.139
4	474	11.28	5345	0.207	86.93	285.3	980.3	1.296	0.183
5	505	14.02	7078	0.274	115.11	198.4	1613.9	0.901	0.228
6	305	16.76	5121	0.198	83.29	83.3	1396.2	0.378	0.273
Σ	2734		25863	1.000	420.62		4886.2		
[a] Approximate Fundamental Period =					0.40	s			
[b] Base Shear/Total Weight =					0.154				

[a] $T_a = C_t h_n^x = 0.0488(16.76)^{0.75} = 0.404\text{s}$

[b] $R = 6.5$

Table 4-4: Comparison between FBD and DDD base shears and overturning moments.

	FBD	DDD		
Performance Level Seismic Hazard	Level 2 [b] 10%/50yr	Level 1 50%/50yr	Level 2 10%/50yr	Level 3 2%/50yr
Base Shear (kN)	421.6	158.2	349.1	2184.6
Base Shear/Total Building Weight[a]	0.154	0.058	0.128	0.799
Base Overturning Moment (m-kN)	4976	1838	4056	25382

[a] Total building weight = 2734 kN (614.7 kip)

[b] The spectral acceleration values for the FBD are computed as 2/3 of the mapped spectral accelerations at the MCE level (2%/50yr).

5. NUMERICAL MODELS FOR THE SIX-STORY CAPSTONE BUILDING

5.1 Pseudo-3D / 2D Model for Nonlinear Time-history Analysis (NLTHA)

A numerical model for the Capstone Building was constructed using the M-SAWS program, a Matlab version of the SAWS (Seismic Analysis of Woodframe Structures) program, which considers only the pure-shear deformation of the shear walls (Folz and Filiatrault, 2001b). In the M-SAWS model, rigid diaphragms with one rotational and two in-plane translational degrees of freedom are assumed for each floor and roof diaphragm (Figure 5-1). Each shear wall was modeled as a zero-height nonlinear SDOF spring using the modified Stewart hysteretic model in the M-CASHEW program (see

Figure **3-3**). Since the height of the shear wall was not explicitly considered, the M-SAWS model is herein referred to as the pseudo-3D or 2D model.

The load-displacement responses for 2.44 m (8 ft) wide standard and midply shear walls built with different nail spacings were predicted using the M-CASHEW and a system identification procedure was used to obtain a set of ten parameters to describe the global hysteretic behavior of each shear wall. The values for parameters K_o, F_o, and F_i were then divided by the width of the shear wall (i.e. 2.44 m or 8 ft) to obtain the unit-width hysteretic parameters (see Appendix E). In the M-SAWS model, only the full-height shear wall segments were considered and the sheathing panel above and below the windows and door openings were ignored. For each full-height shear wall in the Capstone Building, the hysteretic parameters K_o, F_o, and F_i were adjusted for the length of the wall pier while other parameters (r_1, r_2, r_3, r_4, Δ, α and β) were unchanged. All perimeter shear walls were sheathed with one layer of GWB on one side of the wall only while both sides of the interior shear walls were sheathed with GWBs.

The damping matrix used in the NLTHA was determined using the Rayleigh damping model with equal damping ratios assigned to the 1st and 2nd modes. Since the hysteretic damping is accounted for in the nonlinear hysteresis model itself, low level of damping values (2% and 5% of critical dampings) were used in the nonlinear time-history analysis (NLTHA). Assuming a 2% damping in the NLTHA is believed to be a conservative estimate for the viscous damping of the test building since the lateral stiffness of the structural panels above and below the door and window openings were not explicitly considered in the numerical model. On the other hand, assigning a 5% viscous damping in the NLTHA is consistent with the 5% intrinsic damping value assumed in the DDD procedure (see equation (12)). The 2% and 5% damping values approximately bound the actual viscous damping of the test building.

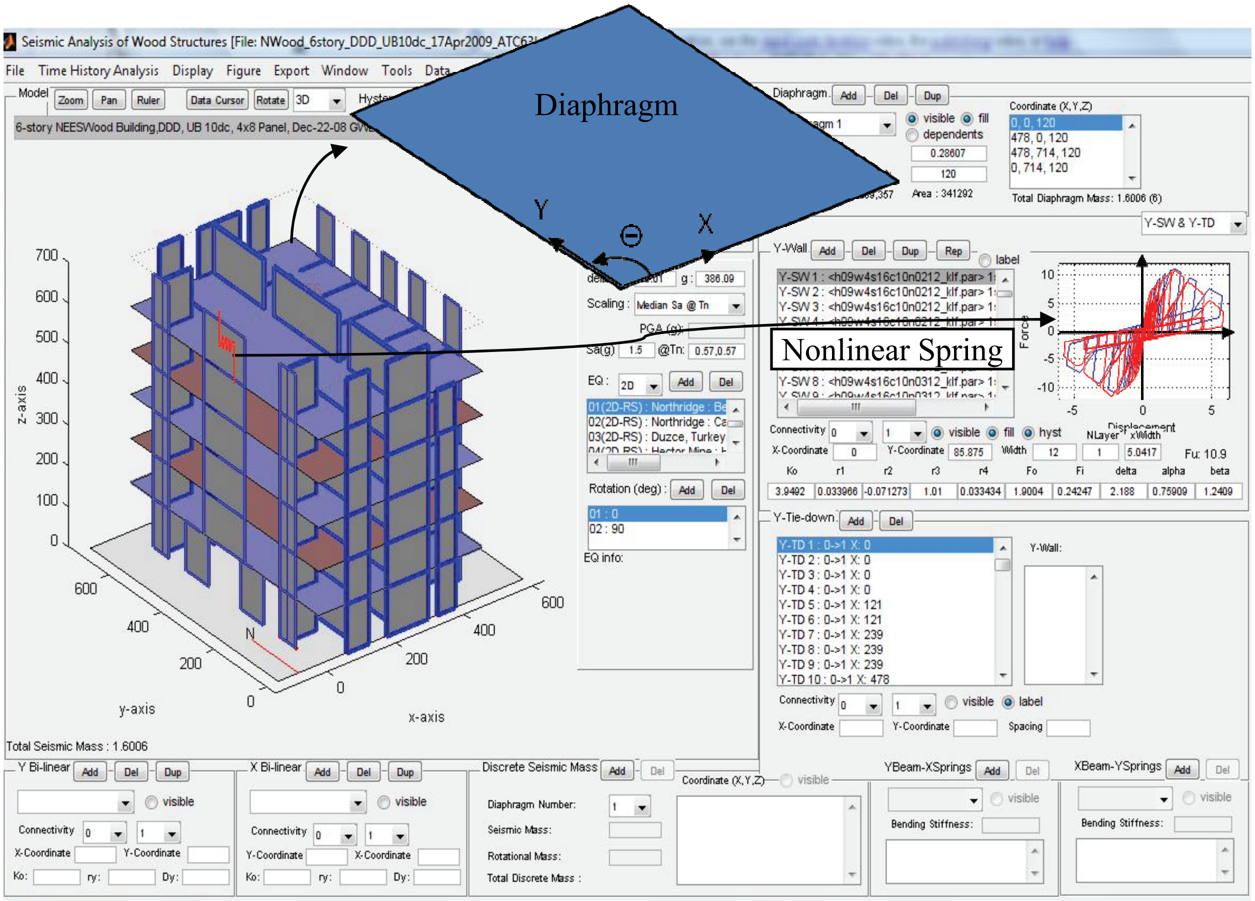

Figure 5-1: M-SAWS model for the six-story NEESWood Capstone Building.

5.2 3D Model for Nonlinear Time-history Analysis (NLTHA)

Although light-frame wood buildings generally are treated as lateral shear-dominant systems in design, they can also be affected by vertical excitation and overturning moment which induces tension forces in the shear wall hold-down system and can cause cumulative elongation of the hold-down rods, especially in buildings exceeding three stories. Pei and van de Lindt (2009) developed a simplified model that is capable of incorporating the effect of overturning and uplift as well as the vertical ground motion excitation in the seismic responses of woodframe structures. The proposed model for wood structures with vertical/uplift effects is quite different from the shear-only model in that the model assigns six degrees-of-freedom at each story diaphragm and includes the stiffness of the hold-down system and the vertical stiffness of shear walls provided by the vertical framing members. The diaphragm is allowed to move and rotate out of the horizontal plane, adding another dimension to the dynamic analysis to make it three-dimensional (3D). Figure 5-2 illustrates the kinematics of the 3D diaphragm model. It is also worth pointing out that the lateral displacement of higher stories will be effected by the out-of-plane rotation (rocking) of lower floors and this effect is cumulative.

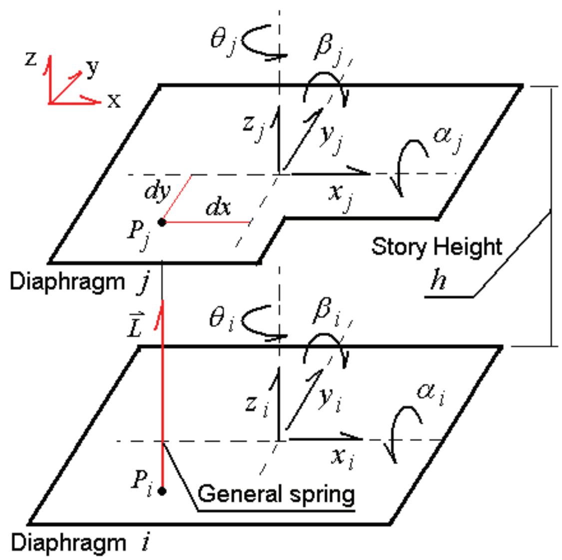

Figure 5-2: Kinematics of six degrees-of-freedom diaphragm model.

The same nonlinear hysteretic shear springs used in the 2D model also were used to model the shear walls in the 3D model. In addition to the nonlinear horizontal shear spring, an un-symmetrical linear vertical spring was used to model the uplift effect of the hold-downs/tie-down rods and the compression of the stud packs (Figure 5-3). The 3D model has been implemented into the SAPWood program, developed as part of the NEESWood project. The SAPWood program also was used to perform the 3D NLTHA to verify the applicability of the DDD procedure.

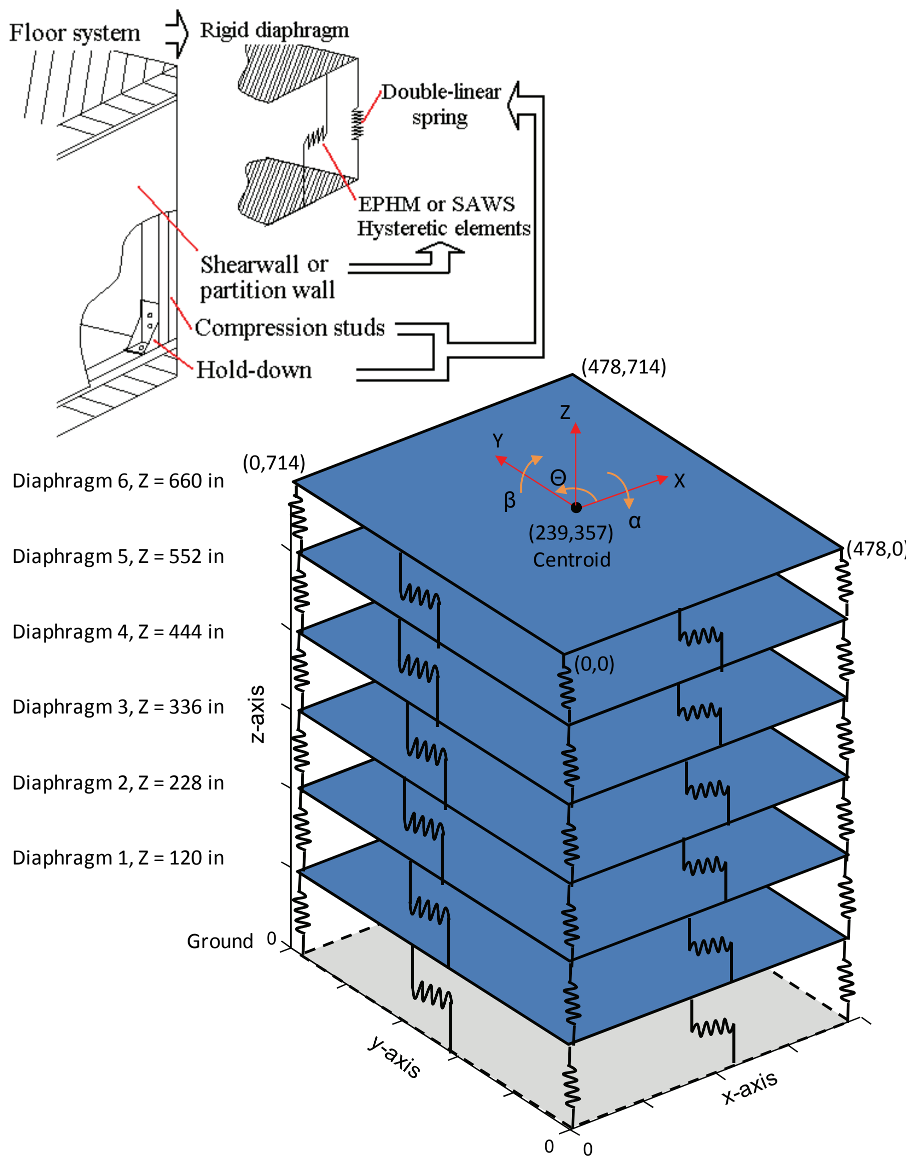

Figure 5-3: SAPWood model for the six-story NEESWood Capstone Building.

5.3 Static Pushover Analyses

Monotonic pushover analyses were performed using the M-SAWS model. Figure 6-3 shows the monotonic pushover curves obtained by applying an inverted triangular lateral load parallel to the transverse (x-axis) and the longitudinal (y-axis) of the test building. The maximum base shears in the transverse and longitudinal directions are 2320 kN (521.6 kips) and 2303 kN (517.5 kips), respectively, which occurs at a roof drift ratio of 1.27% and 1.18%, respectively (roof height is 16.76 m). The model predicted base shear-to-building weight ratios at the peak of the pushover curves, *V/W* are approximately 0.84. It should be noted that the static pushover curves include only the nonlinear restoring force of the shear walls. Therefore, the maximum "dynamic" base shears based on earthquake/shake-table tests are expected to be higher than that predicted by the pushover analyses. For comparison purposes, the design base shear values for the FBD and DDD are also labeled in Figure 6-3. The maximum pushover base shears in both directions are higher than the design base shears thus confirmed that the as-designed six-story Capstone Building has adequate base shear capacity for performance Levels 1 to 3.

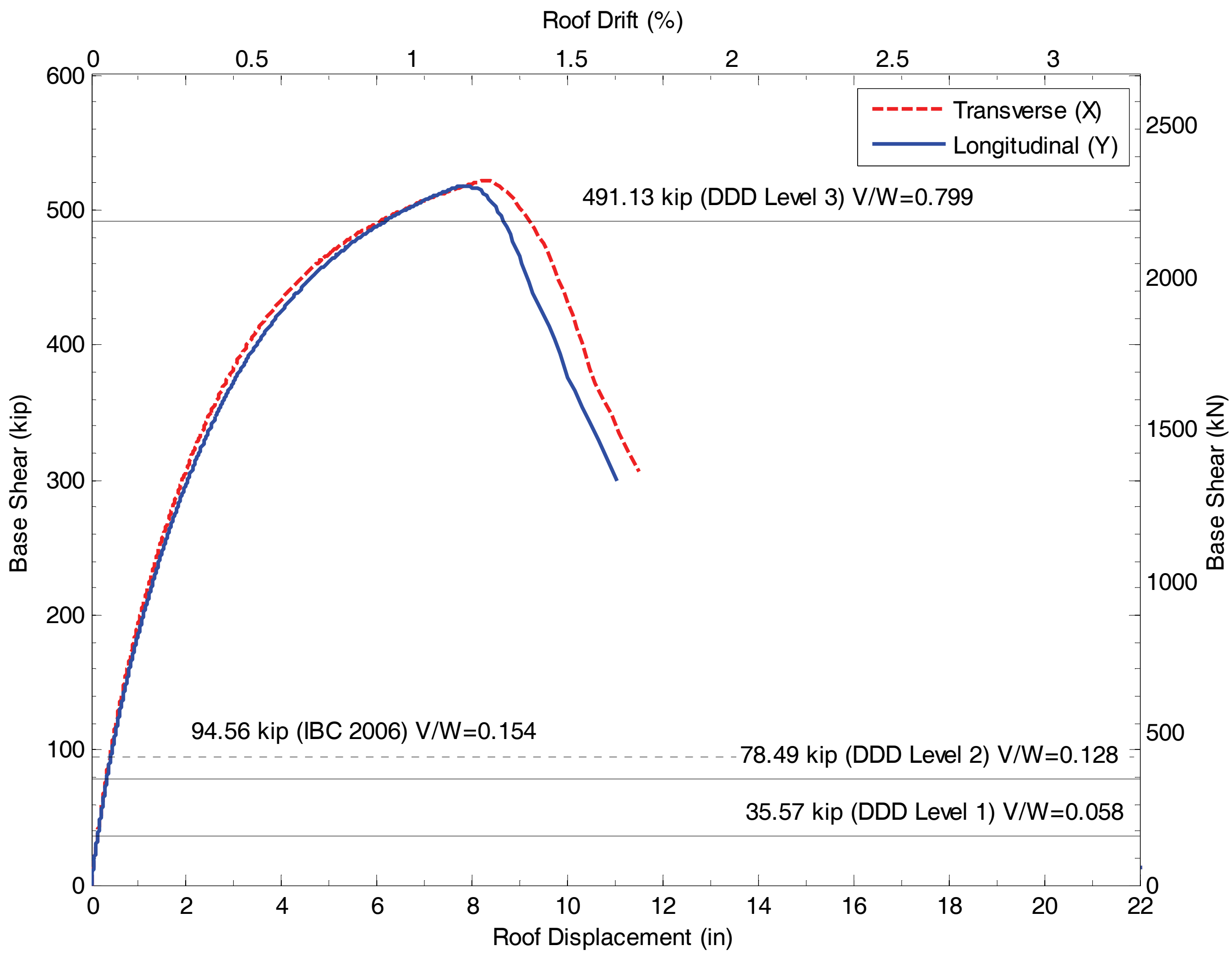

Figure 5-4: Pushover curves of the as-designed six-story Capstone Building (M-SAWS model) and DDD vs. FBD base shear-to-total building weight ratios.

5.4 Modal Analyses

Modal analyses were performed to obtain the periods and mode shapes of the Capstone Building (Appendix F). The fundamental periods calculated using the initial stiffness of the M-SAWS and SAPWood models were 0.375s and 0.398s, respectively (Table 5-1). Including the vertical effects in the SAPWood model results in slightly higher initial periods than those obtained from the 2D M-SAWS model. The models predicted fundamental periods are very close to the approximate fundamental period specified by the design code (0.40s).

Table 5-1: First three periods of the M-SAWS and SAPWood models.

Model	M-SAWS		SAPWood
Mode	Initial Stiffness	Tangent Stiffness at 0.15% Drift	Initial Stiffness
1	0.375	0.537	0.398
2	0.359	0.505	0.391
3	0.320	0.443	0.321

The model predicted periods listed in Table 5-1 include the stiffness contribution of GWBs attached to the shear walls. However, full-scale wall tests show that the stiffness contribution of GWB diminishes quickly at very low drift level (~0.5%, see Figure 3-5). To obtain an upper bound estimate of the fundamental period, modal analysis also was performed using the global tangent stiffness of the M-SAWS model at a very low drift level (0.15% roof drift or 2.54 cm (1 in) roof displacement). Specifically, pushover analysis was first performed at each of the horizontal directions to achieve a 0.15% drift at the roof level. Then, modal analysis was performed using the global tangent stiffness of the lightly "damaged" building. The first three mode shapes and periods of the Capstone Building based on the tangent stiffness at 0.15% drift are shown in

Figure 5-5. The fundamental period at 0.15% drift is about 0.54s which corresponds to a primary translational mode shape drift in the Y (longitudinal) direction. The second mode is a pure translational mode in the X (transverse) direction with negligible rotation. Mode 3 is a pure rotational or torsional mode which causes the building to twist around the center of gravity of the floor diaphragms. The fundamental period at 0.15% drift (0.54s) is relatively close to the upper limit of the approximate period specified by the design code (0.57s, see Appendix G).

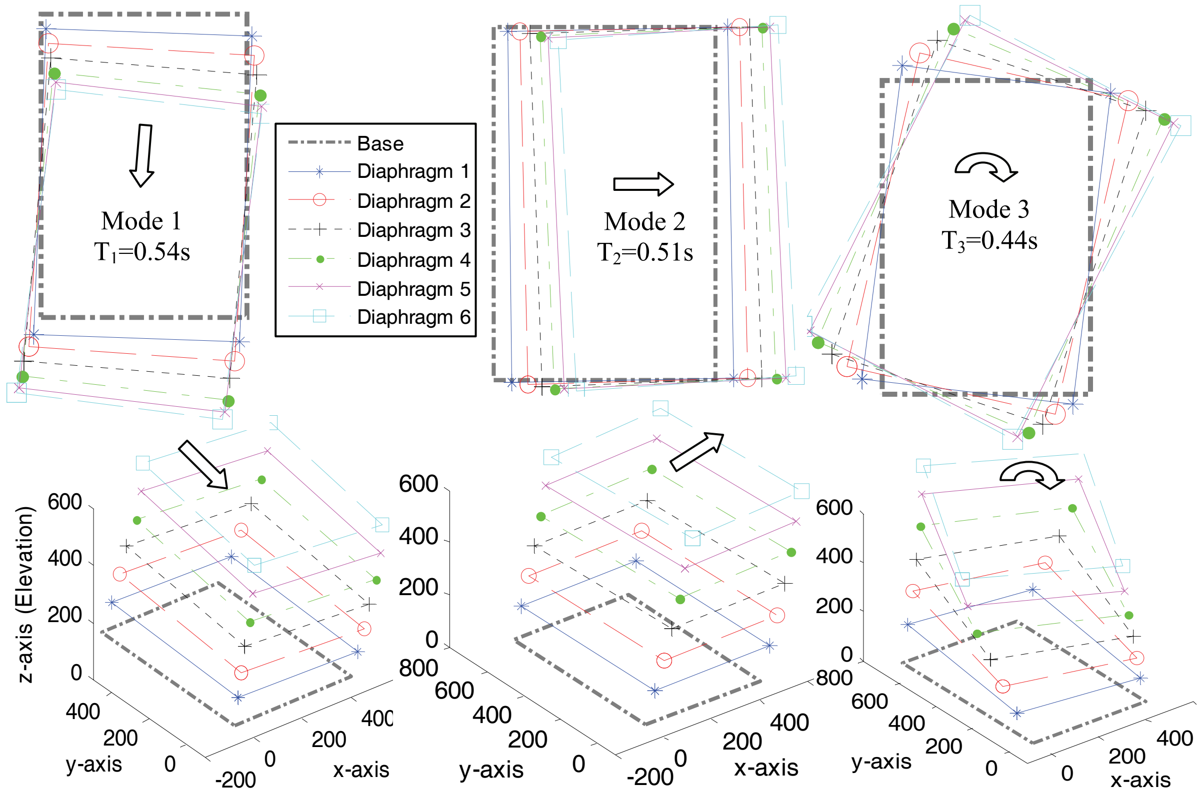

Figure 5-5: First three mode shapes of the M-SAWS model based on tangent stiffness at 0.15% drift.

5.5 Ground Motions

Two sets of ground motion ensembles were considered in the 2D NLTHA: (1) 22 bi-axial ATC-63 far-field ground motions scaled according to the ATC-63 methodology (ATC 2008) for seismic hazard Levels 1-3, and (2) six bi-axial CUREE unscaled near-fault ground motions (Krawinkler et al. 2003) for seismic hazard Level 4 (Appendix H). For hazard Levels 1-3, the median response spectrum of the normalized ground motion ensemble was scaled using a single scaling factor to match the design 5%-damped spectral acceleration at the upper limit of the code prescribed fundamental period of the building (ATC 2008).

According to ASCE-07 (2005), the upper limit of the approximate fundamental period, T_u, of the Capstone Building is 0.57s. The median spectral acceleration, S_a, of the normalized ATC-63 far field ground motion suite at $T_u = 0.57$s is 0.655 g (Figure 5-6). Therefore, the ensemble scaling factor for seismic hazard Level 3 (2%/50yr or MCE) is 1.50g/0.655g = 2.290, where 1.50 g is the code specified spectral acceleration value for the MCE level. The scale factors for adjusting the 22 bi-axial ATC-63 far-field ground motions to match the design seismic hazard Levels 1 to 3 are given in Appendix G.

The ground motions were scaled and the building was analyzed at each of the three performance levels. The bi-axial ground motions also were rotated by 90-degrees and thus, at each performance level, the building was analyzed twice for each of the 22 record pairs for a total of 44 analyses. Similarly, the building was also analyzed using the six pairs of near-fault ground motions rotated at 0 and 90 degrees for seismic hazard Level 4 for a total of 12 analyses. These ground motion ensembles were used in both the 2D and 3D NLTHA to obtain the maximum inter-story drifts of the designed structure at the four design ground motion intensity levels.

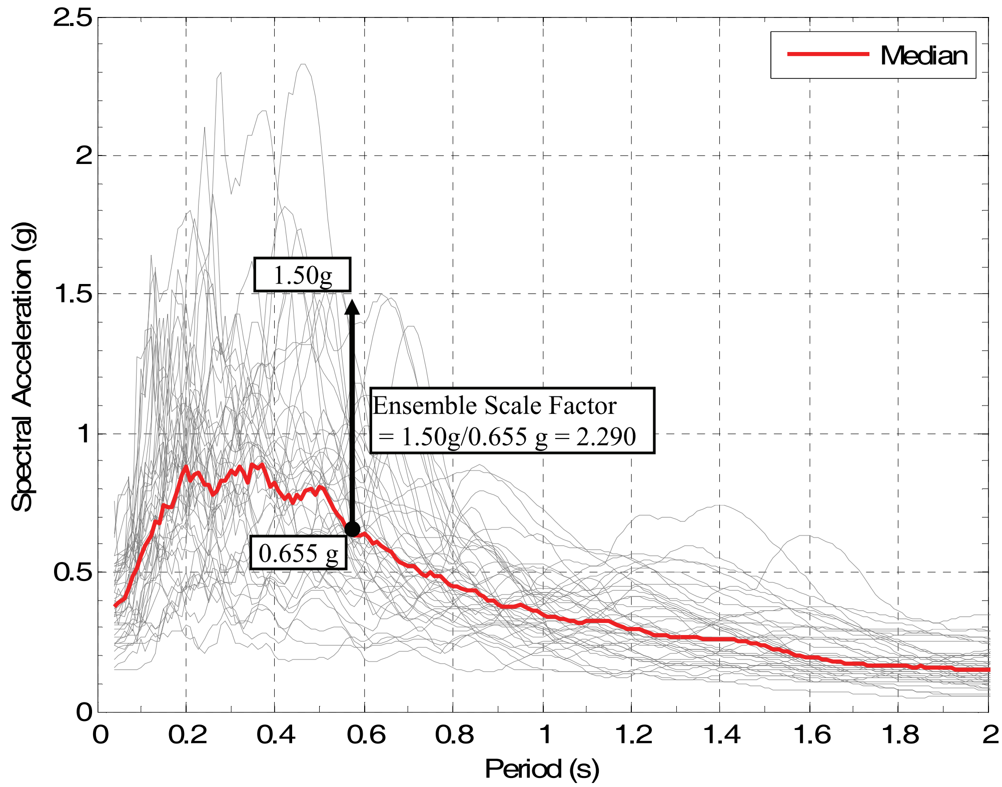

Figure 5-6: Example scaling of the ATC-63 far-field ground motion ensemble.

5.6 Expected Peak Inter-story Drift Distributions

The peak inter-story drifts obtained from the 2D NLTHA for seismic intensity Level 3 (2%/50yr or MCE) are shown in Figure 5-7. Each point represents the maximum inter-story drift recorded from a NLTHA for a particular bi-axial ground motion record rotated at either 0 or 90 degrees. The sample cumulative distribution function (CDF) was constructed from the rank-ordered peak inter-story drifts (dots in Figure 5-7) which were also fitted to a lognormal distribution function given by :

$$P_{NE}(\theta) = \Phi\left(\frac{\ln(\theta) - \lambda}{\xi}\right) \tag{22}$$

where $\Phi(.)$ is the CDF of the standard normal distribution, λ is the logarithmic median, and ξ is the logarithmic standard deviation. The term $P_{NE}(\theta)$ defines the non-exceedance probability at a given inter-story drift, θ.

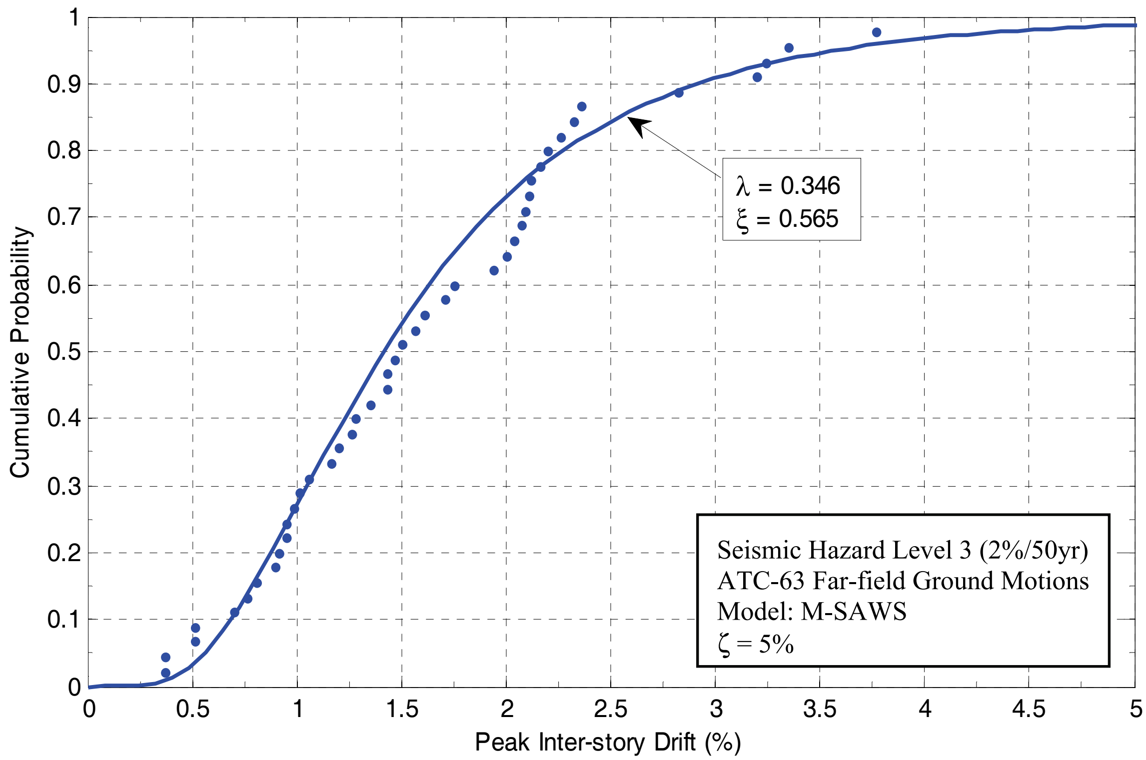

Figure 5-7: Lognormal distribution fit of the peak inter-story drifts for Seismic Hazard Level 3.

The peak inter-story drift distributions based on results from the 3D and 2D NLTHA are shown in Figure 5-8 and the corresponding NE probabilities at the design drift limits are summarized in Table 5-2. Note that the upper and lower bounds of the peak drift distributions are based on the NLTHA results with viscous damping values of 2% and 5%, respectively. For the six-story woodframe structure designed in this study, the differences in the inter-story drifts between the shear-only (2D) model and the three-dimensional model are not felt to be significant. This result is not unexpected because of the aspect ratio (lateral dimension to height ratio approximately equal to one) of the building that makes the dynamic behavior shear-dominant, which is commonly seen in most typical woodframe building floor plans, i.e. multi-unit residential structures.

In summary, both the 2D and 3D NLTHA indicate that the Capstone Building designed using the simplified DDD procedure satisfies all four design objectives. As stated previously, the peak drift distribution curves with 5% viscous damping are felt to be most representative of the actual performance of the test building. As can be seen from the peak drift distribution curves with 5% damping (Figure 5-8), the Capstone Building designed using DDD procedure performs satisfactorily (i.e., meets performance requirements) at all four hazard levels. The median peak drifts at the Levels 1 and 2 were considerably lower than the 1% and 2% drift limits, while the median peak drift at the Level 3 was 1.41% with a 97% probability of not exceeding the 4% drift limit. At Level 4, the probability of exceeding the 7% drift limit was approximately 13% which satisfied the near-fault ground motion performance requirement.

While the peak drift distribution curves with 5% damping were used to verify the seismic performance of the Capstone Building, it should be noted that the design criteria are not tied to the 5% equivalent damping value. An appropriate equivalent viscous damping should be determined for each specific building based on the amount of damping expected from the non-structural elements such as the partition walls and exterior cladding. In addition to the NLTHA with 5% damping, a more conservative assumption of 2% equivalent viscous damping value also was used in the NLTHA to estimate the upper bounds for peak inter-story drifts. The peak drift distribution curves with 2% damping show that the performance requirements are met at all hazard levels except for Level 3 (Table 5-2). Based on the 2D model with 2% equivalent damping, the probability of not exceeding the design drift limit at seismic hazard Level 3 was 75%, which was slightly lower that the design goal (i.e. 80% NE probability). The uncertainties associate with the numerical model and ground motion justify the acceptance of this design since the non-exceedance probability of inter-story drift was within few percents of the design goal and furthermore it was based on a more conservative damping assumption.

The drift profiles (relative to the ground) of two selected earthquake records at the MCE level (2%/50yr) also are shown in Figure 5-8. It can be seen that the drift profiles are relatively uniform which means the seismic demand was distributed evenly among the stories. In other words, the Capstone Building does not have "weak-story".

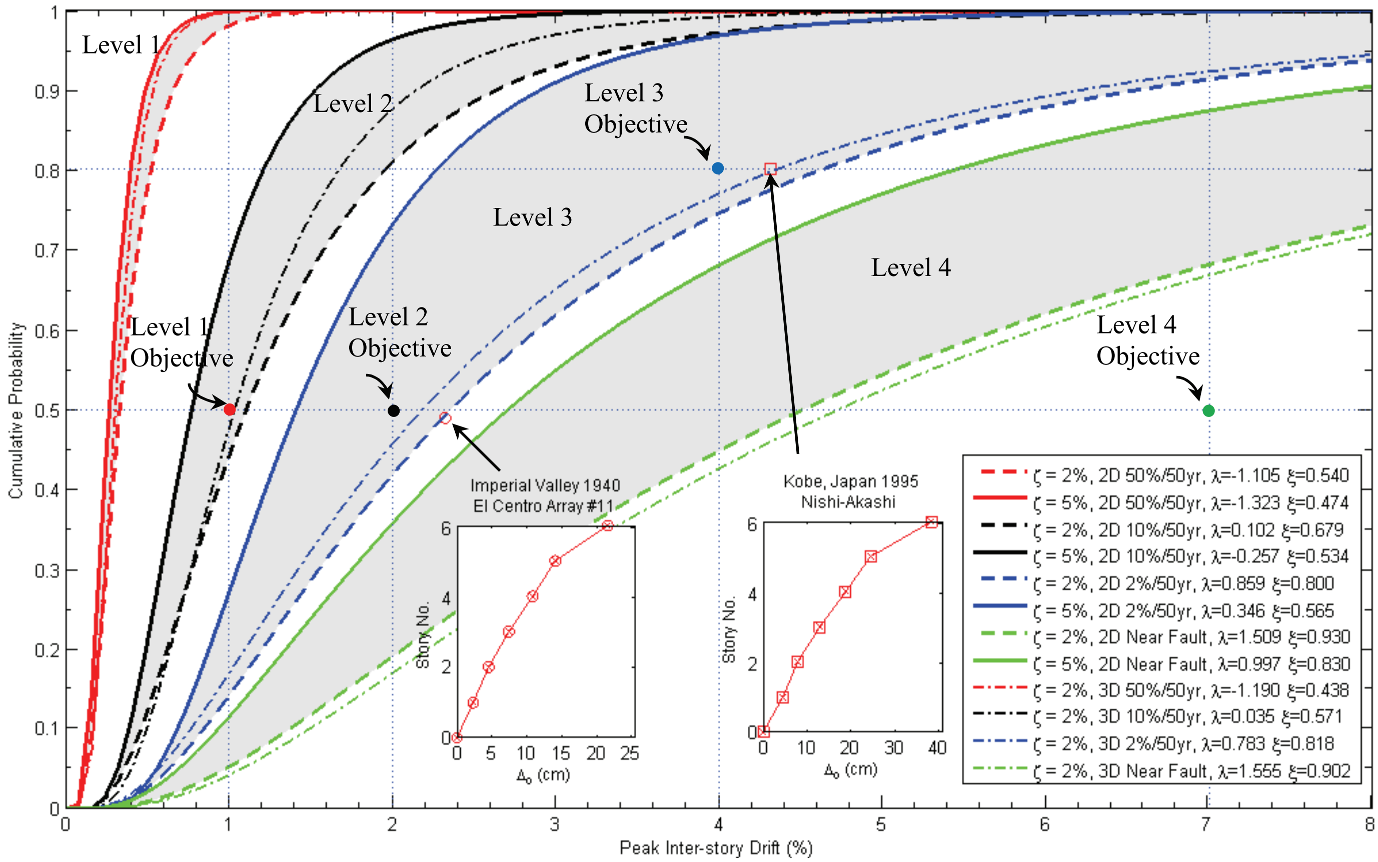

Figure 5-8: Peak inter-story drift distributions of the NEESWood Capstone Building.

Table 5-2: Summary of nonlinear time-history analyses of six-story NEESWood Capstone Building designed using DDD.

Performance Expectation				2D NLTHA (ζ=2%) Upper Bound			2D NLTHA (ζ=5%) Lower Bound			3D NLTHA (ζ=2%)		
Hazard Level	Ground Motion	θ_{lim} (%)	NE_t	θ @ NE_t (%)	P_{NE} @ θ_{lim}	Pass?	θ @ NE_t (%)	P_{NE} @ θ_{lim}	Pass?	θ @ NE_t (%)	P_{NE} @ θ_{lim}	Pass?
Level 1	50%/50yr	1	0.5	0.33	0.98	Yes	0.27	>0.99	Yes	0.30	>0.99	Yes
Level 2	10%/50yr	2	0.5	1.11	0.81	Yes	0.77	0.96	Yes	1.04	0.88	Yes
Level 3	2%/50yr	4	0.8	4.63	0.75	*Almost*	2.27	0.97	Yes	4.36	0.77	*Almost*
Level 4	Near-Fault	7	0.5	4.52	0.68	Yes	2.71	0.87	Yes	4.74	0.67	Yes

6. ATC-63 COLLAPSE MARGIN RATIO

In addition to considering the four NEESWood performance requirements, monotonic pushover and incremental dynamic analyses (IDA) (Vamvatsikos and Cornell 2002) were performed to evaluate the collapse margin ratio of the test building using the ATC-63 methodology (ATC 2008). The ATC-63 methodology was developed for evaluating the collapse risk of structures designed using the current code specified force-based procedures under Maximum Considered Earthquake (MCE) ground motions. An evaluation of the collapse margin ratio using the ATC-63 procedure provides additional perspective on collapse risk of the

Capstone Building designed using the DDD procedure. To compute the collapse capacity, IDA was performed using the ATC-63 far-field ground motions. The spectral intensity of the ground motion causing 50% of the analyses/cases to collapse is 2.57g and the unadjusted collapse margin ratio (CMR) is 2.57/1.50 = 1.71 (Figure 6-1). According to the ATC-63 methodology, the raw CMR must be adjusted for the spectral shape before the acceptance criterion can be determined.

The spectral shape factor (SSF) is a function of the seismic design category (SDC), ductility of the structure which is determined through the pushover curve and the upper limit of the code-defined fundamental period of the structure (ATC 2008). The Capstone Building is designed for SDC D_{max} (Southern California regions) and the code-defined period, determined per ASCE/SEI-07 Section 12.8.2, is 0.57 second. Figure 6-3 shows the monotonic pushover curve obtained by applying an inverted triangular lateral load parallel to the transverse direction (x-axis) of the test building. The maximum base shear in the transverse direction is 2734 kN (514.7 kips) and occurs at a roof drift ratio of 1.27% (roof height is 16.76 m). The seismic coefficient at the peak of the pushover curve, V/W is 0.849. The ultimate drift (1.54%) is defined at the point where the base shear deteriorates to 80% of the maximum value. An idealized elastic-plastic curve is determined by defining the initial stiffness using a secant-stiffness line that passes through the point where the base shear is at 60% of the maximum. From the elastic-plastic curve, the "yield" drift is 0.52% and the ductility factor, μ_c, is computed as 1.54/0.52 = 2.96. Using Table B-4 in the ATC-63 90% draft report, the SSF is 1.22 (ATC 2008). Therefore, the adjusted collapse margin ratio (ACMR), is computed as CMR×SSF = 2.09. While only the pushover response in the transverse direction is discussed herein, it should be noted that the pushover curve in the longitudinal direction is very similar to that in the transverse direction. This is because the inter-story backbone curves of the Capstone Building designed using the

DDD procedure are very similar in two horizontal directions (Figure 4-6). Therefore, the ACMR's are approximately the same in both directions (ACMR in the Y-direction is 2.07).

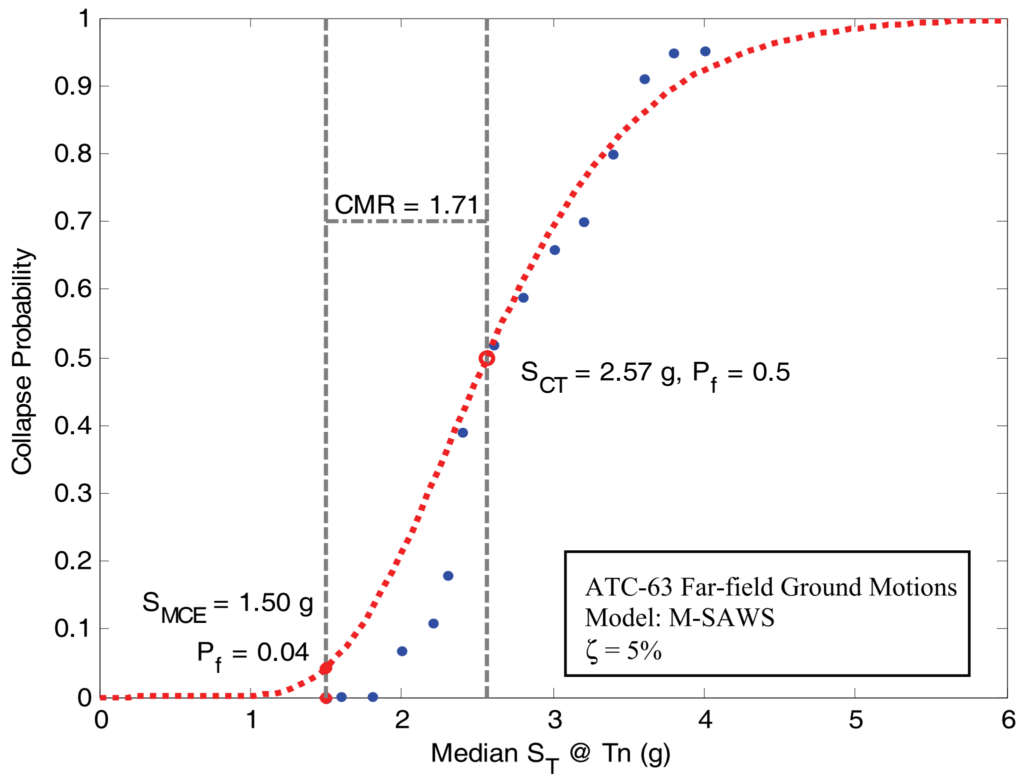

Figure 6-1: Collapse fragility curve of the NEESWood Capstone Building.

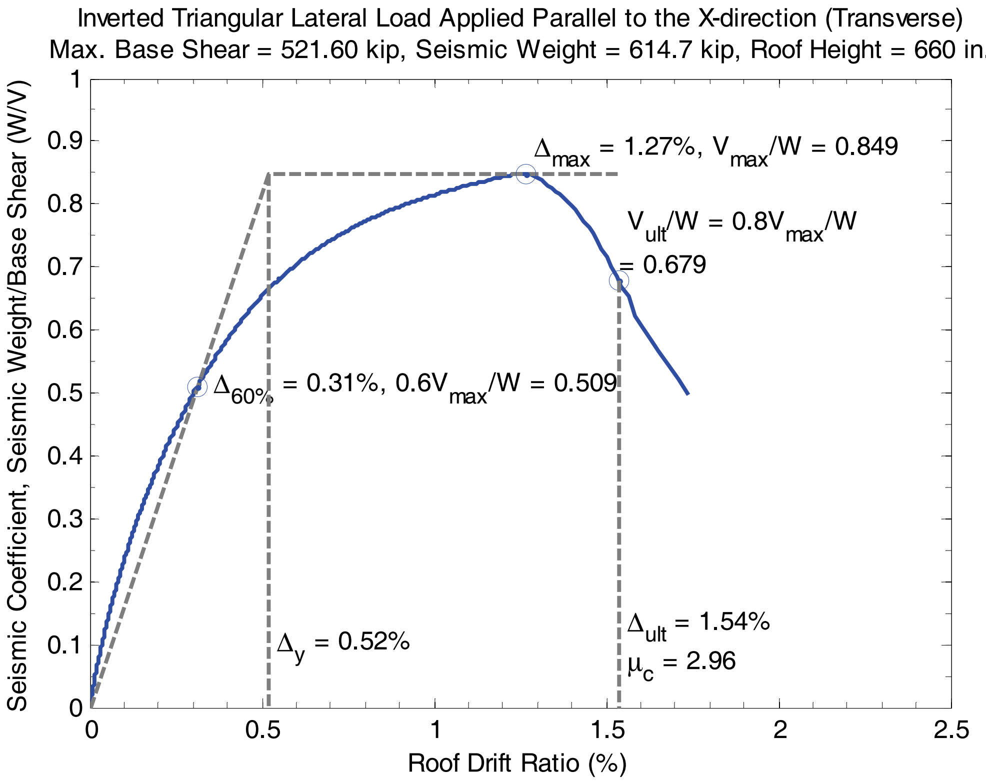

Figure 6-2: Monotonic Pushover curve (transverse, X-direction) of the NEESWood Capstone Building.

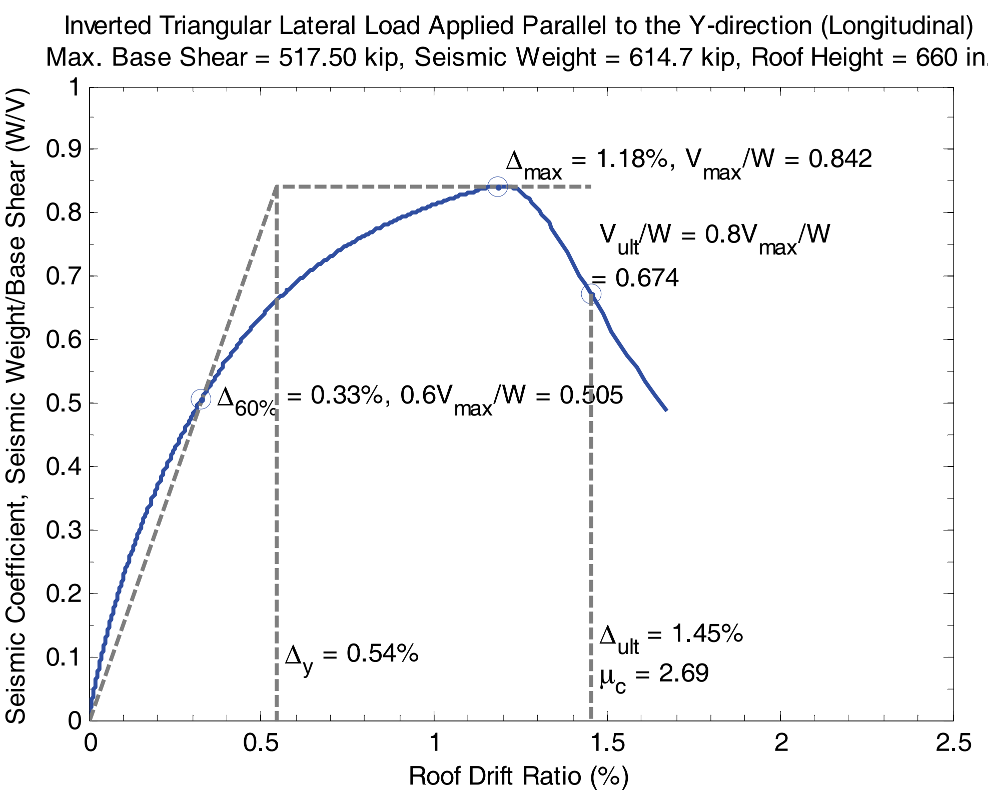

Figure 6-3: Monotonic Pushover curve (longitudinal, Y-direction) of the NEESWood Capstone Building.

The acceptable value for the ACMR of an individual system (i.e., < 20% collapse probability) depends on the uncertainties of the model and the design procedure. Using the same assumptions as the ATC-63 wood building design examples, the uncertainty in ground motion records is 0.40, design requirement uncertainty (B-Good) is 0.30, test data quality (B-Good) is 0.30, and modeling uncertainty (C-Fair) is 0.45. Thus the composite/total uncertainty, β_{TOT}, is 0.75 (Table 7-2c, ATC 2008). The Capstone Building satisfies the ATC-63 collapse margin requirement, since the ACMR of the Capstone Building (2.09) is higher than the acceptable ACMR for individual building with β_{TOT} of 0.75 is 1.88 (determined from Table 7-3, ATC 2008). Based on the adjusted collapse fragility curve, the collapse probability of the Capstone Building at MCE Level is approximately 16% (Figure 6-4).

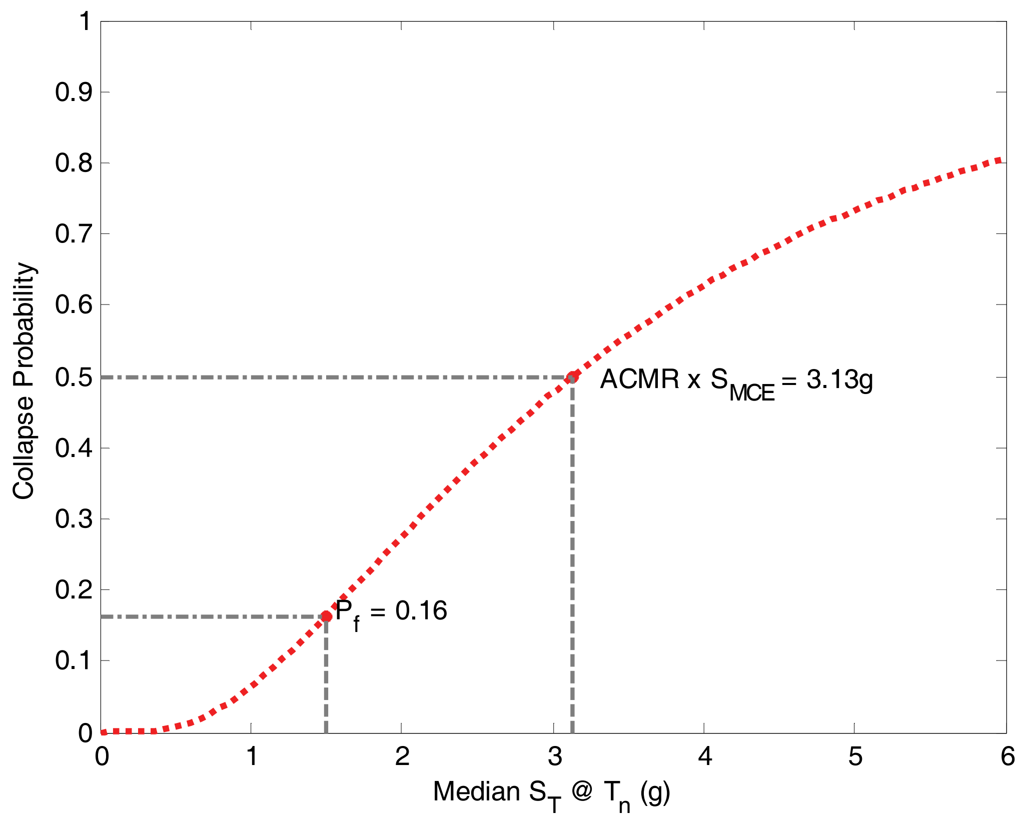

Figure 6-4: Adjusted collapse fragility curve of the 6-story NEESWood Capstone Building.

7. SUMMARY AND DISCUSSION

A simplified direct displacement design (DDD) procedure for performance-based design of multi-story wood buildings is presented. The design procedure can be used to consider drift limit non-exceedance probabilities other than 50%. The proposed design procedure is relatively simple and the shear wall design process can be performed using a spreadsheet. The simplified DDD procedure was used to design the shear walls of the six-story NEESWood Capstone Building. To validate the design procedure, two numerical models (2D and 3D models) were constructed and nonlinear time-history analyses (NLTHA) were performed using the ATC-63 far-field ground motions and a set of near-fault ground motions. The results of the NLTHA confirmed that the Capstone Building designed using the simplified DDD procedure satisfies all four design performance requirements. Additionally, the results of the NLTHA show that the seismic demand was distributed evenly among the stories (uniform drift profiles). Finally, the collapse margin ratio of the Capstone Building under MCE ground motions was determined to be acceptable per the ATC-63 methodology.

In the simplified DDD procedure, an adjustment factor C_{NE} was introduced to design for performance requirements associated with non-exceedance probabilities other than the median. While it is possible to determine C_{NE} for each specific building using the procedure outlined in this study, the current procedure for determining C_{NE} requires the engineers to be familiar with fragility analysis and the treatment of uncertainties at the outset. This may be viewed as a disadvantage of the procedure since most engineers do not have expertise in fragility analysis. One possible way to address this drawback is to pre-analyze a portfolio of buildings (e.g., the ATC-63 woodframe structure archetypes) and develop design charts or tables for determining C_{NE} for use in the simplified DDD procedure. Then, design charts can be created for selection of the adjustment factor considering different non-exceedance probabilities. This would provide a relatively simple procedure for direct displacement design of multi-story woodframe buildings in which the engineer is given flexibility in setting non-exceedance probabilities associated with the different performance requirements/drift limits.

8. REFERENCES

ASCE (2005). *Minimum Design Loads for Buildings and Other Structures* (ASCE/SEI 7-05), American Society of Civil Engineers, Reston, VA.

ASCE (2006). *Seismic Rehabilitation of Existing Buildings* (ASCE/SEI 41-06), American Society of Civil Engineers, Reston, VA.

ATC (2008). *Quantification of Building Seismic Performance Factors*, ATC-63 90%-draft Project Report, Applied Technology Council, Redwood City, CA.

Cheung C.K. (2008). "Multi-storey Timber and Mixed Timber-RC/Steel Construction in the USA," International Association for Bridge and Structural Engineering (IABSE), *Structural Engineering International*, 18(2): 122-125.

Christovasilis, I.P., Filiatrault, A., and Wanitkorkul, A. (2007). *Seismic Testing of a Full-Scale Two-Story Wood Light-frame Building: NEESWood Benchmark Test*, NEESWood Report NW-01, State University of New York at Buffalo, NY.

Coyne, T. (2007). "Framing-to-Sheathing Connection Testing in Support of NEESWood Capstone Test," Network of Earthquake Engineering Simulation Host Institution: State University of New York, Buffalo, NY.

Craig, S. (2008). *Expanding Market Demand for Canadian Wood Products*, Interim Report Phases 1 and 2, Canadian Wood Council, Ottawa, Ontario, Canada.

Gatto, K. and Uang Chia-Ming (2001). *Cyclic Response of Woodframe Shearwalls: Loading Protocol and Rate of Loading Effects*, CUREE Report W-13, Task 1.3.1, Consortium of Universities for Research in Earthquake Engineering, Richmond, CA.

Christovasilis, I.P., Filiatrault, A., Constantinou, M.C., and Wanitkorkul, A. (2009). "Incremental Dynamic Analysis of Woodframe Buildings," Earthquake Engineering and Structural Dynamics, 38(4):477-496.

ICBO (1988). *Uniform Building Code*, International Conference of Building Officials, Whittier, CA.

ICC (2006). *International Building Code*, Building Officials and Code, International Code Council, Country Club Hills, IL.

Martin, Z.A. and Skaggs, T.D. (2003). *Shear Wall Lumber Framing: Double 2x's vs. Single 3x's at Adjoining Panel Edges*, APA Report T2003-22, The Engineer Wood Association, Tacoma, WA.

Martin, Z.A. (2004). *Wood Structural Panel Lateral and Shear Wall Connections with Common, Galvanized Box, and Box Nails*, APA Report T2004-14, The Engineer Wood Association, Tacoma, WA.

Filiatrault, A., and Folz, B. (2002). "Performance-based seismic design of wood framed buildings," *ASCE Journal of Structural Engineering*, 128(1): 39-47.

Filiatrault, A., Isoda, H., and Folz, B. (2003). "Hysteretic Damping of Wood Framed Building," Engineering Structures, 25(4): 461-471.

Folz, B., and Filiatrault, A. (2001a). "Cyclic analysis of wood shear walls," *ASCE J. Struct. Eng.*, 127(4): 433-441.

Folz, B., and Filiatrault, A. (2001b). *A Computer Program for Seismic Analysis of Woodframe Structures*, CUREE Report W-21, Task 1.5.1, Consortium of Universities for Research in Earthquake Engineering, Richmond, CA.

Krawinkler, H., Zareian, F., Ibarra, L., Medina, R., and Lee, S. (2003). *Seismic Demands for Single- and Multi-story Woodframe Buildings*, CUREE Report W-26, Consortium of Universities for Research in Earthquake Engineering, Richmond, C.A.

McMullin, K.M. and Merrick, D. (2001). "Seismic Performance of Gypsum Walls – Experimental Test Program," CUREE Report W-15, Consortium of Universities for Research in Earthquake Engineering, Richmond, C.A.

Pang, W.C., and Rosowsky, D.V. (2009). "Direct Displacement Procedure for Performance-based Seismic Design of Mid-rise Woodframe Structures," *Earthquake Spectra*, accepted for publication**.**

Pardoen, G., Waltman, A., Kazanjy, R., Freund, E., and Hamilton, C. (2003) *Testing and Analysis of One-story and Two-Story Shear Walls Under Cyclic Loading*, CUREE Report W-25, Task 1.4.4, Consortium of Universities for Research in Earthquake Engineering, Richmond, CA.

Pei, S. and van de Lindt, J.W. (2009). "Coupled Shear-bending Formulation for Seismic Analysis of Stacked Wood Shear Wall Systems," *J. of Earthquake Engineering and Structural Dynamics* (in press).

Shama, A.A. and Mander, J.B. (2003). "The Seismic Performance of Braced Timber Pile Bents," *Earthquake Engineering and Structural Dynamic*, 32(3):463-482.

Stewart, W.G. (1987). "The Seismic Design of Plywood Sheathed Shearwall," PhD Thesis, University of Canterbury, Christchurch, New Zealand.

van de Lindt, J.W., Rosowsky, D.V., Filiatrault, A., Symans, M., and Davidson, R. (2006). "Development of a Performance-Based Seismic Design Philosophy for Mid-Rise Woodframe Construction: Progress on the NEESWood Project," *9th World Conference on Timber Engineering*, Portland, OR.

Vamvatsikos, D. and Cornell, A.C. (2002). "The Incremental Dynamic Analysis and Its Application to Performance-based Earthquake Engineering," *12th European Conference on Earthquake Engineering*, London, U.K.

Varoglu, E., Karacabeyli, E., Stiemer, S., Ni, C., Buitelaar, M., and Lungu, D. (2007). "Midply Wood Shear Wall System: Performance in Dynamic Testing," *ASCE Journal of Structural Engineering* 133(7):1035-1042.

White, T. and Ventura, C. (2006). *Seismic Performance of Wood-frame Residential Construction in British Columbia*, EERF Report 06-03, Canada Mortgage and Housing Corporation, Ontario, Canada.

Appendix A

Seismic Hazard for Southern California

Seismic Hazard for Southern California:

- Seismic Design Category D
- Site Class D (stiff soil)
- Spectral values determined following the requirements of ASCE/SEI 7-05 and ASCE/SEI 41-06

Table A-1: Design spectral acceleration parameters for 5% damping.

Hazard Level	Intensity (% of DBE)	Exceedance Probability	Spectral Acceleration Short-period S_{XS}[a] (g)	Spectral Acceleration 1-second S_{X1}[a] (g)	T_0[b] (s)	T_S[c] (s)
Short Return Period Earthquake	44%	50%/50yr	0.44	0.26	0.12	0.59
Design Basis Earthquake (DBE)	100%	10%/50yr	1.00	0.60	0.12	0.60
Maximum Credible Earthquake (MCE)	150%	2%/50yr	1.50	0.90	0.12	0.60

[a] X = M = Maximum Credible Earthquake
D = Design Basis Earthquake
S = Short Return Period Earthquake
[b] $T_0 = 0.2\ S_{XS}/S_{X1}$
[c] $T_S = S_{XS}/S_{X1}$

Mapped values for short and one-second spectral acceleration:
$S_s = 1.5$ g [representative mapped values for Southern California]
$S_1 = 0.6$ g

Site Coefficients:
$F_a = 1.0$ [F_a from ASCE/SEI 7-05, Table 11.4-1]
$F_v = 1.5$ [F_v from ASCE/SEI 7-05, Table 11.4-2]

Maximum Credible Earthquake (MCE) [ASCE/SEI 7-05, Section 11.4]
$S_{MS} = S_s \times F_a = 1.5 \times 1.0 = 1.5$
$S_{M1} = S_1 \times F_v = 0.6 \times 1.5 = 0.9$

Design Basis Earthquake (DBE) [ASCE/SEI 7-05, Section 11.4.4]
$S_{DS} = 2/3 \times S_{MS} = 2/3 \times 1.5 = 1.0$
$S_{D1} = 2/3 \times S_{M1} = 2/3 \times 0.9 = 0.6$

Short Return Period Earthquake (SRE) [ASCE/SEI 41-06, Section 1.6.1.3.2]
10%/50yr spectral value (i.e., S_{DS}) < 1.5 g, use Equation 1-3:

$$S_{50\%/50yr} = S_{10\%/50yr}\left(\frac{P_R}{475}\right)^n$$

where P_R is the mean return period
$n = 0.44$ for California [ASCE/SEI 41-06, Table 1-2]

$$S_{SS} = S_{DS}\left(\frac{72}{475}\right)^{0.44} = 0.44 \text{ g}$$

$$S_{S1} = S_{D1}\left(\frac{72}{475}\right)^{0.44} = 0.26 \text{ g}$$

Appendix B

Displacement-based Shear Wall Design Database

Table B-1: Displacement-based shear wall design table for unit wall width (per ft) in US customary units.

Wall Height (ft)	Wall Type/ Sheathing Layer	Edge Nail Spacing (in)	K_o (kip/in per ft)	F_u (kip per ft)	Backbone Force at Different Drift Levels (kip per ft)					Secant Stiffness, K_s (kip/in per ft)					K_s/K_o				
					Wall Drift					Wall Drift					Wall Drift				
					0.5%	1.0%	2.0%	3.0%	4.0%	0.5%	1.0%	2.0%	3.0%	4.0%	0.5%	1.0%	2.0%	3.0%	4.0%
9	Standard[(a)]	2	3.95	2.17	1.33	1.83	2.17	1.87	1.57	2.464	1.693	1.003	0.579	0.364	0.62	0.43	0.25	0.15	0.09
		3	3.24	1.46	0.99	1.29	1.45	1.24	1.02	1.829	1.190	0.673	0.382	0.236	0.56	0.37	0.21	0.12	0.07
		4	2.76	1.12	0.79	1.00	1.11	0.94	0.77	1.457	0.922	0.512	0.289	0.178	0.53	0.33	0.19	0.10	0.06
		6	1.98	0.77	0.56	0.69	0.75	0.65	0.54	1.030	0.643	0.349	0.200	0.125	0.52	0.32	0.18	0.10	0.06
	Midply[(b)]	2	5.03	4.22	2.04	3.18	4.22	3.64	3.06	3.784	2.943	1.952	1.123	0.708	0.75	0.59	0.39	0.22	0.14
		3	4.38	2.86	1.63	2.38	2.81	2.43	2.06	3.024	2.205	1.299	0.751	0.477	0.69	0.50	0.30	0.17	0.11
		4	3.84	2.18	1.35	1.90	2.11	1.83	1.56	2.508	1.757	0.977	0.566	0.361	0.65	0.46	0.25	0.15	0.09
		6	3.16	1.49	1.02	1.35	1.43	1.25	1.07	1.885	1.249	0.664	0.386	0.248	0.60	0.40	0.21	0.12	0.08
	GWB[(c)]	16	1.29	0.14	0.13	0.13	0.09	0.06	0.03	0.247	0.118	0.043	0.019	0.006	0.19	0.09	0.03	0.01	0.00
8	Standard[(a)]	2	4.23	2.21	1.31	1.84	2.20	1.93	1.63	2.733	1.914	1.144	0.669	0.425	0.65	0.45	0.27	0.16	0.10
		3	3.79	1.50	1.01	1.31	1.50	1.28	1.06	2.113	1.368	0.780	0.445	0.277	0.56	0.36	0.21	0.12	0.07
		4	3.03	1.15	0.80	1.02	1.14	0.97	0.81	1.662	1.064	0.592	0.337	0.210	0.55	0.35	0.20	0.11	0.07
		6	2.36	0.78	0.57	0.71	0.77	0.66	0.55	1.191	0.735	0.402	0.230	0.143	0.50	0.31	0.17	0.10	0.06
	Midply[(b)]	2	5.17	4.35	1.94	3.11	4.30	3.82	3.26	4.037	3.236	2.237	1.328	0.848	0.78	0.63	0.43	0.26	0.16
		3	4.58	2.92	1.57	2.35	2.87	2.51	2.14	3.275	2.450	1.497	0.870	0.557	0.71	0.53	0.33	0.19	0.12
		4	4.17	2.21	1.33	1.89	2.16	1.89	1.62	2.772	1.967	1.124	0.655	0.421	0.66	0.47	0.27	0.16	0.10
		6	3.46	1.52	1.01	1.36	1.47	1.29	1.11	2.112	1.418	0.763	0.446	0.288	0.61	0.41	0.22	0.13	0.08
	GWB[(c)]	16	2.14	0.14	0.14	0.13	0.09	0.05	0.01	0.291	0.134	0.047	0.017	0.003	0.14	0.06	0.02	0.01	0.00

(a) Standard wall model is built with 15/32 in. thick OSB connected to framing members by 10d common nails (0.148 in. diameter) in single-shear.

(b) Midply wall model is built with 15/32 in. \thick OSB connected to framing members by 10d common nails (0.148 in. diameter) in double-shear

(c) Gypsum wall board model is built with 1/2 in. thick GWB connected to framing members by #6 bugle head drywall screws (0.142 in. diameter) in single-shear.

Table B-2: Displacement-based shear wall design table for unit wall width (per m) in SI units.

Wall Height (m)	Wall Type/ Sheathing Layer	Edge Nail Spacing (mm)	K_o (kN/mm per m)	F_u (kN per m)	Backbone Force at Different Drift Levels (kN per m)					Secant Stiffness, K_s (kN/mm per m)					K_s/K_o				
					Wall Drift					Wall Drift					Wall Drift				
					0.5%	1.0%	2.0%	3.0%	4.0%	0.5%	1.0%	2.0%	3.0%	4.0%	0.5%	1.0%	2.0%	3.0%	4.0%
2.74	Standard[a]	51	2.269	31.679	19.418	26.685	31.604	27.357	22.921	1.416	0.973	0.576	0.332	0.209	0.62	0.43	0.25	0.15	0.09
		76	1.861	21.371	14.415	18.754	21.217	18.048	14.879	1.051	0.684	0.387	0.219	0.136	0.56	0.37	0.21	0.12	0.07
		102	1.586	16.397	11.485	14.527	16.131	13.686	11.241	0.837	0.530	0.294	0.166	0.102	0.53	0.33	0.19	0.10	0.06
		152	1.138	11.196	8.116	10.128	11.014	9.441	7.869	0.592	0.369	0.201	0.115	0.072	0.52	0.32	0.18	0.10	0.06
	Midply[b]	51	2.890	61.530	29.818	46.392	61.518	53.089	44.661	2.174	1.691	1.121	0.645	0.407	0.75	0.59	0.39	0.22	0.14
		76	2.514	41.806	23.832	34.746	40.945	35.497	30.049	1.737	1.267	0.746	0.431	0.274	0.69	0.50	0.30	0.17	0.11
		102	2.208	31.833	19.763	27.689	30.791	26.770	22.750	1.441	1.009	0.561	0.325	0.207	0.65	0.46	0.25	0.15	0.09
		152	1.813	21.699	14.855	19.691	20.930	18.267	15.605	1.083	0.718	0.381	0.222	0.142	0.60	0.40	0.21	0.12	0.08
	GWB[c]	406	0.744	2.026	1.947	1.852	1.366	0.879	0.392	0.142	0.068	0.025	0.011	0.004	0.19	0.09	0.03	0.01	0.00
2.44	Standard[a]	51	2.432	32.204	19.146	26.818	32.051	28.130	23.823	1.570	1.100	0.657	0.385	0.244	0.65	0.45	0.27	0.16	0.10
		76	2.176	21.941	14.798	19.169	21.869	18.696	15.523	1.214	0.786	0.448	0.256	0.159	0.56	0.36	0.21	0.12	0.07
		102	1.740	16.753	11.642	14.910	16.578	14.182	11.786	0.955	0.611	0.340	0.194	0.121	0.55	0.35	0.20	0.11	0.07
		152	1.356	11.406	8.345	10.299	11.273	9.652	8.032	0.684	0.422	0.231	0.132	0.082	0.50	0.31	0.17	0.10	0.06
	Midply[b]	51	2.971	63.471	28.277	45.330	62.693	55.795	47.521	2.319	1.859	1.286	0.763	0.487	0.78	0.63	0.43	0.26	0.16
		76	2.633	42.671	22.943	34.326	41.949	36.578	31.208	1.882	1.408	0.860	0.500	0.320	0.71	0.53	0.33	0.19	0.12
		102	2.396	32.263	19.417	27.559	31.500	27.536	23.571	1.593	1.130	0.646	0.376	0.242	0.66	0.47	0.27	0.16	0.10
		152	1.988	22.113	14.794	19.871	21.381	18.761	16.142	1.213	0.815	0.438	0.256	0.165	0.61	0.41	0.22	0.13	0.08
	GWB[c]	406	1.231	2.113	2.036	1.879	1.305	0.731	0.157	0.167	0.077	0.027	0.010	0.002	0.14	0.06	0.02	0.01	0.00

(a) Standard wall model is built with 11.9 mm thick OSB connected to framing members by 10d common nails (3.76 mm diameter) in single-shear.

(b) Midply wall model is built with 11.9 mm thick OSB connected to framing members by 10d common nails (3.76mm diameter) in double-shear

(c) Gypsum wall board model is built with 12.7 mm thick GWB connected to framing members by #6 bugle head drywall screws (3.61 mm diameter) in single-shear.

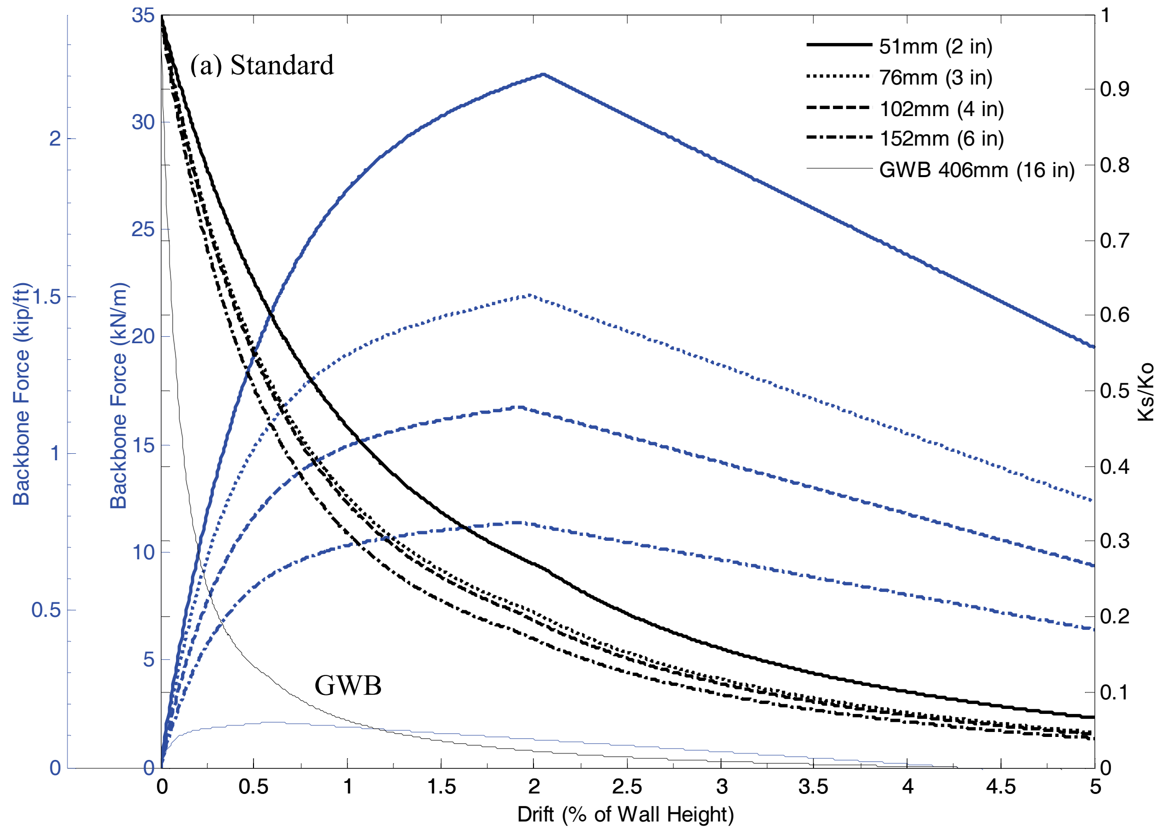

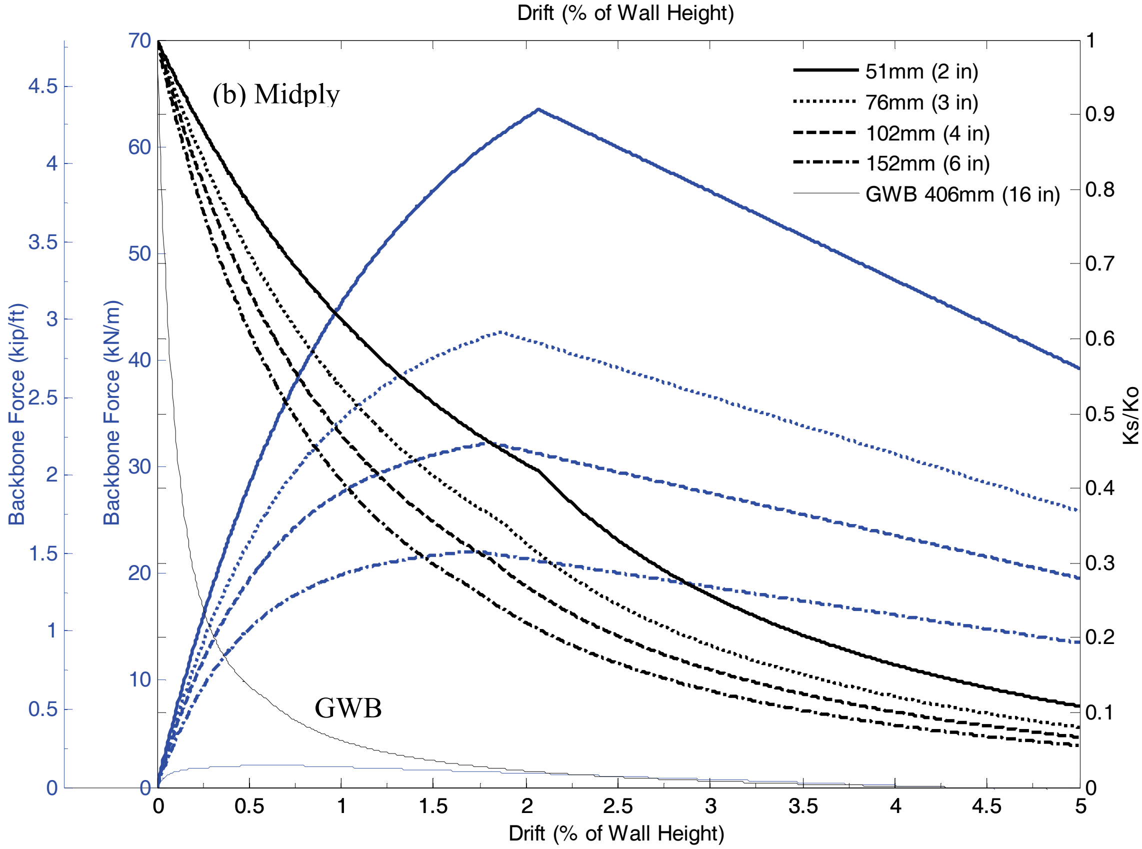

Figure B-1: Shear wall backbone and k_s/k_o curves for 2.44 m (8 ft) tall (a) standard and (b) Midply walls built with 10d common nails and 11.9 mm (15/32 in.) OSB.

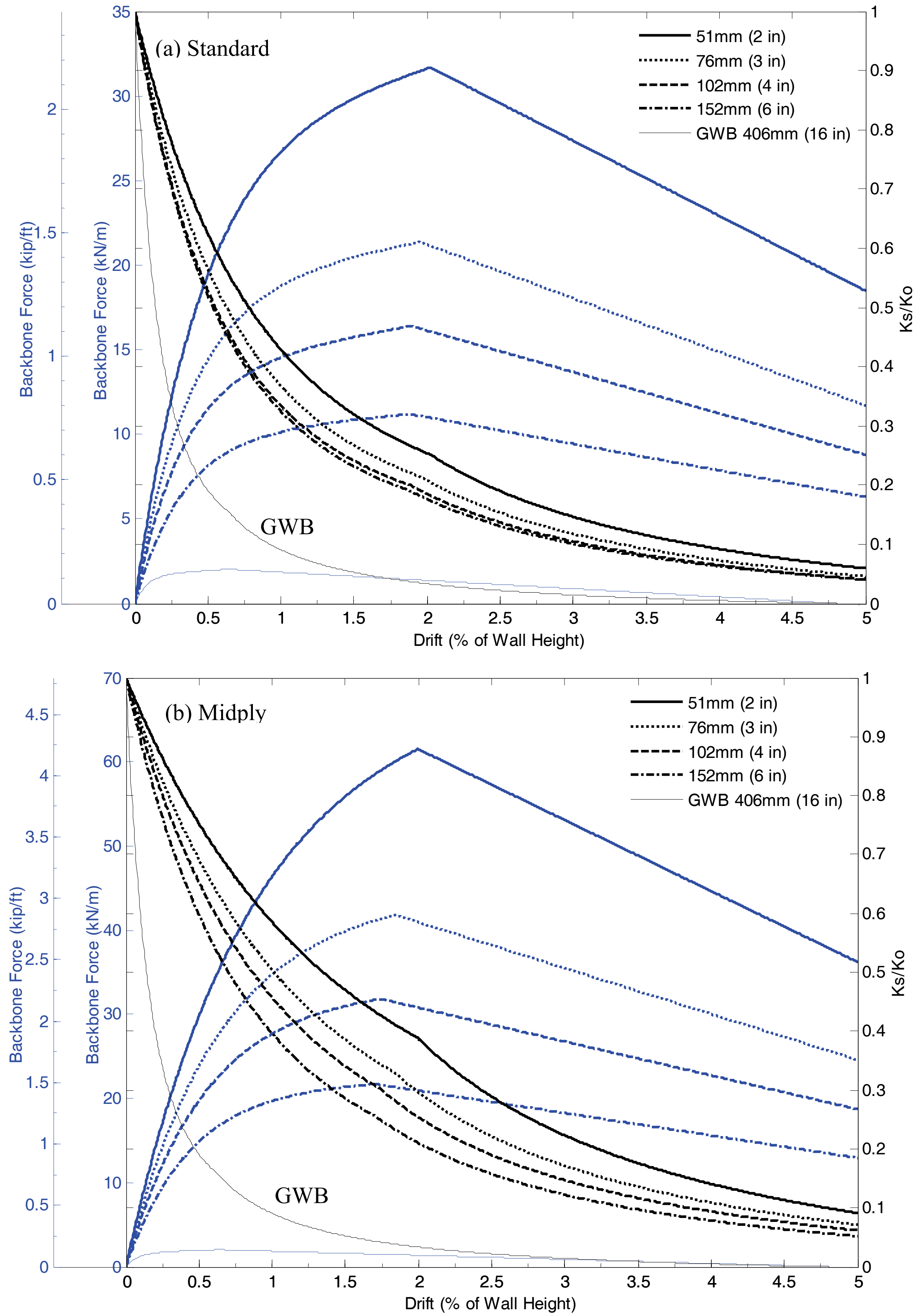

Figure B-2: Shear wall backbone and k_s/k_o curves for 2.74 m (9 ft) tall (a) standard and (b) Midply walls built with 10d common nails and 11.9 mm (15/32 in.) OSB.

Appendix C

Direct Displacement Design Calculations

Table C-1: Determination of DDD base shear coefficient for design Level 1.

Six-story Woodframe NEESWood Capstone Building

Design for Level 1 Seismic Hazard (50%/50yr) and 1% Inter-story Drift Limit (θ_{target}) with 50% Non-exceedance Probability (P_{NE})

Gravitational Constant	g =	386.1	in/s^2	9.807 m/s^2		Date: May-18-2009	W.Pang
Target Drift Limit	θ_{target} =	1	%			Revision: 12	
Target NE Probability	P_{NE} =	0.5			ATC-63 (2008)		
Total Uncertainty	β_R =	0.75	<=		Model, Fair, C		
NE Adjustment Factor	C_{NE} = LogInv(P_{NE},0,β_R) =	1.00			Test Data, Good, B		
Equivalent 50% NE Drift Limit	$\theta_{eq50} = \theta_{target}/C_{NE}$ =	1.00	%		Design Requirement, Good, B		

Parameters for Design Response Spectrum		Damping Coefficient			Dimensions of Diaphragms		
S_1 = 0.26 g	T_0 = 0.12 s	K_s/K_o =	0.75		Floor Width =	39.83 ft	12.15 m
S_S = 0.44 g	T_S = 0.59 s	ζ_{vis} =	0.05		Floor Length =	59.5 ft	18.15 m
	T_L = 8 s	ζ_{hyst} =	0.11		Floor Area (A_F)=	2370.08 ft^2	220.48 m^2
		ζ_{eff} =	0.16				
		B_ζ =	1.43	<= ASCE-41 Section 1.6.1.5			

C_{c1} =		0.071				C_c = min. of C_{c1} and C_{cs}
C_{cS} =		0.309				
C_c =		0.071				
W_{eff} =	$\frac{(\Sigma W^*\Delta_o)^2}{\Sigma(W^*\Delta_o^2)}$ =	500.5	kip	2226	kN	<= See Tables C-2 & C-3
$W_{eff}/\Sigma W$ =		0.81				
h_{eff} =	$\Sigma(Cv^*h_o)$ =	38.11	ft	11.62	m	
h_{eff}/h_t =		0.69				
θ_{eff} =		1.00%				
V_b =	$C_c^*W_{eff}$ =	35.57	kip	158.2	kN	
K_{eff} =	V_b/Δ_{eff} =	7.78	kip/in	1.36	kN/mm	<= Δ_{eff} See Tables C-2 & C-3
T_{eff} =		2.57	s			
K_o =	$K_{eff}^*(Ks/Ko)$ =	10.37	kip/in	1.82	kN/mm	
T_o =	2π/sqrt(g*Ko/W_{eff})=	2.221	s			
$V_b/\Sigma W$ =	$C_c^*W_{eff}/\Sigma W$ =	0.058				
M_o @ base =	$h_{eff}^*F_t$ =	1355.8	kip-ft	1838	kN*m	<= F_t See Tables C-2 & C-3

Table C-2: Summary of simplified DDD calculations for Performance Level 1 in US customary units.

Story	h_s (ft)	h_o (ft)	θ_{it} (%)	W (kip)	Δ_{it} (in)	Δ_o (in)	$W^*\Delta_o$ (kip-in)	C_v	β_v	$C_v^*h_o$ (ft)	$W^*\Delta_o^2$ (kip-in^2)	V_s (kip)	K_s (kip/in)	F (kip)	F^*h_o (kip-ft)	$\beta_{\Delta it}$	β_k	k_o[a] (kip/in)	V_s/A_F (lbs/ft^2)	F/W	Mass (kip-s^2/in)
1	10	10	1.00	112.85	1.20	1.20	135.4	0.059	1.000	0.59	163	35.57	29.64	2.10	21.04	1.00	1.000	39.53	15.0	0.019	0.2923
2	9	19	1.00	106.55	1.08	2.28	242.9	0.106	0.941	2.02	554	33.47	30.99	3.78	71.73	0.90	1.045	41.32	14.1	0.035	0.2760
3	9	28	1.00	106.55	1.08	3.36	358.0	0.156	0.835	4.38	1203	29.69	27.49	5.56	155.78	0.90	0.927	36.66	12.5	0.052	0.2760
4	9	37	1.00	106.55	1.08	4.44	473.1	0.207	0.678	7.65	2101	24.13	22.34	7.35	272.01	0.90	0.754	29.79	10.2	0.069	0.2760
5	9	46	1.00	113.49	1.08	5.52	626.5	0.274	0.472	12.59	3458	16.78	15.54	9.74	447.81	0.90	0.524	20.71	7.1	0.086	0.2939
6	9	55	1.00	68.678	1.08	6.60	453.3	0.198	0.198	10.89	2992	7.04	6.52	7.04	387.41	0.90	0.220	8.70	3.0	0.103	0.1779
Σ				614.7	Δ_{eff} =	4.57	2289.2	1.000		38.11	10469		F_t=	35.57	1355.78						

Δ_{max} = 14.26 in <= deflection @ long period limit, T_L

Table C-3: Summary of simplified DDD calculations for Performance Level 1 in SI units.

Story	h_s (m)	h_o (m)	δ_{ad} (%)	W (kN)	Δ_{it} (mm)	Δ_o (mm)	$W^*\Delta_o$ (kN-mm)	C_v	β_v	$C_v^*h_o$ (m)	$W^*\Delta_o^2$ x10^3 (kN-mm^2)	V_s (kN)	K_s (kN/mm)	F (kN)	F^*h_o (kN-m)	$\beta_{\Delta it}$	β_k	k_o[a] (kN/mm)	V_s/A_F (kN/m^2)	F/W	Mass (kg)
1	3.05	3.05	1.00	502	30	30	15300	0.059	1.000	0.18	466	158	5.19	9	28.5	1.00	1.000	6.92	0.718	0.019	51183
2	2.74	5.79	1.00	474	27	58	27447	0.106	0.941	0.61	1589	149	5.43	17	97.2	0.90	1.045	7.24	0.675	0.035	48327
3	2.74	8.53	1.00	474	27	85	40448	0.156	0.835	1.33	3452	132	4.81	25	211.2	0.90	0.927	6.42	0.599	0.052	48327
4	2.74	11.28	1.00	474	27	113	53449	0.207	0.678	2.33	6028	107	3.91	33	368.8	0.90	0.754	5.22	0.487	0.069	48327
5	2.74	14.02	1.00	505	27	140	70777	0.274	0.472	3.84	9923	75	2.72	43	607.1	0.90	0.524	3.63	0.339	0.086	51473
6	2.74	16.76	1.00	305	27	168	51211	0.198	0.198	3.32	8585	31	1.14	31	525.2	0.90	0.220	1.52	0.142	0.103	31149
Σ				2734	Δ_{eff} =	116	258631	1.000	h_{eff} =	11.62	30044			158	1838.1						

Δ_{max} = 362 mm <= deflection @ long period limit, T_L

[a] k_o = Ks x (Ks/Ko) ratio

Table C-4: Determination of DDD base shear coefficient for design Level 2.

Six-story Woodframe NEESWood Capstone Building

Design for Level 2 Seismic Hazard (10%/50yr) and 2% Inter-story Drift Limit (θ_{target}) with 50% Non-exceedance Probability (P_{NE})

Gravitational Constant	g =	386.1	in/s^2	9.807 m/s^2	Date: May-18-2009	W.Pang
Target Drift Limit	θ_{target} =	$\boxed{2}$	%		Revision: 12	
Target NE Probability	P_{NE} =	$\boxed{0.5}$		ATC-63 (2008)		
Total Uncertainty	β_R =	$\boxed{0.75}$	<=	Model, Fair, C		
NE Adjustment Factor	C_{NE} = LogInv(P_{NE},0,β_R) =	1.00		Test Data, Good, B		
Equivalent 50% NE Drift Limit	$\theta_{eq50} = \theta_{target}/C_{NE}$ =	2.00	%	Design Requirement, Good, B		

Parameters for Design Response Spectrum		Damping Coefficient		Dimensions of Diaphragms		
S_1 = $\boxed{0.60}$ g	T_0 = 0.12 s	K_s/K_o =	$\boxed{0.50}$	Floor Width =	39.83 ft	12.15 m
S_S = $\boxed{1.00}$ g	T_S = 0.60 s	ξ_{vis} =	$\boxed{0.05}$	Floor Length =	59.5 ft	18.15 m
	T_L = 8 s	ξ_{hyst} =	0.16	Floor Area (A_F)=	2370.08 ft^2	220.48 m^2
		ξ_{eff} =	0.21			
		B_1 =	1.57 <= ASCE-41 Section 1.6.1.5			

C_{c1} =		0.157				C_c = min. of C_{c1} and C_{cs}
C_{cS} =		0.638				
C_c =		0.157				
W_{eff} =	$\frac{(\Sigma W^*\Delta_o)^2}{\Sigma(W^*\Delta_o^2)}$ =	500.5	kip	2226	kN	<= See Tables B.1 & B.2
$W_{eff}/\Sigma W$ =		0.81				
h_{eff} =	$\Sigma(Cv^*h_o)$ =	38.11	ft	11.62	m	
h_{eff}/h_t =		0.69				
θ_{eff} =		2.00%				
V_b =	$C_c^*W_{eff}$ =	$\boxed{78.49}$	kip	349.1	kN	
K_{eff} =	V_b/Δ_{eff} =	8.58	kip/in	1.50	kN/mm	<= Δ_{eff} See Tables B.1 & B.2
T_{eff} =		2.44	s			
K_o =	K_{eff}*(Ks/Ko) =	17.16	kip/in	3.01	kN/mm	
T_o =	2π/sqrt(g*Ko/W_{eff})=	1.727	s			
$V_b/\Sigma W$ =	$C_c^*W_{eff}/\Sigma W$ =	0.128				
M_o @ base =	$h_{eff}^*F_t$ =	2991.3	kip-ft	4056	kN*m	<= F_t See Tables B.1 & B.2

Table C-5: Summary of simplified DDD calculations for Performance Level 2 in US customary units.

Story	h_s (ft)	h_o (ft)	θ_{it} (%)	W (kip)	Δ_{it} (in)	Δ_o (in)	$W^*\Delta_o$ (kip-in)	C_v	β_v	$C_v^*h_o$ (ft)	$W^*\Delta_o^2$ (kip-in^2)	V_s (kip)	K_s (kip/in)	F (kip)	F^*h_o (kip-ft)	$\beta_{\Delta it}$	β_k	k_o[a] (kip/in)	V_s/A_F (lbs/ft^2)	F/W	Mass (kip-s^2/in)
1	10	10	2.00	112.85	2.40	2.40	270.8	0.059	1.000	0.59	650	78.49	32.70	4.64	46.43	1.00	1.000	65.41	33.1	0.041	0.2923
2	9	19	2.00	106.55	2.16	4.56	485.9	0.106	0.941	2.02	2216	73.84	34.19	8.33	158.26	0.90	1.045	68.37	31.2	0.078	0.2760
3	9	28	2.00	106.55	2.16	6.72	716.0	0.156	0.835	4.38	4812	65.52	30.33	12.27	343.70	0.90	0.927	60.66	27.6	0.115	0.2760
4	9	37	2.00	106.55	2.16	8.88	946.2	0.207	0.678	7.65	8402	53.24	24.65	16.22	600.15	0.90	0.754	49.30	22.5	0.152	0.2760
5	9	46	2.00	113.49	2.16	11.04	1252.9	0.274	0.472	12.59	13832	37.02	17.14	21.48	988.03	0.90	0.524	34.28	15.6	0.189	0.2939
6	9	55	2.00	68.678	2.16	13.20	906.5	0.198	0.198	10.89	11966	15.54	7.19	15.54	854.76	0.90	0.220	14.39	6.6	0.226	0.1779
Σ				614.7	Δ_{eff} =	9.15	4578.4	1.000		38.11	41878		F_t=	78.49	2991.33						

Δ_{max} = 29.96 in <= deflection @ long period limit, T_L

Table C-6: Summary of simplified DDD calculations for Performance Level 2 in SI units.

Story	h_s (m)	h_o (m)	δ_{ad} (%)	W (kN)	Δ_{it} (mm)	Δ_o (mm)	$W^*\Delta_o$ (kN-mm)	C_v	β_v	$C_v^*h_o$ (m)	$W^*\Delta_o^2$ x10^3 (kN-mm^2)	V_s (kN)	K_s (kN/mm)	F (kN)	F^*h_o (kN-m)	$\beta_{\Delta it}$	β_k	k_o[a] (kN/mm)	V_s/A_F (kN/m^2)	F/W	Mass (kg)
1	3.05	3.05	2.00	502	61	61	30599	0.059	1.000	0.18	1865	349	5.73	21	62.9	1.00	1.000	11.45	1.583	0.041	51183
2	2.74	5.79	2.00	474	55	116	54893	0.106	0.941	0.61	6358	328	5.99	37	214.6	0.90	1.045	11.97	1.490	0.078	48327
3	2.74	8.53	2.00	474	55	171	80896	0.156	0.835	1.33	13808	291	5.31	55	466.0	0.90	0.927	10.62	1.322	0.115	48327
4	2.74	11.28	2.00	474	55	226	106898	0.207	0.678	2.33	24111	237	4.32	72	813.7	0.90	0.754	8.63	1.074	0.152	48327
5	2.74	14.02	2.00	505	55	280	141554	0.274	0.472	3.84	39694	165	3.00	96	1339.5	0.90	0.524	6.00	0.747	0.189	51473
6	2.74	16.76	2.00	305	55	335	102421	0.198	0.198	3.32	34340	69	1.26	69	1158.8	0.90	0.220	2.52	0.314	0.226	31149
Σ				2734	Δ_{eff} =	232	517261	1.000	h_{eff} =	11.62	120176			349	4055.5						

Δ_{max} = 761 mm <= deflection @ long period limit, T_L

[a] k_o = Ks x (Ks/Ko) ratio

Table C-7: Determination of DDD base shear coefficient for design Level 3.

Six-story Woodframe NEESWood Capstone Building

Design for Level 3 Seismic Hazard (2%/50yr) and 4% Inter-story Drift Limit (θ_{target}) with 80% Non-exceedance Probability (P_{NE})

Gravitational Constant	g =	386.1	in/s^2	9.807 m/s^2		Date: May-18-2009	W.Pang
Target Drift Limit	θ_{target} =	$\boxed{4}$	%			Revision: 12	
Target NE Probability	P_{NE} =	$\boxed{0.8}$			ATC-63 (2008)		
Total Uncertainty	β_R =	$\boxed{0.75}$	<=		Model, Fair, C		
NE Adjustment Factor	$C_{NE} = LogInv(P_{NE},0,\beta_R)$ =	1.88			Test Data, Good, B		
Equivalent 50% NE Drift Limit	$\theta_{eq50} = \theta_{target}/C_{NE}$ =	2.13	%		Design Requirement, Good, B		

Parameters for Design Response Spectrum		Damping Coefficient		Dimensions of Diaphragms		
S_1 = $\boxed{0.90}$ g	T_0 = 0.12 s	K_s/K_o =	$\boxed{0.30}$	Floor Width =	39.83 ft	12.15 m
S_S = $\boxed{1.50}$ g	T_S = 0.60 s	ξ_{vis} =	$\boxed{0.05}$	Floor Length =	59.5 ft	18.15 m
	T_L = 8 s	ξ_{hyst} =	0.21	Floor Area (A_F)=	2370.08 ft^2	220.48 m^2
		ξ_{eff} =	0.26			
		B_1 =	1.71 <= ASCE-41 Section 1.6.1.5			

C_{c1} =		0.981				C_c = min. of C_{c1} and C_{cs}
C_{cS} =		1.647				
C_c =		0.981				
W_{eff} =	$\frac{(\Sigma W^*\Delta_o)^2}{\Sigma(W^*\Delta_o^2)}$ =	500.5	kip	2226	kN	<= See Tables B.1 & B.2
$W_{eff}/\Sigma W$ =		0.81				
h_{eff} =	$\Sigma(Cv^*h_o)$ =	38.11	ft	11.62	m	
h_{eff}/h_t =		0.69				
θ_{eff} =		2.13%				
V_b =	$C_c{}^*W_{eff}$ =	$\boxed{491.13}$	kip	2185	kN	
K_{eff} =	V_b/Δ_{eff} =	50.47	kip/in	8.84	kN/mm	<= Δ_{eff} See Tables B.1 & B.2
T_{eff} =		1.01	s			
K_o =	$K_{eff}{}^*(Ks/Ko)$ =	168.23	kip/in	29.46	kN/mm	
T_o =	$2\pi/sqrt(g^*Ko/W_{eff})$=	0.552	s			
$V_b/\Sigma W$ =	$C_c{}^*W_{eff}/\Sigma W$ =	0.799				
M_o @ base =	$h_{eff}{}^*F_t$ =	18718.1	kip-ft	25378	kN*m	<= F_t See Tables B.1 & B.2

Table C-8: Summary of simplified DDD calculations for Performance Level 3 in US customary units.

Story	h_s (ft)	h_o (ft)	θ_{it} (%)	W (kip)	Δ_{it} (in)	Δ_o (in)	$W^*\Delta_o$ (kip-in)	C_v	β_v	$C_v^*h_o$ (ft)	$W^*\Delta_o^2$ (kip-in^2)	V_s (kip)	K_s (kip/in)	F (kip)	F^*h_o (kip-ft)	$\beta_{\Delta it}$	β_k	k_o[(a)] (kip/in)	V_s/A_F (lbs/ft^2)	F/W	Mass (kip-s^2/in)
1	10	10	2.13	112.85	2.55	2.55	288.1	0.059	1.000	0.59	736	491.13	192.35	29.05	290.53	1.00	1.00	641.17	207.2	0.257	0.292288
2	9	19	2.13	106.55	2.30	4.85	516.9	0.106	0.941	2.02	2508	462.08	201.08	52.12	990.29	0.90	1.05	670.26	195.0	0.489	0.275975
3	9	28	2.13	106.55	2.30	7.15	761.8	0.156	0.835	4.38	5446	409.96	178.40	76.81	2150.67	0.90	0.93	594.66	173.0	0.721	0.275975
4	9	37	2.13	106.55	2.30	9.45	1006.6	0.207	0.678	7.65	9510	333.15	144.97	101.50	3755.44	0.90	0.75	483.25	140.6	0.953	0.275975
5	9	46	2.13	113.49	2.30	11.75	1333.0	0.274	0.472	12.59	15656	231.65	100.81	134.40	6182.57	0.90	0.52	336.02	97.7	1.184	0.293945
6	9	55	2.13	68.678	2.30	14.04	964.5	0.198	0.198	10.89	13544	97.25	42.32	97.25	5348.63	0.90	0.22	141.06	41.0	1.416	0.177881
Σ				614.7	Δ_{eff} =	9.73	4870.9	1.000	h_{eff} =	38.11	47400		F_t=	491.13	18718.12						

Δ_{max} = 41.12 in <= deflection @ long period limit, T_L

Table C-9: Summary of simplified DDD calculations for Performance Level 3 in SI units.

Story	h_s (m)	h_o (m)	θ_{it} (%)	W (kN)	Δ_{it} (mm)	Δ_o (mm)	$W^*\Delta_o$ (kN-mm)	C_v	β_v	$C_v^*h_o$ (m)	$W^*\Delta_o^2$ x10^3 (kN-mm^2)	V_s (kN)	K_s (kN/mm)	F (kN)	F^*h_o (kN-m)	$\beta_{\Delta it}$	β_k	k_o[(a)] (kN/mm)	V_s/A_F (kN/m^2)	F/W	Mass (kg)
1	3.05	3.05	2.13	502	65	65	32554	0.059	1.000	0.18	2111	2185	33.68	129	393.9	1.00	1.00	112.28	9.908	0.257	51183
2	2.74	5.79	2.13	474	58	123	58401	0.106	0.941	0.61	7196	2055	35.21	232	1342.6	0.90	1.05	117.38	9.322	0.489	48327
3	2.74	8.53	2.13	474	58	182	86064	0.156	0.835	1.33	15629	1823	31.24	342	2915.8	0.90	0.93	104.14	8.271	0.721	48327
4	2.74	11.28	2.13	474	58	240	113727	0.207	0.678	2.33	27290	1482	25.39	451	5091.4	0.90	0.75	84.63	6.721	0.953	48327
5	2.74	14.02	2.13	505	58	298	150597	0.274	0.472	3.84	44928	1030	17.65	598	8382.0	0.90	0.52	58.84	4.673	1.184	51473
6	2.74	16.76	2.13	305	58	357	108965	0.198	0.198	3.32	38868	433	7.41	433	7251.4	0.90	0.22	24.70	1.962	1.416	31149
Σ				2734	Δ_{eff} =	247	550308	1.000	h_{eff} =	11.62	136022			2185	25377.1						

Δ_{max} = 1045 mm <= deflection @ long period limit, T_L

[(a)] k_o = Ks x (Ks/Ko) ratio

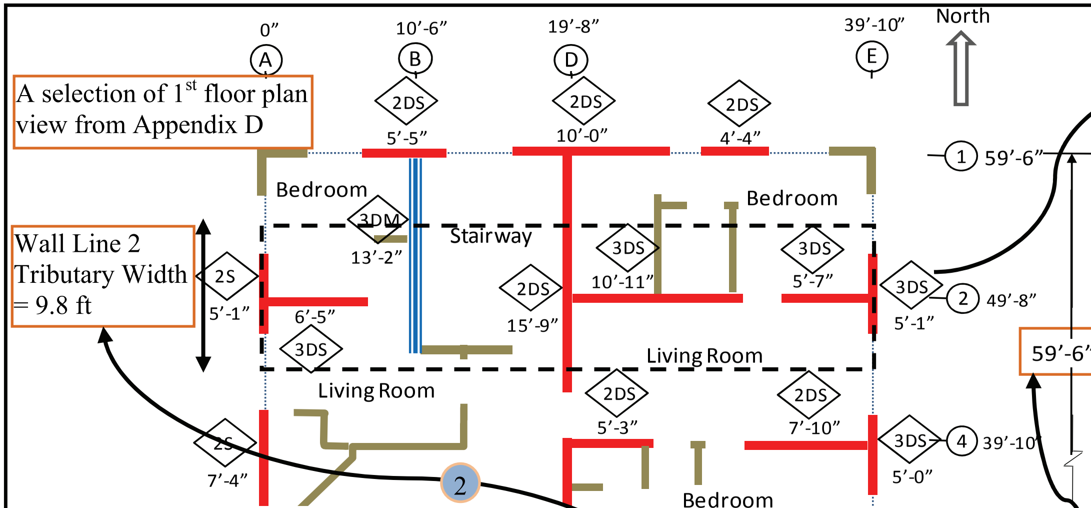

A selection of 1st floor plan view from Appendix D

Wall Line 2
Tributary Width
= 9.8 ft

“3DS”
Double-**S**heathed
Standard Wall
10dc @**3**”/12”

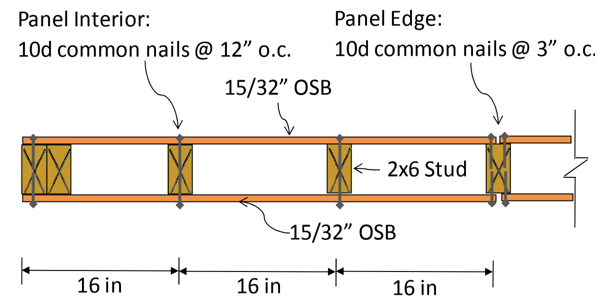

(4) Required story shear for Wall Line 2
$= \frac{\text{Tributary Width}}{\text{Total Diaphragm Length}} \text{Story } V_s$
= 9.8ft / 59.5ft × 491.13 kip
= 81.17 kip

(5) Σ Full-Height Wall Width
= 6’-5” + 10’-11” + 5’-7”
= 22.92 ft
see figure above

(6) Required shear per unit width
= 81.17 k/22.92ft = 3.54k/ft

(8) Select panel edge nail spacing, see Appendix B

(10) 1= single-layer wall
2 = double-layer wall

Shear capacity of GWB layers
= 22.92ft × 2 × 0.09 k/ft
= 4.13k (12)

Story 1
Clear Height 9 ft
Transverse Direction (Parallel to X)

Wall Line			1	2	4	6	8	10	11	sum
Tributary Width (ft)			4.9	9.8	10.0	10.1	10.0	9.8	4.9	59.5
Vs Req' (kip)			40.58	81.17	82.20	83.23	82.20	81.17	40.58	491.13
Full-Height Wall Segment (ft)		1	5.42	6.42	5.25	19.25	5.25	6.42	5.42	
		2	10.00	10.92	7.83		7.83	10.92	10.00	
		3	4.33	5.58				5.58	4.33	
		4								
		5								
Total Length		Σ	19.75	22.92	13.08	19.25	13.08	22.92	19.75	
		Vs Req' (kip per ft)	2.05	3.54	6.28	4.32	6.28	3.54	2.05	
Shear Wall (OSB)	Type		Std	Std	Std	Std	Std	Std	Std	
	Edge Nail	(in)	2	3	2	2	2	3	2	
	Unit Shear	(kip per ft)	2.17	1.45	2.17	2.17	2.17	1.45	2.17	
	Panel Layer		2	2	2	2	2	2	2	
	Shear Cap.	(kip)	85.54	66.63	56.67	83.38	56.67	66.63	85.54	501.06
GWB	Unit Shear	(kip per ft)	0.09	0.09	0.09	0.09	0.09	0.09	0.09	
	Panel Layer		1	2	2	2	2	2	1	
	Shear Cap.		1.78	4.13	2.36	3.47	2.36	4.13	1.78	19.98
	Vs Prov	(kip)	87.32	70.76	59.02	86.84	59.02	70.76	87.32	521.04
	Vs Req/Vs Prov		0.47	1.22	1.45	1.00	1.45	1.22	0.47	0.94

<1 ok

Required story shear see Table C-8 V_s column (3)

Select shear wall type
Std = standard wall
Mply = midply wall (7)

Panel unit shear capacity was taken from Table B-1,
Wall Drift = 2% column (9)
Note: Equivalent 50% NE drift limit, θ_{eq50}= 2.13%

Total shear capacity = Σ Full-Height Wall Width × Panel Layer × Unit Shear Capacity
= 22.92ft × 2 × 1.45 k/ft = 66.63k (11)

Total shear capacity provided for wall line 2 = 66.63k + 4.13k = 70.76k (13)

Σ shear capacity of shear walls in story 1 (14)

Σ shear capacity of GWBs in story 1 (15)

V_s required/ V_s provided (16)
= 491.13kip/521.04 kip = 0.94 < 1 ok!

Figure C-1: Process of selecting shear wall nail spacings.

Table C-10: Determination of shear wall nail patterns for story 1 for seismic hazard Level 3.

Story **1**
Clear Height 9 ft

Transverse Direction (Parallel to X)

		Wall Line	1	2	4	6	8	10	11	sum
		Tributary Width (ft)	4.9	9.8	10.0	10.1	10.0	9.8	4.9	59.5
		Vs Req' (kip)	40.58	81.17	82.20	83.23	82.20	81.17	40.58	491.13
	Full-Height Wall Segment (ft)	1	5.42	6.42	5.25	19.25	5.25	6.42	5.42	
		2	10.00	10.92	7.83		7.83	10.92	10.00	
		3	4.33	5.58				5.58	4.33	
		4								
		5								
	Total Length	Σ	19.75	22.92	13.08	19.25	13.08	22.92	19.75	
		Vs Req' (kip per ft)	2.05	3.54	6.28	4.32	6.28	3.54	2.05	
Shear Wall (OSB)	Type		Std	Std	Std	Std	Std	Std	Std	
	Edge Nail	(in)	2	3	2	2	2	3	2	
	Unit Shear	(kip per ft)	2.17	1.45	2.17	2.17	2.17	1.45	2.17	
	Panel Layer		2	2	2	2	2	2	2	
	Shear Cap.	(kip)	85.54	66.63	56.67	83.38	56.67	66.63	85.54	501.06
GWB	Unit Shear	(kip per ft)	0.09	0.09	0.09	0.09	0.09	0.09	0.09	
	Panel Layer		1	2	2	2	2	2	1	
	Shear Cap.		1.78	4.13	2.36	3.47	2.36	4.13	1.78	19.98
	Vs Prov	(kip)	87.32	70.76	59.02	86.84	59.02	70.76	87.32	521.04
	Vs Req/Vs Prov		0.47	1.22	1.45	1.00	1.45	1.22	0.47	0.94 <1 ok

Longitudinal Direction (Parallel to Y)

Wall Line	A	B	D	E	sum
Tributary Width (ft)	5.2	9.9	14.8	10.1	39.92
Vs Req' (kip)	63.57	121.50	182.00	124.06	491.13
1	5.08	13.17	15.75	5.08	
2	7.33	13.17	20.58	5.00	
3	7.33		15.75	4.58	
4	5.08			5.00	
5				5.08	
Σ	24.83	26.33	52.08	24.75	
Vs Req' (kip per ft)	2.56	4.61	3.49	5.01	
	Std	Mply	Std	Std	
(in)	2	3	2	3	
(kip per ft)	2.17	2.81	2.17	1.45	
	1	2	2	2	
(kip)	53.78	147.76	225.58	71.96	499.09
(kip per ft)	0.09	0.09	0.09	0.09	
	1	2	2	1	
	2.24	4.74	9.38	2.23	
(kip)	56.01	152.50	234.96	74.19	517.66
	1.18	0.82	0.81	1.72	0.95 <1 ok

Table C-11: Determination of shear wall nail patterns for story 2 for seismic hazard Level 3.

Story **2**

Clear Height 8 ft

Transverse Direction (Parallel to X)

		Wall Line	1	2	4	6	8	10	11	sum	
		Tributary Width (ft)	4.9	9.8	10.0	10.1	10.0	9.8	4.9	59.5	
		Vs Req' (kip)	38.18	76.37	77.34	78.31	77.34	76.37	38.18	462.08	
	Full-Height Wall Segment (ft)	1	5.42	6.42	5.25	19.25	5.25	6.42	5.42		
		2	10.00	10.92	7.83		7.83	10.92	10.00		
		3	4.33	5.58				5.58	4.33		
		4									
		5									
	Total Length	∑	19.75	22.92	13.08	19.25	13.08	22.92	19.75		
		Vs Req' (kip per ft)	1.93	3.33	5.91	4.07	5.91	3.33	1.93		
Shear Wall (OSB)	Type		Std	Std	Std	Std	Std	Std	Std		
	Edge Nail	(in)	2	3	2	2	2	3	2		
	Unit Shear	(kip per ft)	2.20	1.50	2.20	2.20	2.20	1.50	2.20		
	Panel Layer		2	2	2	2	2	2	2		
	Shear Cap.	(kip)	86.75	68.68	57.47	84.55	57.47	68.68	86.75	510.35	
GWB	Unit Shear	(kip per ft)	0.09	0.09	0.09	0.09	0.09	0.09	0.09		
	Panel Layer		1	2	2	2	2	2	1		
	Shear Cap.		1.78	4.13	2.36	3.47	2.36	4.13	1.78	19.98	
	Vs Prov	(kip)	88.53	72.81	59.82	88.02	59.82	72.81	88.53	530.33	
	Vs Req/Vs Prov		0.44	1.11	1.35	0.93	1.35	1.11	0.44	0.87	<1 ok

Longitudinal Direction (Parallel to Y)

Wall Line	A	B	D	E	sum	
Tributary Width (ft)	5.2	9.9	14.8	10.1	39.92	
Vs Req' (kip)	59.81	114.31	171.23	116.73	462.08	
1	5.08	13.17	15.75	5.08		
2	13.00	13.17	20.58	5.00		
3	5.08		15.75	4.58		
4				5.00		
5				5.08		
∑	23.17	26.33	52.08	24.75		
Vs Req' (kip per ft)	2.58	4.34	3.29	4.72		
	Std	Mply	Std	Std		
(in)	2	3	2	3		
(kip per ft)	2.20	2.81	2.20	1.50		
	1	2	2	2		
(kip)	50.88	147.76	228.77	74.18	501.59	
(kip per ft)	0.09	0.09	0.09	0.09		
	1	2	2	1		
	2.09	4.74	9.38	2.23		
(kip)	52.96	152.50	238.15	76.40	520.01	
	1.18	0.77	0.75	1.57	0.89	<1 ok

Table C-12: Determination of shear wall nail patterns for story 3 for seismic hazard Level 3.

Story **3**
Clear Height 8 ft

Transverse Direction (Parallel to X)

		Wall Line	1	2	4	6	8	10	11	sum	
		Tributary Width (ft)	4.9	9.8	10.0	10.1	10.0	9.8	4.9	59.5	
		Vs Req' (kip)	33.88	67.75	68.61	69.47	68.61	67.75	33.88	409.96	
	Full-Height Wall Segment (ft)	1	5.42	6.42	5.25	19.25	5.25	6.42	5.42		
		2	10.00	10.92	7.83		7.83	10.92	10.00		
		3	4.33	5.58				5.58	4.33		
		4									
		5									
	Total Length	∑	19.75	22.92	13.08	19.25	13.08	22.92	19.75		
		Vs Req' (kip per ft)	1.72	2.96	5.24	3.61	5.24	2.96	1.72		
Shear Wall (OSB)	Type		Std	Std	Std	Std	Std	Std	Std		
	Edge Nail	(in)	3	3	3	2	3	3	3		
	Unit Shear	(kip per ft)	1.50	1.50	1.50	2.20	1.50	1.50	1.50		
	Panel Layer		2	2	2	2	2	2	2		
	Shear Cap.	(kip)	59.19	68.68	39.21	84.55	39.21	68.68	59.19	418.72	
GWB	Unit Shear	(kip per ft)	0.09	0.09	0.09	0.09	0.09	0.09	0.09		
	Panel Layer		1	2	2	2	2	2	1		
	Shear Cap.		1.78	4.13	2.36	3.47	2.36	4.13	1.78	19.98	
	Vs Prov	(kip)	60.97	72.81	41.57	88.02	41.57	72.81	60.97	438.70	
	Vs Req/Vs Prov		0.57	0.99	1.75	0.82	1.75	0.99	0.57	0.93	<1 ok

Longitudinal Direction (Parallel to Y)

Wall Line	A	B	D	E	sum	
Tributary Width (ft)	5.2	9.9	14.8	10.1	39.92	
Vs Req' (kip)	53.06	101.42	151.92	103.56	409.96	
1	5.08	13.17	15.75	5.08		
2	13.00	13.17	20.58	5.00		
3	5.08		15.75	4.58		
4				5.00		
5				5.08		
∑	23.17	26.33	52.08	24.75		
Vs Req' (kip per ft)	2.29	3.85	2.92	4.18		
	Std	Mply	Std	Std		
(in)	2	3	3	3		
(kip per ft)	2.20	2.87	1.50	1.50		
	1	2	2	2		
(kip)	50.88	151.39	156.09	74.18	432.53	
(kip per ft)	0.09	0.09	0.09	0.09		
	1	2	2	1		
	2.09	4.74	9.38	2.23		
(kip)	52.96	156.13	165.47	76.40	450.96	
	1.04	0.67	0.97	1.40	0.91	<1 ok

Table C-13: Determination of shear wall nail patterns for story 4 for seismic hazard Level 3.

Story **4**

Clear Height 8 ft

Transverse Direction (Parallel to X)

		Wall Line	1	2	4	6	8	10	11	sum
		Tributary Width (ft)	4.9	9.8	10.0	10.1	10.0	9.8	4.9	59.5
		Vs Req' (kip)	27.53	55.06	55.76	56.46	55.76	55.06	27.53	333.15
	Full-Height Wall Segment (ft)	1	5.42	6.42	5.25	19.25	5.25	6.42	5.42	
		2	10.00	10.92	7.83		7.83	10.92	10.00	
		3	4.33	5.58				5.58	4.33	
		4								
		5								
	Total Length	∑	19.75	22.92	13.08	19.25	13.08	22.92	19.75	
		Vs Req' (kip per ft)	1.39	2.40	4.26	2.93	4.26	2.40	1.39	
Shear Wall (OSB)	Type		Std	Std	Std	Std	Std	Std	Std	
	Edge Nail	(in)	4	2	3	2	3	2	4	
	Unit Shear	(kip per ft)	1.14	2.20	1.50	2.20	1.50	2.20	1.14	
	Panel Layer		2	1	2	2	2	1	2	
	Shear Cap.	(kip)	44.87	50.33	39.21	84.55	39.21	50.33	44.87	353.38
GWB	Unit Shear	(kip per ft)	0.09	0.09	0.09	0.09	0.09	0.09	0.09	
	Panel Layer		1	2	2	2	2	2	1	
	Shear Cap.		1.78	4.13	2.36	3.47	2.36	4.13	1.78	19.98
	Vs Prov	(kip)	46.65	54.45	41.57	88.02	41.57	54.45	46.65	373.36
	Vs Req/Vs Prov		0.61	1.09	1.42	0.67	1.42	1.09	0.61	0.89

<1 ok

Longitudinal Direction (Parallel to Y)

Wall Line	A	B	D	E	sum
Tributary Width (ft)	5.2	9.9	14.8	10.1	39.92
Vs Req' (kip)	43.12	82.42	123.45	84.16	333.15
1	5.08	13.17	15.75	5.08	
2	13.00	13.17	20.58	5.00	
3	5.08		15.75	4.58	
4				5.00	
5				5.08	
∑	23.17	26.33	52.08	24.75	
Vs Req' (kip per ft)	1.86	3.13	2.37	3.40	
	Std	Mply	Std	Std	
(in)	2	2	2	3	
(kip per ft)	2.20	4.30	2.20	1.50	
	1	1	1	2	
(kip)	50.88	113.12	114.39	74.18	352.56
(kip per ft)	0.09	0.09	0.09	0.09	
	1	2	2	1	
	2.09	4.74	9.38	2.23	
(kip)	52.96	117.86	123.76	76.40	370.99
	0.85	0.73	1.08	1.13	0.90

<1 ok

Table C-14: Determination of shear wall nail patterns for story 5 for seismic hazard Level 3.

Story **5**
Clear Height 8 ft

Transverse Direction (Parallel to X)

		Wall Line	1	2	4	6	8	10	11	sum	
		Tributary Width (ft)	4.9	9.8	10.0	10.1	10.0	9.8	4.9	59.5	
		Vs Req' (kip)	19.14	38.28	38.77	39.26	38.77	38.28	19.14	231.65	
	Full-Height Wall Segment (ft)	1	5.42	6.42	5.25	19.25	5.25	6.42	5.42		
		2	10.00	10.92	7.83		7.83	10.92	10.00		
		3	4.33	5.58				5.58	4.33		
		4									
		5									
	Total Length	∑	19.75	22.92	13.08	19.25	13.08	22.92	19.75		
		Vs Req' (kip per ft)	0.97	1.67	2.96	2.04	2.96	1.67	0.97		
Shear Wall (OSB)	Type		Std	Std	Std	Std	Std	Std	Std		
	Edge Nail	(in)	4	2	3	2	3	2	4		
	Unit Shear	(kip per ft)	1.14	2.20	1.50	2.20	1.50	2.20	1.14		
	Panel Layer		2	1	1	1	1	1	2		
	Shear Cap.	(kip)	44.87	50.33	19.61	42.28	19.61	50.33	44.87	271.89	
GWB	Unit Shear	(kip per ft)	0.09	0.09	0.09	0.09	0.09	0.09	0.09		
	Panel Layer		1	2	2	2	2	2	1		
	Shear Cap.		1.78	4.13	2.36	3.47	2.36	4.13	1.78	19.98	
	Vs Prov	(kip)	46.65	54.45	21.96	45.74	21.96	54.45	46.65	291.87	
	Vs Req/Vs Prov		0.43	0.76	1.98	0.93	1.98	0.76	0.43	0.79	<1 ok

Longitudinal Direction (Parallel to Y)

Wall Line	A	B	D	E	sum	
Tributary Width (ft)	5.2	9.9	14.8	10.1	39.92	
Vs Req' (kip)	29.98	57.31	85.84	58.52	231.65	
1	5.08	13.17	15.75	5.08		
2	13.00	13.17	20.58	5.00		
3	5.08		15.75	4.58		
4				5.00		
5				5.08		
∑	23.17	26.33	52.08	24.75		
Vs Req' (kip per ft)	1.29	2.18	1.65	2.36		
	Std	Mply	Std	Std		
(in)	3	3	3	3		
(kip per ft)	1.50	2.87	1.50	1.50		
	1	1	1	2		
(kip)	34.72	75.69	78.05	74.18	262.63	
(kip per ft)	0.09	0.09	0.09	0.09		
	1	2	2	1		
	2.09	4.74	9.38	2.23		
(kip)	36.80	80.43	87.42	76.40	281.06	
	0.86	0.76	1.10	0.79	0.82	<1 ok

Table C-15: Determination of shear wall nail patterns for story 6 for seismic hazard Level 3.

Story **6**

Clear Height 8 ft

Transverse Direction (Parallel to X)

		Wall Line	1	2	4	6	8	10	11	sum	
		Tributary Width (ft)	5.0	24.8	0.0	0.0	0.0	24.8	5.0	59.5	
		Vs Req' (kip)	8.17	40.45	0.00	0.00	0.00	40.45	8.17	97.25	
	Full-Height Wall Segment (ft)	1	5.42	6.42				6.42	5.42		
		2	10.00						10.00		
		3	4.33								
		4									
		5									
	Total Length	∑	19.75	6.42				6.42	15.42		
		Vs Req' (kip per ft)	0.41	6.30				6.30	0.53		
Shear Wall (OSB)	Type		Std	Std				Std	Std		
	Edge Nail	(in)	4	2				2	4		
	Unit Shear	(kip per ft)	1.14	2.20				2.20	1.14		
	Panel Layer		2	1				1	2		
	Shear Cap.	(kip)	44.87	14.09				14.09	35.03	108.08	
GWB	Unit Shear	(kip per ft)	0.09	0.09				0.09	0.09		
	Panel Layer		1	2				2	1		
	Shear Cap.		1.78	1.16				1.16	1.39	5.48	
	Vs Prov	(kip)	46.65	15.25				15.25	36.41	113.56	
	Vs Req/Vs Prov		0.18	2.87				2.87	0.23	0.86	<1 ok

Longitudinal Direction (Parallel to Y)

Wall Line	A	B	D	E	sum	
Tributary Width (ft)	5.2	0.0	24.9	10.1	40.13	
Vs Req' (kip)	12.52	0.00	60.29	24.44	97.25	
1	5.08		15.75	5.08		
2	13.00		20.58	5.00		
3	5.08		15.75	4.58		
4				5.00		
5				5.08		
∑	23.17		52.08	24.75		
Vs Req' (kip per ft)	0.54		1.16	0.99		
	Std		Std	Std		
(in)	6		3	6		
(kip per ft)	0.77		1.50	0.77		
	1		1	1		
(kip)	17.89		78.05	19.12	115.06	
(kip per ft)	0.09		0.09	0.09		
	1		2	1		
	2.09		9.38	2.23		
(kip)	19.98		87.42	21.34	128.75	
	0.70		0.77	1.28	0.76	<1 ok

Appendix D

Shear Wall Nail Schedules

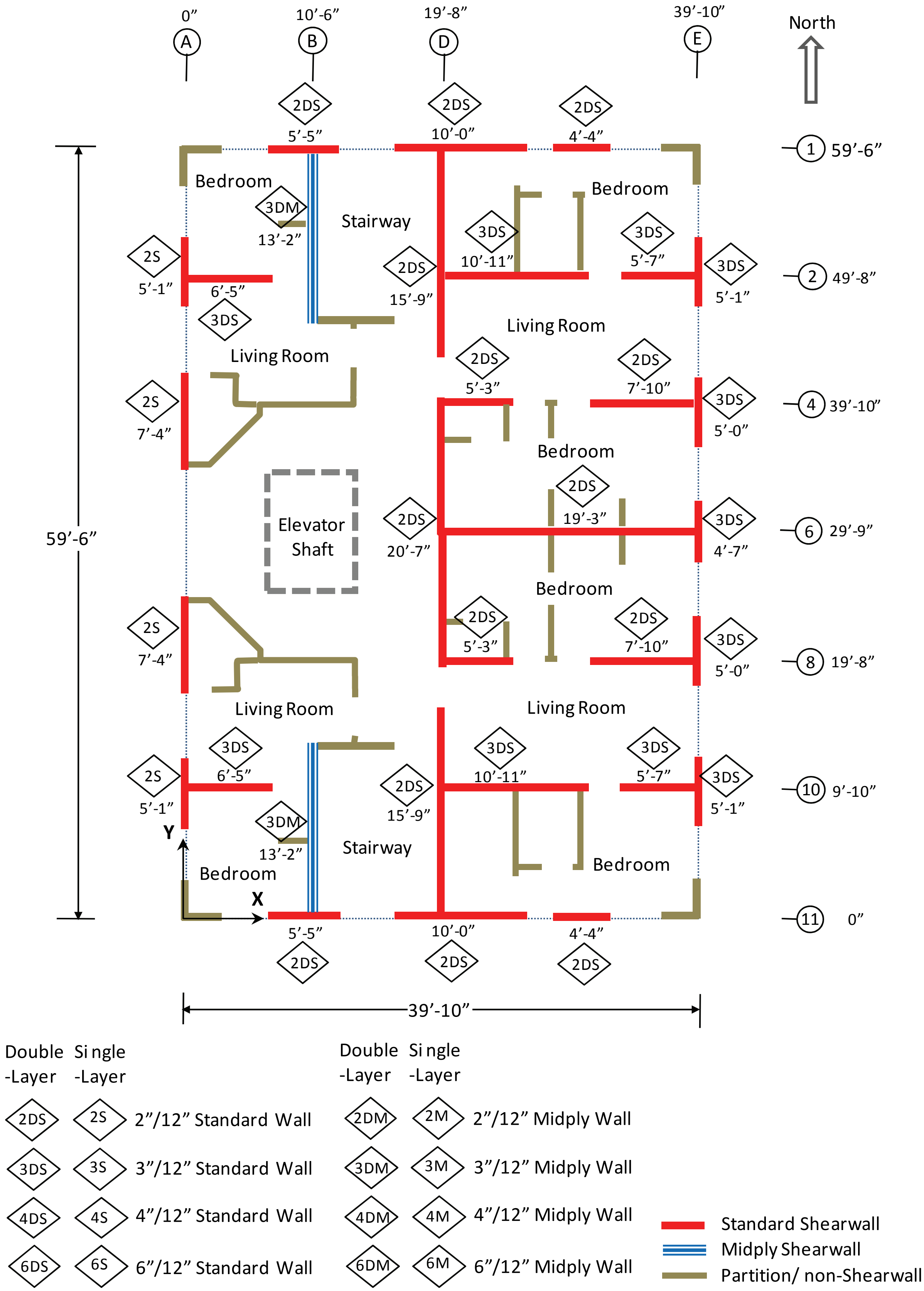

Figure D-1: Story 1 shear wall nail schedule.

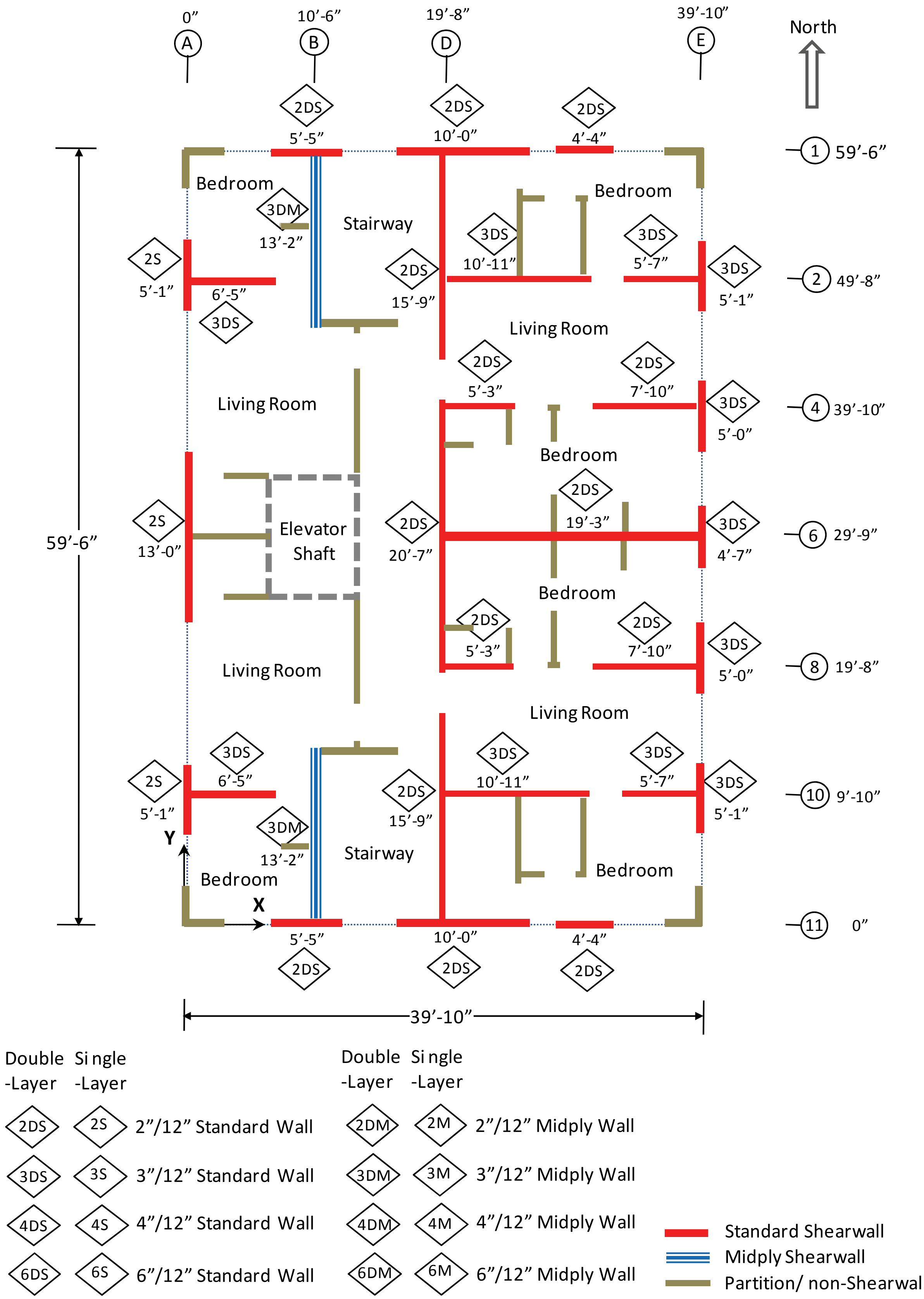

Figure D-2: Story 2 shear wall nail schedule.

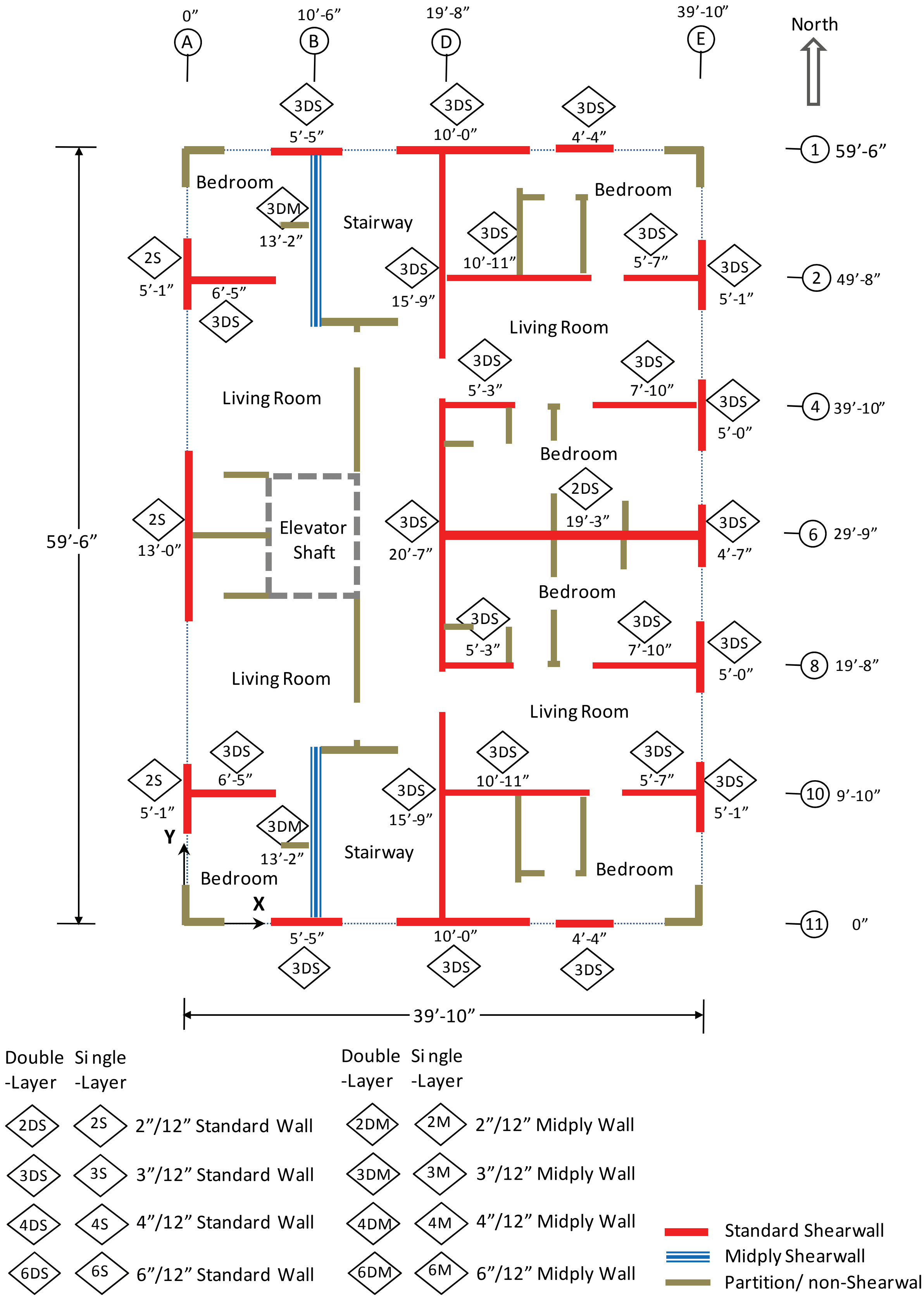

Figure D-3: Story 3 shear wall nail schedule.

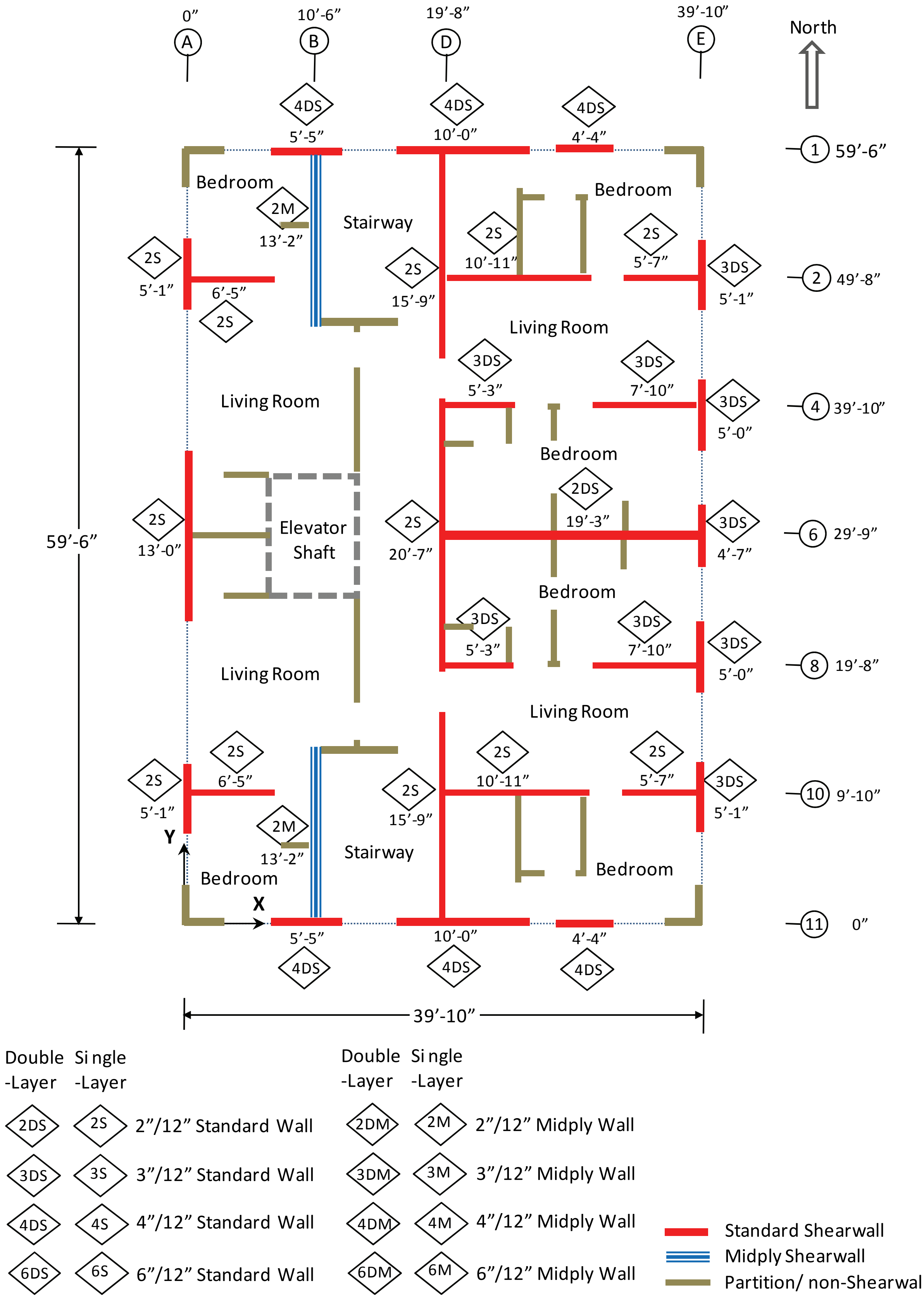

Figure D-4: Story4 shear wall nail schedule.

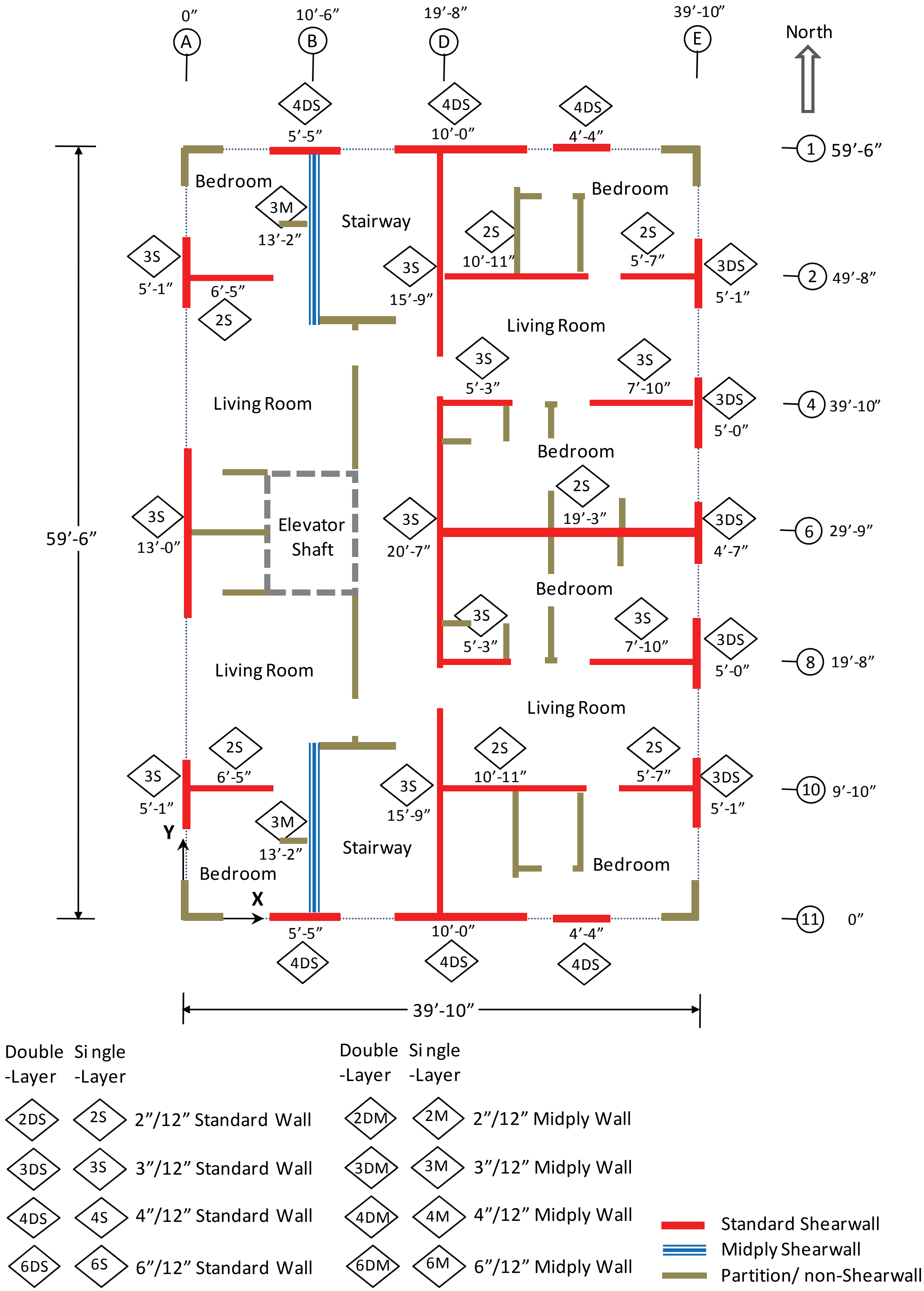

Figure D-5: Story 5 shear wall nail schedule.

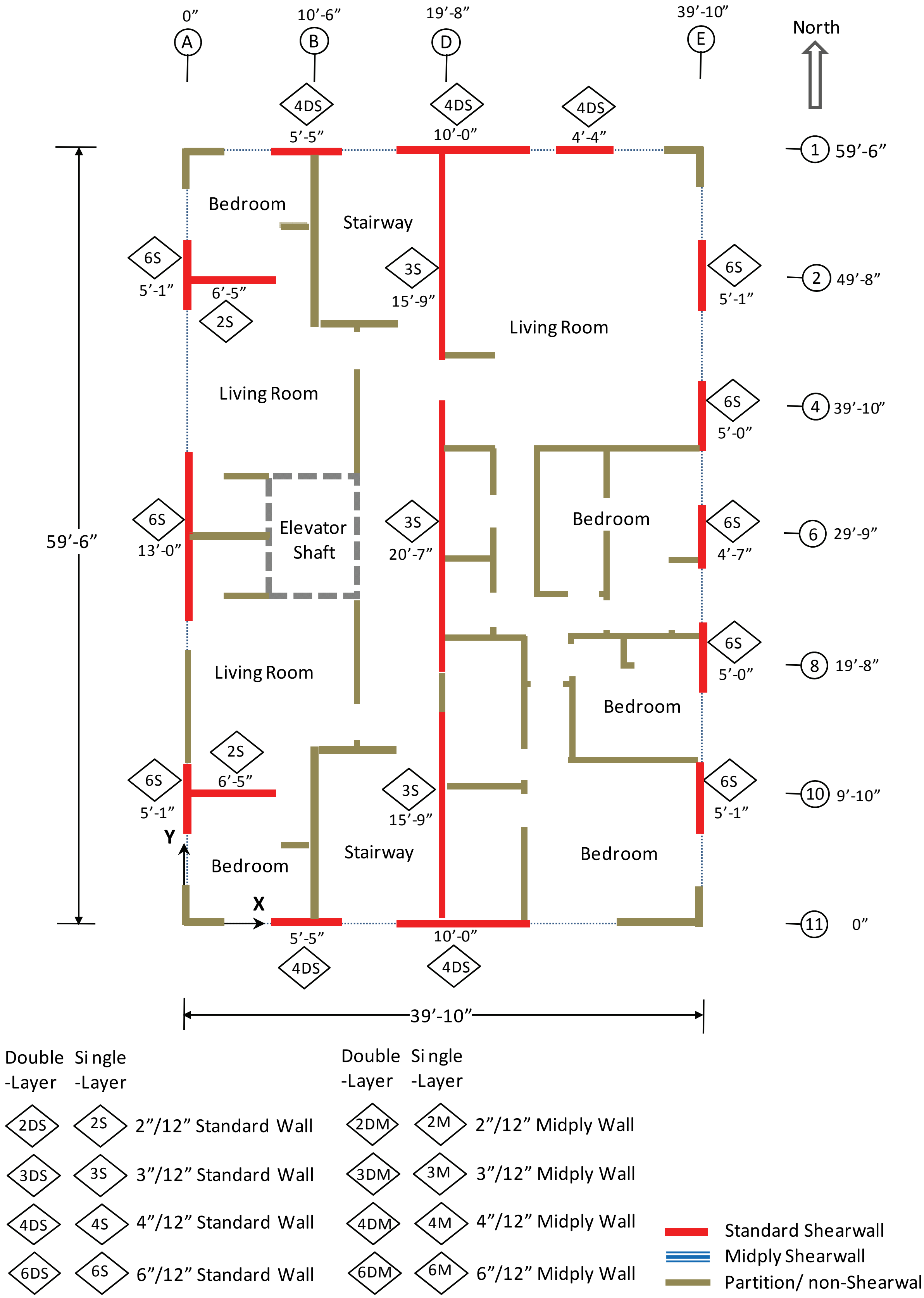

Figure D-6: Story 6 shear wall nail schedule.

Appendix E

Shear Wall Hysteretic Parameters

Table E-1: Shear wall hysteretic parameters for unit wall width (per ft) in US customary units.

Wall Height (ft)	Wall Type/ Sheathing Layer	Edge Nail Spacing (in)	K_o (kip/in per ft)	r_1	r_2	r_3	r_4	F_o (kip per ft)	F_i (kip per ft)	Δ (in)	α	β
9	Standard[a]	2	3.949	0.034	-0.071	1.010	0.033	1.900	0.242	2.188	0.759	1.241
		3	3.239	0.030	-0.062	1.010	0.024	1.268	0.161	2.108	0.759	1.286
		4	2.761	0.033	-0.056	1.010	0.022	0.941	0.127	2.042	0.714	1.286
		6	1.981	0.024	-0.050	1.034	0.021	0.673	0.087	2.035	0.714	1.286
	Midply[b]	2	5.030	0.033	-0.106	1.010	0.048	4.206	0.219	2.159	0.768	1.150
		3	4.375	0.014	-0.079	1.010	0.037	2.895	0.162	1.989	0.759	1.195
		4	3.844	0.011	-0.066	1.010	0.034	2.189	0.133	1.880	0.759	1.241
		6	3.155	0.008	-0.054	1.010	0.027	1.470	0.082	1.848	0.759	1.286
	GWB[c]	16	1.294	0.026	-0.024	1.028	0.005	0.116	0.013	0.694	0.855	1.143
8	Standard[a]	2	4.232	0.030	-0.073	1.010	0.033	1.989	0.247	1.972	0.759	1.241
		3	3.787	0.032	-0.060	1.010	0.023	1.277	0.170	1.898	0.714	1.286
		4	3.028	0.026	-0.056	1.010	0.022	1.006	0.146	1.850	0.759	1.286
		6	2.359	0.025	-0.049	1.010	0.019	0.675	0.091	1.841	0.714	1.286
	Midply[b]	2	5.171	0.046	-0.114	1.010	0.053	4.315	0.255	1.990	0.723	1.150
		3	4.582	0.024	-0.084	1.010	0.040	2.916	0.155	1.791	0.814	1.241
		4	4.171	0.013	-0.068	1.010	0.035	2.202	0.121	1.735	0.759	1.241
		6	3.459	0.009	-0.054	1.010	0.028	1.499	0.087	1.652	0.759	1.286
	GWB[c]	16	2.142	0.028	-0.019	1.010	0.005	0.111	0.015	0.568	0.845	1.141

[a] Standard wall model is built with 15/32 in. thick OSB connected to framing members by 10d common nails (0.148 in. diameter) in single-shear.

[b] Midply wall model is built with 15/32 in. thick OSB connected to framing members by 10d common nails (0.148 in. diameter) in double-shear

[c] Gypsum wall board model is built with 1/2 in. thick GWB connected to framing members by #6 bugle head drywall screws (0.142 in. diameter) in single-shear.

[d] All wall models are built using edge nail distance of 0.5 in. and panel shear modulus of 180 ksi.

[e] In M-CASHEW, each panel-to-frame connection is modeled using two orthogonal uncoupled non-linear springs. The peak backbone forces predicted by M-CASHEW are about 10~15% higher than the peak force predicted by the Fortran version of CASHEW.

Table E-2: Shear wall hysteretic parameters for unit wall width (per m) in SI units.

Wall Height (m)	Wall Type/ Sheathing Layer	Edge Nail Spacing (mm)	K_o (kN/mm per m)	r_1	r_2	r_3	r_4	F_o (kN per m)	F_i (kN per m)	Δ (mm)	α	β
2.74	Standard[a]	51	2.269	0.034	-0.071	1.010	0.033	27.735	3.539	55.575	0.759	1.241
		76	1.861	0.030	-0.062	1.010	0.024	18.500	2.348	53.533	0.759	1.286
		102	1.586	0.033	-0.056	1.010	0.022	13.735	1.857	51.874	0.714	1.286
		152	1.138	0.024	-0.050	1.034	0.021	9.828	1.263	51.692	0.714	1.286
	Midply[b]	51	2.890	0.033	-0.106	1.010	0.048	61.378	3.199	54.826	0.768	1.150
		76	2.514	0.014	-0.079	1.010	0.037	42.246	2.364	50.531	0.759	1.195
		102	2.208	0.011	-0.066	1.010	0.034	31.943	1.947	47.752	0.759	1.241
		152	1.813	0.008	-0.054	1.010	0.027	21.449	1.197	46.939	0.759	1.286
	GWB[c]	406	0.743	0.026	-0.024	1.028	0.005	1.687	0.191	17.631	0.855	1.143
2.44	Standard[a]	51	2.432	0.030	-0.073	1.010	0.033	29.028	3.607	50.086	0.759	1.241
		76	2.176	0.032	-0.060	1.010	0.023	18.641	2.485	48.217	0.714	1.286
		102	1.740	0.026	-0.056	1.010	0.022	14.674	2.128	46.987	0.759	1.286
		152	1.356	0.025	-0.049	1.010	0.019	9.852	1.330	46.764	0.714	1.286
	Midply[b]	51	2.971	0.046	-0.114	1.010	0.053	62.970	3.723	50.533	0.723	1.150
		76	2.633	0.024	-0.084	1.010	0.040	42.561	2.268	45.491	0.814	1.241
		102	2.396	0.013	-0.068	1.010	0.035	32.131	1.768	44.079	0.759	1.241
		152	1.988	0.009	-0.054	1.010	0.028	21.879	1.273	41.953	0.759	1.286
	GWB[c]	406	1.231	0.028	-0.019	1.010	0.005	1.613	0.212	14.425	0.845	1.141

[a] Standard wall model is built with 11.9 mm thick OSB connected to framing members by 10d common nails (3.76 mm diameter) in single-shear.

[b] Midply wall model is built with 11.9 mm thick OSB connected to framing members by 10d common nails (3.76 mm diameter) in double-shear

[c] Gypsum wall board model is built with 12.7 mm thick GWB connected to framing members by #6 bugle head drywall screws (3.61 mm diameter) in single-shear.

[d] All wall models are built using edge nail distance of 12.7 mm and panel shear modulus of 1241 MPa.

[e] In M-CASHEW, each panel-to-frame connection is modeled using two orthogonal uncoupled non-linear springs. The peak backbone force predicted by M-CASHEW are about 10~15% higher than the peak force predicted by the Fortran version of CASHEW.

Appendix F

Modal Analysis Results

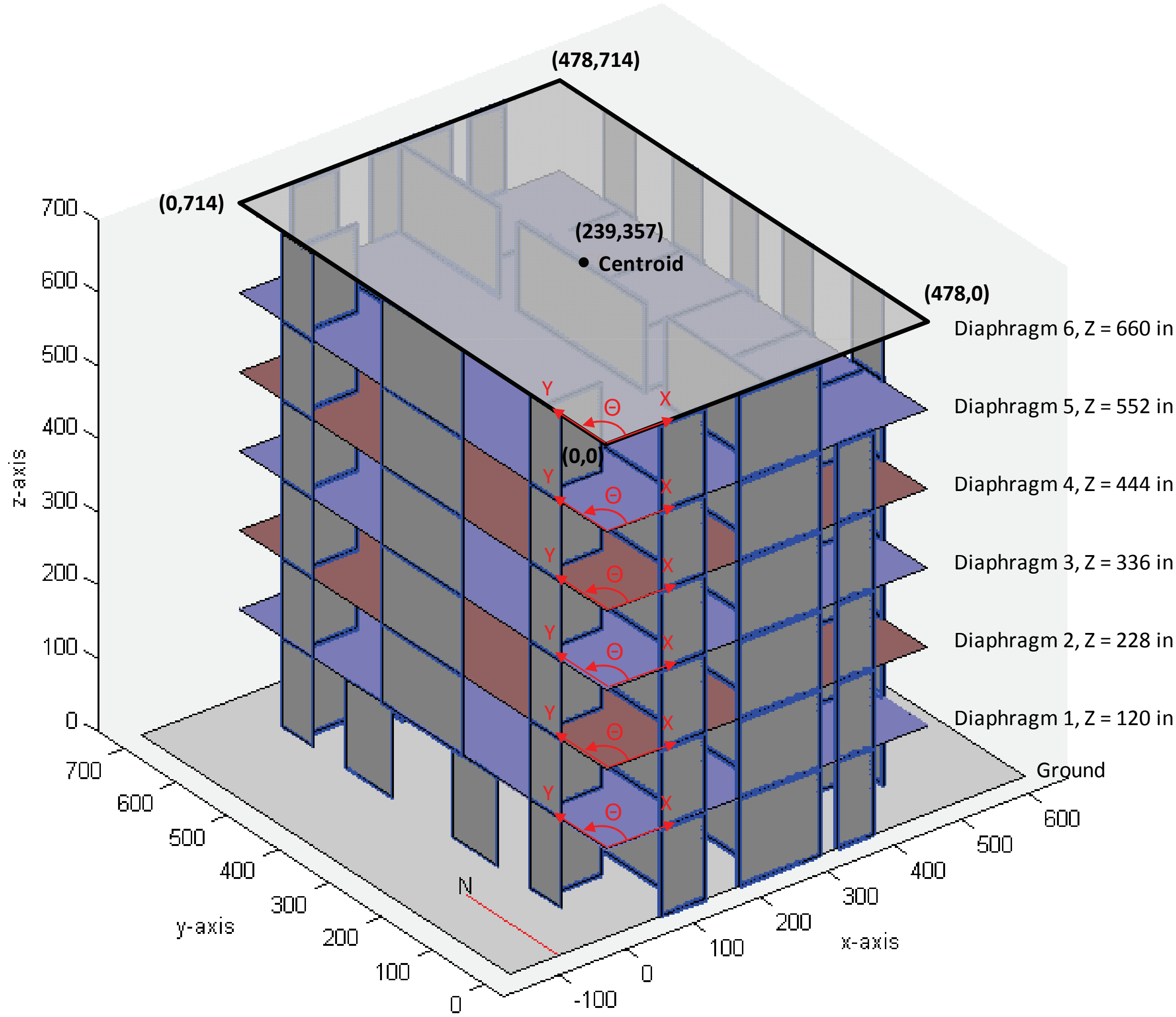

Figure F-1: Diaphragm degrees-of-freedom and corner coordinates in the M-SAWS model.

M-SAWS MODEL (INITIAL STIFFNESS)

Table F-1: Summary of modal analysis based on initial stiffness of the M-SAWS model.

Mode	Frequency (Hz)	Period (s)	Damping (%)	Effective Modal Mass		% of Total Mass		Effective Modal Height		% of Roof Height[a]	
				M^*_X (kip-s^2/in)	M^*_Y (kip-s^2/in)	X (%)	Y (%)	H^*_X (in)	H^*_Y (in)	X (%)	Y (%)
1	2.7	0.3754	5.000	0.0000	1.3423	0.00	84.31	460.9	442.8	68.6	65.9
2	2.8	0.3590	5.000	1.3671	0.0000	85.87	0.00	444.3	445.2	66.1	66.3
3	3.1	0.3201	5.046	0.0001	0.0301	0.01	1.89	396.2	452.0	59.0	67.3
4	7.0	0.1431	7.387	0.1342	0.0000	8.43	0.00	-90.1	-150.4	13.4	22.4
5	7.2	0.1384	7.570	0.0001	0.1539	0.00	9.66	-102.2	-104.7	15.2	15.6
6	8.5	0.1170	8.640	0.0010	0.0012	0.06	0.07	-118.4	-47.8	17.6	7.1
7	10.2	0.0979	10.040	0.0544	0.0000	3.41	0.00	-41.8	500.6	6.2	74.5
8	11.1	0.0897	10.839	0.0000	0.0362	0.00	2.27	15.9	60.5	2.4	9.0
9	13.1	0.0762	12.565	0.0006	0.0000	0.04	0.00	64.6	1000.5	9.6	148.9
10	14.3	0.0697	13.640	0.0213	0.0024	1.34	0.15	7.4	-47.6	1.1	7.1
11	14.4	0.0694	13.701	0.0030	0.0164	0.19	1.03	2.4	-46.2	0.4	6.9
12	16.9	0.0590	15.953	0.0000	0.0000	0.00	0.00	-155.9	-58.3	23.2	8.7
13	17.4	0.0574	16.365	0.0000	0.0067	0.00	0.42	-139.7	-32.8	20.8	4.9
14	18.2	0.0549	17.096	0.0078	0.0000	0.49	0.00	-42.1	-30.2	6.3	4.5
15	20.5	0.0488	19.118	0.0000	0.0011	0.00	0.07	493.1	31.6	73.4	4.7
16	20.7	0.0483	19.337	0.0000	0.0017	0.00	0.11	503.3	6.0	74.9	0.9
17	21.8	0.0460	20.273	0.0024	0.0000	0.15	0.00	5.0	-18.6	0.7	2.8
18	24.1	0.0415	22.376	0.0000	0.0001	0.00	0.00	-11248.1	41.3	1673.8	6.1
sum				1.5920	1.5920	100.0	100.0				

[a] The roof height in M-SAWS model = 660 in.

Table F-2: First 6 mode shapes based on initial stiffness of the M-SAWS model.

Diaphragm	D.O.F.[a]		Mode Shapes					
			1	2	3	4	5	6
1	1	X	-0.0701	0.2376	-0.2540	-0.3309	0.0765	-0.5257
	2	Y	-0.2461	-0.0024	0.1953	0.0085	0.5349	0.3992
	3	θ	-0.0002	0.0000	-0.0007	-0.0001	0.0002	-0.0016
2	4	X	-0.1221	0.4173	-0.4508	-0.4809	0.0957	-0.7325
	5	Y	-0.4381	-0.0042	0.3479	0.0140	0.7566	0.5629
	6	θ	-0.0003	0.0000	-0.0013	-0.0001	0.0003	-0.0022
3	7	X	-0.1696	0.5804	-0.6296	-0.4661	0.0637	-0.6292
	8	Y	-0.6110	-0.0059	0.4865	0.0168	0.6729	0.4934
	9	θ	-0.0005	0.0000	-0.0018	-0.0001	0.0002	-0.0019
4	10	X	-0.2077	0.7323	-0.7989	-0.2556	-0.0053	-0.1791
	11	Y	-0.7894	-0.0077	0.6231	0.0157	0.2073	0.1460
	12	θ	-0.0006	0.0000	-0.0023	-0.0001	0.0000	-0.0005
5	13	X	-0.2330	0.8524	-0.9158	0.1098	-0.0723	0.3773
	14	Y	-0.9172	-0.0091	0.7187	0.0095	-0.4028	-0.2994
	15	θ	-0.0006	0.0000	-0.0026	0.0000	-0.0002	0.0012
6	16	X	-0.2479	1.0000	-1.0000	1.0000	-0.0945	1.0000
	17	Y	-1.0000	-0.0178	0.7831	-0.0529	-1.0000	-0.7616
	18	θ	-0.0007	0.0001	-0.0028	0.0003	-0.0003	0.0028

[a] The units for translational and rotational degrees-of-freedom are inches and radian, respectively.

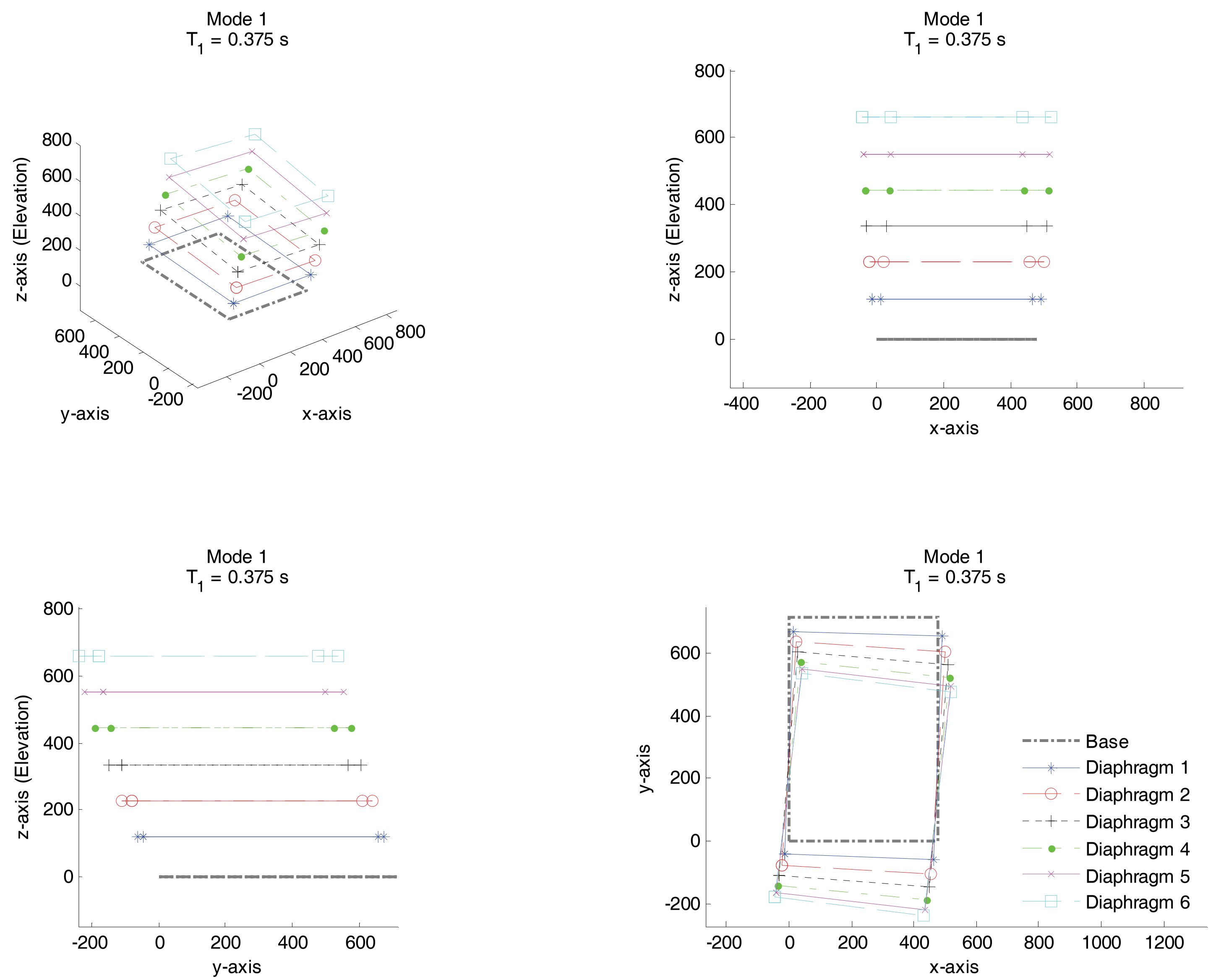

Figure F-2: Mode shape 1 of the M-SAWS model (initial stiffness).

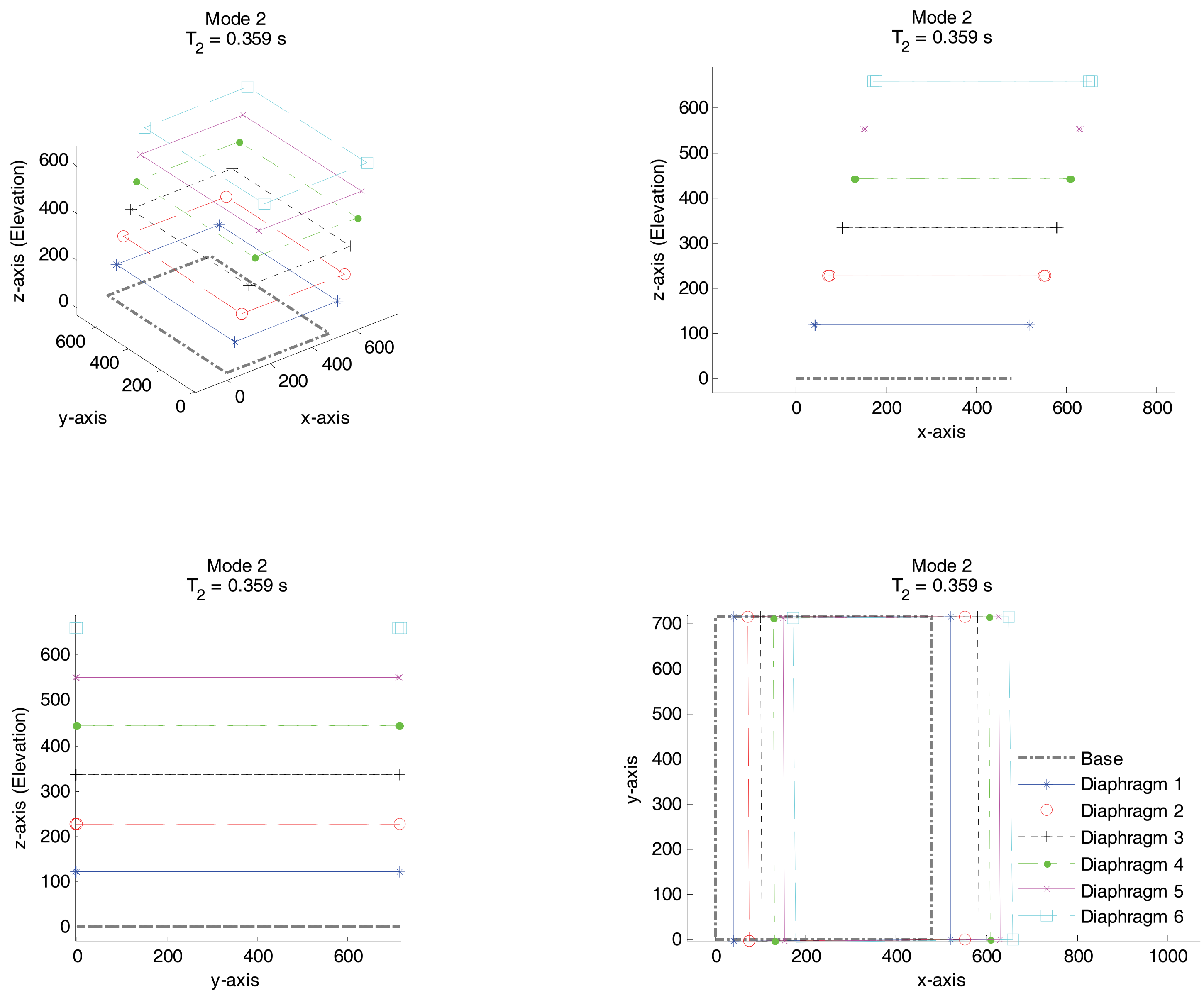

Figure F-3: Mode shape 2 of the M-SAWS model (initial stiffness).

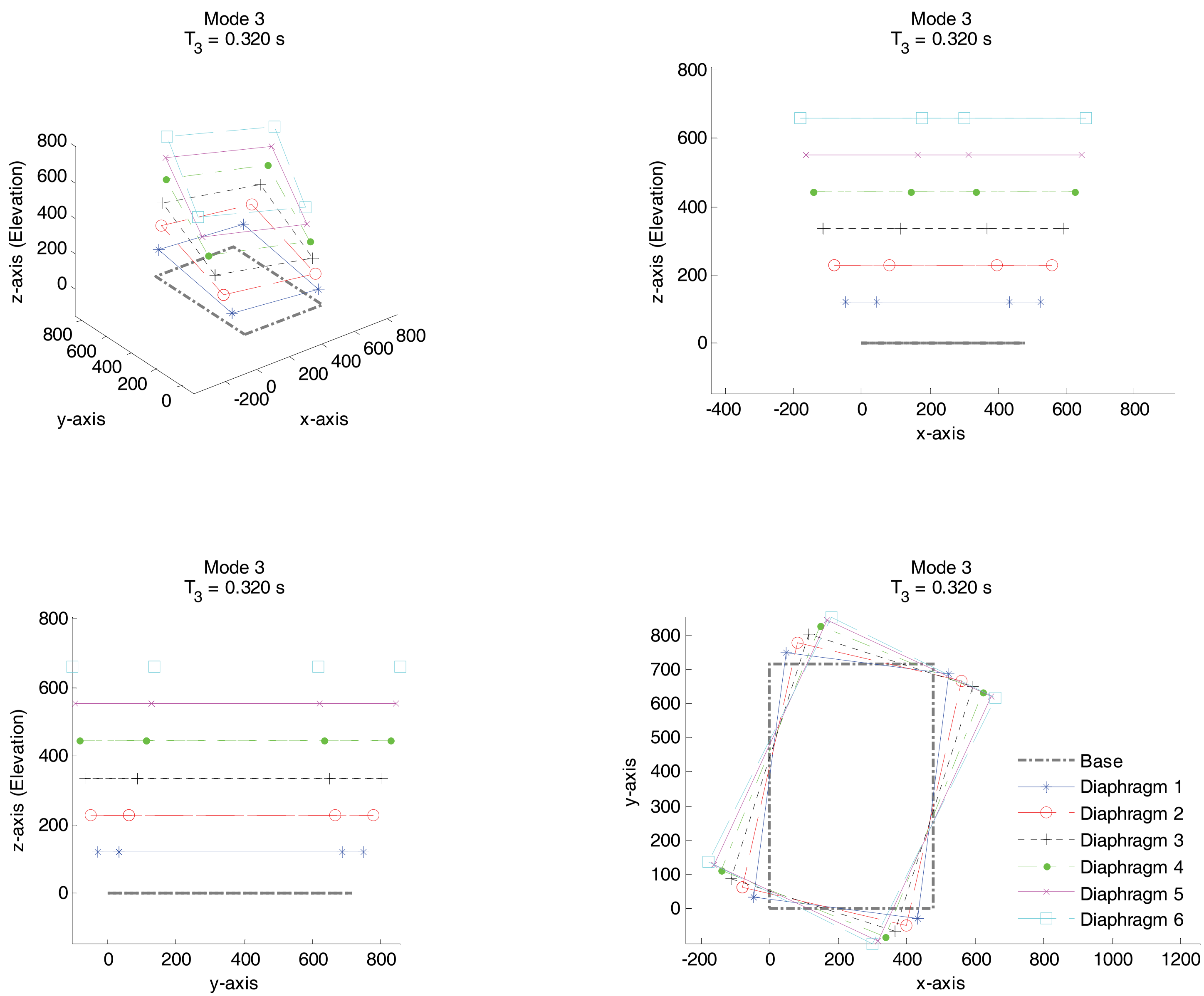

Figure F-4: Mode shape 3 of the M-SAWS model (initial stiffness).

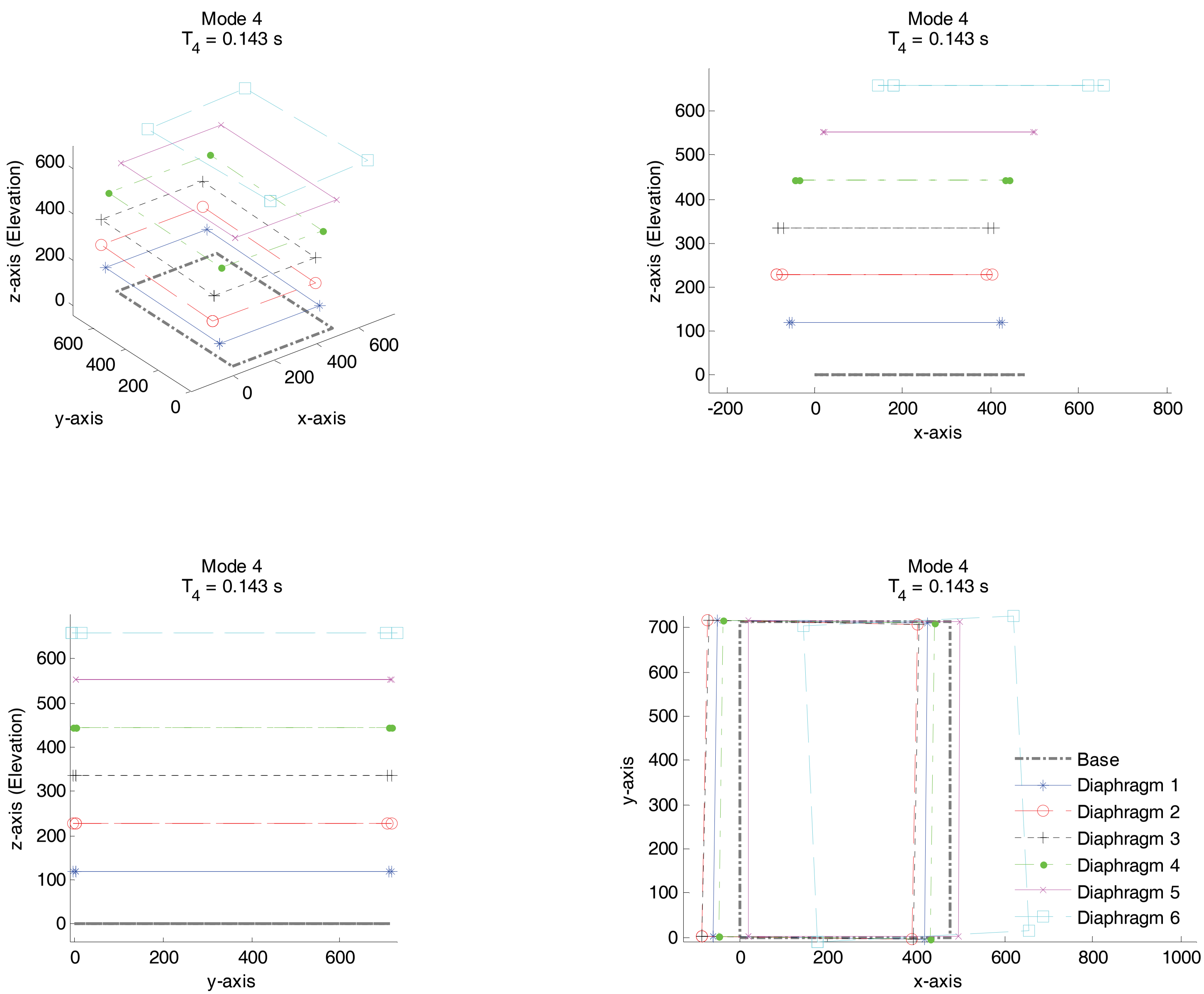

Figure F-5: Mode shape 4 of the M-SAWS model (initial stiffness).

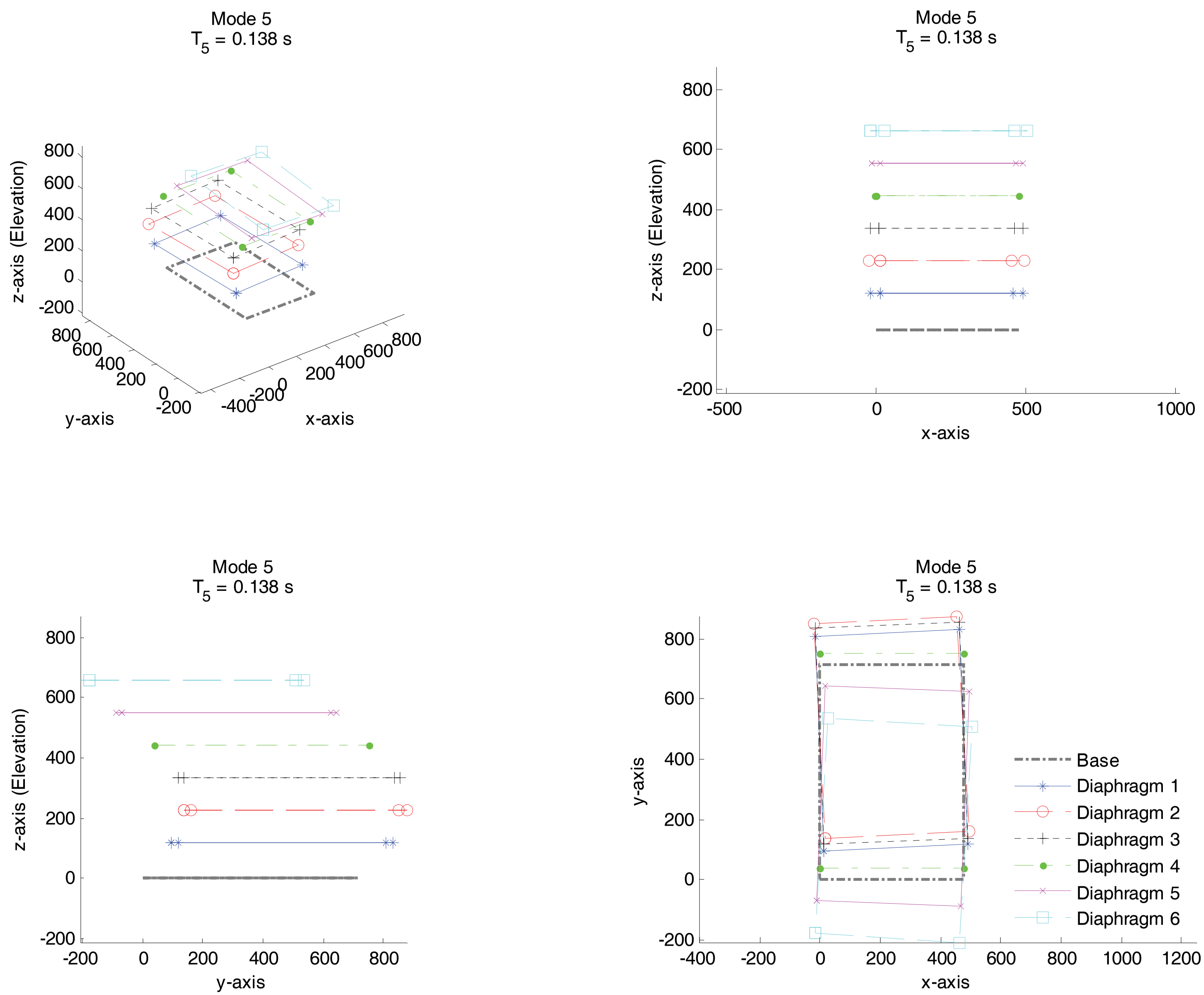

Figure F-6: Mode shape 5 of the M-SAWS model (initial stiffness).

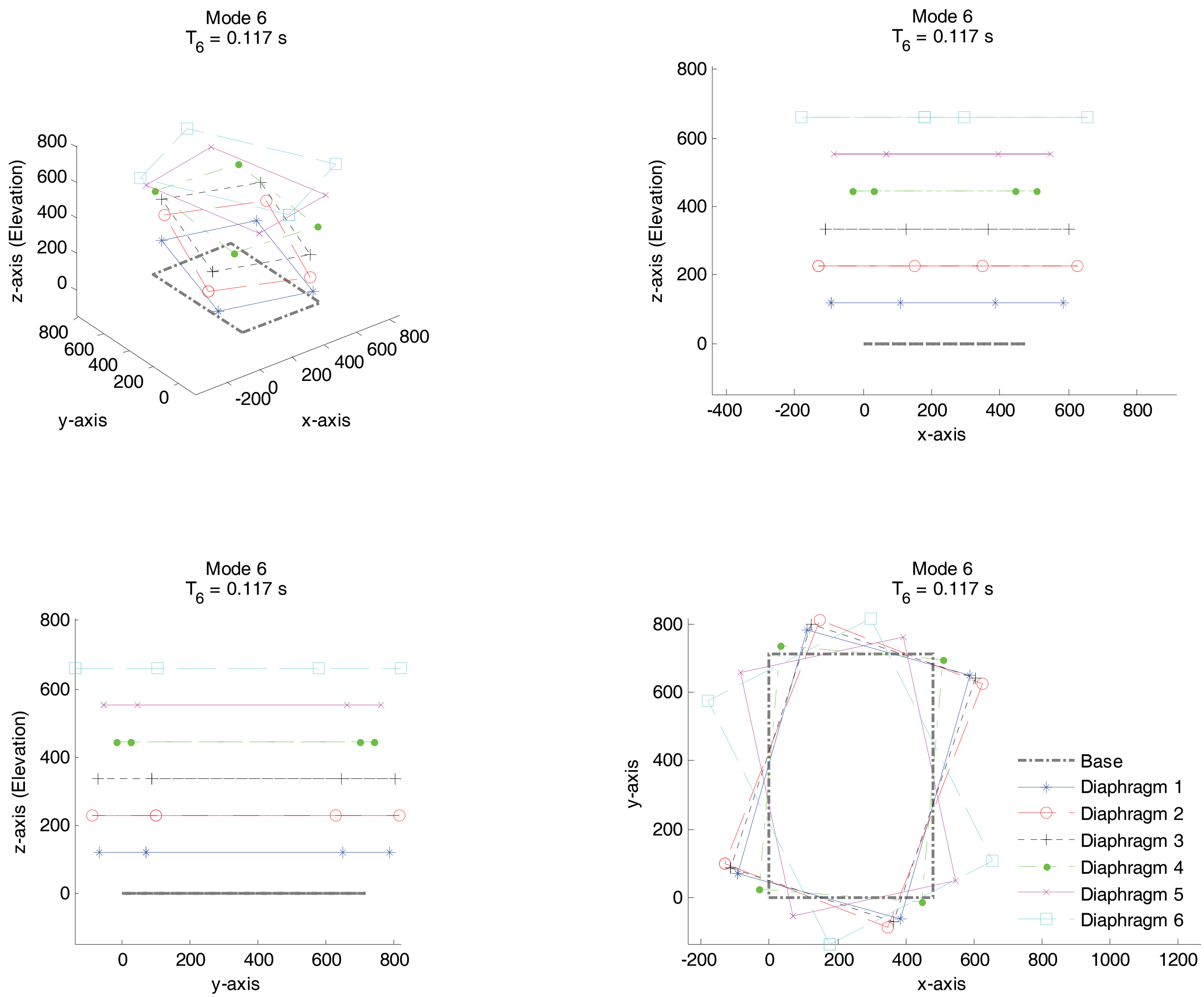

Figure F-7: Mode shape 6 of the M-SAWS model (initial stiffness).

M-SAWS Model (Tangent Stiffness at 0.15% Drift)

Table F-3: Summary of modal analysis based on tangent stiffness at 0.15% drift of the M-SAWS model.

Mode	Frequency (Hz)	Period (s)	Damping (%)	Effective Modal Mass		% of Total Mass		Effective Modal Height		% of Roof Height[a]	
				M^*_X (kip-s^2/in)	M^*_Y (kip-s^2/in)	X (%)	Y (%)	H^*_X (in)	H^*_Y (in)	X (%)	Y (%)
1	1.9	0.5373	5.000	0.0023	1.3104	0.15	82.31	445.9	447.8	66.4	66.6
2	2.0	0.5055	5.000	1.3307	0.0041	83.59	0.26	448.3	452.7	66.7	67.4
3	2.3	0.4429	5.046	0.0126	0.0295	0.79	1.85	451.3	467.0	67.2	69.5
4	5.0	0.2016	7.387	0.1415	0.0026	8.89	0.16	-66.0	-80.7	9.8	12.0
5	5.0	0.1988	7.570	0.0025	0.1716	0.16	10.78	-66.3	-67.3	9.9	10.0
6	6.2	0.1618	8.640	0.0027	0.0008	0.17	0.05	-54.1	51.3	8.1	7.6
7	7.2	0.1386	10.040	0.0575	0.0000	3.61	0.00	-15.3	108.9	2.3	16.2
8	7.8	0.1283	10.839	0.0001	0.0376	0.01	2.36	18.3	92.5	2.7	13.8
9	9.5	0.1056	12.565	0.0015	0.0000	0.09	0.00	68.5	-557.0	10.2	82.9
10	10.0	0.0995	13.640	0.0059	0.0181	0.37	1.13	19.5	-45.1	2.9	6.7
11	10.1	0.0988	13.701	0.0211	0.0046	1.33	0.29	12.6	-44.0	1.9	6.6
12	11.8	0.0846	15.953	0.0000	0.0055	0.00	0.35	-104.6	-34.6	15.6	5.2
13	12.3	0.0811	16.365	0.0001	0.0026	0.00	0.16	-159.9	-44.1	23.8	6.6
14	12.7	0.0785	17.096	0.0097	0.0000	0.61	0.00	-37.3	-59.9	5.6	8.9
15	14.2	0.0705	19.118	0.0000	0.0039	0.00	0.24	-754.7	24.1	112.3	3.6
16	14.8	0.0676	19.337	0.0000	0.0006	0.00	0.04	442.6	27.9	65.9	4.2
17	15.2	0.0657	20.273	0.0037	0.0000	0.23	0.00	5.4	25.4	0.8	3.8
18	17.2	0.0582	22.376	0.0000	0.0002	0.00	0.01	19.0	36.2	2.8	5.4
sum				1.5920	1.5920	100.0	100.0				

[a] The roof height in M-SAWS model = 660 in.

[b] The modal results were obtained after performing pushover analyses parallel to the two horizontal directions at a maximum drift ratio of 0.15% of the building height.

Table F-4: First 6 mode shapes based on tangent stiffness at 0.15% drift of the M-SAWS model.

Diaphragm	D.O.F.[a]		Mode Shapes[b]					
			1	2	3	4	5	6
1	1	X	-0.0833	0.2210	-0.2386	0.3302	-0.0111	-0.5344
	2	Y	-0.2160	-0.0280	0.1900	0.0125	-0.5377	0.3939
	3	θ	-0.0002	0.0001	-0.0007	0.0001	-0.0002	-0.0016
2	4	X	-0.1464	0.4004	-0.4340	0.4944	0.0079	-0.7643
	5	Y	-0.4022	-0.0506	0.3510	0.0193	-0.8084	0.5873
	6	θ	-0.0004	0.0001	-0.0013	0.0002	-0.0002	-0.0024
3	7	X	-0.2081	0.5726	-0.6217	0.4847	0.0495	-0.6638
	8	Y	-0.5766	-0.0726	0.5043	0.0163	-0.7619	0.5435
	9	θ	-0.0005	0.0002	-0.0019	0.0002	-0.0001	-0.0020
4	10	X	-0.2570	0.7346	-0.8074	0.2567	0.0852	-0.1630
	11	Y	-0.7812	-0.0943	0.6698	-0.0049	-0.2404	0.1680
	12	θ	-0.0006	0.0002	-0.0024	0.0001	0.0001	-0.0005
5	13	X	-0.2798	0.8563	-0.9200	-0.1162	0.0381	0.3705
	14	Y	-0.9206	-0.1080	0.7803	-0.0300	0.4220	-0.3126
	15	θ	-0.0007	0.0003	-0.0028	0.0000	0.0002	0.0012
6	16	X	-0.3033	1.0000	-1.0000	-1.0000	-0.0986	1.0000
	17	Y	-1.0000	-0.1266	0.8489	0.0250	1.0000	-0.7733
	18	θ	-0.0007	0.0003	-0.0030	-0.0004	0.0002	0.0029

[a] The units for translational and rotational degrees-of-freedom are inches and radian, respectively.

[b] The mode shapes were obtained using tangent stiffness of the building at 0.15% drift.

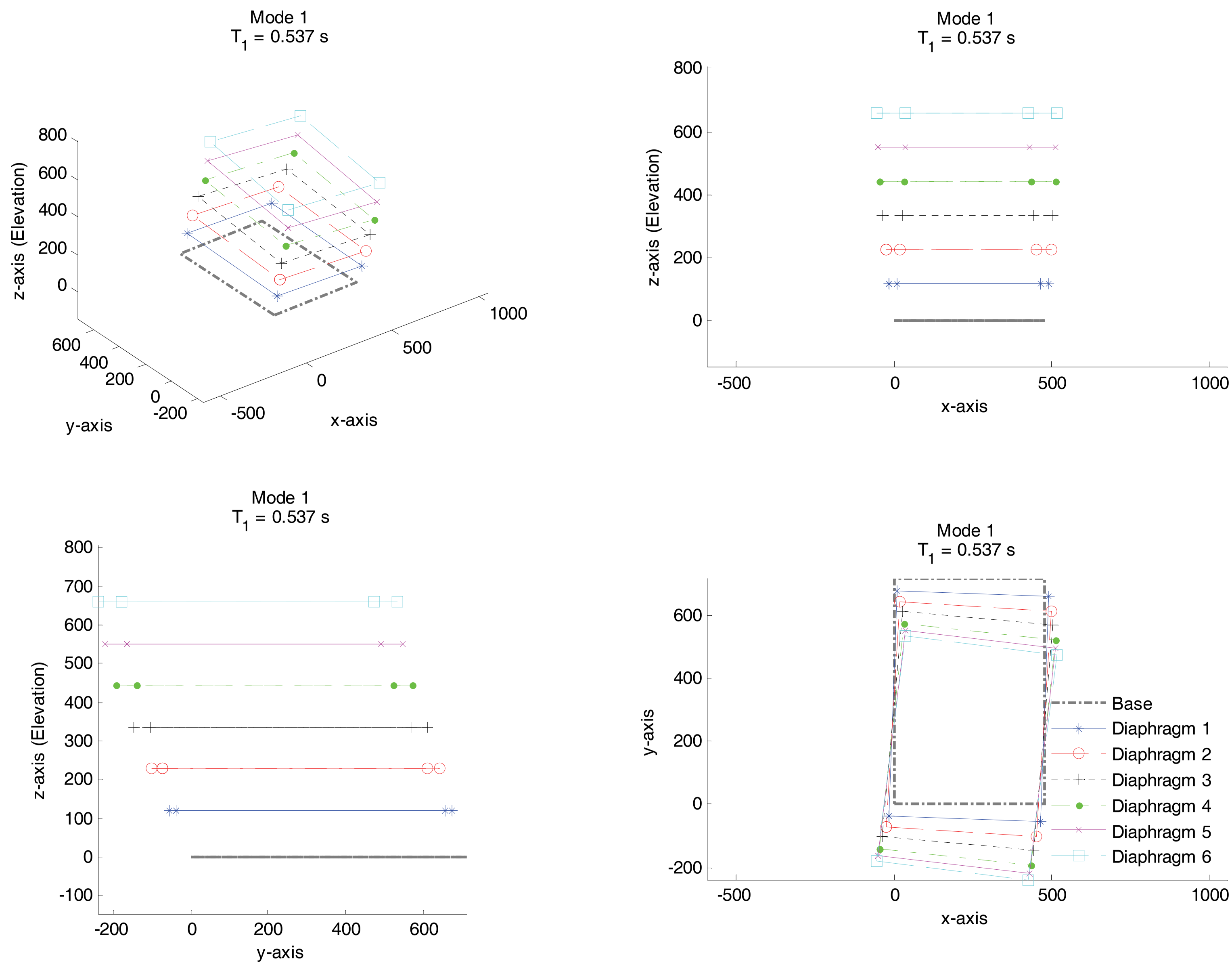

Figure F-8: Mode shape 1 of the M-SAWS model (tangent stiffness at 0.15% drift).

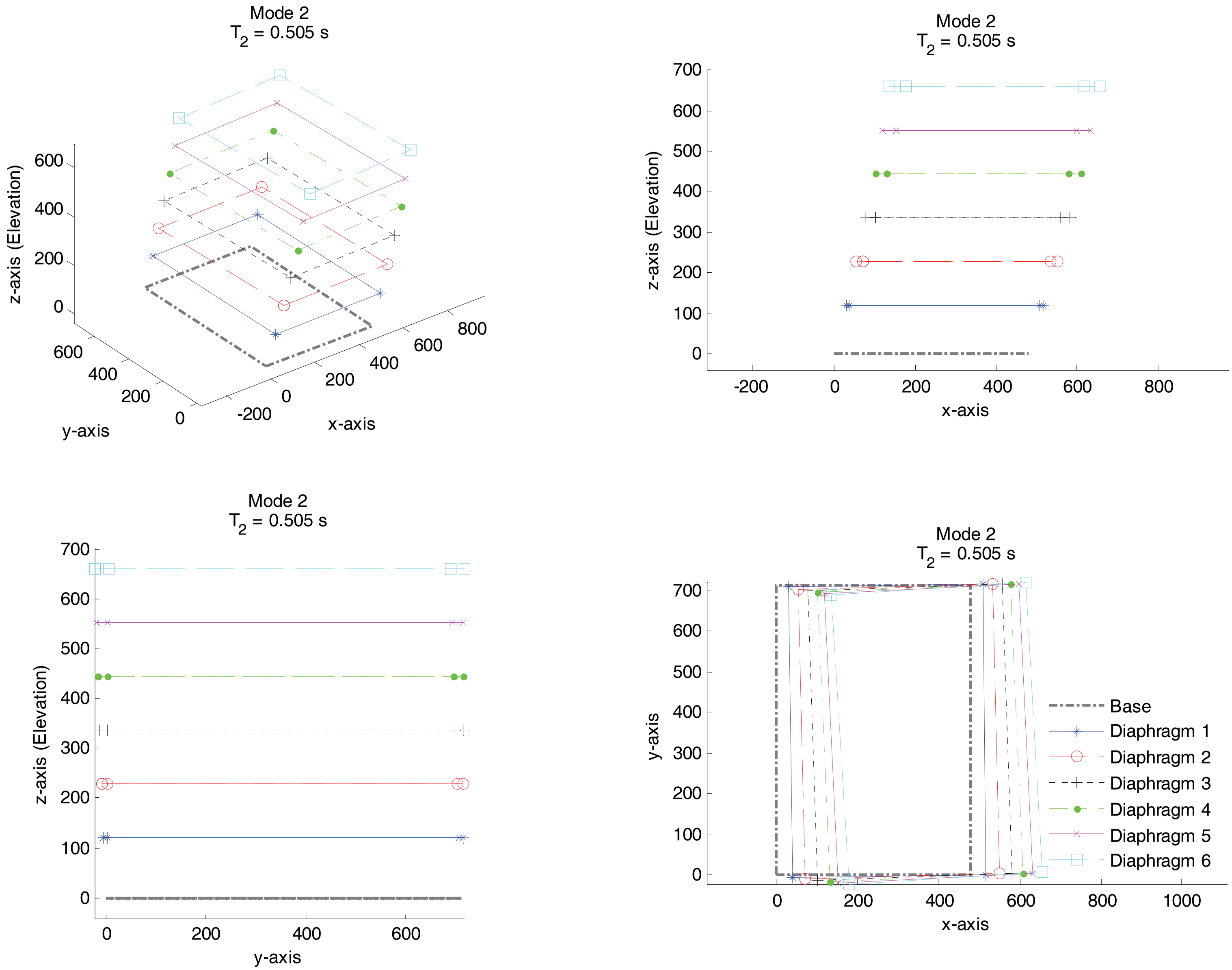

Figure F-9: Mode shape 2 of the M-SAWS model (tangent stiffness at 0.15% drift).

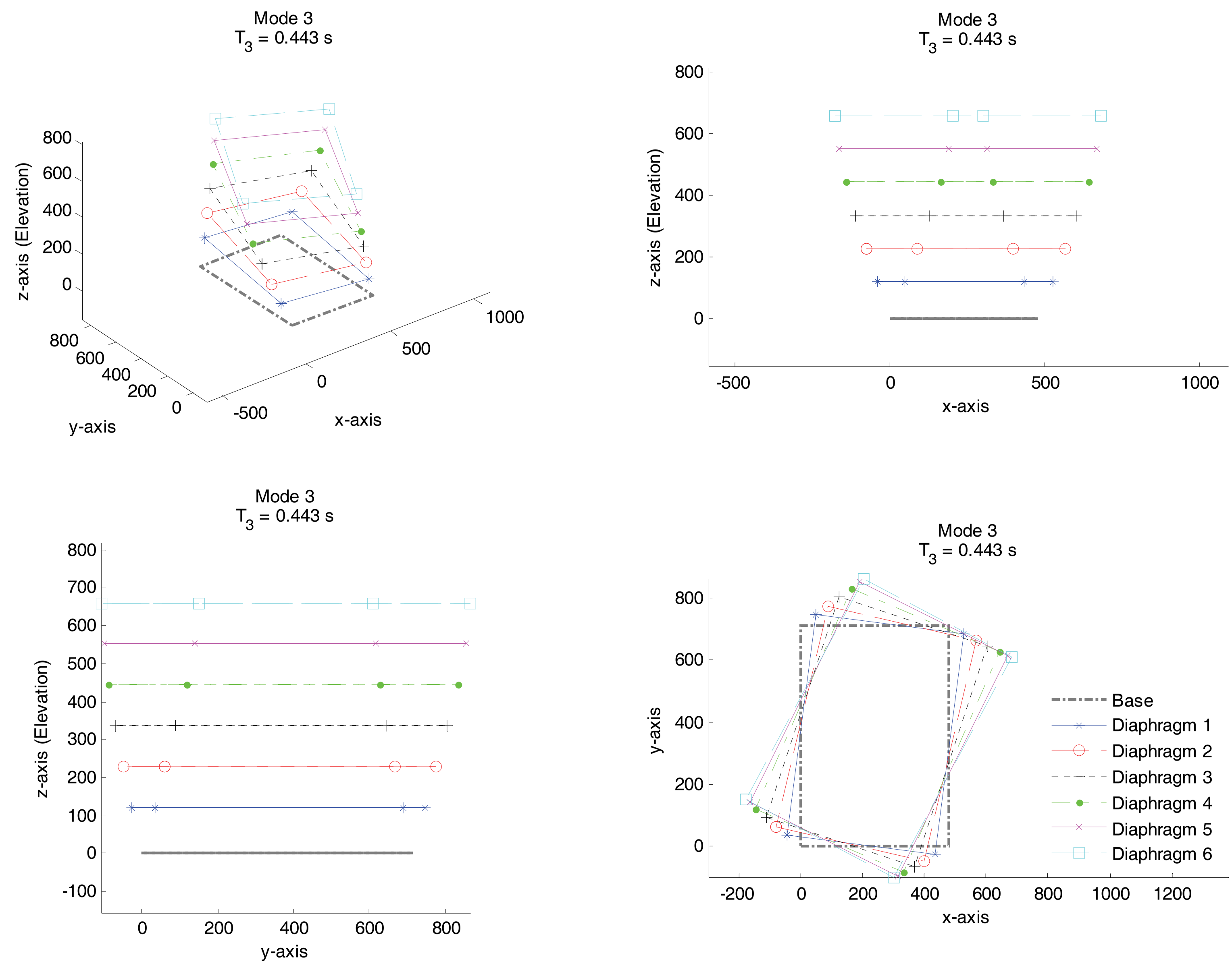

Figure F-10: Mode shape 3 of the M-SAWS model (tangent stiffness at 0.15% drift).

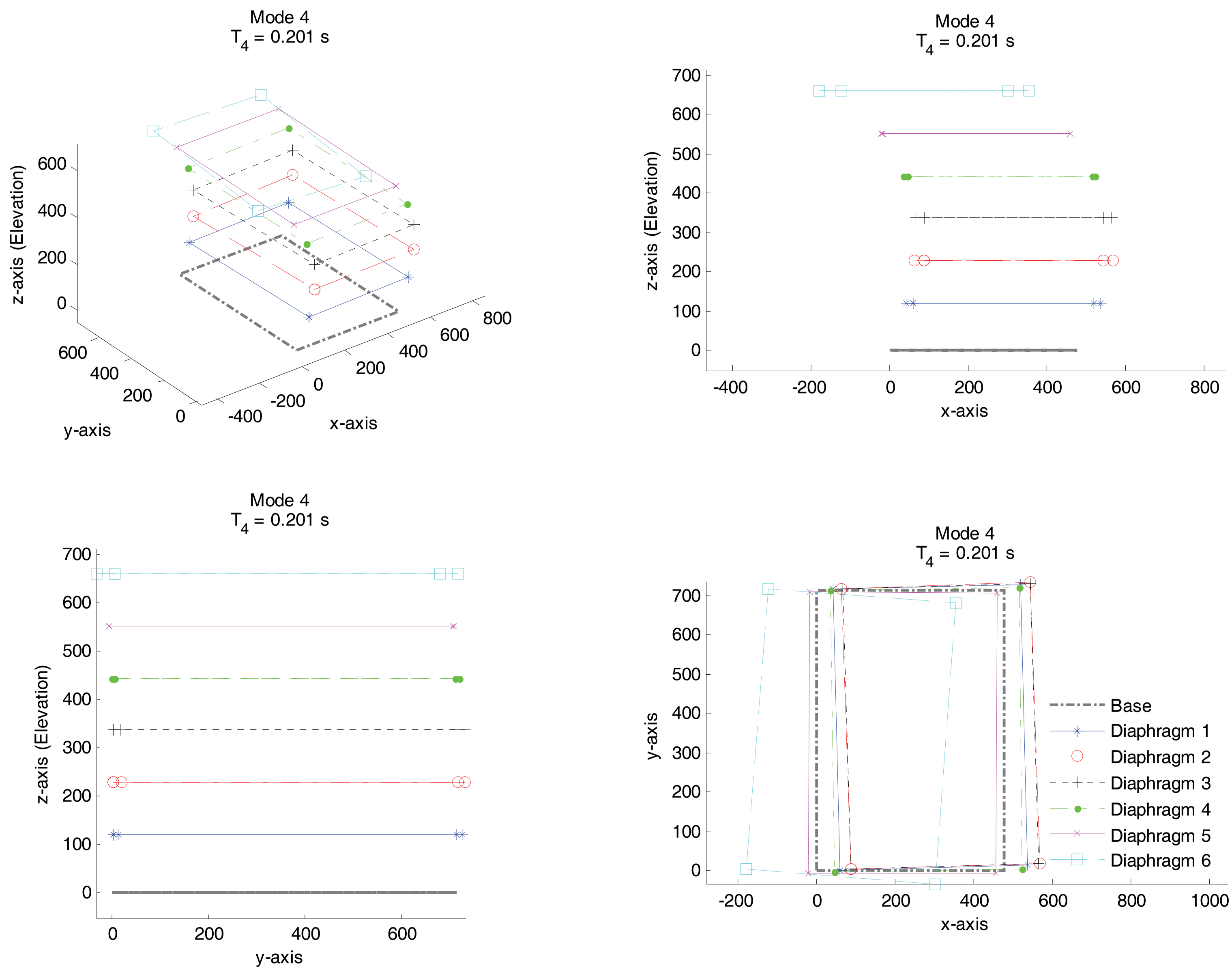

Figure F-11: Mode shape 4 of the M-SAWS model (tangent stiffness at 0.15% drift).

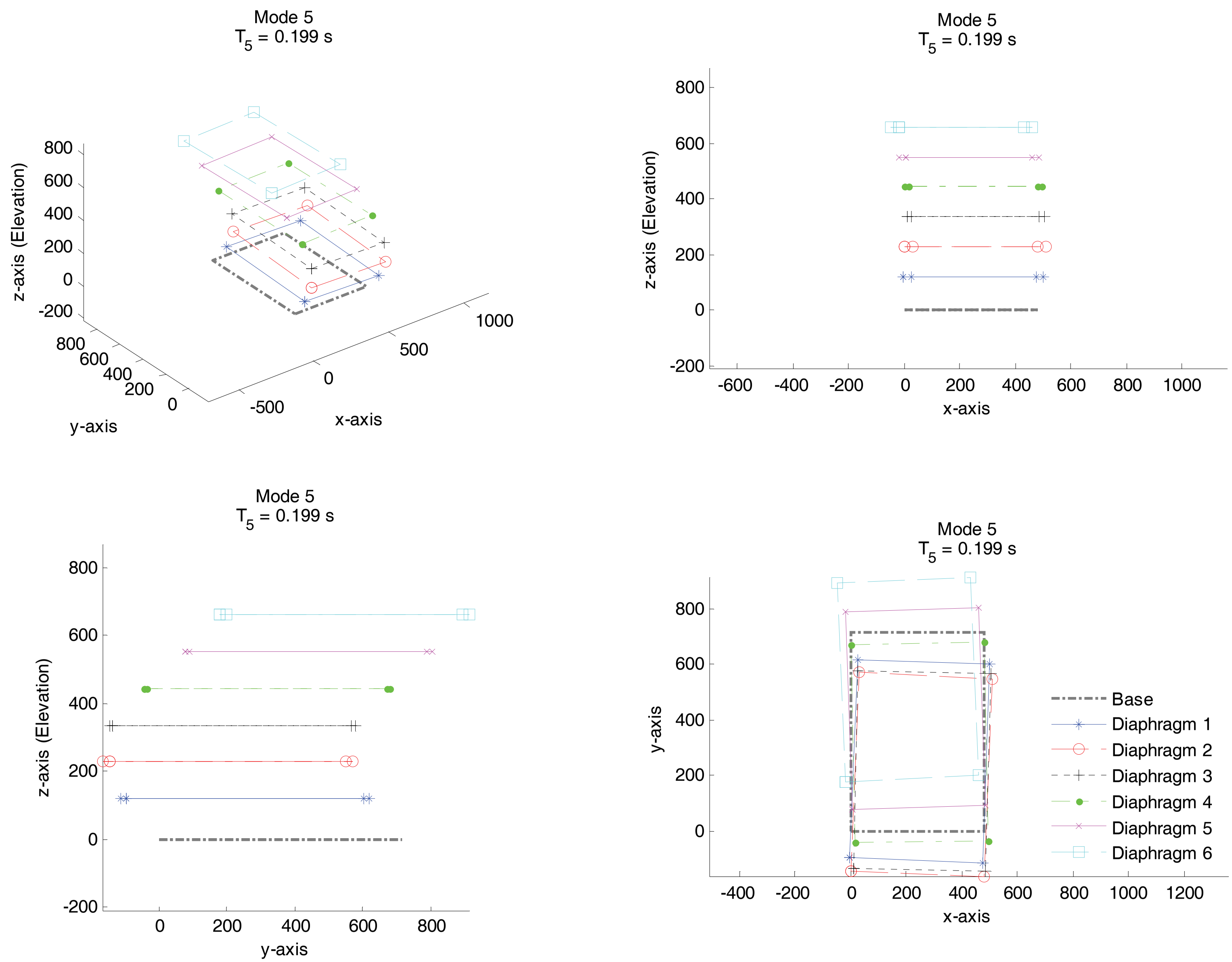

Figure F-12: Mode shape 5 of the M-SAWS model (tangent stiffness at 0.15% drift).

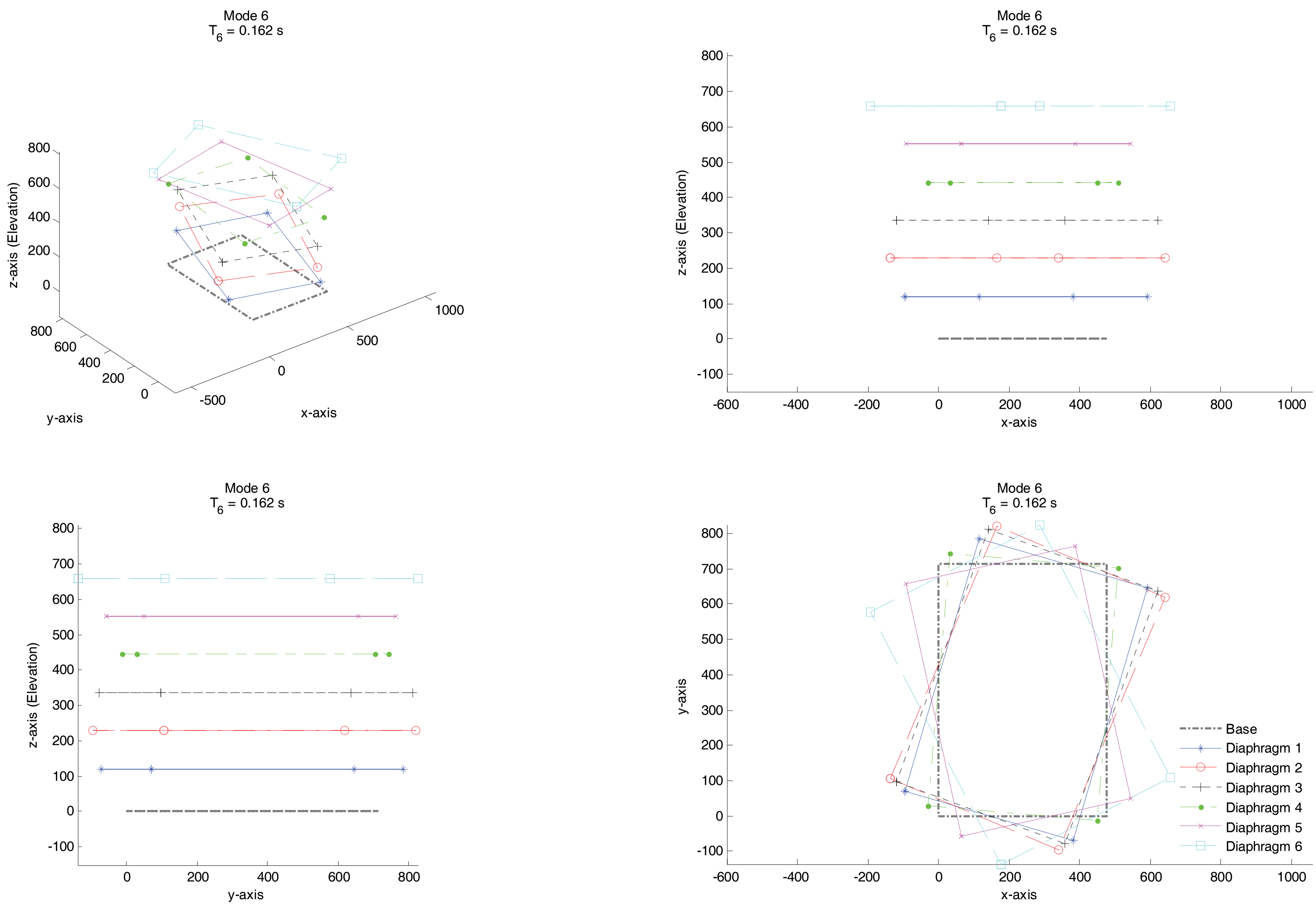

Figure F-13: Mode shape 6 of the M-SAWS model (tangent stiffness at 0.15% drift).

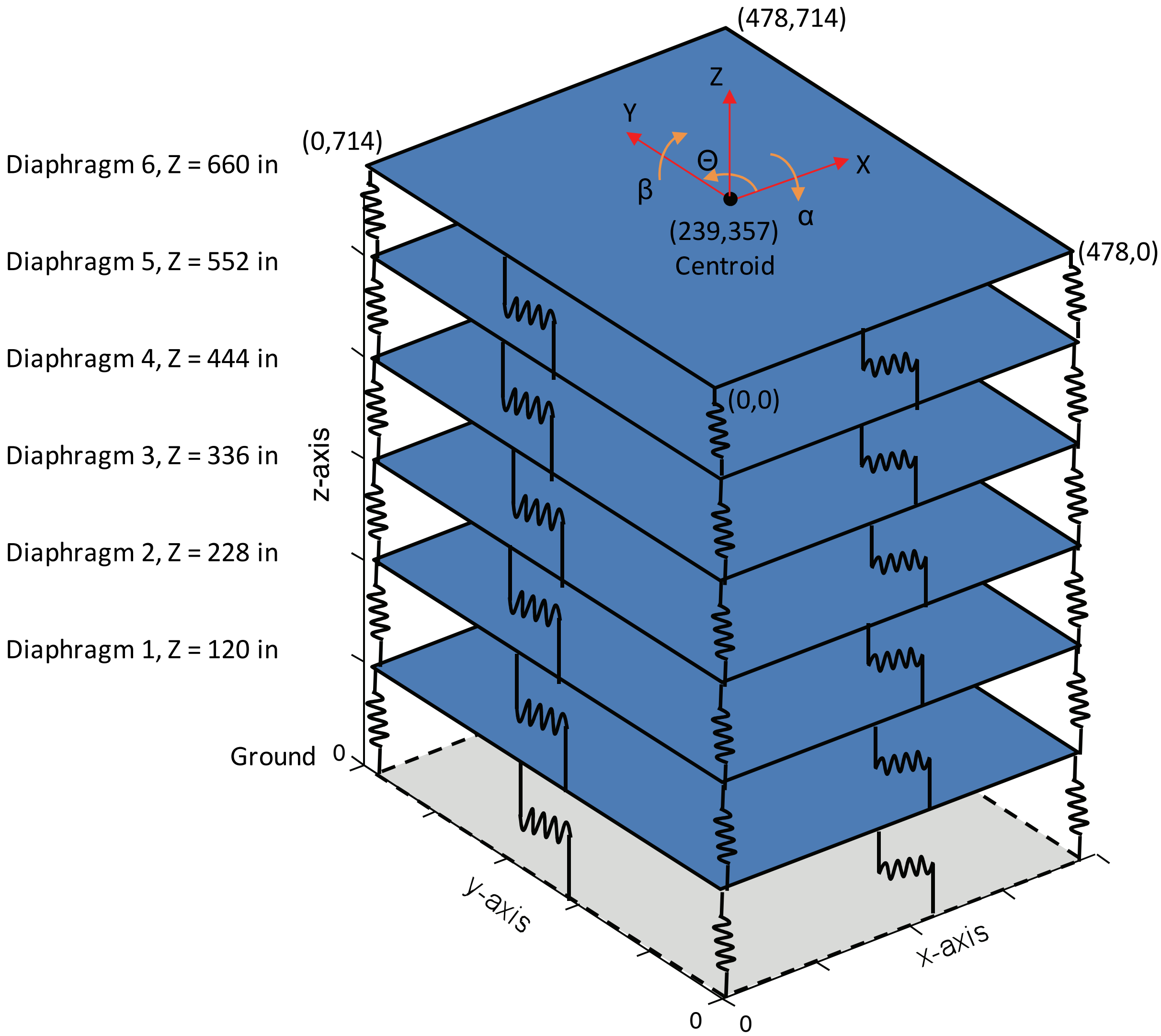

Figure F-14: Diaphragm degrees-of-freedom and corner coordinates in the SAPWood model.

SAPWood 3D Model (Initial Stiffness)

Table F-5: First 6 mode shapes based on initial stiffness of the SAPWood model.

Period (s)			0.398	0.391	0.321	0.162	0.148	0.119
Diaphragm	D.O.F.		Mode 1	Mode 2	Mode 3	Mode 4	Mode 5	Mode 6
1	1	X	-0.1741	0.0009	0.0018	0.2201	0.0004	-0.0491
	2	Y	0.0009	0.2133	0.0133	-0.0002	-0.4302	-0.0020
	3	Z	-0.0050	-0.0002	0.0000	-0.0039	-0.0007	0.0638
	4	α	0.0000	-0.0001	0.0000	0.0000	-0.0001	0.0000
	5	β	-0.0001	0.0000	0.0000	0.0000	0.0000	0.0001
	6	θ	0.0000	0.0001	-0.0007	0.0000	-0.0001	0.0011
2	7	X	-0.3205	0.0016	0.0032	0.3350	0.0004	-0.0480
	8	Y	0.0017	0.3883	0.0262	-0.0003	-0.6302	-0.0117
	9	Z	-0.0110	-0.0004	0.0000	-0.0119	-0.0018	0.1528
	10	α	0.0000	-0.0001	0.0000	0.0000	-0.0002	0.0000
	11	β	-0.0002	0.0000	0.0000	-0.0001	0.0000	0.0003
	12	θ	0.0000	0.0002	-0.0012	0.0000	-0.0001	0.0016
3	13	X	-0.4730	0.0023	0.0045	0.3538	0.0001	-0.0014
	14	Y	0.0025	0.5533	0.0389	-0.0005	-0.6029	-0.0250
	15	Z	-0.0166	-0.0006	0.0000	-0.0243	-0.0034	0.2715
	16	α	0.0000	-0.0002	0.0000	0.0000	-0.0004	0.0000
	17	β	-0.0004	0.0000	0.0000	-0.0003	0.0000	0.0005
	18	θ	0.0000	0.0003	-0.0017	0.0001	-0.0001	0.0015
4	19	X	-0.6317	0.0031	0.0057	0.2486	-0.0006	0.0744
	20	Y	0.0034	0.7267	0.0573	-0.0006	-0.2935	-0.0280
	21	Z	-0.0219	-0.0007	0.0000	-0.0420	-0.0055	0.4352
	22	α	0.0000	-0.0002	0.0000	0.0000	-0.0006	0.0000
	23	β	-0.0005	0.0000	0.0000	-0.0006	0.0000	0.0008
	24	θ	0.0000	0.0003	-0.0022	0.0000	0.0000	0.0006
5	25	X	-0.7843	0.0037	0.0066	0.0126	-0.0013	0.1267
	26	Y	0.0042	0.8650	0.0732	-0.0005	0.1942	-0.0103
	27	Z	-0.0250	-0.0009	0.0000	-0.0594	-0.0080	0.6644
	28	α	0.0000	-0.0003	0.0000	0.0000	-0.0009	0.0000
	29	β	-0.0006	0.0000	0.0000	-0.0010	0.0000	0.0010
	30	θ	0.0000	0.0004	-0.0025	0.0000	0.0001	-0.0006
6	31	X	-1.0000	0.0056	-0.0026	-0.6612	0.0033	-0.3097
	32	Y	0.0051	1.0000	0.0920	0.0004	1.0000	0.0664
	33	Z	-0.0236	-0.0010	0.0000	-0.0585	-0.0110	1.0000
	34	α	0.0000	-0.0003	0.0000	0.0000	-0.0012	0.0000
	35	β	-0.0007	0.0000	0.0000	-0.0015	0.0000	0.0006
	36	θ	0.0000	0.0004	-0.0028	-0.0001	0.0002	-0.0025

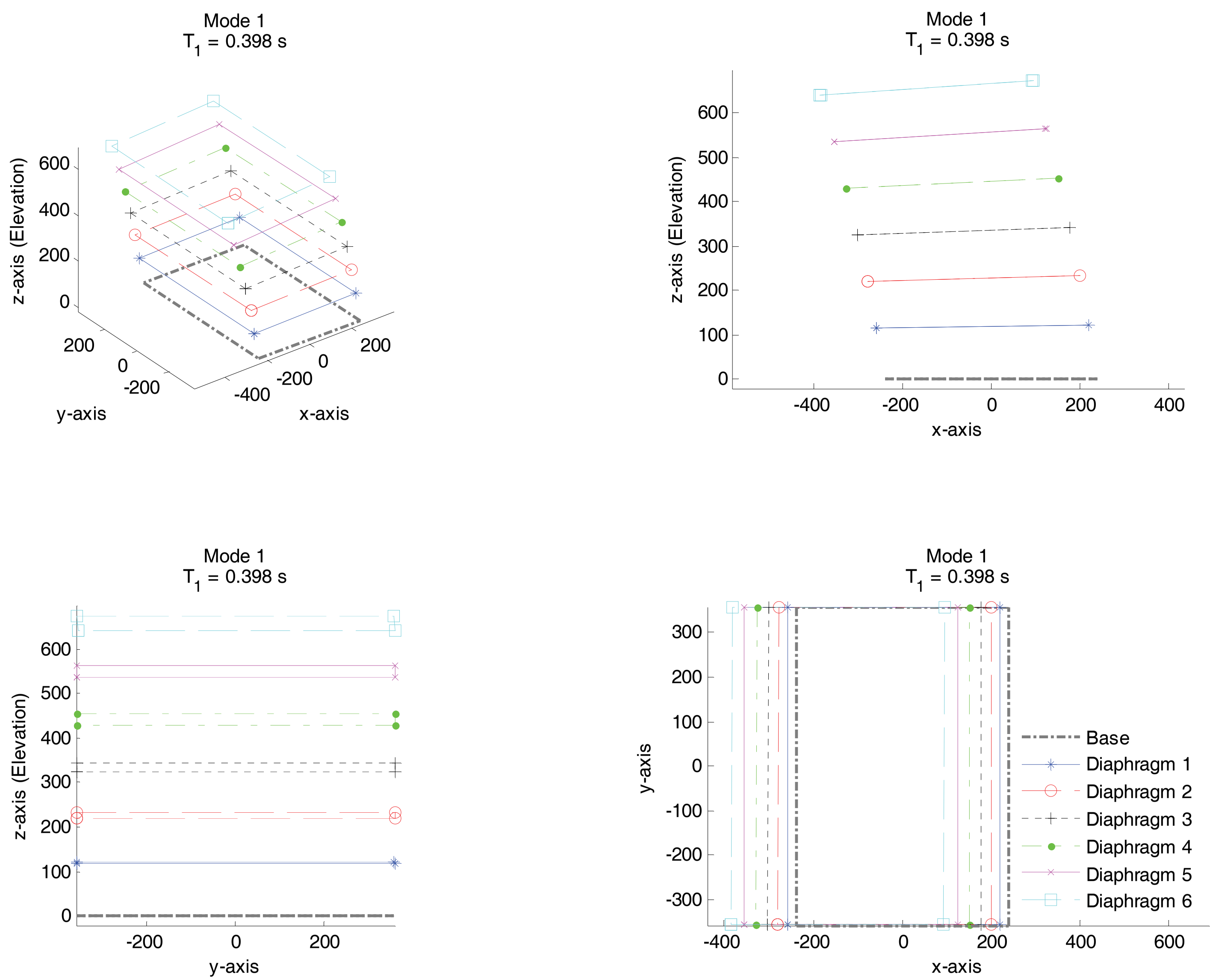

Figure F-15: Mode shape 1 of the SAPWood model (initial stiffness).

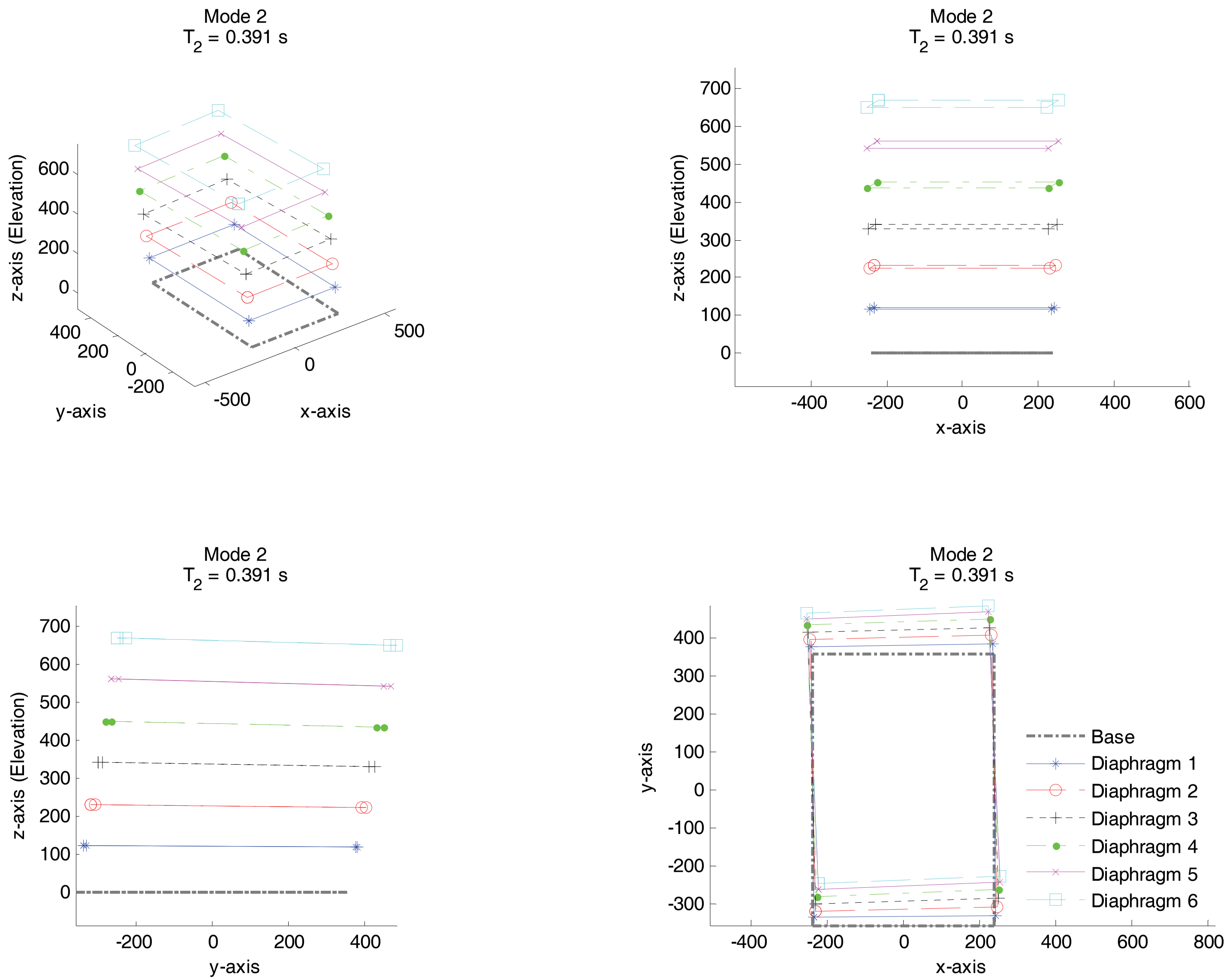

Figure F-16: Mode shape 2 of the SAPWood model (initial stiffness).

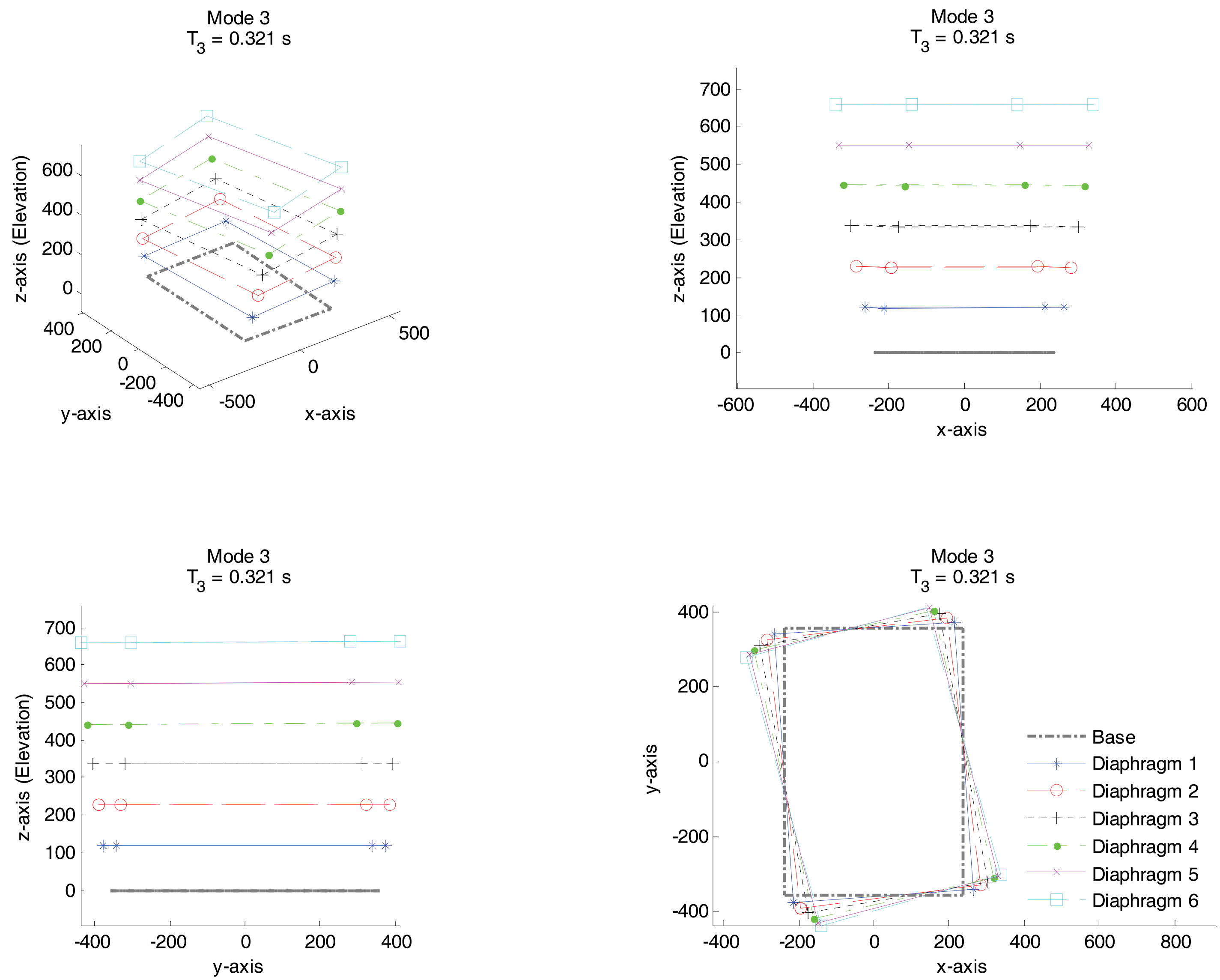

Figure F-17: Mode shape 3 of the SAPWood model (initial stiffness).

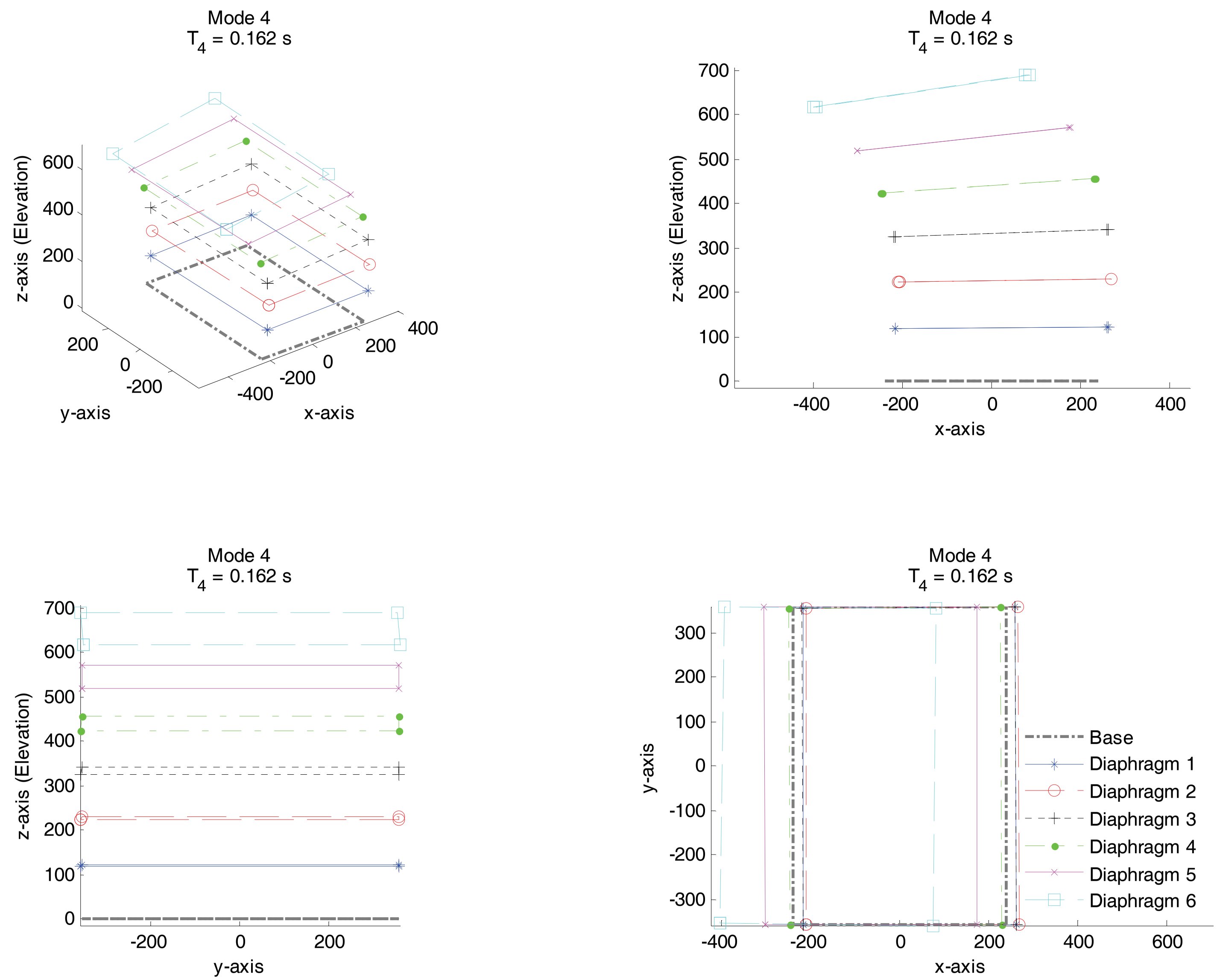

Figure F-18: Mode shape 4 of the SAPWood model (initial stiffness).

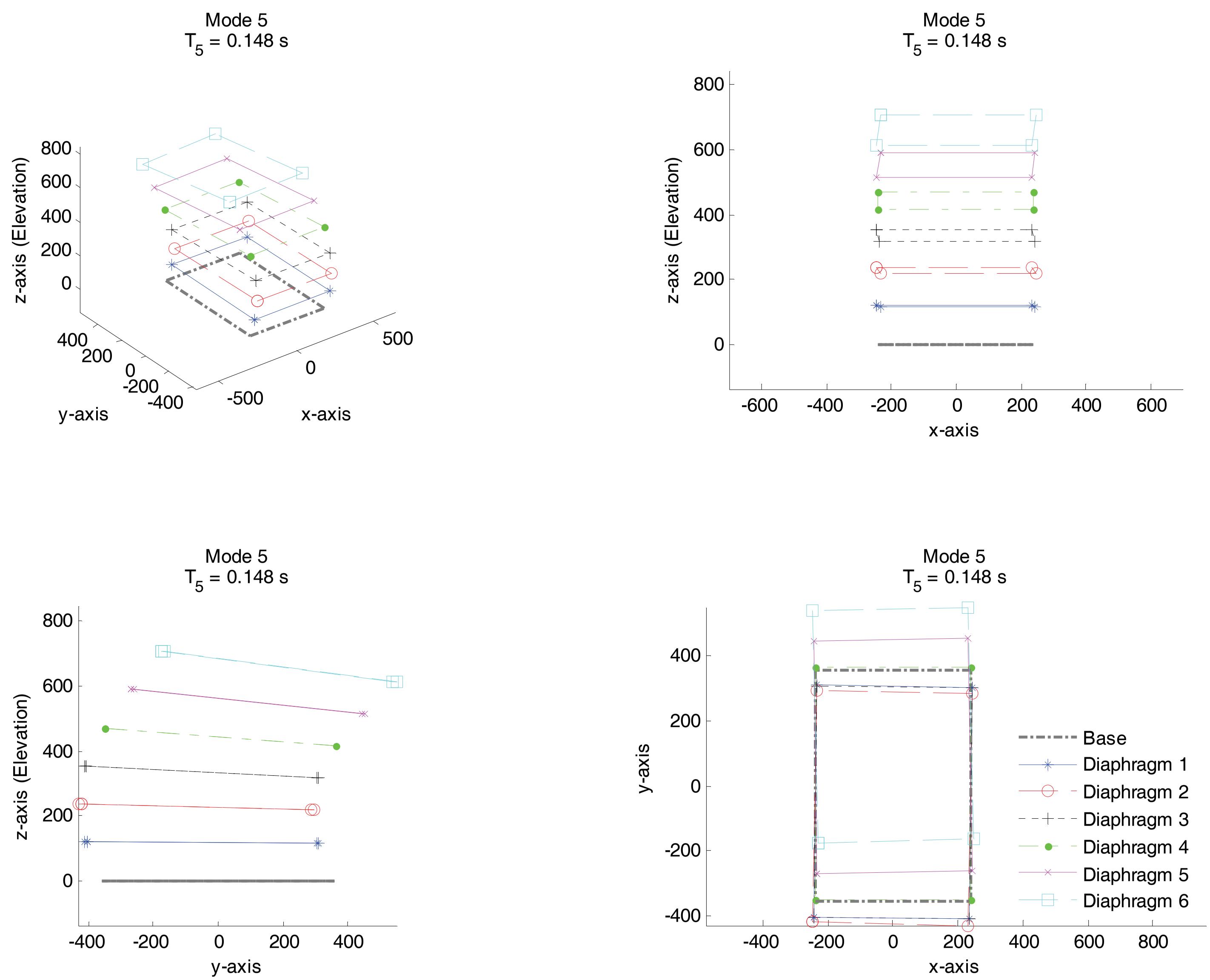

Figure F-19: Mode shape 5 of the SAPWood model (initial stiffness).

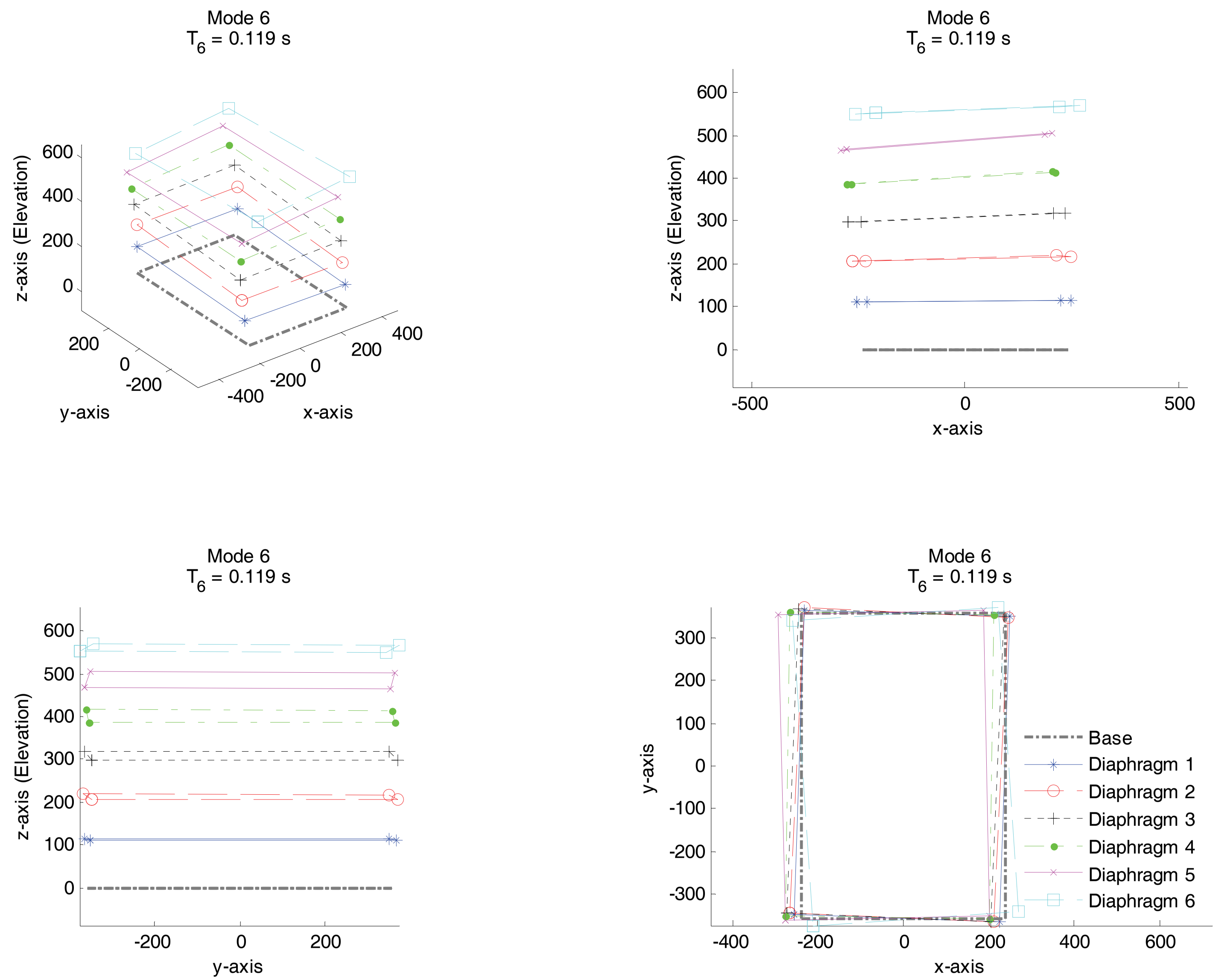

Figure F-20: Mode shape 6 of the SAPWood model (initial stiffness).

Appendix G

Spectral Scaling Factors for ATC-63 Far-Field Ground Motions

Approximate Fundamental Period of the Six-story Capstone Building [ASCE 7-05, 12.8.2]

$T_a = C_t h_n^x$ [ASCE 7-05, Equation 12.8-7]

h_n = total height, measure from ground level to the roof (not including the 3-ft parapet)
= 55 ft

$C_t = 0.02$ [ASCE 7-05, Table 12.8.2]

$x = 0.75$

$T_a = 0.02(55)^{0.75} = 0.404\,\mathrm{s}$

Upper Limit of the Approximate Fundamental Period

C_u = coefficient for upper limit on calculated period [ASCE 7-05, Table 12.8-1]
= 1.4 for $S_{D1} \geq 0.4g$

$T_u = C_u T_a = 1.4 \times 0.404s = 0.57s$

Normalized ATC-63 Far Field Ground Motion Set
Median S_a value @ [T_u=0.57s] = 0.655g

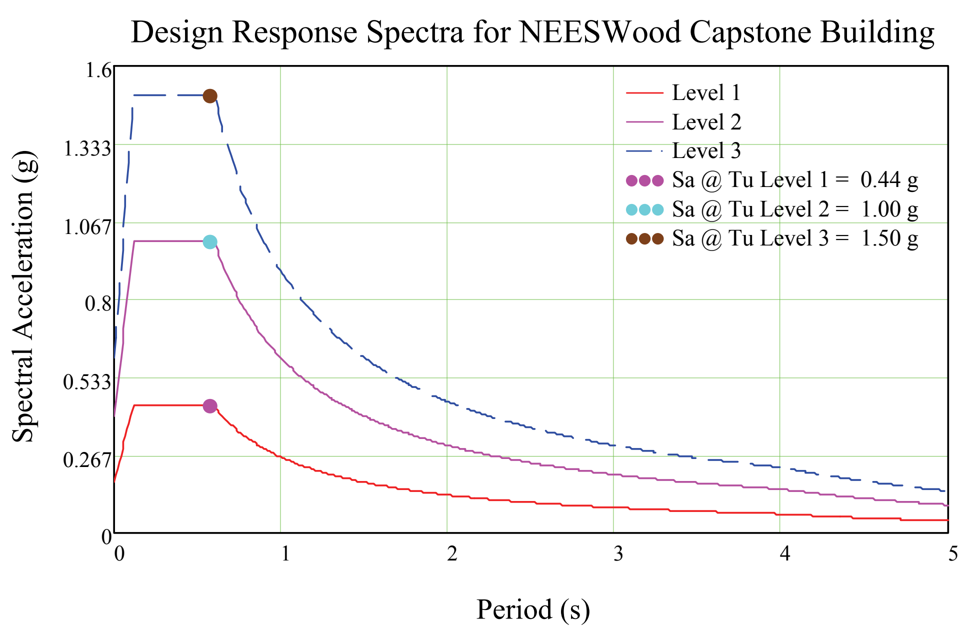

Figure G-1: Design spectral acceleration values at the upper limit of the approximate period for the NEESWood Capstone Building.

Ensemble Scale Factors
Level 1 = 0.44/0.655 = 0.672
Level 2 = 1.00/0.655 = 1.527
Level 3 = 1.50/0.655 = 2.290

Table G-1: Factors for Scaling ATC-63 Far Field Ground Motion Records to the NEESWood Capstone Design Response Spectra.

EQ No.	PEER-NGA Record File Names		ATC-63 Norm. Factor	Scale Factors		
				Level 1	Level 2	Level 3
	Component 1	Component 2		0.672	1.527	2.290
1	NORTHR/MUL009	NORTHR/MUL279	0.651	0.437	0.994	1.490
2	NORTHR/LOS000	NORTHR/LOS270	0.832	0.559	1.270	1.904
3	DUZCE/BOL000	DUZCE/BOL090	0.629	0.423	0.961	1.441
4	HECTOR/HEC000	HECTOR/HEC090	1.092	0.734	1.667	2.500
5	IMPVALL/H-DLT262	IMPVALL/H-DLT352	1.311	0.881	2.003	3.003
6	IMPVALL/H-E11140	IMPVALL/H-E11230	1.014	0.681	1.548	2.322
7	KOBE/NIS000	KOBE/NIS090	1.034	0.695	1.579	2.368
8	KOBE/SHI000	KOBE/SHI090	1.099	0.739	1.678	2.517
9	KOCAELI/DZC180	KOCAELI/DZC270	0.688	0.463	1.051	1.576
10	KOCAELI/ARC000	KOCAELI/ARC090	1.360	0.914	2.077	3.115
11	LANDERS/YER270	LANDERS/YER360	0.987	0.663	1.506	2.259
12	LANDERS/CLW-LN	LANDERS/CLW-TR	1.149	0.772	1.754	2.631
13	LOMAP/CAP000	LOMAP/CAP090	1.089	0.731	1.662	2.493
14	LOMAP/G03000	LOMAP/G03090	0.880	0.592	1.344	2.016
15	MANJIL/ABBAR--L	MANJIL/ABBAR--T	0.787	0.529	1.202	1.803
16	SUPERST/B-ICC000	SUPERST/B-ICC090	0.870	0.584	1.328	1.992
17	SUPERST/B-POE270	SUPERST/B-POE360	1.174	0.789	1.793	2.689
18	CAPEMEND/RIO270	CAPEMEND/RIO360	0.820	0.551	1.252	1.878
19	CHICHI/CHY101-E	CHICHI/CHY101-N	0.410	0.276	0.627	0.940
20	CHICHI/TCU045-E	CHICHI/TCU045-N	0.959	0.645	1.465	2.197
21	SFERN/PEL090	SFERN/PEL180	2.096	1.409	3.201	4.800
22	FRIULI/A-TMZ000	FRIULI/A-TMZ270	1.440	0.968	2.199	3.298

(a) ATC-63 Normalization factors are obtained from Table A-4D of the ATC-63 90% draft report.
(b) Scale factors for individual record are in blue color.

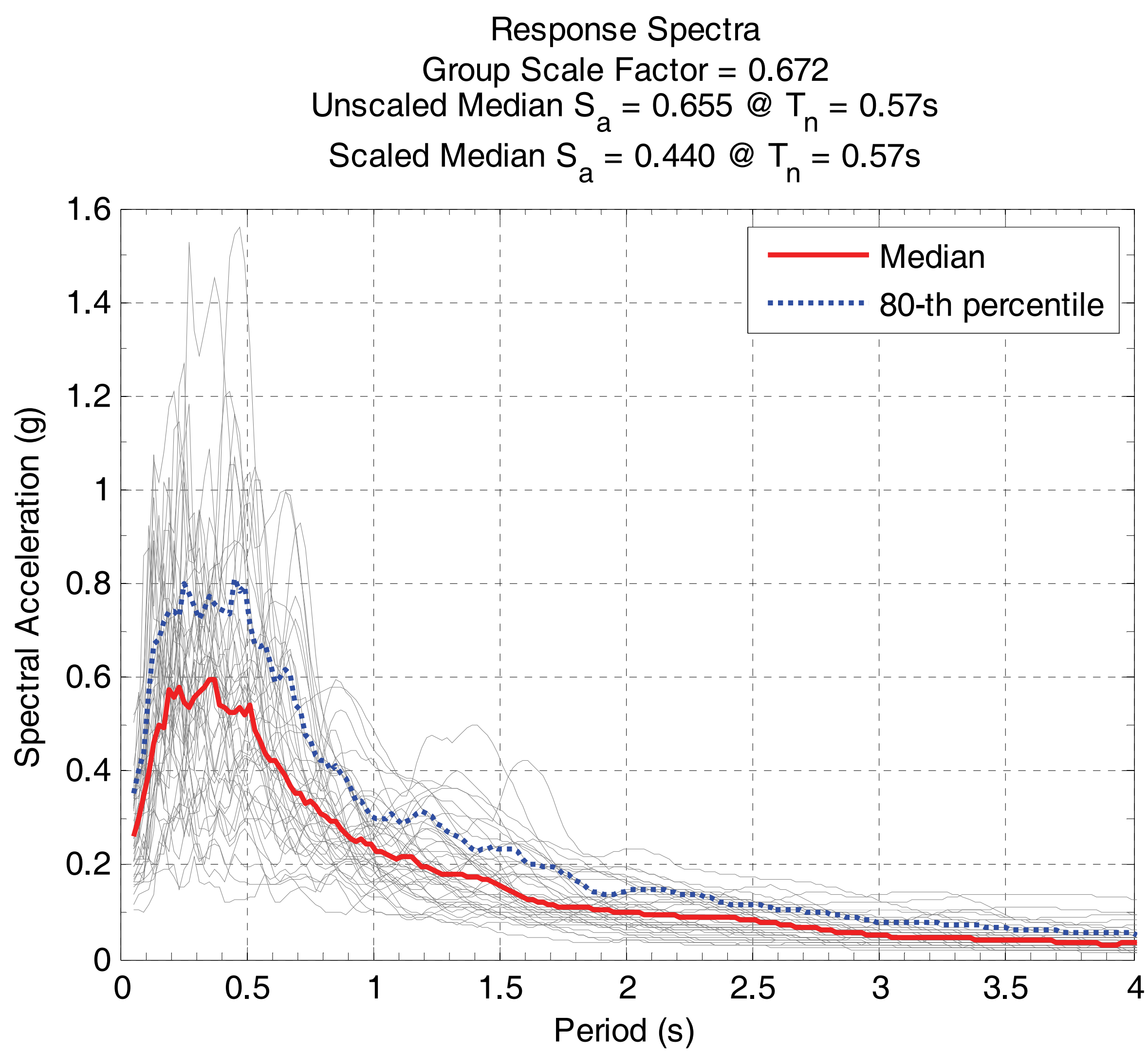

Figure G-2: ATC-63 far-field ground motion ensemble scaled to the design spectrum for seismic hazard Level 1 (50%/50yr).

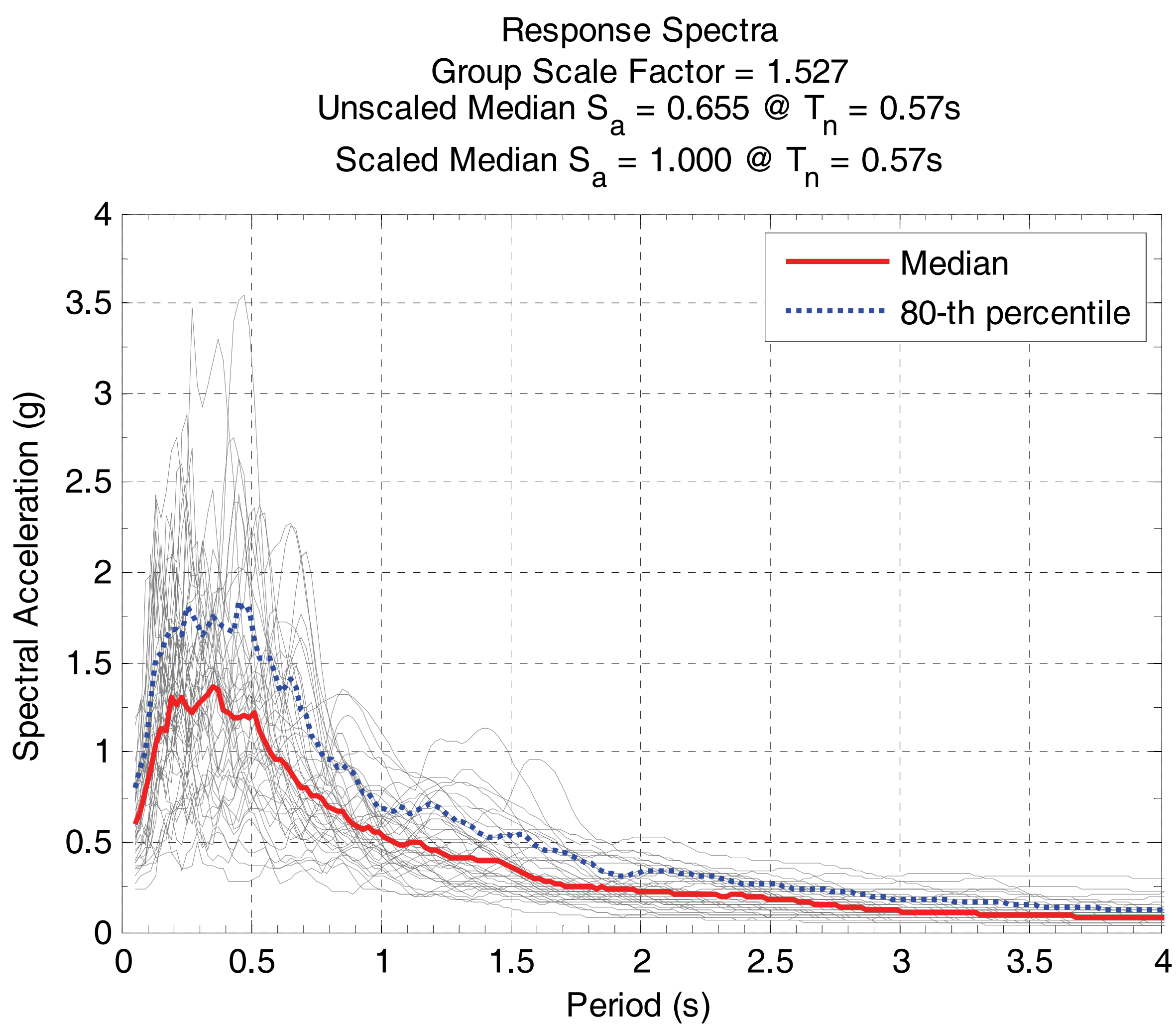

Figure G-3: ATC-63 far-field ground motion ensemble scaled to the design spectrum for seismic hazard Level 2 (10%/50yr).

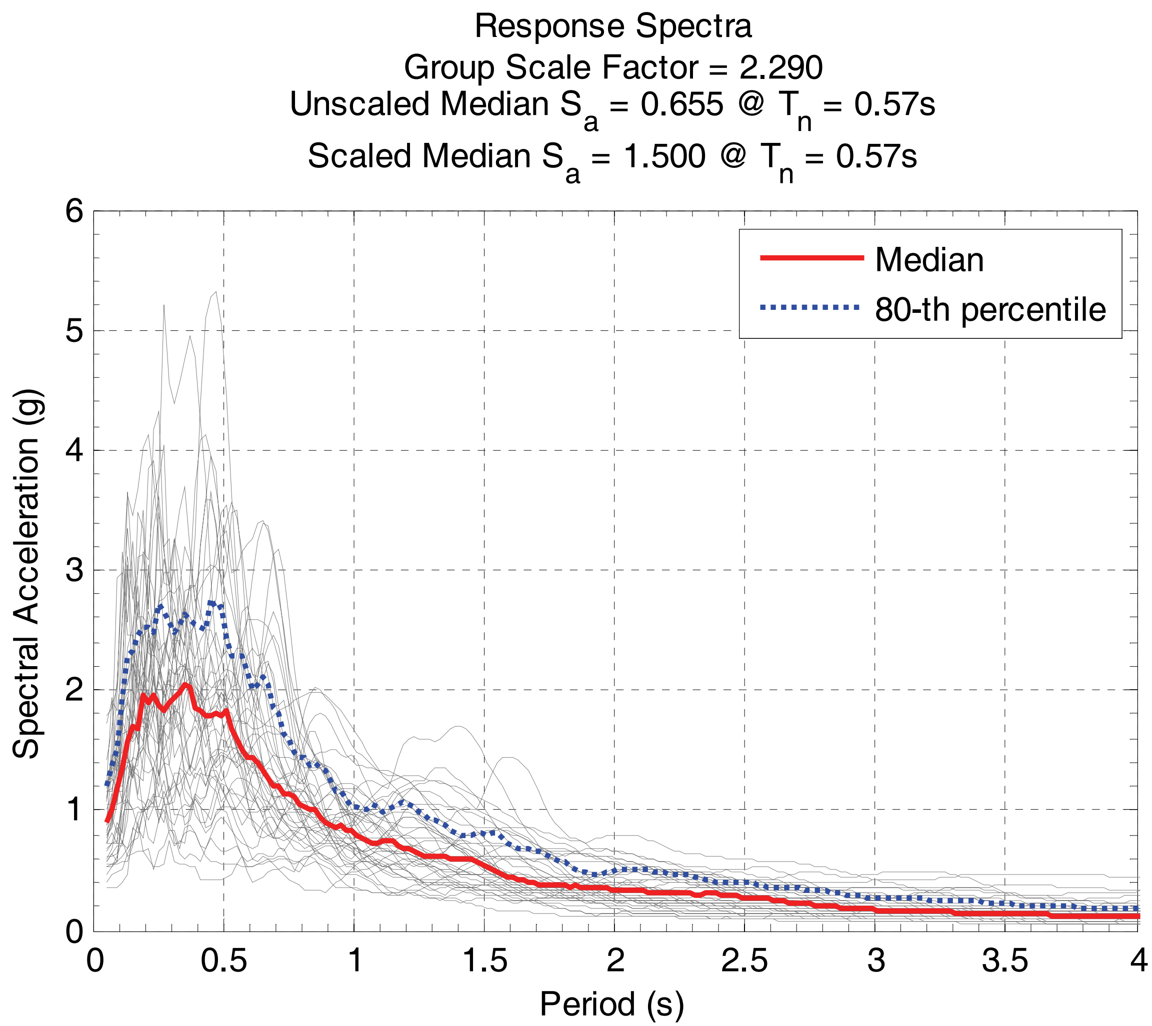

Figure G-4: ATC-63 far-field ground motion ensemble scaled to the design spectrum for seismic hazard Level 3 (2%/50yr).

Appendix H

Near-Fault Ground Motions

No.	Earthquake			Station	NEHRP Soil Type	M-SAWS Input Filename	PGA Component (g)		Record Duration (s)	Source
	M	Year	Name				1	2		
1	6.9	1995	[a]Kobe	n/a	D	KB95kobj.ga2	1.07	0.56	59.96	[b]SAC: NF17 & NF18
2	6.9	1995	[a]Kobe Tato	Takatori	D	KB95tato.ga2	0.77	0.42	40.08	[b]SAC: NF19 & NF20
3	7.0	1989	[a]Loma Prieta	Lex	C	LP89lex.ga2	0.67	0.36	39.97	[b]SAC: NF05 & NF06
4	6.2	1984	Morgan Hill	Coyote Lake Dam	C	MH84cyld.ga2	0.71	1.30	29.95	[c]PEER CYC195.AT2,CYC285.AT2
5	6.7	1994	Northridge	Newhall Fire Station	D	NR94newh.ga2	0.58	0.59	39.98	[c]PEER: NWH090.AT2, NEH360.AT2
6	6.7	1994	Northridge	Rinaldi	D	NR94rrs.ga2	0.84	0.47	14.945	[c]PEER: RRS228.AT2, RRS318.AT2

[a] The individual components of each ground motion have been rotated 45 degrees away from the fault-normal and fault-parallel orientations

[b] Ground motion records were obtained from SAC project website. http://nisee.berkeley.edu/data/strong_motion/sacsteel/motions/nearfault.html

[c] Ground motion records were obtained from PEER Strong Motion Database website. http://peer.berkeley.edu/smcat/index.html

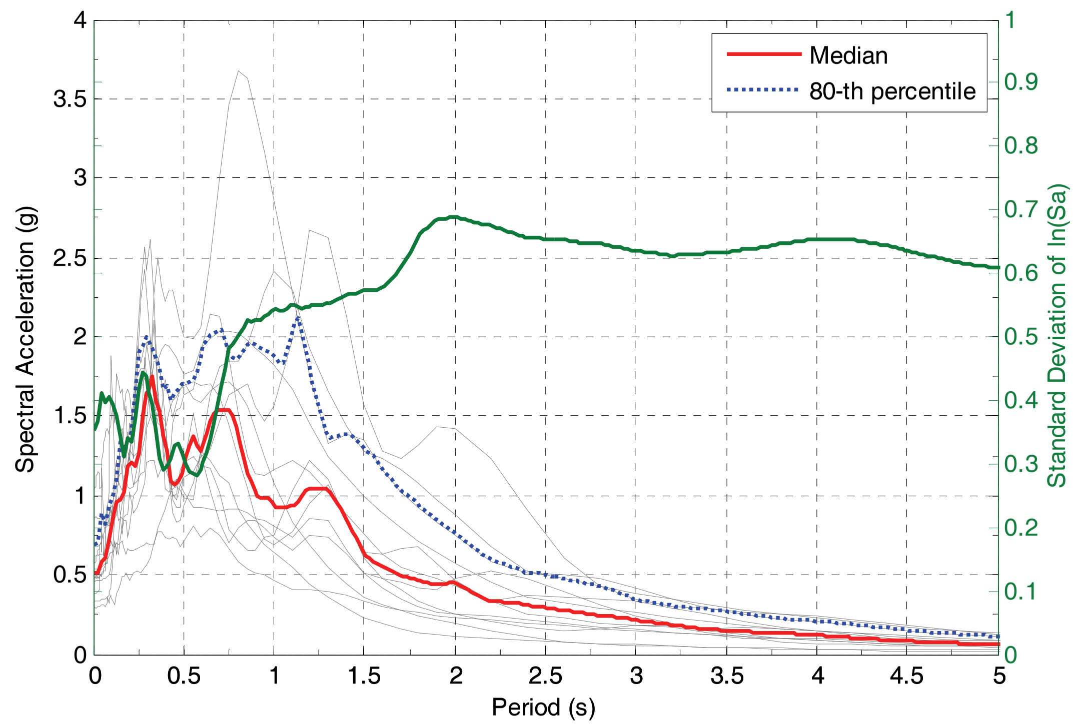

Figure H-1: Response spectra of unscaled near-fault ground motion ensemble.

MCEER Technical Reports

MCEER publishes technical reports on a variety of subjects written by authors funded through MCEER. These reports are available from both MCEER Publications and the National Technical Information Service (NTIS). Requests for reports should be directed to MCEER Publications, MCEER, University at Buffalo, State University of New York, 133A Ketter Hall, Buffalo, New York 14260. Reports can also be requested through NTIS, P.O. Box 1425, Springfield, Virginia 22151. NTIS accession numbers are shown in parenthesis, if available.

NCEER-87-0001 "First-Year Program in Research, Education and Technology Transfer," 3/5/87, (PB88-134275, A04, MF-A01).

NCEER-87-0002 "Experimental Evaluation of Instantaneous Optimal Algorithms for Structural Control," by R.C. Lin, T.T. Soong and A.M. Reinhorn, 4/20/87, (PB88-134341, A04, MF-A01).

NCEER-87-0003 "Experimentation Using the Earthquake Simulation Facilities at University at Buffalo," by A.M. Reinhorn and R.L. Ketter, to be published.

NCEER-87-0004 "The System Characteristics and Performance of a Shaking Table," by J.S. Hwang, K.C. Chang and G.C. Lee, 6/1/87, (PB88-134259, A03, MF-A01). This report is available only through NTIS (see address given above).

NCEER-87-0005 "A Finite Element Formulation for Nonlinear Viscoplastic Material Using a Q Model," by O. Gyebi and G. Dasgupta, 11/2/87, (PB88-213764, A08, MF-A01).

NCEER-87-0006 "Symbolic Manipulation Program (SMP) - Algebraic Codes for Two and Three Dimensional Finite Element Formulations," by X. Lee and G. Dasgupta, 11/9/87, (PB88-218522, A05, MF-A01).

NCEER-87-0007 "Instantaneous Optimal Control Laws for Tall Buildings Under Seismic Excitations," by J.N. Yang, A. Akbarpour and P. Ghaemmaghami, 6/10/87, (PB88-134333, A06, MF-A01). This report is only available through NTIS (see address given above).

NCEER-87-0008 "IDARC: Inelastic Damage Analysis of Reinforced Concrete Frame - Shear-Wall Structures," by Y.J. Park, A.M. Reinhorn and S.K. Kunnath, 7/20/87, (PB88-134325, A09, MF-A01). This report is only available through NTIS (see address given above).

NCEER-87-0009 "Liquefaction Potential for New York State: A Preliminary Report on Sites in Manhattan and Buffalo," by M. Budhu, V. Vijayakumar, R.F. Giese and L. Baumgras, 8/31/87, (PB88-163704, A03, MF-A01). This report is available only through NTIS (see address given above).

NCEER-87-0010 "Vertical and Torsional Vibration of Foundations in Inhomogeneous Media," by A.S. Veletsos and K.W. Dotson, 6/1/87, (PB88-134291, A03, MF-A01). This report is only available through NTIS (see address given above).

NCEER-87-0011 "Seismic Probabilistic Risk Assessment and Seismic Margins Studies for Nuclear Power Plants," by Howard H.M. Hwang, 6/15/87, (PB88-134267, A03, MF-A01). This report is only available through NTIS (see address given above).

NCEER-87-0012 "Parametric Studies of Frequency Response of Secondary Systems Under Ground-Acceleration Excitations," by Y. Yong and Y.K. Lin, 6/10/87, (PB88-134309, A03, MF-A01). This report is only available through NTIS (see address given above).

NCEER-87-0013 "Frequency Response of Secondary Systems Under Seismic Excitation," by J.A. HoLung, J. Cai and Y.K. Lin, 7/31/87, (PB88-134317, A05, MF-A01). This report is only available through NTIS (see address given above).

NCEER-87-0014 "Modelling Earthquake Ground Motions in Seismically Active Regions Using Parametric Time Series Methods," by G.W. Ellis and A.S. Cakmak, 8/25/87, (PB88-134283, A08, MF-A01). This report is only available through NTIS (see address given above).

NCEER-87-0015 "Detection and Assessment of Seismic Structural Damage," by E. DiPasquale and A.S. Cakmak, 8/25/87, (PB88-163712, A05, MF-A01). This report is only available through NTIS (see address given above).

NCEER-87-0016 "Pipeline Experiment at Parkfield, California," by J. Isenberg and E. Richardson, 9/15/87, (PB88-163720, A03, MF-A01). This report is available only through NTIS (see address given above).

NCEER-87-0017 "Digital Simulation of Seismic Ground Motion," by M. Shinozuka, G. Deodatis and T. Harada, 8/31/87, (PB88-155197, A04, MF-A01). This report is available only through NTIS (see address given above).

NCEER-87-0018 "Practical Considerations for Structural Control: System Uncertainty, System Time Delay and Truncation of Small Control Forces," J.N. Yang and A. Akbarpour, 8/10/87, (PB88-163738, A08, MF-A01). This report is only available through NTIS (see address given above).

NCEER-87-0019 "Modal Analysis of Nonclassically Damped Structural Systems Using Canonical Transformation," by J.N. Yang, S. Sarkani and F.X. Long, 9/27/87, (PB88-187851, A04, MF-A01).

NCEER-87-0020 "A Nonstationary Solution in Random Vibration Theory," by J.R. Red-Horse and P.D. Spanos, 11/3/87, (PB88-163746, A03, MF-A01).

NCEER-87-0021 "Horizontal Impedances for Radially Inhomogeneous Viscoelastic Soil Layers," by A.S. Veletsos and K.W. Dotson, 10/15/87, (PB88-150859, A04, MF-A01).

NCEER-87-0022 "Seismic Damage Assessment of Reinforced Concrete Members," by Y.S. Chung, C. Meyer and M. Shinozuka, 10/9/87, (PB88-150867, A05, MF-A01). This report is available only through NTIS (see address given above).

NCEER-87-0023 "Active Structural Control in Civil Engineering," by T.T. Soong, 11/11/87, (PB88-187778, A03, MF-A01).

NCEER-87-0024 "Vertical and Torsional Impedances for Radially Inhomogeneous Viscoelastic Soil Layers," by K.W. Dotson and A.S. Veletsos, 12/87, (PB88-187786, A03, MF-A01).

NCEER-87-0025 "Proceedings from the Symposium on Seismic Hazards, Ground Motions, Soil-Liquefaction and Engineering Practice in Eastern North America," October 20-22, 1987, edited by K.H. Jacob, 12/87, (PB88-188115, A23, MF-A01). This report is available only through NTIS (see address given above).

NCEER-87-0026 "Report on the Whittier-Narrows, California, Earthquake of October 1, 1987," by J. Pantelic and A. Reinhorn, 11/87, (PB88-187752, A03, MF-A01). This report is available only through NTIS (see address given above).

NCEER-87-0027 "Design of a Modular Program for Transient Nonlinear Analysis of Large 3-D Building Structures," by S. Srivastav and J.F. Abel, 12/30/87, (PB88-187950, A05, MF-A01). This report is only available through NTIS (see address given above).

NCEER-87-0028 "Second-Year Program in Research, Education and Technology Transfer," 3/8/88, (PB88-219480, A04, MF-A01).

NCEER-88-0001 "Workshop on Seismic Computer Analysis and Design of Buildings With Interactive Graphics," by W. McGuire, J.F. Abel and C.H. Conley, 1/18/88, (PB88-187760, A03, MF-A01). This report is only available through NTIS (see address given above).

NCEER-88-0002 "Optimal Control of Nonlinear Flexible Structures," by J.N. Yang, F.X. Long and D. Wong, 1/22/88, (PB88-213772, A06, MF-A01).

NCEER-88-0003 "Substructuring Techniques in the Time Domain for Primary-Secondary Structural Systems," by G.D. Manolis and G. Juhn, 2/10/88, (PB88-213780, A04, MF-A01).

NCEER-88-0004 "Iterative Seismic Analysis of Primary-Secondary Systems," by A. Singhal, L.D. Lutes and P.D. Spanos, 2/23/88, (PB88-213798, A04, MF-A01).

NCEER-88-0005 "Stochastic Finite Element Expansion for Random Media," by P.D. Spanos and R. Ghanem, 3/14/88, (PB88-213806, A03, MF-A01).

NCEER-88-0006 "Combining Structural Optimization and Structural Control," by F.Y. Cheng and C.P. Pantelides, 1/10/88, (PB88-213814, A05, MF-A01).

NCEER-88-0007 "Seismic Performance Assessment of Code-Designed Structures," by H.H-M. Hwang, J-W. Jaw and H-J. Shau, 3/20/88, (PB88-219423, A04, MF-A01). This report is only available through NTIS (see address given above).

NCEER-88-0008 "Reliability Analysis of Code-Designed Structures Under Natural Hazards," by H.H-M. Hwang, H. Ushiba and M. Shinozuka, 2/29/88, (PB88-229471, A07, MF-A01). This report is only available through NTIS (see address given above).

NCEER-88-0009 "Seismic Fragility Analysis of Shear Wall Structures," by J-W Jaw and H.H-M. Hwang, 4/30/88, (PB89-102867, A04, MF-A01).

NCEER-88-0010 "Base Isolation of a Multi-Story Building Under a Harmonic Ground Motion - A Comparison of Performances of Various Systems," by F-G Fan, G. Ahmadi and I.G. Tadjbakhsh, 5/18/88, (PB89-122238, A06, MF-A01). This report is only available through NTIS (see address given above).

NCEER-88-0011 "Seismic Floor Response Spectra for a Combined System by Green's Functions," by F.M. Lavelle, L.A. Bergman and P.D. Spanos, 5/1/88, (PB89-102875, A03, MF-A01).

NCEER-88-0012 "A New Solution Technique for Randomly Excited Hysteretic Structures," by G.Q. Cai and Y.K. Lin, 5/16/88, (PB89-102883, A03, MF-A01).

NCEER-88-0013 "A Study of Radiation Damping and Soil-Structure Interaction Effects in the Centrifuge," by K. Weissman, supervised by J.H. Prevost, 5/24/88, (PB89-144703, A06, MF-A01).

NCEER-88-0014 "Parameter Identification and Implementation of a Kinematic Plasticity Model for Frictional Soils," by J.H. Prevost and D.V. Griffiths, to be published.

NCEER-88-0015 "Two- and Three- Dimensional Dynamic Finite Element Analyses of the Long Valley Dam," by D.V. Griffiths and J.H. Prevost, 6/17/88, (PB89-144711, A04, MF-A01).

NCEER-88-0016 "Damage Assessment of Reinforced Concrete Structures in Eastern United States," by A.M. Reinhorn, M.J. Seidel, S.K. Kunnath and Y.J. Park, 6/15/88, (PB89-122220, A04, MF-A01). This report is only available through NTIS (see address given above).

NCEER-88-0017 "Dynamic Compliance of Vertically Loaded Strip Foundations in Multilayered Viscoelastic Soils," by S. Ahmad and A.S.M. Israil, 6/17/88, (PB89-102891, A04, MF-A01).

NCEER-88-0018 "An Experimental Study of Seismic Structural Response With Added Viscoelastic Dampers," by R.C. Lin, Z. Liang, T.T. Soong and R.H. Zhang, 6/30/88, (PB89-122212, A05, MF-A01). This report is available only through NTIS (see address given above).

NCEER-88-0019 "Experimental Investigation of Primary - Secondary System Interaction," by G.D. Manolis, G. Juhn and A.M. Reinhorn, 5/27/88, (PB89-122204, A04, MF-A01).

NCEER-88-0020 "A Response Spectrum Approach For Analysis of Nonclassically Damped Structures," by J.N. Yang, S. Sarkani and F.X. Long, 4/22/88, (PB89-102909, A04, MF-A01).

NCEER-88-0021 "Seismic Interaction of Structures and Soils: Stochastic Approach," by A.S. Veletsos and A.M. Prasad, 7/21/88, (PB89-122196, A04, MF-A01). This report is only available through NTIS (see address given above).

NCEER-88-0022 "Identification of the Serviceability Limit State and Detection of Seismic Structural Damage," by E. DiPasquale and A.S. Cakmak, 6/15/88, (PB89-122188, A05, MF-A01). This report is available only through NTIS (see address given above).

NCEER-88-0023 "Multi-Hazard Risk Analysis: Case of a Simple Offshore Structure," by B.K. Bhartia and E.H. Vanmarcke, 7/21/88, (PB89-145213, A05, MF-A01).

NCEER-88-0024 "Automated Seismic Design of Reinforced Concrete Buildings," by Y.S. Chung, C. Meyer and M. Shinozuka, 7/5/88, (PB89-122170, A06, MF-A01). This report is available only through NTIS (see address given above).

NCEER-88-0025 "Experimental Study of Active Control of MDOF Structures Under Seismic Excitations," by L.L. Chung, R.C. Lin, T.T. Soong and A.M. Reinhorn, 7/10/88, (PB89-122600, A04, MF-A01).

NCEER-88-0026 "Earthquake Simulation Tests of a Low-Rise Metal Structure," by J.S. Hwang, K.C. Chang, G.C. Lee and R.L. Ketter, 8/1/88, (PB89-102917, A04, MF-A01).

NCEER-88-0027 "Systems Study of Urban Response and Reconstruction Due to Catastrophic Earthquakes," by F. Kozin and H.K. Zhou, 9/22/88, (PB90-162348, A04, MF-A01).

NCEER-88-0028 "Seismic Fragility Analysis of Plane Frame Structures," by H.H-M. Hwang and Y.K. Low, 7/31/88, (PB89-131445, A06, MF-A01).

NCEER-88-0029 "Response Analysis of Stochastic Structures," by A. Kardara, C. Bucher and M. Shinozuka, 9/22/88, (PB89-174429, A04, MF-A01).

NCEER-88-0030 "Nonnormal Accelerations Due to Yielding in a Primary Structure," by D.C.K. Chen and L.D. Lutes, 9/19/88, (PB89-131437, A04, MF-A01).

NCEER-88-0031 "Design Approaches for Soil-Structure Interaction," by A.S. Veletsos, A.M. Prasad and Y. Tang, 12/30/88, (PB89-174437, A03, MF-A01). This report is available only through NTIS (see address given above).

NCEER-88-0032 "A Re-evaluation of Design Spectra for Seismic Damage Control," by C.J. Turkstra and A.G. Tallin, 11/7/88, (PB89-145221, A05, MF-A01).

NCEER-88-0033 "The Behavior and Design of Noncontact Lap Splices Subjected to Repeated Inelastic Tensile Loading," by V.E. Sagan, P. Gergely and R.N. White, 12/8/88, (PB89-163737, A08, MF-A01).

NCEER-88-0034 "Seismic Response of Pile Foundations," by S.M. Mamoon, P.K. Banerjee and S. Ahmad, 11/1/88, (PB89-145239, A04, MF-A01).

NCEER-88-0035 "Modeling of R/C Building Structures With Flexible Floor Diaphragms (IDARC2)," by A.M. Reinhorn, S.K. Kunnath and N. Panahshahi, 9/7/88, (PB89-207153, A07, MF-A01).

NCEER-88-0036 "Solution of the Dam-Reservoir Interaction Problem Using a Combination of FEM, BEM with Particular Integrals, Modal Analysis, and Substructuring," by C-S. Tsai, G.C. Lee and R.L. Ketter, 12/31/88, (PB89-207146, A04, MF-A01).

NCEER-88-0037 "Optimal Placement of Actuators for Structural Control," by F.Y. Cheng and C.P. Pantelides, 8/15/88, (PB89-162846, A05, MF-A01).

NCEER-88-0038 "Teflon Bearings in Aseismic Base Isolation: Experimental Studies and Mathematical Modeling," by A. Mokha, M.C. Constantinou and A.M. Reinhorn, 12/5/88, (PB89-218457, A10, MF-A01). This report is available only through NTIS (see address given above).

NCEER-88-0039 "Seismic Behavior of Flat Slab High-Rise Buildings in the New York City Area," by P. Weidlinger and M. Ettouney, 10/15/88, (PB90-145681, A04, MF-A01).

NCEER-88-0040 "Evaluation of the Earthquake Resistance of Existing Buildings in New York City," by P. Weidlinger and M. Ettouney, 10/15/88, to be published.

NCEER-88-0041 "Small-Scale Modeling Techniques for Reinforced Concrete Structures Subjected to Seismic Loads," by W. Kim, A. El-Attar and R.N. White, 11/22/88, (PB89-189625, A05, MF-A01).

NCEER-88-0042 "Modeling Strong Ground Motion from Multiple Event Earthquakes," by G.W. Ellis and A.S. Cakmak, 10/15/88, (PB89-174445, A03, MF-A01).

NCEER-88-0043 "Nonstationary Models of Seismic Ground Acceleration," by M. Grigoriu, S.E. Ruiz and E. Rosenblueth, 7/15/88, (PB89-189617, A04, MF-A01).

NCEER-88-0044 "SARCF User's Guide: Seismic Analysis of Reinforced Concrete Frames," by Y.S. Chung, C. Meyer and M. Shinozuka, 11/9/88, (PB89-174452, A08, MF-A01).

NCEER-88-0045 "First Expert Panel Meeting on Disaster Research and Planning," edited by J. Pantelic and J. Stoyle, 9/15/88, (PB89-174460, A05, MF-A01).

NCEER-88-0046 "Preliminary Studies of the Effect of Degrading Infill Walls on the Nonlinear Seismic Response of Steel Frames," by C.Z. Chrysostomou, P. Gergely and J.F. Abel, 12/19/88, (PB89-208383, A05, MF-A01).

NCEER-88-0047 "Reinforced Concrete Frame Component Testing Facility - Design, Construction, Instrumentation and Operation," by S.P. Pessiki, C. Conley, T. Bond, P. Gergely and R.N. White, 12/16/88, (PB89-174478, A04, MF-A01).

NCEER-89-0001 "Effects of Protective Cushion and Soil Compliancy on the Response of Equipment Within a Seismically Excited Building," by J.A. HoLung, 2/16/89, (PB89-207179, A04, MF-A01).

NCEER-89-0002 "Statistical Evaluation of Response Modification Factors for Reinforced Concrete Structures," by H.H-M. Hwang and J-W. Jaw, 2/17/89, (PB89-207187, A05, MF-A01).

NCEER-89-0003 "Hysteretic Columns Under Random Excitation," by G-Q. Cai and Y.K. Lin, 1/9/89, (PB89-196513, A03, MF-A01).

NCEER-89-0004 "Experimental Study of `Elephant Foot Bulge' Instability of Thin-Walled Metal Tanks," by Z-H. Jia and R.L. Ketter, 2/22/89, (PB89-207195, A03, MF-A01).

NCEER-89-0005 "Experiment on Performance of Buried Pipelines Across San Andreas Fault," by J. Isenberg, E. Richardson and T.D. O'Rourke, 3/10/89, (PB89-218440, A04, MF-A01). This report is available only through NTIS (see address given above).

NCEER-89-0006 "A Knowledge-Based Approach to Structural Design of Earthquake-Resistant Buildings," by M. Subramani, P. Gergely, C.H. Conley, J.F. Abel and A.H. Zaghw, 1/15/89, (PB89-218465, A06, MF-A01).

NCEER-89-0007 "Liquefaction Hazards and Their Effects on Buried Pipelines," by T.D. O'Rourke and P.A. Lane, 2/1/89, (PB89-218481, A09, MF-A01).

NCEER-89-0008 "Fundamentals of System Identification in Structural Dynamics," by H. Imai, C-B. Yun, O. Maruyama and M. Shinozuka, 1/26/89, (PB89-207211, A04, MF-A01).

NCEER-89-0009 "Effects of the 1985 Michoacan Earthquake on Water Systems and Other Buried Lifelines in Mexico," by A.G. Ayala and M.J. O'Rourke, 3/8/89, (PB89-207229, A06, MF-A01).

NCEER-89-R010 "NCEER Bibliography of Earthquake Education Materials," by K.E.K. Ross, Second Revision, 9/1/89, (PB90-125352, A05, MF-A01). This report is replaced by NCEER-92-0018.

NCEER-89-0011 "Inelastic Three-Dimensional Response Analysis of Reinforced Concrete Building Structures (IDARC-3D), Part I - Modeling," by S.K. Kunnath and A.M. Reinhorn, 4/17/89, (PB90-114612, A07, MF-A01). This report is available only through NTIS (see address given above).

NCEER-89-0012 "Recommended Modifications to ATC-14," by C.D. Poland and J.O. Malley, 4/12/89, (PB90-108648, A15, MF-A01).

NCEER-89-0013 "Repair and Strengthening of Beam-to-Column Connections Subjected to Earthquake Loading," by M. Corazao and A.J. Durrani, 2/28/89, (PB90-109885, A06, MF-A01).

NCEER-89-0014 "Program EXKAL2 for Identification of Structural Dynamic Systems," by O. Maruyama, C-B. Yun, M. Hoshiya and M. Shinozuka, 5/19/89, (PB90-109877, A09, MF-A01).

NCEER-89-0015 "Response of Frames With Bolted Semi-Rigid Connections, Part I - Experimental Study and Analytical Predictions," by P.J. DiCorso, A.M. Reinhorn, J.R. Dickerson, J.B. Radziminski and W.L. Harper, 6/1/89, to be published.

NCEER-89-0016 "ARMA Monte Carlo Simulation in Probabilistic Structural Analysis," by P.D. Spanos and M.P. Mignolet, 7/10/89, (PB90-109893, A03, MF-A01).

NCEER-89-P017 "Preliminary Proceedings from the Conference on Disaster Preparedness - The Place of Earthquake Education in Our Schools," Edited by K.E.K. Ross, 6/23/89, (PB90-108606, A03, MF-A01).

NCEER-89-0017 "Proceedings from the Conference on Disaster Preparedness - The Place of Earthquake Education in Our Schools," Edited by K.E.K. Ross, 12/31/89, (PB90-207895, A012, MF-A02). This report is available only through NTIS (see address given above).

NCEER-89-0018 "Multidimensional Models of Hysteretic Material Behavior for Vibration Analysis of Shape Memory Energy Absorbing Devices, by E.J. Graesser and F.A. Cozzarelli, 6/7/89, (PB90-164146, A04, MF-A01).

NCEER-89-0019 "Nonlinear Dynamic Analysis of Three-Dimensional Base Isolated Structures (3D-BASIS)," by S. Nagarajaiah, A.M. Reinhorn and M.C. Constantinou, 8/3/89, (PB90-161936, A06, MF-A01). This report has been replaced by NCEER-93-0011.

NCEER-89-0020 "Structural Control Considering Time-Rate of Control Forces and Control Rate Constraints," by F.Y. Cheng and C.P. Pantelides, 8/3/89, (PB90-120445, A04, MF-A01).

NCEER-89-0021 "Subsurface Conditions of Memphis and Shelby County," by K.W. Ng, T-S. Chang and H-H.M. Hwang, 7/26/89, (PB90-120437, A03, MF-A01).

NCEER-89-0022 "Seismic Wave Propagation Effects on Straight Jointed Buried Pipelines," by K. Elhmadi and M.J. O'Rourke, 8/24/89, (PB90-162322, A10, MF-A02).

NCEER-89-0023 "Workshop on Serviceability Analysis of Water Delivery Systems," edited by M. Grigoriu, 3/6/89, (PB90-127424, A03, MF-A01).

NCEER-89-0024 "Shaking Table Study of a 1/5 Scale Steel Frame Composed of Tapered Members," by K.C. Chang, J.S. Hwang and G.C. Lee, 9/18/89, (PB90-160169, A04, MF-A01).

NCEER-89-0025 "DYNA1D: A Computer Program for Nonlinear Seismic Site Response Analysis - Technical Documentation," by Jean H. Prevost, 9/14/89, (PB90-161944, A07, MF-A01). This report is available only through NTIS (see address given above).

NCEER-89-0026 "1:4 Scale Model Studies of Active Tendon Systems and Active Mass Dampers for Aseismic Protection," by A.M. Reinhorn, T.T. Soong, R.C. Lin, Y.P. Yang, Y. Fukao, H. Abe and M. Nakai, 9/15/89, (PB90-173246, A10, MF-A02). This report is available only through NTIS (see address given above).

NCEER-89-0027 "Scattering of Waves by Inclusions in a Nonhomogeneous Elastic Half Space Solved by Boundary Element Methods," by P.K. Hadley, A. Askar and A.S. Cakmak, 6/15/89, (PB90-145699, A07, MF-A01).

NCEER-89-0028 "Statistical Evaluation of Deflection Amplification Factors for Reinforced Concrete Structures," by H.H.M. Hwang, J-W. Jaw and A.L. Ch'ng, 8/31/89, (PB90-164633, A05, MF-A01).

NCEER-89-0029 "Bedrock Accelerations in Memphis Area Due to Large New Madrid Earthquakes," by H.H.M. Hwang, C.H.S. Chen and G. Yu, 11/7/89, (PB90-162330, A04, MF-A01).

NCEER-89-0030 "Seismic Behavior and Response Sensitivity of Secondary Structural Systems," by Y.Q. Chen and T.T. Soong, 10/23/89, (PB90-164658, A08, MF-A01).

NCEER-89-0031 "Random Vibration and Reliability Analysis of Primary-Secondary Structural Systems," by Y. Ibrahim, M. Grigoriu and T.T. Soong, 11/10/89, (PB90-161951, A04, MF-A01).

NCEER-89-0032 "Proceedings from the Second U.S. - Japan Workshop on Liquefaction, Large Ground Deformation and Their Effects on Lifelines, September 26-29, 1989," Edited by T.D. O'Rourke and M. Hamada, 12/1/89, (PB90-209388, A22, MF-A03).

NCEER-89-0033 "Deterministic Model for Seismic Damage Evaluation of Reinforced Concrete Structures," by J.M. Bracci, A.M. Reinhorn, J.B. Mander and S.K. Kunnath, 9/27/89, (PB91-108803, A06, MF-A01).

NCEER-89-0034 "On the Relation Between Local and Global Damage Indices," by E. DiPasquale and A.S. Cakmak, 8/15/89, (PB90-173865, A05, MF-A01).

NCEER-89-0035 "Cyclic Undrained Behavior of Nonplastic and Low Plasticity Silts," by A.J. Walker and H.E. Stewart, 7/26/89, (PB90-183518, A10, MF-A01).

NCEER-89-0036 "Liquefaction Potential of Surficial Deposits in the City of Buffalo, New York," by M. Budhu, R. Giese and L. Baumgrass, 1/17/89, (PB90-208455, A04, MF-A01).

NCEER-89-0037 "A Deterministic Assessment of Effects of Ground Motion Incoherence," by A.S. Veletsos and Y. Tang, 7/15/89, (PB90-164294, A03, MF-A01).

NCEER-89-0038 "Workshop on Ground Motion Parameters for Seismic Hazard Mapping," July 17-18, 1989, edited by R.V. Whitman, 12/1/89, (PB90-173923, A04, MF-A01).

NCEER-89-0039 "Seismic Effects on Elevated Transit Lines of the New York City Transit Authority," by C.J. Costantino, C.A. Miller and E. Heymsfield, 12/26/89, (PB90-207887, A06, MF-A01).

NCEER-89-0040 "Centrifugal Modeling of Dynamic Soil-Structure Interaction," by K. Weissman, Supervised by J.H. Prevost, 5/10/89, (PB90-207879, A07, MF-A01).

NCEER-89-0041 "Linearized Identification of Buildings With Cores for Seismic Vulnerability Assessment," by I-K. Ho and A.E. Aktan, 11/1/89, (PB90-251943, A07, MF-A01).

NCEER-90-0001 "Geotechnical and Lifeline Aspects of the October 17, 1989 Loma Prieta Earthquake in San Francisco," by T.D. O'Rourke, H.E. Stewart, F.T. Blackburn and T.S. Dickerman, 1/90, (PB90-208596, A05, MF-A01).

NCEER-90-0002 "Nonnormal Secondary Response Due to Yielding in a Primary Structure," by D.C.K. Chen and L.D. Lutes, 2/28/90, (PB90-251976, A07, MF-A01).

NCEER-90-0003 "Earthquake Education Materials for Grades K-12," by K.E.K. Ross, 4/16/90, (PB91-251984, A05, MF-A05). This report has been replaced by NCEER-92-0018.

NCEER-90-0004 "Catalog of Strong Motion Stations in Eastern North America," by R.W. Busby, 4/3/90, (PB90-251984, A05, MF-A01).

NCEER-90-0005 "NCEER Strong-Motion Data Base: A User Manual for the GeoBase Release (Version 1.0 for the Sun3)," by P. Friberg and K. Jacob, 3/31/90 (PB90-258062, A04, MF-A01).

NCEER-90-0006 "Seismic Hazard Along a Crude Oil Pipeline in the Event of an 1811-1812 Type New Madrid Earthquake," by H.H.M. Hwang and C-H.S. Chen, 4/16/90, (PB90-258054, A04, MF-A01).

NCEER-90-0007 "Site-Specific Response Spectra for Memphis Sheahan Pumping Station," by H.H.M. Hwang and C.S. Lee, 5/15/90, (PB91-108811, A05, MF-A01).

NCEER-90-0008 "Pilot Study on Seismic Vulnerability of Crude Oil Transmission Systems," by T. Ariman, R. Dobry, M. Grigoriu, F. Kozin, M. O'Rourke, T. O'Rourke and M. Shinozuka, 5/25/90, (PB91-108837, A06, MF-A01).

NCEER-90-0009 "A Program to Generate Site Dependent Time Histories: EQGEN," by G.W. Ellis, M. Srinivasan and A.S. Cakmak, 1/30/90, (PB91-108829, A04, MF-A01).

NCEER-90-0010 "Active Isolation for Seismic Protection of Operating Rooms," by M.E. Talbott, Supervised by M. Shinozuka, 6/8/9, (PB91-110205, A05, MF-A01).

NCEER-90-0011 "Program LINEARID for Identification of Linear Structural Dynamic Systems," by C-B. Yun and M. Shinozuka, 6/25/90, (PB91-110312, A08, MF-A01).

NCEER-90-0012 "Two-Dimensional Two-Phase Elasto-Plastic Seismic Response of Earth Dams," by A.N. Yiagos, Supervised by J.H. Prevost, 6/20/90, (PB91-110197, A13, MF-A02).

NCEER-90-0013 "Secondary Systems in Base-Isolated Structures: Experimental Investigation, Stochastic Response and Stochastic Sensitivity," by G.D. Manolis, G. Juhn, M.C. Constantinou and A.M. Reinhorn, 7/1/90, (PB91-110320, A08, MF-A01).

NCEER-90-0014 "Seismic Behavior of Lightly-Reinforced Concrete Column and Beam-Column Joint Details," by S.P. Pessiki, C.H. Conley, P. Gergely and R.N. White, 8/22/90, (PB91-108795, A11, MF-A02).

NCEER-90-0015 "Two Hybrid Control Systems for Building Structures Under Strong Earthquakes," by J.N. Yang and A. Danielians, 6/29/90, (PB91-125393, A04, MF-A01).

NCEER-90-0016 "Instantaneous Optimal Control with Acceleration and Velocity Feedback," by J.N. Yang and Z. Li, 6/29/90, (PB91-125401, A03, MF-A01).

NCEER-90-0017 "Reconnaissance Report on the Northern Iran Earthquake of June 21, 1990," by M. Mehrain, 10/4/90, (PB91-125377, A03, MF-A01).

NCEER-90-0018 "Evaluation of Liquefaction Potential in Memphis and Shelby County," by T.S. Chang, P.S. Tang, C.S. Lee and H. Hwang, 8/10/90, (PB91-125427, A09, MF-A01).

NCEER-90-0019 "Experimental and Analytical Study of a Combined Sliding Disc Bearing and Helical Steel Spring Isolation System," by M.C. Constantinou, A.S. Mokha and A.M. Reinhorn, 10/4/90, (PB91-125385, A06, MF-A01). This report is available only through NTIS (see address given above).

NCEER-90-0020 "Experimental Study and Analytical Prediction of Earthquake Response of a Sliding Isolation System with a Spherical Surface," by A.S. Mokha, M.C. Constantinou and A.M. Reinhorn, 10/11/90, (PB91-125419, A05, MF-A01).

NCEER-90-0021 "Dynamic Interaction Factors for Floating Pile Groups," by G. Gazetas, K. Fan, A. Kaynia and E. Kausel, 9/10/90, (PB91-170381, A05, MF-A01).

NCEER-90-0022 "Evaluation of Seismic Damage Indices for Reinforced Concrete Structures," by S. Rodriguez-Gomez and A.S. Cakmak, 9/30/90, PB91-171322, A06, MF-A01).

NCEER-90-0023 "Study of Site Response at a Selected Memphis Site," by H. Desai, S. Ahmad, E.S. Gazetas and M.R. Oh, 10/11/90, (PB91-196857, A03, MF-A01).

NCEER-90-0024 "A User's Guide to Strongmo: Version 1.0 of NCEER's Strong-Motion Data Access Tool for PCs and Terminals," by P.A. Friberg and C.A.T. Susch, 11/15/90, (PB91-171272, A03, MF-A01).

NCEER-90-0025 "A Three-Dimensional Analytical Study of Spatial Variability of Seismic Ground Motions," by L-L. Hong and A.H.-S. Ang, 10/30/90, (PB91-170399, A09, MF-A01).

NCEER-90-0026 "MUMOID User's Guide - A Program for the Identification of Modal Parameters," by S. Rodriguez-Gomez and E. DiPasquale, 9/30/90, (PB91-171298, A04, MF-A01).

NCEER-90-0027 "SARCF-II User's Guide - Seismic Analysis of Reinforced Concrete Frames," by S. Rodriguez-Gomez, Y.S. Chung and C. Meyer, 9/30/90, (PB91-171280, A05, MF-A01).

NCEER-90-0028 "Viscous Dampers: Testing, Modeling and Application in Vibration and Seismic Isolation," by N. Makris and M.C. Constantinou, 12/20/90 (PB91-190561, A06, MF-A01).

NCEER-90-0029 "Soil Effects on Earthquake Ground Motions in the Memphis Area," by H. Hwang, C.S. Lee, K.W. Ng and T.S. Chang, 8/2/90, (PB91-190751, A05, MF-A01).

NCEER-91-0001 "Proceedings from the Third Japan-U.S. Workshop on Earthquake Resistant Design of Lifeline Facilities and Countermeasures for Soil Liquefaction, December 17-19, 1990," edited by T.D. O'Rourke and M. Hamada, 2/1/91, (PB91-179259, A99, MF-A04).

NCEER-91-0002 "Physical Space Solutions of Non-Proportionally Damped Systems," by M. Tong, Z. Liang and G.C. Lee, 1/15/91, (PB91-179242, A04, MF-A01).

NCEER-91-0003 "Seismic Response of Single Piles and Pile Groups," by K. Fan and G. Gazetas, 1/10/91, (PB92-174994, A04, MF-A01).

NCEER-91-0004 "Damping of Structures: Part 1 - Theory of Complex Damping," by Z. Liang and G. Lee, 10/10/91, (PB92-197235, A12, MF-A03).

NCEER-91-0005 "3D-BASIS - Nonlinear Dynamic Analysis of Three Dimensional Base Isolated Structures: Part II," by S. Nagarajaiah, A.M. Reinhorn and M.C. Constantinou, 2/28/91, (PB91-190553, A07, MF-A01). This report has been replaced by NCEER-93-0011.

NCEER-91-0006 "A Multidimensional Hysteretic Model for Plasticity Deforming Metals in Energy Absorbing Devices," by E.J. Graesser and F.A. Cozzarelli, 4/9/91, (PB92-108364, A04, MF-A01).

NCEER-91-0007 "A Framework for Customizable Knowledge-Based Expert Systems with an Application to a KBES for Evaluating the Seismic Resistance of Existing Buildings," by E.G. Ibarra-Anaya and S.J. Fenves, 4/9/91, (PB91-210930, A08, MF-A01).

NCEER-91-0008 "Nonlinear Analysis of Steel Frames with Semi-Rigid Connections Using the Capacity Spectrum Method," by G.G. Deierlein, S-H. Hsieh, Y-J. Shen and J.F. Abel, 7/2/91, (PB92-113828, A05, MF-A01).

NCEER-91-0009 "Earthquake Education Materials for Grades K-12," by K.E.K. Ross, 4/30/91, (PB91-212142, A06, MF-A01). This report has been replaced by NCEER-92-0018.

NCEER-91-0010 "Phase Wave Velocities and Displacement Phase Differences in a Harmonically Oscillating Pile," by N. Makris and G. Gazetas, 7/8/91, (PB92-108356, A04, MF-A01).

NCEER-91-0011 "Dynamic Characteristics of a Full-Size Five-Story Steel Structure and a 2/5 Scale Model," by K.C. Chang, G.C. Yao, G.C. Lee, D.S. Hao and Y.C. Yeh," 7/2/91, (PB93-116648, A06, MF-A02).

NCEER-91-0012 "Seismic Response of a 2/5 Scale Steel Structure with Added Viscoelastic Dampers," by K.C. Chang, T.T. Soong, S-T. Oh and M.L. Lai, 5/17/91, (PB92-110816, A05, MF-A01).

NCEER-91-0013 "Earthquake Response of Retaining Walls; Full-Scale Testing and Computational Modeling," by S. Alampalli and A-W.M. Elgamal, 6/20/91, to be published.

NCEER-91-0014 "3D-BASIS-M: Nonlinear Dynamic Analysis of Multiple Building Base Isolated Structures," by P.C. Tsopelas, S. Nagarajaiah, M.C. Constantinou and A.M. Reinhorn, 5/28/91, (PB92-113885, A09, MF-A02).

NCEER-91-0015 "Evaluation of SEAOC Design Requirements for Sliding Isolated Structures," by D. Theodossiou and M.C. Constantinou, 6/10/91, (PB92-114602, A11, MF-A03).

NCEER-91-0016 "Closed-Loop Modal Testing of a 27-Story Reinforced Concrete Flat Plate-Core Building," by H.R. Somaprasad, T. Toksoy, H. Yoshiyuki and A.E. Aktan, 7/15/91, (PB92-129980, A07, MF-A02).

NCEER-91-0017 "Shake Table Test of a 1/6 Scale Two-Story Lightly Reinforced Concrete Building," by A.G. El-Attar, R.N. White and P. Gergely, 2/28/91, (PB92-222447, A06, MF-A02).

NCEER-91-0018 "Shake Table Test of a 1/8 Scale Three-Story Lightly Reinforced Concrete Building," by A.G. El-Attar, R.N. White and P. Gergely, 2/28/91, (PB93-116630, A08, MF-A02).

NCEER-91-0019 "Transfer Functions for Rigid Rectangular Foundations," by A.S. Veletsos, A.M. Prasad and W.H. Wu, 7/31/91, to be published.

NCEER-91-0020 "Hybrid Control of Seismic-Excited Nonlinear and Inelastic Structural Systems," by J.N. Yang, Z. Li and A. Danielians, 8/1/91, (PB92-143171, A06, MF-A02).

NCEER-91-0021 "The NCEER-91 Earthquake Catalog: Improved Intensity-Based Magnitudes and Recurrence Relations for U.S. Earthquakes East of New Madrid," by L. Seeber and J.G. Armbruster, 8/28/91, (PB92-176742, A06, MF-A02).

NCEER-91-0022 "Proceedings from the Implementation of Earthquake Planning and Education in Schools: The Need for Change - The Roles of the Changemakers," by K.E.K. Ross and F. Winslow, 7/23/91, (PB92-129998, A12, MF-A03).

NCEER-91-0023 "A Study of Reliability-Based Criteria for Seismic Design of Reinforced Concrete Frame Buildings," by H.H.M. Hwang and H-M. Hsu, 8/10/91, (PB92-140235, A09, MF-A02).

NCEER-91-0024 "Experimental Verification of a Number of Structural System Identification Algorithms," by R.G. Ghanem, H. Gavin and M. Shinozuka, 9/18/91, (PB92-176577, A18, MF-A04).

NCEER-91-0025 "Probabilistic Evaluation of Liquefaction Potential," by H.H.M. Hwang and C.S. Lee," 11/25/91, (PB92-143429, A05, MF-A01).

NCEER-91-0026 "Instantaneous Optimal Control for Linear, Nonlinear and Hysteretic Structures - Stable Controllers," by J.N. Yang and Z. Li, 11/15/91, (PB92-163807, A04, MF-A01).

NCEER-91-0027 "Experimental and Theoretical Study of a Sliding Isolation System for Bridges," by M.C. Constantinou, A. Kartoum, A.M. Reinhorn and P. Bradford, 11/15/91, (PB92-176973, A10, MF-A03).

NCEER-92-0001 "Case Studies of Liquefaction and Lifeline Performance During Past Earthquakes, Volume 1: Japanese Case Studies," Edited by M. Hamada and T. O'Rourke, 2/17/92, (PB92-197243, A18, MF-A04).

NCEER-92-0002 "Case Studies of Liquefaction and Lifeline Performance During Past Earthquakes, Volume 2: United States Case Studies," Edited by T. O'Rourke and M. Hamada, 2/17/92, (PB92-197250, A20, MF-A04).

NCEER-92-0003 "Issues in Earthquake Education," Edited by K. Ross, 2/3/92, (PB92-222389, A07, MF-A02).

NCEER-92-0004 "Proceedings from the First U.S. - Japan Workshop on Earthquake Protective Systems for Bridges," Edited by I.G. Buckle, 2/4/92, (PB94-142239, A99, MF-A06).

NCEER-92-0005 "Seismic Ground Motion from a Haskell-Type Source in a Multiple-Layered Half-Space," A.P. Theoharis, G. Deodatis and M. Shinozuka, 1/2/92, to be published.

NCEER-92-0006 "Proceedings from the Site Effects Workshop," Edited by R. Whitman, 2/29/92, (PB92-197201, A04, MF-A01).

NCEER-92-0007 "Engineering Evaluation of Permanent Ground Deformations Due to Seismically-Induced Liquefaction," by M.H. Baziar, R. Dobry and A-W.M. Elgamal, 3/24/92, (PB92-222421, A13, MF-A03).

NCEER-92-0008 "A Procedure for the Seismic Evaluation of Buildings in the Central and Eastern United States," by C.D. Poland and J.O. Malley, 4/2/92, (PB92-222439, A20, MF-A04).

NCEER-92-0009 "Experimental and Analytical Study of a Hybrid Isolation System Using Friction Controllable Sliding Bearings," by M.Q. Feng, S. Fujii and M. Shinozuka, 5/15/92, (PB93-150282, A06, MF-A02).

NCEER-92-0010 "Seismic Resistance of Slab-Column Connections in Existing Non-Ductile Flat-Plate Buildings," by A.J. Durrani and Y. Du, 5/18/92, (PB93-116812, A06, MF-A02).

NCEER-92-0011 "The Hysteretic and Dynamic Behavior of Brick Masonry Walls Upgraded by Ferrocement Coatings Under Cyclic Loading and Strong Simulated Ground Motion," by H. Lee and S.P. Prawel, 5/11/92, to be published.

NCEER-92-0012 "Study of Wire Rope Systems for Seismic Protection of Equipment in Buildings," by G.F. Demetriades, M.C. Constantinou and A.M. Reinhorn, 5/20/92, (PB93-116655, A08, MF-A02).

NCEER-92-0013 "Shape Memory Structural Dampers: Material Properties, Design and Seismic Testing," by P.R. Witting and F.A. Cozzarelli, 5/26/92, (PB93-116663, A05, MF-A01).

NCEER-92-0014 "Longitudinal Permanent Ground Deformation Effects on Buried Continuous Pipelines," by M.J. O'Rourke, and C. Nordberg, 6/15/92, (PB93-116671, A08, MF-A02).

NCEER-92-0015 "A Simulation Method for Stationary Gaussian Random Functions Based on the Sampling Theorem," by M. Grigoriu and S. Balopoulou, 6/11/92, (PB93-127496, A05, MF-A01).

NCEER-92-0016 "Gravity-Load-Designed Reinforced Concrete Buildings: Seismic Evaluation of Existing Construction and Detailing Strategies for Improved Seismic Resistance," by G.W. Hoffmann, S.K. Kunnath, A.M. Reinhorn and J.B. Mander, 7/15/92, (PB94-142007, A08, MF-A02).

NCEER-92-0017 "Observations on Water System and Pipeline Performance in the Limón Area of Costa Rica Due to the April 22, 1991 Earthquake," by M. O'Rourke and D. Ballantyne, 6/30/92, (PB93-126811, A06, MF-A02).

NCEER-92-0018 "Fourth Edition of Earthquake Education Materials for Grades K-12," Edited by K.E.K. Ross, 8/10/92, (PB93-114023, A07, MF-A02).

NCEER-92-0019 "Proceedings from the Fourth Japan-U.S. Workshop on Earthquake Resistant Design of Lifeline Facilities and Countermeasures for Soil Liquefaction," Edited by M. Hamada and T.D. O'Rourke, 8/12/92, (PB93-163939, A99, MF-E11).

NCEER-92-0020 "Active Bracing System: A Full Scale Implementation of Active Control," by A.M. Reinhorn, T.T. Soong, R.C. Lin, M.A. Riley, Y.P. Wang, S. Aizawa and M. Higashino, 8/14/92, (PB93-127512, A06, MF-A02).

NCEER-92-0021 "Empirical Analysis of Horizontal Ground Displacement Generated by Liquefaction-Induced Lateral Spreads," by S.F. Bartlett and T.L. Youd, 8/17/92, (PB93-188241, A06, MF-A02).

NCEER-92-0022 "IDARC Version 3.0: Inelastic Damage Analysis of Reinforced Concrete Structures," by S.K. Kunnath, A.M. Reinhorn and R.F. Lobo, 8/31/92, (PB93-227502, A07, MF-A02).

NCEER-92-0023 "A Semi-Empirical Analysis of Strong-Motion Peaks in Terms of Seismic Source, Propagation Path and Local Site Conditions, by M. Kamiyama, M.J. O'Rourke and R. Flores-Berrones, 9/9/92, (PB93-150266, A08, MF-A02).

NCEER-92-0024 "Seismic Behavior of Reinforced Concrete Frame Structures with Nonductile Details, Part I: Summary of Experimental Findings of Full Scale Beam-Column Joint Tests," by A. Beres, R.N. White and P. Gergely, 9/30/92, (PB93-227783, A05, MF-A01).

NCEER-92-0025 "Experimental Results of Repaired and Retrofitted Beam-Column Joint Tests in Lightly Reinforced Concrete Frame Buildings," by A. Beres, S. El-Borgi, R.N. White and P. Gergely, 10/29/92, (PB93-227791, A05, MF-A01).

NCEER-92-0026 "A Generalization of Optimal Control Theory: Linear and Nonlinear Structures," by J.N. Yang, Z. Li and S. Vongchavalitkul, 11/2/92, (PB93-188621, A05, MF-A01).

NCEER-92-0027 "Seismic Resistance of Reinforced Concrete Frame Structures Designed Only for Gravity Loads: Part I - Design and Properties of a One-Third Scale Model Structure," by J.M. Bracci, A.M. Reinhorn and J.B. Mander, 12/1/92, (PB94-104502, A08, MF-A02).

NCEER-92-0028 "Seismic Resistance of Reinforced Concrete Frame Structures Designed Only for Gravity Loads: Part II - Experimental Performance of Subassemblages," by L.E. Aycardi, J.B. Mander and A.M. Reinhorn, 12/1/92, (PB94-104510, A08, MF-A02).

NCEER-92-0029 "Seismic Resistance of Reinforced Concrete Frame Structures Designed Only for Gravity Loads: Part III - Experimental Performance and Analytical Study of a Structural Model," by J.M. Bracci, A.M. Reinhorn and J.B. Mander, 12/1/92, (PB93-227528, A09, MF-A01).

NCEER-92-0030 "Evaluation of Seismic Retrofit of Reinforced Concrete Frame Structures: Part I - Experimental Performance of Retrofitted Subassemblages," by D. Choudhuri, J.B. Mander and A.M. Reinhorn, 12/8/92, (PB93-198307, A07, MF-A02).

NCEER-92-0031 "Evaluation of Seismic Retrofit of Reinforced Concrete Frame Structures: Part II - Experimental Performance and Analytical Study of a Retrofitted Structural Model," by J.M. Bracci, A.M. Reinhorn and J.B. Mander, 12/8/92, (PB93-198315, A09, MF-A03).

NCEER-92-0032 "Experimental and Analytical Investigation of Seismic Response of Structures with Supplemental Fluid Viscous Dampers," by M.C. Constantinou and M.D. Symans, 12/21/92, (PB93-191435, A10, MF-A03). This report is available only through NTIS (see address given above).

NCEER-92-0033 "Reconnaissance Report on the Cairo, Egypt Earthquake of October 12, 1992," by M. Khater, 12/23/92, (PB93-188621, A03, MF-A01).

NCEER-92-0034 "Low-Level Dynamic Characteristics of Four Tall Flat-Plate Buildings in New York City," by H. Gavin, S. Yuan, J. Grossman, E. Pekelis and K. Jacob, 12/28/92, (PB93-188217, A07, MF-A02).

NCEER-93-0001 "An Experimental Study on the Seismic Performance of Brick-Infilled Steel Frames With and Without Retrofit," by J.B. Mander, B. Nair, K. Wojtkowski and J. Ma, 1/29/93, (PB93-227510, A07, MF-A02).

NCEER-93-0002 "Social Accounting for Disaster Preparedness and Recovery Planning," by S. Cole, E. Pantoja and V. Razak, 2/22/93, (PB94-142114, A12, MF-A03).

NCEER-93-0003 "Assessment of 1991 NEHRP Provisions for Nonstructural Components and Recommended Revisions," by T.T. Soong, G. Chen, Z. Wu, R-H. Zhang and M. Grigoriu, 3/1/93, (PB93-188639, A06, MF-A02).

NCEER-93-0004 "Evaluation of Static and Response Spectrum Analysis Procedures of SEAOC/UBC for Seismic Isolated Structures," by C.W. Winters and M.C. Constantinou, 3/23/93, (PB93-198299, A10, MF-A03).

NCEER-93-0005 "Earthquakes in the Northeast - Are We Ignoring the Hazard? A Workshop on Earthquake Science and Safety for Educators," edited by K.E.K. Ross, 4/2/93, (PB94-103066, A09, MF-A02).

NCEER-93-0006 "Inelastic Response of Reinforced Concrete Structures with Viscoelastic Braces," by R.F. Lobo, J.M. Bracci, K.L. Shen, A.M. Reinhorn and T.T. Soong, 4/5/93, (PB93-227486, A05, MF-A02).

NCEER-93-0007 "Seismic Testing of Installation Methods for Computers and Data Processing Equipment," by K. Kosar, T.T. Soong, K.L. Shen, J.A. HoLung and Y.K. Lin, 4/12/93, (PB93-198299, A07, MF-A02).

NCEER-93-0008 "Retrofit of Reinforced Concrete Frames Using Added Dampers," by A. Reinhorn, M. Constantinou and C. Li, to be published.

NCEER-93-0009 "Seismic Behavior and Design Guidelines for Steel Frame Structures with Added Viscoelastic Dampers," by K.C. Chang, M.L. Lai, T.T. Soong, D.S. Hao and Y.C. Yeh, 5/1/93, (PB94-141959, A07, MF-A02).

NCEER-93-0010 "Seismic Performance of Shear-Critical Reinforced Concrete Bridge Piers," by J.B. Mander, S.M. Waheed, M.T.A. Chaudhary and S.S. Chen, 5/12/93, (PB93-227494, A08, MF-A02).

NCEER-93-0011 "3D-BASIS-TABS: Computer Program for Nonlinear Dynamic Analysis of Three Dimensional Base Isolated Structures," by S. Nagarajaiah, C. Li, A.M. Reinhorn and M.C. Constantinou, 8/2/93, (PB94-141819, A09, MF-A02).

NCEER-93-0012 "Effects of Hydrocarbon Spills from an Oil Pipeline Break on Ground Water," by O.J. Helweg and H.H.M. Hwang, 8/3/93, (PB94-141942, A06, MF-A02).

NCEER-93-0013 "Simplified Procedures for Seismic Design of Nonstructural Components and Assessment of Current Code Provisions," by M.P. Singh, L.E. Suarez, E.E. Matheu and G.O. Maldonado, 8/4/93, (PB94-141827, A09, MF-A02).

NCEER-93-0014 "An Energy Approach to Seismic Analysis and Design of Secondary Systems," by G. Chen and T.T. Soong, 8/6/93, (PB94-142767, A11, MF-A03).

NCEER-93-0015 "Proceedings from School Sites: Becoming Prepared for Earthquakes - Commemorating the Third Anniversary of the Loma Prieta Earthquake," Edited by F.E. Winslow and K.E.K. Ross, 8/16/93, (PB94-154275, A16, MF-A02).

NCEER-93-0016 "Reconnaissance Report of Damage to Historic Monuments in Cairo, Egypt Following the October 12, 1992 Dahshur Earthquake," by D. Sykora, D. Look, G. Croci, E. Karaesmen and E. Karaesmen, 8/19/93, (PB94-142221, A08, MF-A02).

NCEER-93-0017 "The Island of Guam Earthquake of August 8, 1993," by S.W. Swan and S.K. Harris, 9/30/93, (PB94-141843, A04, MF-A01).

NCEER-93-0018 "Engineering Aspects of the October 12, 1992 Egyptian Earthquake," by A.W. Elgamal, M. Amer, K. Adalier and A. Abul-Fadl, 10/7/93, (PB94-141983, A05, MF-A01).

NCEER-93-0019 "Development of an Earthquake Motion Simulator and its Application in Dynamic Centrifuge Testing," by I. Krstelj, Supervised by J.H. Prevost, 10/23/93, (PB94-181773, A-10, MF-A03).

NCEER-93-0020 "NCEER-Taisei Corporation Research Program on Sliding Seismic Isolation Systems for Bridges: Experimental and Analytical Study of a Friction Pendulum System (FPS)," by M.C. Constantinou, P. Tsopelas, Y-S. Kim and S. Okamoto, 11/1/93, (PB94-142775, A08, MF-A02).

NCEER-93-0021 "Finite Element Modeling of Elastomeric Seismic Isolation Bearings," by L.J. Billings, Supervised by R. Shepherd, 11/8/93, to be published.

NCEER-93-0022 "Seismic Vulnerability of Equipment in Critical Facilities: Life-Safety and Operational Consequences," by K. Porter, G.S. Johnson, M.M. Zadeh, C. Scawthorn and S. Eder, 11/24/93, (PB94-181765, A16, MF-A03).

NCEER-93-0023 "Hokkaido Nansei-oki, Japan Earthquake of July 12, 1993, by P.I. Yanev and C.R. Scawthorn, 12/23/93, (PB94-181500, A07, MF-A01).

NCEER-94-0001 "An Evaluation of Seismic Serviceability of Water Supply Networks with Application to the San Francisco Auxiliary Water Supply System," by I. Markov, Supervised by M. Grigoriu and T. O'Rourke, 1/21/94, (PB94-204013, A07, MF-A02).

NCEER-94-0002 "NCEER-Taisei Corporation Research Program on Sliding Seismic Isolation Systems for Bridges: Experimental and Analytical Study of Systems Consisting of Sliding Bearings, Rubber Restoring Force Devices and Fluid Dampers," Volumes I and II, by P. Tsopelas, S. Okamoto, M.C. Constantinou, D. Ozaki and S. Fujii, 2/4/94, (PB94-181740, A09, MF-A02 and PB94-181757, A12, MF-A03).

NCEER-94-0003 "A Markov Model for Local and Global Damage Indices in Seismic Analysis," by S. Rahman and M. Grigoriu, 2/18/94, (PB94-206000, A12, MF-A03).

NCEER-94-0004 "Proceedings from the NCEER Workshop on Seismic Response of Masonry Infills," edited by D.P. Abrams, 3/1/94, (PB94-180783, A07, MF-A02).

NCEER-94-0005 "The Northridge, California Earthquake of January 17, 1994: General Reconnaissance Report," edited by J.D. Goltz, 3/11/94, (PB94-193943, A10, MF-A03).

NCEER-94-0006 "Seismic Energy Based Fatigue Damage Analysis of Bridge Columns: Part I - Evaluation of Seismic Capacity," by G.A. Chang and J.B. Mander, 3/14/94, (PB94-219185, A11, MF-A03).

NCEER-94-0007 "Seismic Isolation of Multi-Story Frame Structures Using Spherical Sliding Isolation Systems," by T.M. Al-Hussaini, V.A. Zayas and M.C. Constantinou, 3/17/94, (PB94-193745, A09, MF-A02).

NCEER-94-0008 "The Northridge, California Earthquake of January 17, 1994: Performance of Highway Bridges," edited by I.G. Buckle, 3/24/94, (PB94-193851, A06, MF-A02).

NCEER-94-0009 "Proceedings of the Third U.S.-Japan Workshop on Earthquake Protective Systems for Bridges," edited by I.G. Buckle and I. Friedland, 3/31/94, (PB94-195815, A99, MF-A06).

NCEER-94-0010 "3D-BASIS-ME: Computer Program for Nonlinear Dynamic Analysis of Seismically Isolated Single and Multiple Structures and Liquid Storage Tanks," by P.C. Tsopelas, M.C. Constantinou and A.M. Reinhorn, 4/12/94, (PB94-204922, A09, MF-A02).

NCEER-94-0011 "The Northridge, California Earthquake of January 17, 1994: Performance of Gas Transmission Pipelines," by T.D. O'Rourke and M.C. Palmer, 5/16/94, (PB94-204989, A05, MF-A01).

NCEER-94-0012 "Feasibility Study of Replacement Procedures and Earthquake Performance Related to Gas Transmission Pipelines," by T.D. O'Rourke and M.C. Palmer, 5/25/94, (PB94-206638, A09, MF-A02).

NCEER-94-0013 "Seismic Energy Based Fatigue Damage Analysis of Bridge Columns: Part II - Evaluation of Seismic Demand," by G.A. Chang and J.B. Mander, 6/1/94, (PB95-18106, A08, MF-A02).

NCEER-94-0014 "NCEER-Taisei Corporation Research Program on Sliding Seismic Isolation Systems for Bridges: Experimental and Analytical Study of a System Consisting of Sliding Bearings and Fluid Restoring Force/Damping Devices," by P. Tsopelas and M.C. Constantinou, 6/13/94, (PB94-219144, A10, MF-A03).

NCEER-94-0015 "Generation of Hazard-Consistent Fragility Curves for Seismic Loss Estimation Studies," by H. Hwang and J-R. Huo, 6/14/94, (PB95-181996, A09, MF-A02).

NCEER-94-0016 "Seismic Study of Building Frames with Added Energy-Absorbing Devices," by W.S. Pong, C.S. Tsai and G.C. Lee, 6/20/94, (PB94-219136, A10, A03).

NCEER-94-0017 "Sliding Mode Control for Seismic-Excited Linear and Nonlinear Civil Engineering Structures," by J. Yang, J. Wu, A. Agrawal and Z. Li, 6/21/94, (PB95-138483, A06, MF-A02).

NCEER-94-0018 "3D-BASIS-TABS Version 2.0: Computer Program for Nonlinear Dynamic Analysis of Three Dimensional Base Isolated Structures," by A.M. Reinhorn, S. Nagarajaiah, M.C. Constantinou, P. Tsopelas and R. Li, 6/22/94, (PB95-182176, A08, MF-A02).

NCEER-94-0019 "Proceedings of the International Workshop on Civil Infrastructure Systems: Application of Intelligent Systems and Advanced Materials on Bridge Systems," Edited by G.C. Lee and K.C. Chang, 7/18/94, (PB95-252474, A20, MF-A04).

NCEER-94-0020 "Study of Seismic Isolation Systems for Computer Floors," by V. Lambrou and M.C. Constantinou, 7/19/94, (PB95-138533, A10, MF-A03).

NCEER-94-0021 "Proceedings of the U.S.-Italian Workshop on Guidelines for Seismic Evaluation and Rehabilitation of Unreinforced Masonry Buildings," Edited by D.P. Abrams and G.M. Calvi, 7/20/94, (PB95-138749, A13, MF-A03).

NCEER-94-0022 "NCEER-Taisei Corporation Research Program on Sliding Seismic Isolation Systems for Bridges: Experimental and Analytical Study of a System Consisting of Lubricated PTFE Sliding Bearings and Mild Steel Dampers," by P. Tsopelas and M.C. Constantinou, 7/22/94, (PB95-182184, A08, MF-A02).

NCEER-94-0023 "Development of Reliability-Based Design Criteria for Buildings Under Seismic Load," by Y.K. Wen, H. Hwang and M. Shinozuka, 8/1/94, (PB95-211934, A08, MF-A02).

NCEER-94-0024 "Experimental Verification of Acceleration Feedback Control Strategies for an Active Tendon System," by S.J. Dyke, B.F. Spencer, Jr., P. Quast, M.K. Sain, D.C. Kaspari, Jr. and T.T. Soong, 8/29/94, (PB95-212320, A05, MF-A01).

NCEER-94-0025 "Seismic Retrofitting Manual for Highway Bridges," Edited by I.G. Buckle and I.F. Friedland, published by the Federal Highway Administration (PB95-212676, A15, MF-A03).

NCEER-94-0026 "Proceedings from the Fifth U.S.-Japan Workshop on Earthquake Resistant Design of Lifeline Facilities and Countermeasures Against Soil Liquefaction," Edited by T.D. O'Rourke and M. Hamada, 11/7/94, (PB95-220802, A99, MF-E08).

NCEER-95-0001 "Experimental and Analytical Investigation of Seismic Retrofit of Structures with Supplemental Damping: Part 1 - Fluid Viscous Damping Devices," by A.M. Reinhorn, C. Li and M.C. Constantinou, 1/3/95, (PB95-266599, A09, MF-A02).

NCEER-95-0002 "Experimental and Analytical Study of Low-Cycle Fatigue Behavior of Semi-Rigid Top-And-Seat Angle Connections," by G. Pekcan, J.B. Mander and S.S. Chen, 1/5/95, (PB95-220042, A07, MF-A02).

NCEER-95-0003 "NCEER-ATC Joint Study on Fragility of Buildings," by T. Anagnos, C. Rojahn and A.S. Kiremidjian, 1/20/95, (PB95-220026, A06, MF-A02).

NCEER-95-0004 "Nonlinear Control Algorithms for Peak Response Reduction," by Z. Wu, T.T. Soong, V. Gattulli and R.C. Lin, 2/16/95, (PB95-220349, A05, MF-A01).

NCEER-95-0005 "Pipeline Replacement Feasibility Study: A Methodology for Minimizing Seismic and Corrosion Risks to Underground Natural Gas Pipelines," by R.T. Eguchi, H.A. Seligson and D.G. Honegger, 3/2/95, (PB95-252326, A06, MF-A02).

NCEER-95-0006 "Evaluation of Seismic Performance of an 11-Story Frame Building During the 1994 Northridge Earthquake," by F. Naeim, R. DiSulio, K. Benuska, A. Reinhorn and C. Li, to be published.

NCEER-95-0007 "Prioritization of Bridges for Seismic Retrofitting," by N. Basöz and A.S. Kiremidjian, 4/24/95, (PB95-252300, A08, MF-A02).

NCEER-95-0008 "Method for Developing Motion Damage Relationships for Reinforced Concrete Frames," by A. Singhal and A.S. Kiremidjian, 5/11/95, (PB95-266607, A06, MF-A02).

NCEER-95-0009 "Experimental and Analytical Investigation of Seismic Retrofit of Structures with Supplemental Damping: Part II - Friction Devices," by C. Li and A.M. Reinhorn, 7/6/95, (PB96-128087, A11, MF-A03).

NCEER-95-0010 "Experimental Performance and Analytical Study of a Non-Ductile Reinforced Concrete Frame Structure Retrofitted with Elastomeric Spring Dampers," by G. Pekcan, J.B. Mander and S.S. Chen, 7/14/95, (PB96-137161, A08, MF-A02).

NCEER-95-0011 "Development and Experimental Study of Semi-Active Fluid Damping Devices for Seismic Protection of Structures," by M.D. Symans and M.C. Constantinou, 8/3/95, (PB96-136940, A23, MF-A04).

NCEER-95-0012 "Real-Time Structural Parameter Modification (RSPM): Development of Innervated Structures," by Z. Liang, M. Tong and G.C. Lee, 4/11/95, (PB96-137153, A06, MF-A01).

NCEER-95-0013 "Experimental and Analytical Investigation of Seismic Retrofit of Structures with Supplemental Damping: Part III - Viscous Damping Walls," by A.M. Reinhorn and C. Li, 10/1/95, (PB96-176409, A11, MF-A03).

NCEER-95-0014 "Seismic Fragility Analysis of Equipment and Structures in a Memphis Electric Substation," by J-R. Huo and H.H.M. Hwang, 8/10/95, (PB96-128087, A09, MF-A02).

NCEER-95-0015 "The Hanshin-Awaji Earthquake of January 17, 1995: Performance of Lifelines," Edited by M. Shinozuka, 11/3/95, (PB96-176383, A15, MF-A03).

NCEER-95-0016 "Highway Culvert Performance During Earthquakes," by T.L. Youd and C.J. Beckman, available as NCEER-96-0015.

NCEER-95-0017 "The Hanshin-Awaji Earthquake of January 17, 1995: Performance of Highway Bridges," Edited by I.G. Buckle, 12/1/95, to be published.

NCEER-95-0018 "Modeling of Masonry Infill Panels for Structural Analysis," by A.M. Reinhorn, A. Madan, R.E. Valles, Y. Reichmann and J.B. Mander, 12/8/95, (PB97-110886, MF-A01, A06).

NCEER-95-0019 "Optimal Polynomial Control for Linear and Nonlinear Structures," by A.K. Agrawal and J.N. Yang, 12/11/95, (PB96-168737, A07, MF-A02).

NCEER-95-0020 "Retrofit of Non-Ductile Reinforced Concrete Frames Using Friction Dampers," by R.S. Rao, P. Gergely and R.N. White, 12/22/95, (PB97-133508, A10, MF-A02).

NCEER-95-0021 "Parametric Results for Seismic Response of Pile-Supported Bridge Bents," by G. Mylonakis, A. Nikolaou and G. Gazetas, 12/22/95, (PB97-100242, A12, MF-A03).

NCEER-95-0022 "Kinematic Bending Moments in Seismically Stressed Piles," by A. Nikolaou, G. Mylonakis and G. Gazetas, 12/23/95, (PB97-113914, MF-A03, A13).

NCEER-96-0001 "Dynamic Response of Unreinforced Masonry Buildings with Flexible Diaphragms," by A.C. Costley and D.P. Abrams," 10/10/96, (PB97-133573, MF-A03, A15).

NCEER-96-0002 "State of the Art Review: Foundations and Retaining Structures," by I. Po Lam, to be published.

NCEER-96-0003 "Ductility of Rectangular Reinforced Concrete Bridge Columns with Moderate Confinement," by N. Wehbe, M. Saiidi, D. Sanders and B. Douglas, 11/7/96, (PB97-133557, A06, MF-A02).

NCEER-96-0004 "Proceedings of the Long-Span Bridge Seismic Research Workshop," edited by I.G. Buckle and I.M. Friedland, to be published.

NCEER-96-0005 "Establish Representative Pier Types for Comprehensive Study: Eastern United States," by J. Kulicki and Z. Prucz, 5/28/96, (PB98-119217, A07, MF-A02).

NCEER-96-0006 "Establish Representative Pier Types for Comprehensive Study: Western United States," by R. Imbsen, R.A. Schamber and T.A. Osterkamp, 5/28/96, (PB98-118607, A07, MF-A02).

NCEER-96-0007 "Nonlinear Control Techniques for Dynamical Systems with Uncertain Parameters," by R.G. Ghanem and M.I. Bujakov, 5/27/96, (PB97-100259, A17, MF-A03).

NCEER-96-0008 "Seismic Evaluation of a 30-Year Old Non-Ductile Highway Bridge Pier and Its Retrofit," by J.B. Mander, B. Mahmoodzadegan, S. Bhadra and S.S. Chen, 5/31/96, (PB97-110902, MF-A03, A10).

NCEER-96-0009 "Seismic Performance of a Model Reinforced Concrete Bridge Pier Before and After Retrofit," by J.B. Mander, J.H. Kim and C.A. Ligozio, 5/31/96, (PB97-110910, MF-A02, A10).

NCEER-96-0010 "IDARC2D Version 4.0: A Computer Program for the Inelastic Damage Analysis of Buildings," by R.E. Valles, A.M. Reinhorn, S.K. Kunnath, C. Li and A. Madan, 6/3/96, (PB97-100234, A17, MF-A03).

NCEER-96-0011 "Estimation of the Economic Impact of Multiple Lifeline Disruption: Memphis Light, Gas and Water Division Case Study," by S.E. Chang, H.A. Seligson and R.T. Eguchi, 8/16/96, (PB97-133490, A11, MF-A03).

NCEER-96-0012 "Proceedings from the Sixth Japan-U.S. Workshop on Earthquake Resistant Design of Lifeline Facilities and Countermeasures Against Soil Liquefaction, Edited by M. Hamada and T. O'Rourke, 9/11/96, (PB97-133581, A99, MF-A06).

NCEER-96-0013 "Chemical Hazards, Mitigation and Preparedness in Areas of High Seismic Risk: A Methodology for Estimating the Risk of Post-Earthquake Hazardous Materials Release," by H.A. Seligson, R.T. Eguchi, K.J. Tierney and K. Richmond, 11/7/96, (PB97-133565, MF-A02, A08).

NCEER-96-0014 "Response of Steel Bridge Bearings to Reversed Cyclic Loading," by J.B. Mander, D-K. Kim, S.S. Chen and G.J. Premus, 11/13/96, (PB97-140735, A12, MF-A03).

NCEER-96-0015 "Highway Culvert Performance During Past Earthquakes," by T.L. Youd and C.J. Beckman, 11/25/96, (PB97-133532, A06, MF-A01).

NCEER-97-0001 "Evaluation, Prevention and Mitigation of Pounding Effects in Building Structures," by R.E. Valles and A.M. Reinhorn, 2/20/97, (PB97-159552, A14, MF-A03).

NCEER-97-0002 "Seismic Design Criteria for Bridges and Other Highway Structures," by C. Rojahn, R. Mayes, D.G. Anderson, J. Clark, J.H. Hom, R.V. Nutt and M.J. O'Rourke, 4/30/97, (PB97-194658, A06, MF-A03).

NCEER-97-0003 “Proceedings of the U.S.-Italian Workshop on Seismic Evaluation and Retrofit,” Edited by D.P. Abrams and G.M. Calvi, 3/19/97, (PB97-194666, A13, MF-A03).

NCEER-97-0004 "Investigation of Seismic Response of Buildings with Linear and Nonlinear Fluid Viscous Dampers," by A.A. Seleemah and M.C. Constantinou, 5/21/97, (PB98-109002, A15, MF-A03).

NCEER-97-0005 "Proceedings of the Workshop on Earthquake Engineering Frontiers in Transportation Facilities," edited by G.C. Lee and I.M. Friedland, 8/29/97, (PB98-128911, A25, MR-A04).

NCEER-97-0006 "Cumulative Seismic Damage of Reinforced Concrete Bridge Piers," by S.K. Kunnath, A. El-Bahy, A. Taylor and W. Stone, 9/2/97, (PB98-108814, A11, MF-A03).

NCEER-97-0007 "Structural Details to Accommodate Seismic Movements of Highway Bridges and Retaining Walls," by R.A. Imbsen, R.A. Schamber, E. Thorkildsen, A. Kartoum, B.T. Martin, T.N. Rosser and J.M. Kulicki, 9/3/97, (PB98-108996, A09, MF-A02).

NCEER-97-0008 "A Method for Earthquake Motion-Damage Relationships with Application to Reinforced Concrete Frames," by A. Singhal and A.S. Kiremidjian, 9/10/97, (PB98-108988, A13, MF-A03).

NCEER-97-0009 "Seismic Analysis and Design of Bridge Abutments Considering Sliding and Rotation," by K. Fishman and R. Richards, Jr., 9/15/97, (PB98-108897, A06, MF-A02).

NCEER-97-0010 "Proceedings of the FHWA/NCEER Workshop on the National Representation of Seismic Ground Motion for New and Existing Highway Facilities," edited by I.M. Friedland, M.S. Power and R.L. Mayes, 9/22/97, (PB98-128903, A21, MF-A04).

NCEER-97-0011 "Seismic Analysis for Design or Retrofit of Gravity Bridge Abutments," by K.L. Fishman, R. Richards, Jr. and R.C. Divito, 10/2/97, (PB98-128937, A08, MF-A02).

NCEER-97-0012 "Evaluation of Simplified Methods of Analysis for Yielding Structures," by P. Tsopelas, M.C. Constantinou, C.A. Kircher and A.S. Whittaker, 10/31/97, (PB98-128929, A10, MF-A03).

NCEER-97-0013 "Seismic Design of Bridge Columns Based on Control and Repairability of Damage," by C-T. Cheng and J.B. Mander, 12/8/97, (PB98-144249, A11, MF-A03).

NCEER-97-0014 "Seismic Resistance of Bridge Piers Based on Damage Avoidance Design," by J.B. Mander and C-T. Cheng, 12/10/97, (PB98-144223, A09, MF-A02).

NCEER-97-0015 “Seismic Response of Nominally Symmetric Systems with Strength Uncertainty,” by S. Balopoulou and M. Grigoriu, 12/23/97, (PB98-153422, A11, MF-A03).

NCEER-97-0016 “Evaluation of Seismic Retrofit Methods for Reinforced Concrete Bridge Columns,” by T.J. Wipf, F.W. Klaiber and F.M. Russo, 12/28/97, (PB98-144215, A12, MF-A03).

NCEER-97-0017 “Seismic Fragility of Existing Conventional Reinforced Concrete Highway Bridges,” by C.L. Mullen and A.S. Cakmak, 12/30/97, (PB98-153406, A08, MF-A02).

NCEER-97-0018 “Loss Asssessment of Memphis Buildings,” edited by D.P. Abrams and M. Shinozuka, 12/31/97, (PB98-144231, A13, MF-A03).

NCEER-97-0019 “Seismic Evaluation of Frames with Infill Walls Using Quasi-static Experiments,” by K.M. Mosalam, R.N. White and P. Gergely, 12/31/97, (PB98-153455, A07, MF-A02).

NCEER-97-0020 “Seismic Evaluation of Frames with Infill Walls Using Pseudo-dynamic Experiments,” by K.M. Mosalam, R.N. White and P. Gergely, 12/31/97, (PB98-153430, A07, MF-A02).

NCEER-97-0021 “Computational Strategies for Frames with Infill Walls: Discrete and Smeared Crack Analyses and Seismic Fragility,” by K.M. Mosalam, R.N. White and P. Gergely, 12/31/97, (PB98-153414, A10, MF-A02).

NCEER-97-0022 "Proceedings of the NCEER Workshop on Evaluation of Liquefaction Resistance of Soils," edited by T.L. Youd and I.M. Idriss, 12/31/97, (PB98-155617, A15, MF-A03).

MCEER-98-0001 "Extraction of Nonlinear Hysteretic Properties of Seismically Isolated Bridges from Quick-Release Field Tests," by Q. Chen, B.M. Douglas, E.M. Maragakis and I.G. Buckle, 5/26/98, (PB99-118838, A06, MF-A01).

MCEER-98-0002 "Methodologies for Evaluating the Importance of Highway Bridges," by A. Thomas, S. Eshenaur and J. Kulicki, 5/29/98, (PB99-118846, A10, MF-A02).

MCEER-98-0003 "Capacity Design of Bridge Piers and the Analysis of Overstrength," by J.B. Mander, A. Dutta and P. Goel, 6/1/98, (PB99-118853, A09, MF-A02).

MCEER-98-0004 "Evaluation of Bridge Damage Data from the Loma Prieta and Northridge, California Earthquakes," by N. Basoz and A. Kiremidjian, 6/2/98, (PB99-118861, A15, MF-A03).

MCEER-98-0005 "Screening Guide for Rapid Assessment of Liquefaction Hazard at Highway Bridge Sites," by T. L. Youd, 6/16/98, (PB99-118879, A06, not available on microfiche).

MCEER-98-0006 "Structural Steel and Steel/Concrete Interface Details for Bridges," by P. Ritchie, N. Kauhl and J. Kulicki, 7/13/98, (PB99-118945, A06, MF-A01).

MCEER-98-0007 "Capacity Design and Fatigue Analysis of Confined Concrete Columns," by A. Dutta and J.B. Mander, 7/14/98, (PB99-118960, A14, MF-A03).

MCEER-98-0008 "Proceedings of the Workshop on Performance Criteria for Telecommunication Services Under Earthquake Conditions," edited by A.J. Schiff, 7/15/98, (PB99-118952, A08, MF-A02).

MCEER-98-0009 "Fatigue Analysis of Unconfined Concrete Columns," by J.B. Mander, A. Dutta and J.H. Kim, 9/12/98, (PB99-123655, A10, MF-A02).

MCEER-98-0010 "Centrifuge Modeling of Cyclic Lateral Response of Pile-Cap Systems and Seat-Type Abutments in Dry Sands," by A.D. Gadre and R. Dobry, 10/2/98, (PB99-123606, A13, MF-A03).

MCEER-98-0011 "IDARC-BRIDGE: A Computational Platform for Seismic Damage Assessment of Bridge Structures," by A.M. Reinhorn, V. Simeonov, G. Mylonakis and Y. Reichman, 10/2/98, (PB99-162919, A15, MF-A03).

MCEER-98-0012 "Experimental Investigation of the Dynamic Response of Two Bridges Before and After Retrofitting with Elastomeric Bearings," by D.A. Wendichansky, S.S. Chen and J.B. Mander, 10/2/98, (PB99-162927, A15, MF-A03).

MCEER-98-0013 "Design Procedures for Hinge Restrainers and Hinge Sear Width for Multiple-Frame Bridges," by R. Des Roches and G.L. Fenves, 11/3/98, (PB99-140477, A13, MF-A03).

MCEER-98-0014 "Response Modification Factors for Seismically Isolated Bridges," by M.C. Constantinou and J.K. Quarshie, 11/3/98, (PB99-140485, A14, MF-A03).

MCEER-98-0015 "Proceedings of the U.S.-Italy Workshop on Seismic Protective Systems for Bridges," edited by I.M. Friedland and M.C. Constantinou, 11/3/98, (PB2000-101711, A22, MF-A04).

MCEER-98-0016 "Appropriate Seismic Reliability for Critical Equipment Systems: Recommendations Based on Regional Analysis of Financial and Life Loss," by K. Porter, C. Scawthorn, C. Taylor and N. Blais, 11/10/98, (PB99-157265, A08, MF-A02).

MCEER-98-0017 "Proceedings of the U.S. Japan Joint Seminar on Civil Infrastructure Systems Research," edited by M. Shinozuka and A. Rose, 11/12/98, (PB99-156713, A16, MF-A03).

MCEER-98-0018 "Modeling of Pile Footings and Drilled Shafts for Seismic Design," by I. PoLam, M. Kapuskar and D. Chaudhuri, 12/21/98, (PB99-157257, A09, MF-A02).

MCEER-99-0001 "Seismic Evaluation of a Masonry Infilled Reinforced Concrete Frame by Pseudodynamic Testing," by S.G. Buonopane and R.N. White, 2/16/99, (PB99-162851, A09, MF-A02).

MCEER-99-0002 "Response History Analysis of Structures with Seismic Isolation and Energy Dissipation Systems: Verification Examples for Program SAP2000," by J. Scheller and M.C. Constantinou, 2/22/99, (PB99-162869, A08, MF-A02).

MCEER-99-0003 "Experimental Study on the Seismic Design and Retrofit of Bridge Columns Including Axial Load Effects," by A. Dutta, T. Kokorina and J.B. Mander, 2/22/99, (PB99-162877, A09, MF-A02).

MCEER-99-0004 "Experimental Study of Bridge Elastomeric and Other Isolation and Energy Dissipation Systems with Emphasis on Uplift Prevention and High Velocity Near-source Seismic Excitation," by A. Kasalanati and M. C. Constantinou, 2/26/99, (PB99-162885, A12, MF-A03).

MCEER-99-0005 "Truss Modeling of Reinforced Concrete Shear-flexure Behavior," by J.H. Kim and J.B. Mander, 3/8/99, (PB99-163693, A12, MF-A03).

MCEER-99-0006 "Experimental Investigation and Computational Modeling of Seismic Response of a 1:4 Scale Model Steel Structure with a Load Balancing Supplemental Damping System," by G. Pekcan, J.B. Mander and S.S. Chen, 4/2/99, (PB99-162893, A11, MF-A03).

MCEER-99-0007 "Effect of Vertical Ground Motions on the Structural Response of Highway Bridges," by M.R. Button, C.J. Cronin and R.L. Mayes, 4/10/99, (PB2000-101411, A10, MF-A03).

MCEER-99-0008 "Seismic Reliability Assessment of Critical Facilities: A Handbook, Supporting Documentation, and Model Code Provisions," by G.S. Johnson, R.E. Sheppard, M.D. Quilici, S.J. Eder and C.R. Scawthorn, 4/12/99, (PB2000-101701, A18, MF-A04).

MCEER-99-0009 "Impact Assessment of Selected MCEER Highway Project Research on the Seismic Design of Highway Structures," by C. Rojahn, R. Mayes, D.G. Anderson, J.H. Clark, D'Appolonia Engineering, S. Gloyd and R.V. Nutt, 4/14/99, (PB99-162901, A10, MF-A02).

MCEER-99-0010 "Site Factors and Site Categories in Seismic Codes," by R. Dobry, R. Ramos and M.S. Power, 7/19/99, (PB2000-101705, A08, MF-A02).

MCEER-99-0011 "Restrainer Design Procedures for Multi-Span Simply-Supported Bridges," by M.J. Randall, M. Saiidi, E. Maragakis and T. Isakovic, 7/20/99, (PB2000-101702, A10, MF-A02).

MCEER-99-0012 "Property Modification Factors for Seismic Isolation Bearings," by M.C. Constantinou, P. Tsopelas, A. Kasalanati and E. Wolff, 7/20/99, (PB2000-103387, A11, MF-A03).

MCEER-99-0013 "Critical Seismic Issues for Existing Steel Bridges," by P. Ritchie, N. Kauhl and J. Kulicki, 7/20/99, (PB2000-101697, A09, MF-A02).

MCEER-99-0014 "Nonstructural Damage Database," by A. Kao, T.T. Soong and A. Vender, 7/24/99, (PB2000-101407, A06, MF-A01).

MCEER-99-0015 "Guide to Remedial Measures for Liquefaction Mitigation at Existing Highway Bridge Sites," by H.G. Cooke and J. K. Mitchell, 7/26/99, (PB2000-101703, A11, MF-A03).

MCEER-99-0016 "Proceedings of the MCEER Workshop on Ground Motion Methodologies for the Eastern United States," edited by N. Abrahamson and A. Becker, 8/11/99, (PB2000-103385, A07, MF-A02).

MCEER-99-0017 "Quindío, Colombia Earthquake of January 25, 1999: Reconnaissance Report," by A.P. Asfura and P.J. Flores, 10/4/99, (PB2000-106893, A06, MF-A01).

MCEER-99-0018 "Hysteretic Models for Cyclic Behavior of Deteriorating Inelastic Structures," by M.V. Sivaselvan and A.M. Reinhorn, 11/5/99, (PB2000-103386, A08, MF-A02).

MCEER-99-0019 "Proceedings of the 7th U.S.- Japan Workshop on Earthquake Resistant Design of Lifeline Facilities and Countermeasures Against Soil Liquefaction," edited by T.D. O'Rourke, J.P. Bardet and M. Hamada, 11/19/99, (PB2000-103354, A99, MF-A06).

MCEER-99-0020 "Development of Measurement Capability for Micro-Vibration Evaluations with Application to Chip Fabrication Facilities," by G.C. Lee, Z. Liang, J.W. Song, J.D. Shen and W.C. Liu, 12/1/99, (PB2000-105993, A08, MF-A02).

MCEER-99-0021 "Design and Retrofit Methodology for Building Structures with Supplemental Energy Dissipating Systems," by G. Pekcan, J.B. Mander and S.S. Chen, 12/31/99, (PB2000-105994, A11, MF-A03).

MCEER-00-0001 "The Marmara, Turkey Earthquake of August 17, 1999: Reconnaissance Report," edited by C. Scawthorn; with major contributions by M. Bruneau, R. Eguchi, T. Holzer, G. Johnson, J. Mander, J. Mitchell, W. Mitchell, A. Papageorgiou, C. Scaethorn, and G. Webb, 3/23/00, (PB2000-106200, A11, MF-A03).

MCEER-00-0002 "Proceedings of the MCEER Workshop for Seismic Hazard Mitigation of Health Care Facilities," edited by G.C. Lee, M. Ettouney, M. Grigoriu, J. Hauer and J. Nigg, 3/29/00, (PB2000-106892, A08, MF-A02).

MCEER-00-0003 "The Chi-Chi, Taiwan Earthquake of September 21, 1999: Reconnaissance Report," edited by G.C. Lee and C.H. Loh, with major contributions by G.C. Lee, M. Bruneau, I.G. Buckle, S.E. Chang, P.J. Flores, T.D. O'Rourke, M. Shinozuka, T.T. Soong, C-H. Loh, K-C. Chang, Z-J. Chen, J-S. Hwang, M-L. Lin, G-Y. Liu, K-C. Tsai, G.C. Yao and C-L. Yen, 4/30/00, (PB2001-100980, A10, MF-A02).

MCEER-00-0004 "Seismic Retrofit of End-Sway Frames of Steel Deck-Truss Bridges with a Supplemental Tendon System: Experimental and Analytical Investigation," by G. Pekcan, J.B. Mander and S.S. Chen, 7/1/00, (PB2001-100982, A10, MF-A02).

MCEER-00-0005 "Sliding Fragility of Unrestrained Equipment in Critical Facilities," by W.H. Chong and T.T. Soong, 7/5/00, (PB2001-100983, A08, MF-A02).

MCEER-00-0006 "Seismic Response of Reinforced Concrete Bridge Pier Walls in the Weak Direction," by N. Abo-Shadi, M. Saiidi and D. Sanders, 7/17/00, (PB2001-100981, A17, MF-A03).

MCEER-00-0007 "Low-Cycle Fatigue Behavior of Longitudinal Reinforcement in Reinforced Concrete Bridge Columns," by J. Brown and S.K. Kunnath, 7/23/00, (PB2001-104392, A08, MF-A02).

MCEER-00-0008 "Soil Structure Interaction of Bridges for Seismic Analysis," I. PoLam and H. Law, 9/25/00, (PB2001-105397, A08, MF-A02).

MCEER-00-0009 "Proceedings of the First MCEER Workshop on Mitigation of Earthquake Disaster by Advanced Technologies (MEDAT-1), edited by M. Shinozuka, D.J. Inman and T.D. O'Rourke, 11/10/00, (PB2001-105399, A14, MF-A03).

MCEER-00-0010 "Development and Evaluation of Simplified Procedures for Analysis and Design of Buildings with Passive Energy Dissipation Systems, Revision 01," by O.M. Ramirez, M.C. Constantinou, C.A. Kircher, A.S. Whittaker, M.W. Johnson, J.D. Gomez and C. Chrysostomou, 11/16/01, (PB2001-105523, A23, MF-A04).

MCEER-00-0011 "Dynamic Soil-Foundation-Structure Interaction Analyses of Large Caissons," by C-Y. Chang, C-M. Mok, Z-L. Wang, R. Settgast, F. Waggoner, M.A. Ketchum, H.M. Gonnermann and C-C. Chin, 12/30/00, (PB2001-104373, A07, MF-A02).

MCEER-00-0012 "Experimental Evaluation of Seismic Performance of Bridge Restrainers," by A.G. Vlassis, E.M. Maragakis and M. Saiid Saiidi, 12/30/00, (PB2001-104354, A09, MF-A02).

MCEER-00-0013 "Effect of Spatial Variation of Ground Motion on Highway Structures," by M. Shinozuka, V. Saxena and G. Deodatis, 12/31/00, (PB2001-108755, A13, MF-A03).

MCEER-00-0014 "A Risk-Based Methodology for Assessing the Seismic Performance of Highway Systems," by S.D. Werner, C.E. Taylor, J.E. Moore, II, J.S. Walton and S. Cho, 12/31/00, (PB2001-108756, A14, MF-A03).

MCEER-01-0001 "Experimental Investigation of P-Delta Effects to Collapse During Earthquakes," by D. Vian and M. Bruneau, 6/25/01, (PB2002-100534, A17, MF-A03).

MCEER-01-0002 "Proceedings of the Second MCEER Workshop on Mitigation of Earthquake Disaster by Advanced Technologies (MEDAT-2)," edited by M. Bruneau and D.J. Inman, 7/23/01, (PB2002-100434, A16, MF-A03).

MCEER-01-0003 "Sensitivity Analysis of Dynamic Systems Subjected to Seismic Loads," by C. Roth and M. Grigoriu, 9/18/01, (PB2003-100884, A12, MF-A03).

MCEER-01-0004 "Overcoming Obstacles to Implementing Earthquake Hazard Mitigation Policies: Stage 1 Report," by D.J. Alesch and W.J. Petak, 12/17/01, (PB2002-107949, A07, MF-A02).

MCEER-01-0005 "Updating Real-Time Earthquake Loss Estimates: Methods, Problems and Insights," by C.E. Taylor, S.E. Chang and R.T. Eguchi, 12/17/01, (PB2002-107948, A05, MF-A01).

MCEER-01-0006 "Experimental Investigation and Retrofit of Steel Pile Foundations and Pile Bents Under Cyclic Lateral Loadings," by A. Shama, J. Mander, B. Blabac and S. Chen, 12/31/01, (PB2002-107950, A13, MF-A03).

MCEER-02-0001 "Assessment of Performance of Bolu Viaduct in the 1999 Duzce Earthquake in Turkey" by P.C. Roussis, M.C. Constantinou, M. Erdik, E. Durukal and M. Dicleli, 5/8/02, (PB2003-100883, A08, MF-A02).

MCEER-02-0002 "Seismic Behavior of Rail Counterweight Systems of Elevators in Buildings," by M.P. Singh, Rildova and L.E. Suarez, 5/27/02. (PB2003-100882, A11, MF-A03).

MCEER-02-0003 "Development of Analysis and Design Procedures for Spread Footings," by G. Mylonakis, G. Gazetas, S. Nikolaou and A. Chauncey, 10/02/02, (PB2004-101636, A13, MF-A03, CD-A13).

MCEER-02-0004 "Bare-Earth Algorithms for Use with SAR and LIDAR Digital Elevation Models," by C.K. Huyck, R.T. Eguchi and B. Houshmand, 10/16/02, (PB2004-101637, A07, CD-A07).

MCEER-02-0005 "Review of Energy Dissipation of Compression Members in Concentrically Braced Frames," by K.Lee and M. Bruneau, 10/18/02, (PB2004-101638, A10, CD-A10).

MCEER-03-0001 "Experimental Investigation of Light-Gauge Steel Plate Shear Walls for the Seismic Retrofit of Buildings" by J. Berman and M. Bruneau, 5/2/03, (PB2004-101622, A10, MF-A03, CD-A10).

MCEER-03-0002 "Statistical Analysis of Fragility Curves," by M. Shinozuka, M.Q. Feng, H. Kim, T. Uzawa and T. Ueda, 6/16/03, (PB2004-101849, A09, CD-A09).

MCEER-03-0003 "Proceedings of the Eighth U.S.-Japan Workshop on Earthquake Resistant Design f Lifeline Facilities and Countermeasures Against Liquefaction," edited by M. Hamada, J.P. Bardet and T.D. O'Rourke, 6/30/03, (PB2004-104386, A99, CD-A99).

MCEER-03-0004 "Proceedings of the PRC-US Workshop on Seismic Analysis and Design of Special Bridges," edited by L.C. Fan and G.C. Lee, 7/15/03, (PB2004-104387, A14, CD-A14).

MCEER-03-0005 "Urban Disaster Recovery: A Framework and Simulation Model," by S.B. Miles and S.E. Chang, 7/25/03, (PB2004-104388, A07, CD-A07).

MCEER-03-0006 "Behavior of Underground Piping Joints Due to Static and Dynamic Loading," by R.D. Meis, M. Maragakis and R. Siddharthan, 11/17/03, (PB2005-102194, A13, MF-A03, CD-A00).

MCEER-04-0001 "Experimental Study of Seismic Isolation Systems with Emphasis on Secondary System Response and Verification of Accuracy of Dynamic Response History Analysis Methods," by E. Wolff and M. Constantinou, 1/16/04 (PB2005-102195, A99, MF-E08, CD-A00).

MCEER-04-0002 "Tension, Compression and Cyclic Testing of Engineered Cementitious Composite Materials," by K. Kesner and S.L. Billington, 3/1/04, (PB2005-102196, A08, CD-A08).

MCEER-04-0003 "Cyclic Testing of Braces Laterally Restrained by Steel Studs to Enhance Performance During Earthquakes," by O.C. Celik, J.W. Berman and M. Bruneau, 3/16/04, (PB2005-102197, A13, MF-A03, CD-A00).

MCEER-04-0004 "Methodologies for Post Earthquake Building Damage Detection Using SAR and Optical Remote Sensing: Application to the August 17, 1999 Marmara, Turkey Earthquake," by C.K. Huyck, B.J. Adams, S. Cho, R.T. Eguchi, B. Mansouri and B. Houshmand, 6/15/04, (PB2005-104888, A10, CD-A00).

MCEER-04-0005 "Nonlinear Structural Analysis Towards Collapse Simulation: A Dynamical Systems Approach," by M.V. Sivaselvan and A.M. Reinhorn, 6/16/04, (PB2005-104889, A11, MF-A03, CD-A00).

MCEER-04-0006 "Proceedings of the Second PRC-US Workshop on Seismic Analysis and Design of Special Bridges," edited by G.C. Lee and L.C. Fan, 6/25/04, (PB2005-104890, A16, CD-A00).

MCEER-04-0007 "Seismic Vulnerability Evaluation of Axially Loaded Steel Built-up Laced Members," by K. Lee and M. Bruneau, 6/30/04, (PB2005-104891, A16, CD-A00).

MCEER-04-0008 "Evaluation of Accuracy of Simplified Methods of Analysis and Design of Buildings with Damping Systems for Near-Fault and for Soft-Soil Seismic Motions," by E.A. Pavlou and M.C. Constantinou, 8/16/04, (PB2005-104892, A08, MF-A02, CD-A00).

MCEER-04-0009 "Assessment of Geotechnical Issues in Acute Care Facilities in California," by M. Lew, T.D. O'Rourke, R. Dobry and M. Koch, 9/15/04, (PB2005-104893, A08, CD-A00).

MCEER-04-0010 "Scissor-Jack-Damper Energy Dissipation System," by A.N. Sigaher-Boyle and M.C. Constantinou, 12/1/04 (PB2005-108221).

MCEER-04-0011 "Seismic Retrofit of Bridge Steel Truss Piers Using a Controlled Rocking Approach," by M. Pollino and M. Bruneau, 12/20/04 (PB2006-105795).

MCEER-05-0001 "Experimental and Analytical Studies of Structures Seismically Isolated with an Uplift-Restraint Isolation System," by P.C. Roussis and M.C. Constantinou, 1/10/05 (PB2005-108222).

MCEER-05-0002 "A Versatile Experimentation Model for Study of Structures Near Collapse Applied to Seismic Evaluation of Irregular Structures," by D. Kusumastuti, A.M. Reinhorn and A. Rutenberg, 3/31/05 (PB2006-101523).

MCEER-05-0003 "Proceedings of the Third PRC-US Workshop on Seismic Analysis and Design of Special Bridges," edited by L.C. Fan and G.C. Lee, 4/20/05, (PB2006-105796).

MCEER-05-0004 "Approaches for the Seismic Retrofit of Braced Steel Bridge Piers and Proof-of-Concept Testing of an Eccentrically Braced Frame with Tubular Link," by J.W. Berman and M. Bruneau, 4/21/05 (PB2006-101524).

MCEER-05-0005 "Simulation of Strong Ground Motions for Seismic Fragility Evaluation of Nonstructural Components in Hospitals," by A. Wanitkorkul and A. Filiatrault, 5/26/05 (PB2006-500027).

MCEER-05-0006 "Seismic Safety in California Hospitals: Assessing an Attempt to Accelerate the Replacement or Seismic Retrofit of Older Hospital Facilities," by D.J. Alesch, L.A. Arendt and W.J. Petak, 6/6/05 (PB2006-105794).

MCEER-05-0007 "Development of Seismic Strengthening and Retrofit Strategies for Critical Facilities Using Engineered Cementitious Composite Materials," by K. Kesner and S.L. Billington, 8/29/05 (PB2006-111701).

MCEER-05-0008 "Experimental and Analytical Studies of Base Isolation Systems for Seismic Protection of Power Transformers," by N. Murota, M.Q. Feng and G-Y. Liu, 9/30/05 (PB2006-111702).

MCEER-05-0009 "3D-BASIS-ME-MB: Computer Program for Nonlinear Dynamic Analysis of Seismically Isolated Structures," by P.C. Tsopelas, P.C. Roussis, M.C. Constantinou, R. Buchanan and A.M. Reinhorn, 10/3/05 (PB2006-111703).

MCEER-05-0010 "Steel Plate Shear Walls for Seismic Design and Retrofit of Building Structures," by D. Vian and M. Bruneau, 12/15/05 (PB2006-111704).

MCEER-05-0011 "The Performance-Based Design Paradigm," by M.J. Astrella and A. Whittaker, 12/15/05 (PB2006-111705).

MCEER-06-0001 "Seismic Fragility of Suspended Ceiling Systems," H. Badillo-Almaraz, A.S. Whittaker, A.M. Reinhorn and G.P. Cimellaro, 2/4/06 (PB2006-111706).

MCEER-06-0002 "Multi-Dimensional Fragility of Structures," by G.P. Cimellaro, A.M. Reinhorn and M. Bruneau, 3/1/06 (PB2007-106974, A09, MF-A02, CD A00).

MCEER-06-0003 "Built-Up Shear Links as Energy Dissipators for Seismic Protection of Bridges," by P. Dusicka, A.M. Itani and I.G. Buckle, 3/15/06 (PB2006-111708).

MCEER-06-0004 "Analytical Investigation of the Structural Fuse Concept," by R.E. Vargas and M. Bruneau, 3/16/06 (PB2006-111709).

MCEER-06-0005 "Experimental Investigation of the Structural Fuse Concept," by R.E. Vargas and M. Bruneau, 3/17/06 (PB2006-111710).

MCEER-06-0006 "Further Development of Tubular Eccentrically Braced Frame Links for the Seismic Retrofit of Braced Steel Truss Bridge Piers," by J.W. Berman and M. Bruneau, 3/27/06 (PB2007-105147).

MCEER-06-0007 "REDARS Validation Report," by S. Cho, C.K. Huyck, S. Ghosh and R.T. Eguchi, 8/8/06 (PB2007-106983).

MCEER-06-0008 "Review of Current NDE Technologies for Post-Earthquake Assessment of Retrofitted Bridge Columns," by J.W. Song, Z. Liang and G.C. Lee, 8/21/06 (PB2007-106984).

MCEER-06-0009 "Liquefaction Remediation in Silty Soils Using Dynamic Compaction and Stone Columns," by S. Thevanayagam, G.R. Martin, R. Nashed, T. Shenthan, T. Kanagalingam and N. Ecemis, 8/28/06 (PB2007-106985).

MCEER-06-0010 "Conceptual Design and Experimental Investigation of Polymer Matrix Composite Infill Panels for Seismic Retrofitting," by W. Jung, M. Chiewanichakorn and A.J. Aref, 9/21/06 (PB2007-106986).

MCEER-06-0011 "A Study of the Coupled Horizontal-Vertical Behavior of Elastomeric and Lead-Rubber Seismic Isolation Bearings," by G.P. Warn and A.S. Whittaker, 9/22/06 (PB2007-108679).

MCEER-06-0012 "Proceedings of the Fourth PRC-US Workshop on Seismic Analysis and Design of Special Bridges: Advancing Bridge Technologies in Research, Design, Construction and Preservation," Edited by L.C. Fan, G.C. Lee and L. Ziang, 10/12/06 (PB2007-109042).

MCEER-06-0013 "Cyclic Response and Low Cycle Fatigue Characteristics of Plate Steels," by P. Dusicka, A.M. Itani and I.G. Buckle, 11/1/06 06 (PB2007-106987).

MCEER-06-0014 "Proceedings of the Second US-Taiwan Bridge Engineering Workshop," edited by W.P. Yen, J. Shen, J-Y. Chen and M. Wang, 11/15/06 (PB2008-500041).

MCEER-06-0015 "User Manual and Technical Documentation for the REDARS™ Import Wizard," by S. Cho, S. Ghosh, C.K. Huyck and S.D. Werner, 11/30/06 (PB2007-114766).

MCEER-06-0016 "Hazard Mitigation Strategy and Monitoring Technologies for Urban and Infrastructure Public Buildings: Proceedings of the China-US Workshops," edited by X.Y. Zhou, A.L. Zhang, G.C. Lee and M. Tong, 12/12/06 (PB2008-500018).

MCEER-07-0001 "Static and Kinetic Coefficients of Friction for Rigid Blocks," by C. Kafali, S. Fathali, M. Grigoriu and A.S. Whittaker, 3/20/07 (PB2007-114767).

MCEER-07-0002 "Hazard Mitigation Investment Decision Making: Organizational Response to Legislative Mandate," by L.A. Arendt, D.J. Alesch and W.J. Petak, 4/9/07 (PB2007-114768).

MCEER-07-0003 "Seismic Behavior of Bidirectional-Resistant Ductile End Diaphragms with Unbonded Braces in Straight or Skewed Steel Bridges," by O. Celik and M. Bruneau, 4/11/07 (PB2008-105141).

MCEER-07-0004 “Modeling Pile Behavior in Large Pile Groups Under Lateral Loading,” by A.M. Dodds and G.R. Martin, 4/16/07(PB2008-105142).

MCEER-07-0005 “Experimental Investigation of Blast Performance of Seismically Resistant Concrete-Filled Steel Tube Bridge Piers,” by S. Fujikura, M. Bruneau and D. Lopez-Garcia, 4/20/07 (PB2008-105143).

MCEER-07-0006 “Seismic Analysis of Conventional and Isolated Liquefied Natural Gas Tanks Using Mechanical Analogs,” by I.P. Christovasilis and A.S. Whittaker, 5/1/07.

MCEER-07-0007 “Experimental Seismic Performance Evaluation of Isolation/Restraint Systems for Mechanical Equipment – Part 1: Heavy Equipment Study,” by S. Fathali and A. Filiatrault, 6/6/07 (PB2008-105144).

MCEER-07-0008 “Seismic Vulnerability of Timber Bridges and Timber Substructures,” by A.A. Sharma, J.B. Mander, I.M. Friedland and D.R. Allicock, 6/7/07 (PB2008-105145).

MCEER-07-0009 “Experimental and Analytical Study of the XY-Friction Pendulum (XY-FP) Bearing for Bridge Applications,” by C.C. Marin-Artieda, A.S. Whittaker and M.C. Constantinou, 6/7/07 (PB2008-105191).

MCEER-07-0010 “Proceedings of the PRC-US Earthquake Engineering Forum for Young Researchers,” Edited by G.C. Lee and X.Z. Qi, 6/8/07 (PB2008-500058).

MCEER-07-0011 “Design Recommendations for Perforated Steel Plate Shear Walls,” by R. Purba and M. Bruneau, 6/18/07, (PB2008-105192).

MCEER-07-0012 “Performance of Seismic Isolation Hardware Under Service and Seismic Loading,” by M.C. Constantinou, A.S. Whittaker, Y. Kalpakidis, D.M. Fenz and G.P. Warn, 8/27/07, (PB2008-105193).

MCEER-07-0013 “Experimental Evaluation of the Seismic Performance of Hospital Piping Subassemblies,” by E.R. Goodwin, E. Maragakis and A.M. Itani, 9/4/07, (PB2008-105194).

MCEER-07-0014 “A Simulation Model of Urban Disaster Recovery and Resilience: Implementation for the 1994 Northridge Earthquake,” by S. Miles and S.E. Chang, 9/7/07, (PB2008-106426).

MCEER-07-0015 “Statistical and Mechanistic Fragility Analysis of Concrete Bridges,” by M. Shinozuka, S. Banerjee and S-H. Kim, 9/10/07, (PB2008-106427).

MCEER-07-0016 “Three-Dimensional Modeling of Inelastic Buckling in Frame Structures,” by M. Schachter and AM. Reinhorn, 9/13/07, (PB2008-108125).

MCEER-07-0017 “Modeling of Seismic Wave Scattering on Pile Groups and Caissons,” by I. Po Lam, H. Law and C.T. Yang, 9/17/07 (PB2008-108150).

MCEER-07-0018 “Bridge Foundations: Modeling Large Pile Groups and Caissons for Seismic Design,” by I. Po Lam, H. Law and G.R. Martin (Coordinating Author), 12/1/07 (PB2008-111190).

MCEER-07-0019 “Principles and Performance of Roller Seismic Isolation Bearings for Highway Bridges,” by G.C. Lee, Y.C. Ou, Z. Liang, T.C. Niu and J. Song, 12/10/07 (PB2009-110466).

MCEER-07-0020 “Centrifuge Modeling of Permeability and Pinning Reinforcement Effects on Pile Response to Lateral Spreading,” by L.L Gonzalez-Lagos, T. Abdoun and R. Dobry, 12/10/07 (PB2008-111191).

MCEER-07-0021 “Damage to the Highway System from the Pisco, Perú Earthquake of August 15, 2007,” by J.S. O’Connor, L. Mesa and M. Nykamp, 12/10/07, (PB2008-108126).

MCEER-07-0022 “Experimental Seismic Performance Evaluation of Isolation/Restraint Systems for Mechanical Equipment – Part 2: Light Equipment Study,” by S. Fathali and A. Filiatrault, 12/13/07 (PB2008-111192).

MCEER-07-0023 “Fragility Considerations in Highway Bridge Design,” by M. Shinozuka, S. Banerjee and S.H. Kim, 12/14/07 (PB2008-111193).

MCEER-07-0024 "Performance Estimates for Seismically Isolated Bridges," by G.P. Warn and A.S. Whittaker, 12/30/07 (PB2008-112230).

MCEER-08-0001 "Seismic Performance of Steel Girder Bridge Superstructures with Conventional Cross Frames," by L.P. Carden, A.M. Itani and I.G. Buckle, 1/7/08, (PB2008-112231).

MCEER-08-0002 "Seismic Performance of Steel Girder Bridge Superstructures with Ductile End Cross Frames with Seismic Isolators," by L.P. Carden, A.M. Itani and I.G. Buckle, 1/7/08 (PB2008-112232).

MCEER-08-0003 "Analytical and Experimental Investigation of a Controlled Rocking Approach for Seismic Protection of Bridge Steel Truss Piers," by M. Pollino and M. Bruneau, 1/21/08 (PB2008-112233).

MCEER-08-0004 "Linking Lifeline Infrastructure Performance and Community Disaster Resilience: Models and Multi-Stakeholder Processes," by S.E. Chang, C. Pasion, K. Tatebe and R. Ahmad, 3/3/08 (PB2008-112234).

MCEER-08-0005 "Modal Analysis of Generally Damped Linear Structures Subjected to Seismic Excitations," by J. Song, Y-L. Chu, Z. Liang and G.C. Lee, 3/4/08 (PB2009-102311).

MCEER-08-0006 "System Performance Under Multi-Hazard Environments," by C. Kafali and M. Grigoriu, 3/4/08 (PB2008-112235).

MCEER-08-0007 "Mechanical Behavior of Multi-Spherical Sliding Bearings," by D.M. Fenz and M.C. Constantinou, 3/6/08 (PB2008-112236).

MCEER-08-0008 "Post-Earthquake Restoration of the Los Angeles Water Supply System," by T.H.P. Tabucchi and R.A. Davidson, 3/7/08 (PB2008-112237).

MCEER-08-0009 "Fragility Analysis of Water Supply Systems," by A. Jacobson and M. Grigoriu, 3/10/08 (PB2009-105545).

MCEER-08-0010 "Experimental Investigation of Full-Scale Two-Story Steel Plate Shear Walls with Reduced Beam Section Connections," by B. Qu, M. Bruneau, C-H. Lin and K-C. Tsai, 3/17/08 (PB2009-106368).

MCEER-08-0011 "Seismic Evaluation and Rehabilitation of Critical Components of Electrical Power Systems," S. Ersoy, B. Feizi, A. Ashrafi and M. Ala Saadeghvaziri, 3/17/08 (PB2009-105546).

MCEER-08-0012 "Seismic Behavior and Design of Boundary Frame Members of Steel Plate Shear Walls," by B. Qu and M. Bruneau, 4/26/08 . (PB2009-106744).

MCEER-08-0013 "Development and Appraisal of a Numerical Cyclic Loading Protocol for Quantifying Building System Performance," by A. Filiatrault, A. Wanitkorkul and M. Constantinou, 4/27/08 (PB2009-107906).

MCEER-08-0014 "Structural and Nonstructural Earthquake Design: The Challenge of Integrating Specialty Areas in Designing Complex, Critical Facilities," by W.J. Petak and D.J. Alesch, 4/30/08 (PB2009-107907).

MCEER-08-0015 "Seismic Performance Evaluation of Water Systems," by Y. Wang and T.D. O'Rourke, 5/5/08 (PB2009-107908).

MCEER-08-0016 "Seismic Response Modeling of Water Supply Systems," by P. Shi and T.D. O'Rourke, 5/5/08 (PB2009-107910).

MCEER-08-0017 "Numerical and Experimental Studies of Self-Centering Post-Tensioned Steel Frames," by D. Wang and A. Filiatrault, 5/12/08 (PB2009-110479).

MCEER-08-0018 "Development, Implementation and Verification of Dynamic Analysis Models for Multi-Spherical Sliding Bearings," by D.M. Fenz and M.C. Constantinou, 8/15/08 (PB2009-107911).

MCEER-08-0019 "Performance Assessment of Conventional and Base Isolated Nuclear Power Plants for Earthquake Blast Loadings," by Y.N. Huang, A.S. Whittaker and N. Luco, 10/28/08 (PB2009-107912).

MCEER-08-0020 “Remote Sensing for Resilient Multi-Hazard Disaster Response – Volume I: Introduction to Damage Assessment Methodologies,” by B.J. Adams and R.T. Eguchi, 11/17/08 (PB2010-102695).

MCEER-08-0021 “Remote Sensing for Resilient Multi-Hazard Disaster Response – Volume II: Counting the Number of Collapsed Buildings Using an Object-Oriented Analysis: Case Study of the 2003 Bam Earthquake,” by L. Gusella, C.K. Huyck and B.J. Adams, 11/17/08 (PB2010-100925).

MCEER-08-0022 “Remote Sensing for Resilient Multi-Hazard Disaster Response – Volume III: Multi-Sensor Image Fusion Techniques for Robust Neighborhood-Scale Urban Damage Assessment,” by B.J. Adams and A. McMillan, 11/17/08 (PB2010-100926).

MCEER-08-0023 “Remote Sensing for Resilient Multi-Hazard Disaster Response – Volume IV: A Study of Multi-Temporal and Multi-Resolution SAR Imagery for Post-Katrina Flood Monitoring in New Orleans,” by A. McMillan, J.G. Morley, B.J. Adams and S. Chesworth, 11/17/08 (PB2010-100927).

MCEER-08-0024 “Remote Sensing for Resilient Multi-Hazard Disaster Response – Volume V: Integration of Remote Sensing Imagery and VIEWS^{TM} Field Data for Post-Hurricane Charley Building Damage Assessment,” by J.A. Womble, K. Mehta and B.J. Adams, 11/17/08 (PB2009-115532).

MCEER-08-0025 “Building Inventory Compilation for Disaster Management: Application of Remote Sensing and Statistical Modeling,” by P. Sarabandi, A.S. Kiremidjian, R.T. Eguchi and B. J. Adams, 11/20/08 (PB2009-110484).

MCEER-08-0026 “New Experimental Capabilities and Loading Protocols for Seismic Qualification and Fragility Assessment of Nonstructural Systems,” by R. Retamales, G. Mosqueda, A. Filiatrault and A. Reinhorn, 11/24/08 (PB2009-110485).

MCEER-08-0027 “Effects of Heating and Load History on the Behavior of Lead-Rubber Bearings,” by I.V. Kalpakidis and M.C. Constantinou, 12/1/08 (PB2009-115533).

MCEER-08-0028 “Experimental and Analytical Investigation of Blast Performance of Seismically Resistant Bridge Piers,” by S.Fujikura and M. Bruneau, 12/8/08 (PB2009-115534).

MCEER-08-0029 “Evolutionary Methodology for Aseismic Decision Support,” by Y. Hu and G. Dargush, 12/15/08.

MCEER-08-0030 “Development of a Steel Plate Shear Wall Bridge Pier System Conceived from a Multi-Hazard Perspective,” by D. Keller and M. Bruneau, 12/19/08 (PB2010-102696).

MCEER-09-0001 “Modal Analysis of Arbitrarily Damped Three-Dimensional Linear Structures Subjected to Seismic Excitations,” by Y.L. Chu, J. Song and G.C. Lee, 1/31/09 (PB2010-100922).

MCEER-09-0002 “Air-Blast Effects on Structural Shapes,” by G. Ballantyne, A.S. Whittaker, A.J. Aref and G.F. Dargush, 2/2/09 (PB2010-102697).

MCEER-09-0003 “Water Supply Performance During Earthquakes and Extreme Events,” by A.L. Bonneau and T.D. O’Rourke, 2/16/09 (PB2010-100923).

MCEER-09-0004 “Generalized Linear (Mixed) Models of Post-Earthquake Ignitions,” by R.A. Davidson, 7/20/09 (PB2010-102698).

MCEER-09-0005 “Seismic Testing of a Full-Scale Two-Story Light-Frame Wood Building: NEESWood Benchmark Test,” by I.P. Christovasilis, A. Filiatrault and A. Wanitkorkul, 7/22/09.

MCEER-09-0006 “IDARC2D Version 7.0: A Program for the Inelastic Damage Analysis of Structures,” by A.M. Reinhorn, H. Roh, M. Sivaselvan, S.K. Kunnath, R.E. Valles, A. Madan, C. Li, R. Lobo and Y.J. Park, 7/28/09 (PB2010-103199).

MCEER-09-0007 “Enhancements to Hospital Resiliency: Improving Emergency Planning for and Response to Hurricanes,” by D.B. Hess and L.A. Arendt, 7/30/09 (PB2010-100924).

MCEER-09-0008 "Assessment of Base-Isolated Nuclear Structures for Design and Beyond-Design Basis Earthquake Shaking," by Y.N. Huang, A.S. Whittaker, R.P. Kennedy and R.L. Mayes, 8/20/09 (PB2010-102699).

MCEER-09-0009 "Quantification of Disaster Resilience of Health Care Facilities," by G.P. Cimellaro, C. Fumo, A.M Reinhorn and M. Bruneau, 9/14/09.

MCEER-09-0010 "Performance-Based Assessment and Design of Squat Reinforced Concrete Shear Walls," by C.K. Gulec and A.S. Whittaker, 9/15/09 (PB2010-102700).

MCEER-09-0011 "Proceedings of the Fourth US-Taiwan Bridge Engineering Workshop," edited by W.P. Yen, J.J. Shen, T.M. Lee and R.B. Zheng, 10/27/09 (PB2010-500009).

MCEER-09-0012 "Proceedings of the Special International Workshop on Seismic Connection Details for Segmental Bridge Construction," edited by W. Phillip Yen and George C. Lee, 12/21/09.

MCEER-10-0001 "Direct Displacement Procedure for Performance-Based Seismic Design of Multistory Woodframe Structures," by W. Pang and D. Rosowsky, 4/26/10.

MCEER-10-0002 "Simplified Direct Displacement Design of Six-Story NEESWood Capstone Building and Pre-Test Seismic Performance Assessment," by W. Pang, D. Rosowsky, J. van de Lindt and S. Pei, 5/28/10.

MCEER

EARTHQUAKE ENGINEERING TO EXTREME EVENTS

University at Buffalo, The State University of New York
Red Jacket Quadrangle ▪ Buffalo, New York 14261
Phone: (716) 645-3391 ▪ Fax: (716) 645-3399
E-mail: *mceer@buffalo.edu* ▪ WWW Site *http://mceer.buffalo.edu*

University at Buffalo *The State University of New York*

ISSN 1520-295X